

ABSTRACT

Title of Document: **THE IMPORTANCE OF SORTING CALCIUM IN PLANT CELLS: UNCOVERING THE ROLES OF A SARCOPLASMIC/ENDOPLASMIC RETICULUM-LIKE CALCIUM ATPASE**

Xiyan Li

Doctor of Philosophy, 2006

Directed By: Professor Heven Sze
Department of Cell Biology & Molecular Genetics

The spatial and temporal dynamics of intracellular Ca^{2+} in response to environmental and hormonal cues underscore the importance of Ca^{2+} transport during plant growth and development. The *Arabidopsis thaliana* genome predicts multiple genes encoding Ca^{2+} transporters, though the biological roles of most are unknown. Here I determine the function of AtECA3 which represents the first plant P-type 2A ATPase resembling mammalian sarcoplasmic/endoplasmic reticulum Ca ATPase (SERCA).

AtECA3 (At1g10130) expressed in a yeast mutant lacking its endogenous Ca^{2+} pumps functionally substitutes for the defective Ca^{2+} -ATPases. AtECA3-dependent yeast growth is blocked by thapsigargin, a specific SERCA inhibitor. The results suggest that AtECA3 is a cation pump with specificity for Ca^{2+} and Mn^{2+} , and that AtECA3 enhances yeast growth on Ca^{2+} -depleted medium or on medium with high Mn^{2+} by sequestering

Ca²⁺ or Mn²⁺, respectively, into endomembrane compartments. AtECA3 is expressed in pollen grains as revealed by promoter::GUS analyses and a green fluorescence protein (GFP)-tagged to AtECA3 labels endomembranes at the pollen tip. *In vitro* tube growth of wild-type pollen is enhanced by 10 mM Ca²⁺, and inhibited by thapsigargin, suggesting that AtECA3 supports tube elongation by sorting intracellular Ca²⁺ to appropriate compartments. This idea is supported by genetic evidence, where three T-DNA insertional mutants show 33% reduction in pollen tube length. This defect lowers sperm transmission shown as segregation distortion and decreased seed set.

AtECA3 is also expressed in vascular tissues of young roots and leaves, and the GFP-tagged protein colocalizes with two Golgi markers. Three millimolar Ca²⁺ stimulate root growth of wild-type but not of mutants, indicating that Ca²⁺ accumulation in Golgi lumen is critical for growth. Root growth of *eca3-4*, but not of wild-type, is hypersensitive to 50 μM Mn²⁺. Thus loading Mn²⁺ into Golgi lumen by AtECA3 supports root growth. Intriguingly, mutant roots show 80% increase in apoplastic peroxidase suggesting that secretory activities became deregulated.

In conclusion, I provide molecular evidence for a Golgi Ca²⁺/Mn²⁺ pump in plants. Ca²⁺ and Mn²⁺ accumulation into Golgi/secretory compartments by AtECA3 and perhaps cation release from these stores affect secretory activities critical for root growth, pollen tube elongation and male fertility.

THE IMPORTANCE OF SORTING CALCIUM IN PLANT CELLS:
UNCOVERING THE ROLES OF A SARCOPLASMIC/ENDOPLASMIC
RETICULUM-LIKE CALCIUM ATPASE

By

Xiyan Li

Dissertation submitted to the Faculty of the Graduate School of the
University of Maryland, College Park, in partial fulfillment
of the requirements for the degree of
Doctor of Philosophy
2006

Advisory Committee:

Professor Heven Sze, Chair/Advisor
Associate Professor Gerald Deitzer
Associate Professor Zhongchi Liu
Professor Ian Mather
Professor Rajini Rao
Professor Stephen M. Wolniak

© Copyright by
Xiyang Li
2006

DEDICATION

To my parents, grandparents, and my wife Zhixin.

ACKNOWLEDGEMENTS

The sincerest gratitude goes to my advisor, Dr. Heven Sze, for enlightening advices in logical reasoning, critical thinking, and interest-driven research. Her rigorous training has helped me through to be an independent researcher and will remain as a paradigmatic virtue in my academic career in the future.

I would also like to thank Dr. Jeffrey Harper and his technician Shawn Romanowsky for discussion and help in this study. I also want to extend my appreciation to my dissertation committee members, Dr. Stephen M. Wolniak, Dr. Rajini Rao, Dr. Ian Mather, Dr. Zhongchi Liu and Dr. Gerald Deitzer for the advice, encouragement and support.

My special appreciation goes to my current and former colleagues, Drs. Senthilkumar Padmanaban, Zhongyi Wu, and Guoying Wang, Yukio Kawamura, DorothyBell Poli, graduate students Yongxian Lu, Salil Chanroj, research assistant Kevin Bock, for the wonderful chance to work, talk and share.

I am always deeply grateful to my parents for constant encouragement, understanding and reassurance and to my wife for her love and tolerance.

TABLE OF CONTENTS

ABSTRACT	
DEDICATION	ii
ACKNOWLEDGEMENTS	iii
TABLE OF CONTENTS	iv
LIST OF TABLES	viii
LIST OF FIGURES	ix
ABBREVIATIONS	xi
I. GENERAL INTRODUCTION	1
1. LITERATURE REVIEW	1
1.1. Calcium: a special element for biological functionality	1
1.2. Ca ²⁺ uptake and long-distance transport in plants	4
1.3. Ca ²⁺ and cell wall remodeling	6
1.4. Functions of Ca ²⁺ in ER and Golgi apparatus	10
1.5. Functions of Ca ²⁺ in endocytosis and exocytosis	12
1.6. Ca ²⁺ in signaling and tip growth	14
1.7. Transporters that control the entry and extrusion of cellular Ca ²⁺	18
1.8. Research Questions: What are the biological roles of AtECAs?	29
2. STATEMENT OF RESEARCH GOALS	29
II. BIOINFORMATIC ANALYSES AND TISSUE EXPRESSION PATTERNS OF <i>ARABIDOPSIS</i> ECAs	31
1. ABSTRACT	31
2. INTRODUCTION	32
3. RESULTS	33
3.1. Molecular cloning of At ECAs	33
3.2. Bioinformatic analyses of AtECAs	35
3.3. Tissue expression of AtECA1-4	54
4. DISCUSSION	68
4.1. Divergent AtECA genes suggest functional diversity	68
4.2. Differential gene expression of multiple <i>Arabidopsis</i> ECAs	69
4.3. The multiplicity of AtECA genes may reflect the importance of their functional divergence in multicellular organisms	70
5. MATERIALS AND METHODS	72
5.1. Molecular cloning of AtECA cDNAs	72
5.2. Bioinformatic analyses	72
5.3. Promoter::GUS constructs for tissue expression pattern of ECAs	76
5.4. RT-PCR for tissue expression of AtECAs	77
III. A THAPSIGARGIN-SENSITIVE CA²⁺/MN²⁺ PUMP ATECA3, SUPPORTS POLLEN TUBE GROWTH AND MALE FERTILITY	78
1. ABSTRACT	78

2.	INTRODUCTION	79
3.	RESULTS	81
3.1.	AtECA3 diverges from other <i>Arabidopsis</i> ECA and shares high identity with animal SERCAs	81
3.2.	AtECA3 confers tolerance to low Ca ²⁺ / high Mn ²⁺ in yeast	84
3.3.	AtECA3-dependent yeast growth is inhibited by cyclopiazonic acid and thapsigargin	87
3.4.	AtECA3 confers hypersensitivity to high Ca ²⁺ and toxic Mn ²⁺ when expressed in K667	90
3.5.	A functional GFP-tagged AtECA3 is localized to structures resembling ER-Golgi compartments in yeast	92
3.6.	Inhibition of <i>Arabidopsis</i> pollen growth by cyclopiazonic acid and thapsigargin	92
3.7.	Identification and analyses of T-DNA insertional mutants of AtECA3	94
3.8.	Pollen tube growth is impaired in <i>eca3</i> mutants	95
3.9.	Pollen tube growth of <i>eca3-4</i> is insensitive to cyclopiazonic acid	100
3.10.	AtECA3 T-DNA mutants have reduced seed set and male gamete transmission	101
3.11.	AtECA3-GFP exhibits tip-concentrated punctate locations in pollen tubes	104
4.	DISCUSSION	104
4.1.	AtECA3 is a Ca ²⁺ /Mn ²⁺ -ATPase on the endomembrane	104
4.2.	AtECA3 is a thapsigargin-sensitive Ca ²⁺ pump that supports pollen tube growth	107
4.3.	Proposed roles of AtECA3 in pollen tube growth	109
5.	MATERIALS AND METHODS	111
5.1.	Plant Growth, and Mutants	111
5.2.	DNA manipulations	112
5.3.	Bioinformatic analyses	116
5.4.	Agrobacterium-mediated plant transformation & Histochemical GUS staining	116
5.5.	Expression analysis using RT-PCR	117
5.6.	Yeast strains, plasmids and transformation	117
5.7.	Yeast growth assays	119
5.8.	Confocal microscopy	120
5.9.	Analyses of plants	120
IV. A GOLGI Ca²⁺/Mn²⁺ PUMP AFFECTS ROOT GROWTH THROUGH SECRETION		123
1.	ABSTRACT	123
2.	INTRODUCTION	124
3.	RESULTS	126
3.1.	AtECA3 affects root growth	126
3.2.	AtECA3 is expressed in vascular tissues of <i>Arabidopsis</i> root and leaf	132

3.3.	AtECA3 localized to Golgi membranes in plant cells	132
3.4.	Enhanced apoplastic peroxidase (APX) activity and protein secretion in <i>eca3</i> mutants	138
4.	DISCUSSION	139
4.1.	AtECA3 the first plant gene encoding a Golgi-bound Ca ²⁺ /Mn ²⁺ pump	139
4.2.	Functions of a Golgi Ca ²⁺ pump in plants	143
4.3.	Role of Mn ²⁺ in the Golgi	145
4.4.	Possible roles of Golgi Ca ²⁺ in secretion and wall remodeling	146
5.	MATERIALS AND METHODS	147
5.1.	Plant Growth	147
5.2.	DNA manipulations.	148
5.3.	Transient expression in <i>Arabidopsis</i> mesophyll protoplast.	150
5.4.	Extraction of wall fluid and measurement of Apoplastic peroxidase activity.	151
V.	CONCLUSIONS AND FUTURE PROSPECTS	153
1.	CONCLUSIONS	153
1.1.	<i>Arabidopsis</i> ECA3 is a plant P-type ATPase transporting Ca ²⁺ and Mn ²⁺	153
1.2.	AtECA3 is the first plant Ca ²⁺ pump localized to Golgi membrane	154
1.3.	AtECA3 function is important for root growth and male sterility	155
1.4.	AtECA3 is the first plant Ca ²⁺ pump inhibited by thapsigargin	156
1.5.	Protein secretion is affected by a Golgi Ca ²⁺ pump, AtECA3	157
2.	FUTURE DIRECTIONS	157
2.1.	To study how Ca ²⁺ dynamics are controlled by AtECA3	158
2.2.	To study the significance of multiple ECA/SERCA in multicellular organisms	158
2.3.	To identify the regulators of ECA pumps	159
2.4.	To determine the biological functions of AtECA2	160
2.5.	To identify Ca ²⁺ -permeable channels in higher plants	160
2.6.	To identify the processed apoplastic protein that mediate intercellular communication	161
APPENDICES		163
A.	RESULTS	163
1.	Sequences of cloned ECA cDNA	163
2.	Ion content in Mutants of AtECA	172
3.	Pollen germination of <i>eca1</i> and <i>eca2</i> mutants.	174
4.	Root growth of <i>eca1</i> and <i>eca2</i> mutants.	177
5.	Generation of Gateway destination vectors for heterologous expression in yeast.	178
B.	METHODS	180
1.	Home-made Murashige and Skoog medium for <i>Arabidopsis</i> plants under different Ca ²⁺ /Mn ²⁺ conditions	180
2.	Modified ¼ Hoagland medium for <i>Arabidopsis</i> growth	182

3.	GUS staining protocol (fool-proof version)	182
4.	<i>Arabidopsis</i> pollen tube germination protocol	187
5.	Transient expression in <i>Arabidopsis</i> mesophyll protoplasts	190
6.	Extraction of apoplastic wall fluid for apoplastic peroxidase activity assay.	195
C.	Materials used in this study	197
1.	Plant Materials	197
2.	Yeast Strains and Transformants	199
3.	Vectors used in this study	199
	REFERENCES	201

LIST OF TABLES

I-1.	Summary of characterized Ca ²⁺ transporters in plants	21
II-1.	<i>Arabidopsis</i> ECA/ACA Genomic DNA	34
II-2.	Similarity and identity of AtECA to mammalian SERCA pumps	63
II-3.	PCR primers used in Chapter 2	73
II-4.	Web-based databases and software used in this research	75
III-1.	AtECA3-dependent yeast growth is sensitive to cyclopiazonic acid and to thapsigargin	89
III-2.	Primer sequences used in this study	114
IV-1.	The summary of 3 experiments measuring APX activity and total apoplastic protein	142

LIST OF FIGURES

I-1.	Chemical properties of common cations found in cells	3
I-2.	Free Ca ²⁺ concentration in a typical plant cells	7
I-3.	Membrane transporters maintain Ca ²⁺ homeostasis in plant cells	19
II-1.	Phylogenetic tree of Ca ²⁺ -ATPases from cyanobacteria, yeast, protozoan, plants, nematode, insect, fish, amphibian, and mammal	36
II-2.	Primary sequence alignment of endomembrane-type Ca ²⁺ -ATPases from eukaryote organisms human, <i>Arabidopsis</i> , rice, tomato, <i>Drosophila</i> , and yeast	39
II-3.	Predicted Topology of AtECA3	46
II-4.	Structural alignment of SERCA1a and plant ECAs	47
II-5.	Gene structures of <i>Arabidopsis</i> Ca ²⁺ -ATPases	49
II-6.	Chromosome position of <i>Arabidopsis</i> Ca ²⁺ -ATPases	51
II-7.	Multiple sequence alignment of animal phospholambans (PLN) and sarcolipins (SLN) with putative plant phospholamban	52
II-8.	Topology of putative <i>Arabidopsis</i> PLN	53
II-9.	ECA1::GUS expression in <i>Arabidopsis</i>	55
II-10.	ECA2::GUS expression in <i>Arabidopsis</i>	56
II-11.	ECA3::GUS expression in <i>Arabidopsis</i>	58
II-12.	ECA4::GUS expression in <i>Arabidopsis</i>	59
II-13.	Presence of AtECA transcripts in plant body parts	60
II-14.	Summary of tissue expression patterns of AtECAs	64
II-15.	Summary of expression of AtECAs over developmental stages.	65
II-16.	Summary of expression of AtECAs responding to various signals	66
II-17.	Expression of AtECAs and AtACAs on different pollen developmental stages	67
III-1.	AtECA3 shares high similarity with animal SERCA	82
III-2.	AtECA3 confers tolerance of K616 yeast growing on medium depleted of Ca ²⁺ or supplemented with high Mn ²⁺	86
III-3.	Growth of yeast mutants and AtECA3 transformants in medium with or without EGTA	88
III-4.	Growth of K667 yeast expressing AtECA3 is hypersensitive to high Ca ²⁺	91
III-5.	AtECA3-GFP expressed in yeast exhibits an ER-Golgi pattern	93
III-6.	<i>In vitro Arabidopsis</i> pollen tube growth is inhibited by cyclopiazonic acid (A) and by thapsigargin (B)	96
III-7.	Three alleles of AtECA3 mutants were identified	97
III-8.	Ca ²⁺ -dependent pollen tube growth is impaired in <i>eca3</i> mutants	98
III-9.	<i>In vitro</i> pollen tube growth of <i>eca3-4</i> is insensitive to inhibition by cyclopiazonic acid (A) and by thapsigargin (B)	102
III-10.	AtECA3 T-DNA mutants show reduced seed set	103
III-11.	AtECA3 fused to GFP show cortical punctate fluorescence in pollen tubes	105

IV-1.	Ca ²⁺ -stimulated root growth is inhibited in <i>Ateca3</i> mutants	128
IV-2.	Root growth of mutants is sensitive to 50 μM Mn ²⁺	129
IV-3.	Expression pattern of AtECA3 promoter::GUS in root and leaf	133
IV-4.	Free AtECA3 or ECA3-GFP fusion protein confers tolerance to toxic levels of Mn ²⁺ in K616 yeast	135
IV-5.	AtECA3 is localized to Golgi membranes in <i>Arabidopsis</i> mesophyll protoplasts	136
IV-6.	Apoplastic peroxidase (APX) activity and general protein secretion were enhanced in <i>Ateca3</i> mutant	140

ABBREVIATIONS

$[Ca^{2+}]_{\text{cyt}}$	free Ca^{2+} concentration in the cytosol
$[Ca^{2+}]_{\text{ext}}$	extracellular free Ca^{2+} concentration
$[Ca^{2+}]_{\text{lum}}$	luminal free Ca^{2+} concentration
ABA	Abscisic acid
ACA	autoinhibitory-type Ca^{2+} -ATPase
APX	apoplastic peroxidase
ATP	adenosine 5'-triphosphate
AWF	apoplastic wall fluid
CaM	calmodulin
CAX	Ca^{2+}/H^{+} exchanger
cDNA	complementary deoxyribonucleic acid
CPA	cyclopiazonic acid
DIC	differential interference contrast
DNA	deoxyribonucleic acid
ECA	endomembrane-type Ca^{2+} -ATPase
EGTA	ethylene glycol-bis(β -aminoethyl ether)-N,N,N',N'-tetraacetic acid
ER	endoplasmic reticulum
EST	expressed sequence tag
GFP	green fluorescent protein
GmMan1	soybean α -1,2 mannosidase 1
GUS	β -Glucuronidase
MES	2-(N-Morpholino)ethanesulfonic acid
mRNA	messenger ribonucleic acid
OD600	optical density at wavelength of 600 nm
ORF	open reading frame
PCR	polymerase chain reaction
PLN	phospholamban

PM	plasma membrane
PMCA	plasma membrane Ca^{2+} -ATPase
RFP	red fluorescent protein
RNA	ribonucleic acid
RT	reverse transcriptase or transcription
SERCA	sarcoplasmic/endoplasmic reticulum Ca^{2+} -ATPase
SLN	sarcolipin
SNARE	soluble NSF attachment receptor
SPCA	secretory pathway Ca^{2+} -ATPase
ST	rat sialyltransferase
SV	secretory vesicle
T-DNA	Transfer DNA (Agrobacterium)
TG	thapsigargin
TM	transmembrane domain
X-Gluc	5-bromo-4-chloro-3-indolyl-beta-D-glucuronic acidacidicyclohexylammonium salt

I. GENERAL INTRODUCTION

1. LITERATURE REVIEW

The research described in this dissertation focuses on a group of plant proteins carrying out Ca^{2+} translocation across biomembranes. Since Ca^{2+} is implicated in various biological processes, I give a broad introduction to include all the possible functions of a Ca^{2+} transporter. This section starts with a comparison of Ca^{2+} and cation chemical properties, which is followed by an introduction of the roles of Ca^{2+} in plant biology from a few different perspectives and by a review of Ca^{2+} transporter activities and biological functions. It provides a general knowledge base for the research presented in this dissertation.

1.1. Calcium: a special element for biological functionality

In biological systems, cations are discriminated by their chemical properties in membrane transport. The transport specificity and efficiency of a given transporter is determined by the Coulomb interaction of its key amino acid residues with cations. Therefore, a comparison of the electrochemical properties of different cations provides fundamental understandings of how each cation is used in a specific and efficient way to sustain the biological processes.

Calcium is the third most abundant metal element in the earth's crust, only less than aluminum (Al) and iron (Fe) (Lutgens and Tarbuck, 1995). Unlike Al^{3+} or $\text{Fe}^{2+}/\text{Fe}^{3+}$, ionic Ca^{2+} is relatively stable in that its aqueous chemical form is independent of proton concentration or reducing/oxidizing status. Furthermore, divalent Ca^{2+} can be used to bridge two negatively charged organic molecules to form matrix structures.

These features may account for the compositional essentiality of Ca^{2+} in all cellular structures, such as for plant cell wall and animal extracellular matrix (Maurer and Hohenester, 1997; Periz and Fortini, 1999; Hepler, 2005).

Ca^{2+} is unique in its mild electric field strength at the surface, large unhydrated ionic radius, and relatively small hydrated ionic radius (Fig. I-1). In aqueous solutions, cations are hydrated and move along with bound H_2O molecules as a whole (Chang, 2005). The hydrated cations are stripped of bound H_2O before being translocated within membrane-spanning tunnel of cation transporters. Within the tunnel, cations are screened by their width and the electric field formed from protruding side chains of amino acid residues. The properties contribute to the ion specificity of a given ion transporter at three distinct steps: 1) recognition of hydrated ions of proper size and shedding of bound H_2O ; 2) translocation of “naked” ions within the tunnel; and 3) release and re-hydration of cations at the other side.

A summary of relative surface electric field strength, ionic size, and hydration energy of common cations illustrates the distinct features of Ca^{2+} ions (Fig. I-1). Both Na^+ and K^+ have similar hydrated cation size as Ca^{2+} . However, the hydration energy of Ca^{2+} (-1579 kJ/mol) is strong compared with Na^+ (-405 kJ/mol) and K^+ (-314 kJ/mol) so that Ca^{2+} ion is associated selectively and firmly with anionic molecules. On the other hand, the hydration energy of Ca^{2+} is still mild enough so that bound Ca^{2+} is readily disassociated from anions by alternation in ionic strength and pH when compared with other strong binders such as -4665 kJ/mol of Al^{3+} , -4355 kJ/mol of Fe^{3+} , -1950 kJ/mol of Fe^{2+} , -1926 kJ/mol of Mg^{2+} (Chang, 2005). This reversibility is universally utilized to

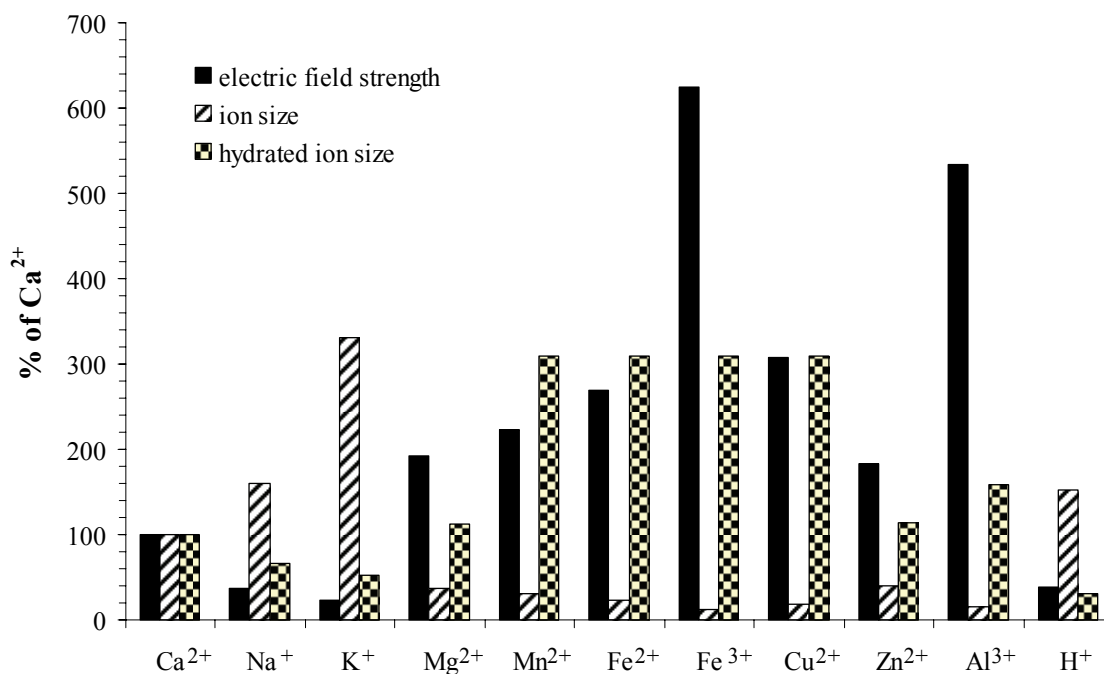


Figure I-1. Chemical properties of common cations found in cells.

Relative diameters of unhydrated and hydrated ions were obtained from Shannon (1976) and Kielland (1937). Hydration energy values of cations were from Chang (2005). All values were normalized to those of Ca²⁺. Electric field strength was calculated as Ze/r^2 , where Z is the number of charges, e is the electron charge, and r is the ionic radius. Ion size and hydrated ion size were based on $4\pi r^3/3$ while r is ionic radius. The unhydrated and hydrated ionic radii for Ca²⁺ are 1 Å and 4.12 Å, respectively. The size is based on the spherical volume of each ion. 100 % are 32.04 C/m², 4.2 x 10⁻³⁰ m³, and 2.9 x 10⁻²⁸ m³ for electric field strength, ion size, and hydrated ion size, respectively.

relay informational flux within the cell and at the cell surface. Not surprisingly, Ca^{2+} has been linked in plants to hormonal and environmental reactions as membrane potential modulator (membrane-crossing flux) and enzymatic regulator (cytosolic fluctuation and binding). Perturbation in Ca^{2+} homeostasis compromises a wide range of signaling circuits, such as ABA-regulated guard cell movement, nodulation, and pollen tube guidance in plants (Taylor and Hepler, 1997; Sanders et al., 1999; Hepler et al., 2001; Sanders et al., 2002).

The unique chemical features and natural abundance may underline the widely observed involvement of Ca^{2+} in organisms. The roles Ca^{2+} may play in plants can be divided into three aspects: 1) structural components such as bridging of pectate molecules in cell wall, most of Ca^{2+} is used for this purpose; 2) enzymatic co-factors or ligands such as Ca^{2+} -dependent proteins, like protein-folding aide calnexin in ER lumen, and signaling components Ca^{2+} -dependent kinases in the cytosol; and 3) as a second messenger, which is often expressed and recorded as localized distinctive Ca^{2+} oscillations that relay signal response in the cytoplasm.

1.2. Ca^{2+} uptake and long-distance transport in plants

Ca^{2+} is an essential macronutrient required at millimolar levels in growth medium for plants (Marschner, 1986). For multicellular organisms like higher land plants, Ca^{2+} is taken up at the root surface from the soil, which usually contains sufficient Ca^{2+} due to the natural abundance of Ca^{2+} in the earth's crust. Available Ca^{2+} may be limited occasionally when the soil solution has a limited basic buffering capacity and has a high pH, because Ca^{2+} precipitates with many organic/inorganic weak acids when the pH is above neutral. However, Ca^{2+} deficiency is more commonly caused by insufficient Ca^{2+}

supply within the plant body, especially in growing and developing tissues, mainly because new walls demand a large quantity of Ca^{2+} to maintain the functionality of the cell wall (White and Broadley, 2003).

Based on the Ca^{2+} content in root and in shoot, it was estimated that a Ca^{2+} flux of $\sim 30 \text{ mmol (m}^2 \text{ axis)}^{-1} \text{ s}^{-1}$ is required for a hypocotyl of 20 mm^2 when growing at 0.1 relative length per day (Raven, 1986). Therefore, it is thought that Ca^{2+} is mainly transported in the apoplast over a long distance ($>$ several millimeters) (Raven, 1986; White, 2001). This type of Ca^{2+} mass flow occurs in the xylem, which is driven by transpiration occurring in photosynthetic regions (Storey and Leigh, 2004). For growing tissues with low transpiration rates, Ca^{2+} is transported via the relatively slow symplastic system, which may account for Ca^{2+} deficiency symptoms in young growing regions, and a Ca^{2+} gradient between vascular terminus (high in the bundle sheath) and epidermal tissue in leaves (Storey and Leigh, 2004). Because of the presence of water-impermeable suberized Casparian band in the longitudinal side of endodermal cells above the root differentiation zone, plants accomplish apoplastic Ca^{2+} transport from soil to root xylem only at undifferentiated root tip region (White, 2001). Ca^{2+} enters the cell via cation-permeable channels on the plasma membrane. Redistribution of Ca^{2+} into internal organelles is carried out by Ca^{2+} pumps and $\text{Ca}^{2+}/\text{H}^+$ exchangers residing on endomembranes (Sze et al., 2000).

Within plant cells, calcium is distributed in an apparently controlled manner. The free calcium concentration in cytosol ($[\text{Ca}^{2+}]_{\text{cyt}}$) is estimated at 10^{-7} M level while the calcium concentration outside cells or in intracellular compartments, such as endoplasmic reticulum (ER), mitochondria, and vacuole, can be as high as 10^{-3} M (Fig. I-2) (Hepler,

2005). When internal transport and distribution is inadequate, Ca^{2+} starvation at certain locations results in calcium deficiency symptoms, manifested by necrosis of young meristematic regions, general chlorosis, deformed and downward hooking of young leaves, and brownish, short, and highly branched root systems, or even severe stunting (Taiz and Zeiger, 2002). Therefore, proteins that regulate the entry and extrusion of cytosolic calcium levels have to be exquisitely regulated to achieve the critical balance required for plant development and survival (Sanders et al., 2002).

1.3. Ca^{2+} and cell wall remodeling

The immobility of plants necessitates a fortified protective scaffold to support a multicellular body plan and to accommodate environmental challenges such as wind, light, and drought conditions. A typical plant is composed of ~ 35 cell types, each of which is made of a pliable protoplasm enclosed by a rigid but flexible carbohydrate-rich wall layer (Cosgrove, 2005). In spite of distinctive variations in shape, size, and function between different cell types, all plant cells are subject to a demanding task of: construction and maintenance of its supporting and protective wall by the control of developmental and environmental cues.

Young plant cells start with a thin layer of primary cell wall which is primarily composed of microfibril bundles (cellulose polymer) and cross-linking hemicellulose and pectin molecules. The growing wall yields in tensile strength to turgor pressure from the protoplasm, and the cross-linking of hemicellulose or pectin is loosened by pH-dependent enzymes such as expansins and pectin methylesterases (Cosgrove, 1997; Bosch et al., 2005; Jiang et al., 2005). Except for cellulose, and callose occasionally, which are synthesized at the cell surface, all other wall polymers are synthesized *de novo* by

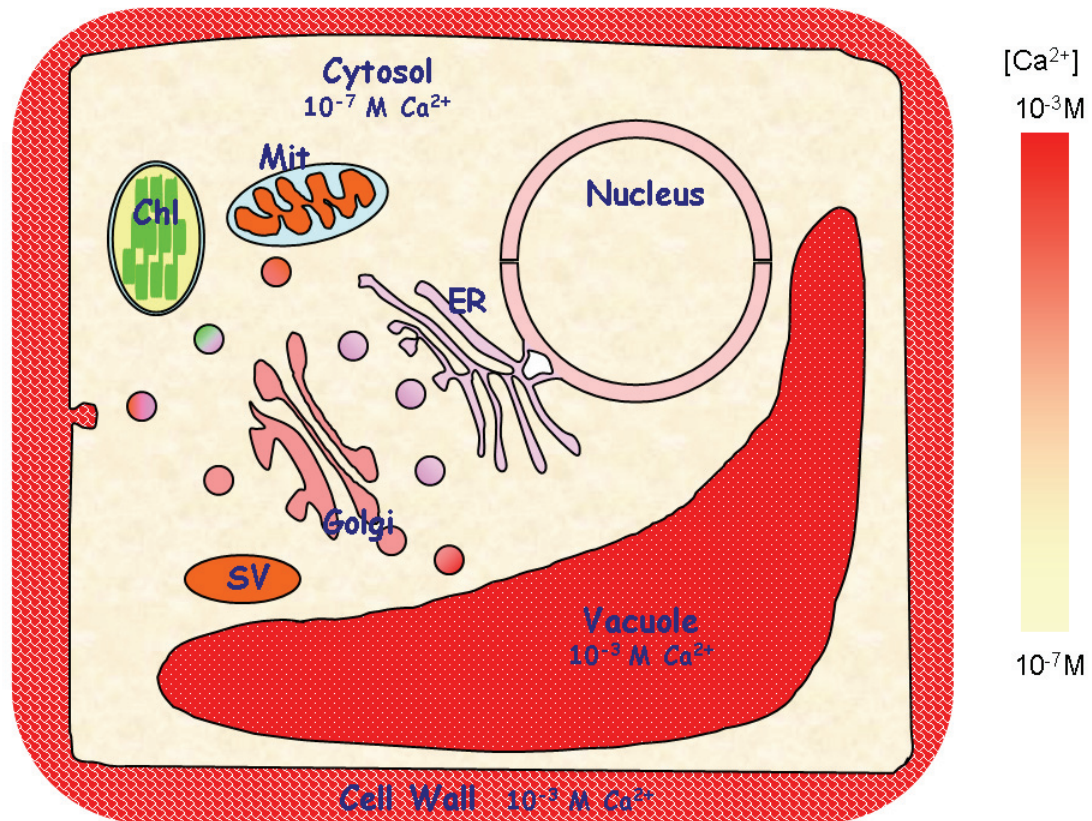


Figure I-2. Free Ca^{2+} concentration in a typical plant cells.

Free Ca^{2+} concentration ($[\text{Ca}^{2+}]$) is drawn in a heat map pattern. Warmer color indicates higher free $[\text{Ca}^{2+}]$. In unexcited cells, the cytosolic $[\text{Ca}^{2+}]$ is maintained at 10^{-7} M to avoid precipitation with other anions whereas organellar lumens are filled with 10^{-3} M $[\text{Ca}^{2+}]$.

nucleotide sugar interconversion within the Golgi apparatus, and secreted in vesicles along the secretory pathway (Buchanan et al., 2000; Taiz and Zeiger, 2002). The secretory system poses a demanding pressure on protein folding, post-translational modification, and vesicular trafficking process, especially for those cells with active wall modeling and remodeling such as dividing cells, vascular cells and growing pollen tubes (Cosgrove, 1997; Cosgrove, 2005).

a. Pectin biosynthesis

Calcium is an abundant constituent in the cell walls where the majority of Ca^{2+} is bound to pectins forming a homogalacturonan (HGA, pectin constituent) in the junction zones of pectin macromolecular structure (Ridley et al., 2001). The spacing of the junction zones, combined with other cross-linking sugar residues, defines a cell-specific pore size in the wall matrix that permits free diffusion of molecules within the apoplast (Buchanan et al., 2000; Willats et al., 2001). It is estimated that at least 53 enzymatic activities are required to produce complex structure of pectin (Ridley et al., 2001). However, very little is known of these enzymes. Immuno-cytochemical evidence has revealed that HGA is synthesized in cis-Golgi, and esterified in medial/trans-Golgi apparatus (Ridley et al., 2001). Pectin is secreted and inserted into cell wall in a highly methylesterified form although some cell types also secrete an unesterified form. Methylated pectins are more soluble and can withstand higher tensile stress, which may be necessary for young cell enlargement and elongation. A pH-dependent secreted protein pectin methylesterase (PME) activity regulates pectin matrix structure by exposing carboxyl groups which are then crosslinked into tighter and stiffer 3-dimensional structure by apoplastic Ca^{2+} (Willats et al., 2001; Hepler, 2005). Given that

all pectin-synthesizing enzymes are located in the Golgi and all pectin mass and modifying enzymes are secreted through the Golgi, it is very likely that pectin biogenesis is largely dependent on the correct maintenance and functionality of the Golgi (Hawes, 2005).

Processes involving pectin deposition or pectin cross-linking require Ca^{2+} either as components or indirectly as biogenesis co-factor (such as Golgi protein folding and modification). These include cell elongation, ripening, and pollen tube growth where pectins are secreted or assembled in wall-forming phragmoplast. Calcium deficiency causes disintegration of cell walls which is expressed as the collapse of petioles and the upper parts of the stems (Marschner, 1986).

b. Cellulose production

$\text{Ca}^{2+}/\text{Mg}^{2+}$ are also required as effectors for *in vitro* cellulose synthesis (Doblin et al., 2002). Cellulose synthase complex (CesA) in higher plants is large (>500kDa), integral to the membrane, and composed of 36 cellulose synthase catalytic subunits (CesA, three isoforms) in a six-fold symmetric rosette architecture. The assembly of CesA occurs in the Golgi. A Ca^{2+} -activated membrane-bound cellulase in *Arabidopsis*, the Korrigan cellulase (Kor) is required for cellulose synthesis, possibly by transferring cellobiose or larger units from the lipid donor to the growing cellulose chain (Doblin et al., 2002; Robert et al., 2005). Glycosylation is found in CesA and is required for Kor to function properly. Cortical microtubule arrays are also involved in directing the alignment and the orientation of cellulose deposition (Salnikov et al., 2001; Gardiner et al., 2003). Considering both cytoskeleton organization and protein glycosylation depend

on changes in Ca^{2+} concentration, cellulose biosynthesis may also be affected by Ca^{2+} at multiple steps.

c. Secreted wall proteins

In plant cells, there are four major classes of structural proteins in the cell wall: the hydroxy-proline-rich glycoproteins (HRGPs), the proline-rich proteins (PRPs), the glycine-rich proteins (GRPs), and arabinogalactan proteins (AGPs) (Buchanan et al., 2000; Showalter, 2001). These proteins are glycosylated to varying extent and exhibit distinctive abundance in the cell wall of different cell types, implying specific functions. Members of these protein groups are involved in structure, morphogenesis, intercellular interactions (Cassab, 1998). The functions of wall proteins depend on a bona fide secretory system and extracellular Ca^{2+} homeostasis.

1.4. Functions of Ca^{2+} in ER and Golgi apparatus

All membrane, luminal, and secreted proteins are synthesized and co-translationally inserted into the lumen of the rough ER. These proteins are then progressively processed along the ER-to Golgi system. The Golgi apparatus is also where most of wall carbohydrates are synthesized and modified. ER luminal Ca^{2+} is maintained at near mM concentrations so that Ca^{2+} -dependent chaperones such as calnexin and calreticulin help nascent protein folding. In the Golgi, luminal Ca^{2+} is at similar levels, which ranges from 0.1-1.0 mM free Ca^{2+} in contrast to $\sim 0.2 \mu\text{M}$ in cytosol. However, in spite of lack of quantitative evidence, the majority of the Ca^{2+} in the Golgi is in bound form, which is acting as a co-factor for enzymatic activities that control glycosylation and other post-translational protein modification. Retrograde membrane trafficking from Golgi to ER, secreted protein aggregating and sorting in the trans-Golgi

network (TGN) are also dependent on sufficient presence of luminal Ca^{2+} (Chanat and Huttner, 1991; Ivessa et al., 1995). Nevertheless, the presence and importance of Ca^{2+} -binding proteins in ER-Golgi lumen such as plant Golgi resident calreticulin (Borisjuk et al., 1998) and ER resident calnexin (Nash et al., 1994), both of which are activated by Ca^{2+} -binding, impose another critical requirement for sufficient loading of Ca^{2+} .

When animal cells are starved of Ca^{2+} , insufficient luminal Ca^{2+} negatively affects protein folding chaperones, calnexin and calreticulin, which in turn results in accumulation of unfolded/misfolded nascent proteins in ER. Unfolded protein response thus incurs and leads to export of the unfolded proteins to the cytosol via translocons (protein-transporting complex on ER membrane) for degradation. The opening of translocons is accompanied by ER-luminal Ca^{2+} release into cytosol which in turn leads to activation of caspases and then induction of cell death (Wuytack et al., 2003).

Excessive Ca^{2+} in the soil is rarely a problem for plants. The plants attenuate this situation by decreasing membrane permeability, like what is observed in zygotes of the alga *Pelvetia* (Robinson, 1977), or by restoring excessive Ca^{2+} in the vacuole using H^{+} -coupled transporters (Hirschi, 2001).

As mentioned above, Ca^{2+} is involved in many steps during the cell wall synthesis and expansion. Deficient Ca^{2+} loading ability into the ER-Golgi-SV (secretory vesicles) lumen, therefore, could cause insufficient folding and modification of wall assembling enzymes, thus a decrease in wall secretion, synthesis, and expansion, which is evidenced in various assays (Cosgrove, 1997).

1.5. Functions of Ca^{2+} in endocytosis and exocytosis

Exocytosis occurs in all growing cells, and in cells specialized in secretory activities. For example, growing cells delivery wall polysaccharides, membrane proteins and lipids, and structural and enzymatic proteins from trans-Golgi network to the cell surface. Recent advances in cell biology show that many exocytotic events are coupled to endocytotic processes, though the extent of such “kiss-and-run” events is poorly documented in plant cells.

During exocytosis, there are generally 2 types of membrane fusion: transient fusion for cargo release only during secretion, and permanent fusion for membrane incorporation during cell expansion. The ratio of these two processes within the cell varies greatly between cell types for functional purpose. Exocytosis, as monitored by change in membrane capacitance in barley aleurone protoplast, involves at least 2 types of vesicles targeted to the PM: Ca^{2+} -stimulated vesicles which are also modulated by Ca^{2+} -binding protein; and Ca^{2+} -independent vesicles which are thought to contribute to cell expansion during cell growth (Homann and Tester, 1997). Although technical difficulties limit our understanding of the mechanism controlling exocytosis, Ca^{2+} is thought to be involved in several aspects. The first is likely through a Ca^{2+} -dependent binding of synaptotagmin to v-/t-SNARE complex-primed vesicle fusion observed in synapses (Goda and Sudhof, 1997). It is thought that both Ca^{2+} -dependent activator protein for secretion (CAPS) and annexin promote membrane fusion by Ca^{2+} -dependent binding to phospholipids (Martin, 1997; Battey et al., 1999).

In plant cells as in animal cells, endocytosis is thought to serve several purposes, such as membrane recycling, internalization of receptor and ligand, and cell volume

regulation (Battey et al., 1999). While most genes and proteins involved in endocytosis are found in plants (Battey et al., 1999), direct evidence relating secretion and development is still lacking. A large portion of endocytosis seems to retrieve membranes used for exocytosis in nongrowing cells (Battey et al., 1999). In pollen tube elongation of self-incompatible plants, endocytosis is used to internalize and compartmentalize S-locus determinants, a group of S-RNases (Sijacic et al., 2004; Goldraij et al., 2006). Osmoregulation of cell volume occurs in guard cells whose size changes greatly in response to light or drought over the short term. A reversible surface area change was observed in guard cells treated hypoosmotically suggesting that pressure-driven membrane turnover involved exo- and endocytosis of the plasma membrane which is accompanied by the addition and removal of K channels (Homann, 1998; Meckel et al., 2005).

Endocytosis and exocytosis are often coupled to maximize material transport while minimizing the energy and material cost to the cells. In rat adrenaline-containing chromaffin cells, in the presence of high $[Ca^{2+}]_{cyt}$, endocytosis occurs immediately after exocytosis in <1 ms (Ales et al., 1999). This kiss-and-run fusion provides a fast and recurrent means to release its cargo upon a Ca^{2+} spike. This strategy may also be used in signal-responding cells in plants, such as guard cell movement and pollen tube growth, in which the $[Ca^{2+}]_{cyt}$ spike may regulate the secretion on the PM and thus the cellular response to signals from outside. However, additional studies are needed to disclose the mechanisms involved.

1.6. Ca^{2+} in signaling and tip growth

a. Ca^{2+} is a ubiquitous second messenger

Many studies show that in response to a stimulus, there is a local and transient increase in $[\text{Ca}^{2+}]_{\text{cyt}}$. The increase in $[\text{Ca}^{2+}]_{\text{cyt}}$ is due to Ca^{2+} influx from outside the cells and/or Ca^{2+} released from intracellular compartments to the cytosol, and the decrease in $[\text{Ca}^{2+}]_{\text{cyt}}$ has been attributed to stimulation of transporters that either sequester Ca^{2+} into endomembrane stores or pump the ion outside the cell. Cytosolic Ca^{2+} signal is in turn decoded by proteins sensing distinct Ca^{2+} spikes and other downstream signaling components which include phosphorelay and transcriptional regulation (Sanders et al., 2002).

Signal transduction pathways induced by biotic stimuli, such as abscisic acid (ABA), gibberellin (GA), fungal elicitors, and nodulation factors (Nod), elicit $[\text{Ca}^{2+}]_{\text{cyt}}$ increase. For example, a sustained steady state $[\text{Ca}^{2+}]_{\text{cyt}}$ increase from exterior and/or vacuole is induced by ABA treatment, which may be mediated by IP_3 , cyclic ADP-ribose, sphingosine-1-phosphate, hyperpolarization activation of plasma membrane Ca^{2+} channels, and reactive oxygen species (ROS). However, these responses are not mutually exclusive. Instead, each response may be interpreted in the cells into distinctive Ca^{2+} signals with different oscillation frequencies, amplitudes, and localizations (Finkelstein et al., 2002). How plants manage this mission is still largely unclear.

There are generally 2 types of Ca^{2+} signaling following conditional influx and release of Ca^{2+} into the cytosol: calmodulin (CaM)-dependent and CaM-independent. In calmodulin (CaM)-dependent pathways, released Ca^{2+} binds to CaM to induce the conformational change of the latter. The resultant Ca^{2+} /CaM complex binds to and

activates various Ca^{2+} -dependent protein kinases (CDPKs), phosphatases (e.g. a calcineurin, SOS3 in *Arabidopsis* (Ishitani et al., 2000)), and thus other enzymes, thus relaying the signal to downstream components. Auto-inhibitory Calcium ATPases (ACAs) in *Arabidopsis*, which will be discussed later, are thought to be involved in this type of signaling pathway because of the presence of CaM-activated domains (Hwang et al., 2000).

How do these different signals share a key common messenger but result in distinct responses? One working hypothesis is that Ca^{2+} signals are spatially and temporally regulated within specific cell-types, due to spatial localization of the transporters which give rise to distinct frequencies and amplitudes of $[\text{Ca}^{2+}]_{\text{cyt}}$ oscillations (Ca^{2+} signature). It is thought that Ca^{2+} signature designates specificity of signal properties (Sanders et al., 1999; Plieth, 2005). Therefore, regardless of what other signaling components are involved, a specifically patterned regulation of Ca^{2+} entry and extrusion in the cells is necessary to encode and decode each stimulus the cells perceive. A detailed biochemical, cellular, and physiological study of Ca^{2+} transporters would help to understand these signaling mechanisms.

b. Ca^{2+} is the major ionic regulator in pollen germination and tube growth

Several systems have been well established to study the roles of Ca^{2+} in plants including polarized growth models of pollen and root hair growth (Hepler et al., 2001; Carol and Dolan, 2002), signal sensing models in guard cell movement and root growth tropisms (Assmann and Wang, 2001; Massa et al., 2003). Here I focus mainly on pollen tube growth.

In vitro pollen growth has been a robust system to dissect the roles of Ca^{2+} by combining direct observation of ion dynamics using a Ca^{2+} imaging approach, direct observation of ion flux using a patch-clamp approach, direct observation of change in growth rate, and, more recently, direct link to the function of a gene when combined with reverse or forward genetic approaches.

Pollen is the male gametophyte that delivers sperm cells to the ovule in a process of polarized cell expansion (tube growth) driven by internal outward turgor pressure in higher plants. Depending on species, the time it takes for pollen tubes to grow from the stigma surface to the fertilization location near the ovules varies markedly from 5 hours of continuous expansion in *Arabidopsis* (Faure et al., 2002) to around 8 weeks of intermittent expansion in alder trees (Sogo and Tobe, 2005). This process is strictly regulated by developmental and environmental cues and carried out by an exquisitely coordinated functional hierarchy of signaling, cellular streaming, membrane trafficking, and wall deposition.

Ca^{2+} is essential for pollen germination and tube growth (Brewbaker and Kwack, 1963). The first report of the presence of Ca^{2+} came from the Ca^{2+} radiograph of growing lily pollen tubes (Jaffe et al., 1975). $^{45}\text{Ca}^{2+}$ was found to be 100 times higher in the tip region ($\sim 20 \mu\text{m}$) than in the shank, and concentrated in the cytoplasm. It was later found that the Ca^{2+} influx at the tube tip is essential for sustained tube growth because the $[\text{Ca}^{2+}]_{\text{cyt}}$ maximum at the tube tip is decreased when Ca^{2+} channel inhibitor, La^{3+} , is added to the medium (Obermeyer and Weisenseel, 1991). The channel activity also correlates well in spatial and temporal dynamics with $[\text{Ca}^{2+}]_{\text{cyt}}$. Interestingly, the Ca^{2+} influx only comprises a small portion of the observed cation influx at the tip when

compared with the K^+ influx (Weisenseel and Jaffe, 1976), suggesting Ca^{2+} is not used for membrane potential modulation. These observations have been reexamined by fluorescence ratiometric Ca^{2+} imaging using Ca^{2+} -specific dyes fura-2 and quin-2 (Obermeyer and Weisenseel, 1991; Miller et al., 1992) and using indo-1 (Rathore et al., 1991). Changes in the direction of apical Ca^{2+} influx also re-orient the tube growth direction (Malho et al., 1995; Malho and Trewavas, 1996).

In addition, the tip-focused free Ca^{2+} gradient, which decreases sharply from 5 μM beneath the tip apex to 0.1 μM within 20 μm along the tube axis as revealed by microinjected dextran-conjugated Ca^{2+} fluorescence dye (Holdaway-Clarke and Hepler, 2003), is correlated with active tube growth (Miller et al., 1992). This gradient is oscillating in phase with the peak growth rate with a period of ~ 42 seconds and an amplitude of 0.75-3.0 μM (Pierson et al., 1994; Holdaway-Clarke et al., 1997; Messerli and Robinson, 1997). This observation is confirmed by using a proteinaceous Ca^{2+} sensor, cameleon, in *Arabidopsis* pollen tube (Iwano et al., 2004). This tip-focused Ca^{2+} gradient may set up a chemotactic scheme to direct tube growth because of the lack of cytoskeleton in the apical region (clear zone), which is supported by the observation that a Ca^{2+} ionophore applied to the lateral-apical region changed the direction of tube growth (Malho and Trewavas, 1996). The gradients and fluxes of other cations, such as H^+ and K^+ are also required for fast tube growth, but for different purposes (Holdaway-Clarke and Hepler, 2003). For example, massive K^+ flux is used to rectify membrane potential and to control osmotic potential in cytosol. A scenario of how these ions are maintained in growing tube apex was reviewed recently (Sze, et al. 2006).

A challenging question is how the oscillating free cytosolic Ca^{2+} gradient at the pollen tube tip is generated and maintained. Ca^{2+} most likely enters by passive flow through ion channels on the PM or is released from endomembranes, given the negative inside membrane potential (-130 mV) and existing pH gradient across the PM. The prompt sequestering of Ca^{2+} into endomembrane compartments, or its extrusion outside of the cell, is needed to restrict the Ca^{2+} gradient to the extreme apex of growing tubes. Since large organelles such as mitochondria, plastids, and vacuoles are blocked by an actin mesh behind the clear zone (thus the Ca^{2+} gradient), it is very likely that active Ca^{2+} transporters, ATPases and H^+ -coupled antiporters on the abundant small vesicles derived from secretory pathway (e.g. the Golgi), as observed under electron microscope using a freeze substitution method (Lancelle et al., 1997), help lower the $[\text{Ca}^{2+}]_{\text{cyt}}$ by 50 fold along a short distance of 20 μm .

However, the molecular mechanism underlying how this critical gradient is generated and the oscillation maintained, e.g. what Ca^{2+} transporters are involved, is still not well understood but pieces of evidence have appeared recently (see next section).

1.7. Transporters that control the entry and extrusion of cellular Ca^{2+}

Using *Arabidopsis* as a model, plants have 3 groups of calcium-conducting transporters:

1) Ca^{2+} -permeable channels, 2) $\text{H}^+/\text{Ca}^{2+}$ antiporters, and 3) Ca^{2+} -ATPases (Ca^{2+} pumps).

Ca^{2+} -permeable channels allow the Ca^{2+} influx and release into the cytosol under certain conditions, while both Ca^{2+} antiporters and Ca^{2+} pumps extrude Ca^{2+} from the cytosol into endomembrane compartments and to the exterior of the cells (Fig. I-3). The

coordination of the activities by these 3 groups serves two highly demanding missions:

1) to maintain the Ca^{2+} homeostasis in cells (e.g. low in cytosol and high in the

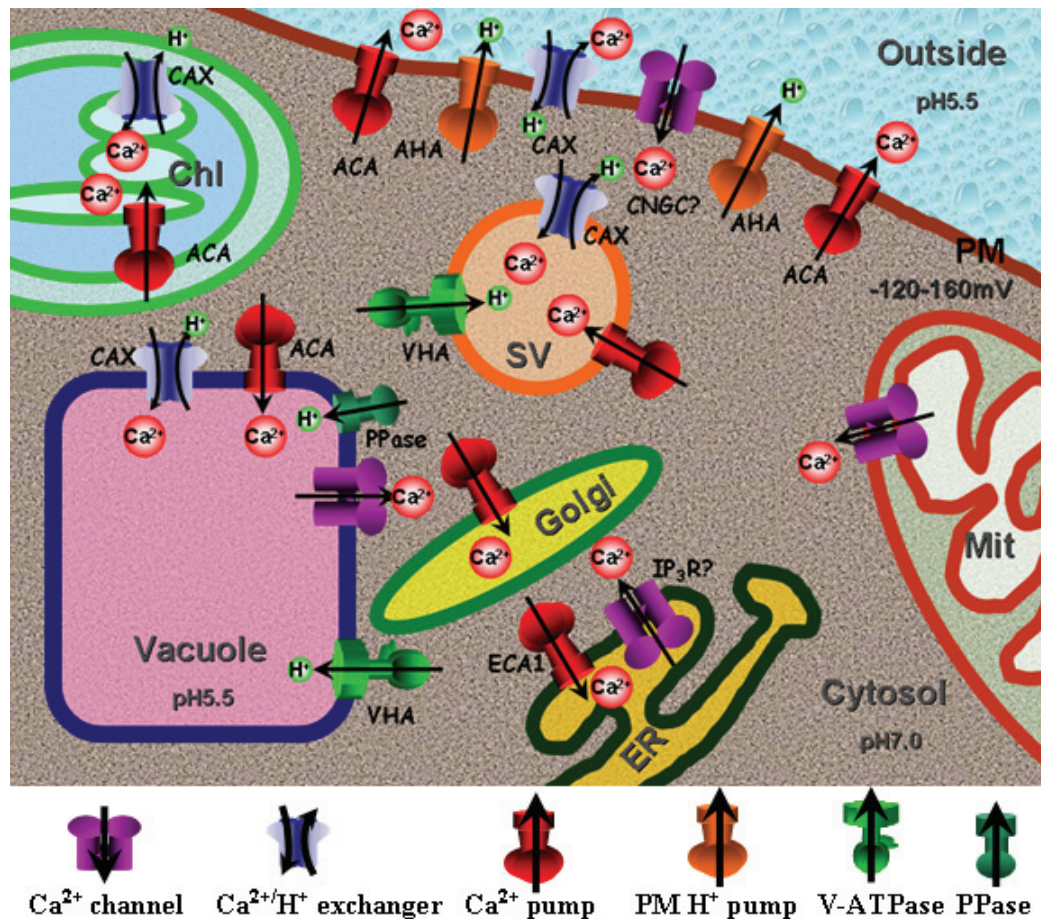


Figure I-3. Membrane transporters maintain Ca²⁺ homeostasis in plant cells.

There are 3 types of Ca²⁺ transporters. Ca²⁺ permeable channels may be gated by cNTP or IP₃ to allow Ca²⁺ entry on PM or Ca²⁺ release on endomembranes. Ca²⁺-ATPases (ACA (for auto-inhibitory Ca²⁺-ATPase) and ECA (for endomembrane Ca²⁺-ATPase)) hydrolyze ATP to load Ca²⁺ into endomembrane lumen or to extrude to outside of the cell. Ca²⁺/H⁺ exchangers (CAX) also load and extrude Ca²⁺, but by coupling H⁺ transport in reverse direction, which is dependent on the H⁺ gradient maintained by proton pumps on PM (AHA (for *Arabidopsis* H⁺-ATPase)) or on vacuolar membrane (VHA (for vacuole H⁺-ATPase) and PPase (for pyrophosphatase)).

endomembrane compartment lumen); 2) to activate many proteins and enzymes in the secretory pathway; 3) to encode specific Ca^{2+} signals by directly controlling Ca^{2+} flux across the various subcellular membranes in response to a wide range of stimuli. A summary of characterized Ca^{2+} -transporting proteins in *Arabidopsis* is given in Table I-1.

a. Ca^{2+} -permeable channels

The presence of channels gated by hyperpolarization and depolarization of plasma membranes have been shown using electrophysiological or biochemical approaches (Navazio et al., 2000; Sze et al., 2006), although evidence of calcium channels at the molecular level is sparse in plants. The first putative Ca^{2+} -permeable channel identified in *Arabidopsis*, is a unique gene TPC1 (two pore channel, At4g03560) encoding a protein that resembles pore-forming subunits of mammalian and yeast Ca^{2+} channels, and has been characterized in yeast (Furuichi et al., 2001). TPC1 is a slow vacuolar channel which conducts a Ca^{2+} -dependent Ca^{2+} release. Disruption of the TPC1 gene in *Arabidopsis* leads to a defect in ABA-repressed seed germination and in stomata responses to extracellular Ca^{2+} and to the absence of a functional slow vacuole channel activity recorded by an electrophysiological approach (Peiter et al., 2005).

The genomic annotation also identifies a group of >20 cyclic nucleotide-gated channels (CNGCs) and a group of 30 glutamate receptors (GLRs) in *Arabidopsis* (Sanders et al., 1999; Sanders et al., 2002). These genes provide the best candidates for a functional study of Ca^{2+} -conducting and ligand-switched channels because some of their animal counterparts are characterized as Ca^{2+} channels.

In endomembrane compartments, Ca^{2+} channel activities have been found on the vacuole and ER. The vacuolar Ca^{2+} channels include two ligand-gated channels, which

Table I-1. Summary of characterized Ca^{2+} transporters in plants. n.d. not determined.

Name	Tissue expression	Membrane location	Ca^{2+} affinity	Functions		Reference
				Yeast	Plant	
Ca^{2+}-permeable channels						
TPC1	ubiquitous	vacuole	2.2 μM	Ca^{2+} uptake	ABA-suppressed seed germination; $[\text{Ca}^{2+}]_{\text{ext}}$ -induced guard cell opening	(Furuichi et al., 2001; Peiter et al., 2005)
$\text{Ca}^{2+}/\text{H}^{+}$ exchangers						
CAX1	leaves, flowers, seeds; induced by Mn^{2+} , Na^{+} , Ni^{2+}	vacuole	13 μM	High Ca^{2+} tolerance	Regulation of other vacuolar transporters. Null mutants exhibit enhanced growth under high $\text{Mn}^{2+}/\text{Mg}^{2+}$, synergistic with CAX3.	(Hirschi et al., 1996; Cheng et al., 2003; Cheng et al., 2005)
CAX2	n.d.	vacuole	>100 μM	High $\text{Ca}^{2+}/\text{Mn}^{2+}/\text{Cd}^{2+}$ tolerance	$\text{Mn}^{2+}/\text{Cd}^{2+}$ tolerance	(Hirschi et al., 1996; Koren'kov et al., 2006; Shigaki and Hirschi, 2006)
CAX3	roots, flowers, seeds; induced by Mn^{2+} , Na^{+} , Ni^{2+}	vacuole	n.d.	High Ca^{2+} tolerance	Synergistic with CAX1.	(Shigaki and Hirschi, 2000; Cheng et al., 2002; Cheng et al., 2005; Koren'kov et al., 2006)
CAX4	low; induced by Mn^{2+} , Na^{+} , Ni^{2+}	vacuole	Cd^{2+} -transporting	High Ca^{2+} tolerance	n.d.	(Cheng et al., 2002; Koren'kov et al., 2006)
Ca^{2+}-ATPases						
Type IIA Endomembrane Ca^{2+}-ATPases						
ECA1	ubiquitous	ER	30 nM; Mn^{2+} -transporting	Ca^{2+} uptake; Mn^{2+} detoxification	Plant growth under low Ca^{2+} and toxic Mn^{2+} ; Root hair growth under toxic Mn^{2+} .	(Liang et al., 1997; Liang and Sze, 1998; Wu et al., 2002), this study
ECA2	vasculature	n.d.	n.d.	n.d.	n.d.	This study

ECA3	vasculature and pollen	Golgi, SV	n.d.; Mn ²⁺ - transporting	Ca ²⁺ uptake ; Mn ²⁺ detoxification	Root growth and pollen tube elongation; support root growth under toxic Mn ²⁺ .	This study
ECA4	vasculature, root tip	n.d.	n.d.	Ca ²⁺ uptake.	n.d.	This study
Type IIB Autoinhibitory Ca²⁺-ATPases						
ACA1	Root, preferential	chloroplast, inner envelope	n.d.	n.d.	n.d.	(Huang et al., 1993b)
ACA2	n.d.	ER	0.25-0.67 μM	Ca ²⁺ uptake, stimulated by CaM	n.d.	(Harper et al., 1998; Hong et al., 1999; Hwang et al., 2000)
ACA4	Ubiquitous, NaCl- induced	small vacuole	n.d.	Tolerance to osmotic stresses (high NaCl, KCl, and mannitol)	n.d.	(Geisler et al., 2000)
ACA8	n.d.	PM	n.d.	n.d.	n.d.	(Bonza et al., 2000)
ACA9	pollen	PM	n.d.	Ca ²⁺ uptake	Pollen tube elongation and sperm cell discharge	(Schirott et al., 2004)

are activated by inositol trisphosphate and by cyclic ADP-ribose, and two voltage-gated channels which are activated either by membrane hyperpolarization or by membrane depolarization. Ca^{2+} channel activity, gated by a similar mechanism, as well as an ER-only NAADP (nicotinic acid adenine dinucleotide phosphate)-activated Ca^{2+} channel, are also found in ER (Navazio et al., 2000; Sanders et al., 2002). It has been recently found in mammalian cells that an ER luminal thioredoxin protein, ERp44, directly binds to the ER-localized Ca^{2+} channel, inositol 1,4,5-trisphosphate receptors (IP_3Rs) and inhibits its channel activity in a redox status-dependent manner (Higo et al., 2005). Therefore, Ca^{2+} release from intracellular stores is also regulated by the cytosolic redox status through the sensor thioredoxin. The mechanism may also be conserved in plants since ER-residing thioredoxins are also found in *Arabidopsis* (Houston et al., 2005).

b. $\text{Ca}^{2+}/\text{H}^+$ antiporters

$\text{H}^+/\text{Ca}^{2+}$ antiporters (CAXs, 12 members) are mainly localized on the vacuole membrane (Maser et al., 2001; Sanders et al., 2002). They are now divided into two groups including CAX1-6 as *bona fide* CAX genes and CAX7-11 that have been re-categorized as K^+ -dependent $\text{N}^+/\text{Ca}^{2+}$ exchangers (Shigaki and Hirschi, 2006).

Promoter::GUS analyses suggest that CAXs are expressed in different locations. For example, CAX1 is expressed preferentially in the shoot while CAX3 is detected mainly in the root (Cheng et al., 2005). Nevertheless, many CAXs are also expressed in the inflorescence (Cheng et al., 2005), suggesting a role of CAXs in reproductive growth. CAX1 is also involved in cold adaptation. *Arabidopsis* mutants deficient of CAX1 exhibited increased freezing tolerance after cold acclimation, which coincides with enhanced expression of the transcription factor CBF/DREB gene in the mutants,

suggesting a role of CAX1 in controlling accurate cold-acclimation response (Catala et al., 2003).

Arabidopsis CAX1 is the best studied plant CAX. The Ca^{2+} transport activity of CAX1 has a low affinity ($K_m = 10\text{-}15 \mu\text{M}$) and high capacity in comparison with Ca^{2+} -ATPases (Hirschi et al., 1996). Unlike Ca^{2+} -ATPases, CAXs exhibit a wide range of ion substrates such as Mn^{2+} , Cd^{2+} and Zn^{2+} in addition to Ca^{2+} , which prompted renaming CAX as Cation eXchanger. CAX1-6 possess an autoinhibitory domain at the N-terminus. Removal of this N-terminal domain from CAX1-5 results in constitutively active CAX, whose expression improves the tolerance of yeast mutant K667 to high Ca^{2+} , while expression of full-length CAX failed to show growth improvements in yeast (Shigaki and Hirschi, 2006). However, the identity of the regulator binding to the N-terminal domains of CAXs is unknown.

Biological functions of CAX were inferred from genetic studies. Overexpression of the constitutively active form of CAX1 with an N-terminal truncation in tobacco resulted in increased accumulation of Ca^{2+} in the vacuole, and also caused Ca^{2+} deficiency symptoms, hypersensitivity to K^+ and Mg^{2+} , and increased cold sensitivity (Hirschi, 1999), probably by oversorting Ca^{2+} into the vacuole and dissipating the H^+ gradient across the vacuolar membrane which is also used to drive other cation co-transporters. Recent evidence also showed the vacuolar Ca^{2+} -ATPase activity is increased by 36% in the *cax1* mutant, which may be related to the enhanced $\text{Mn}^{2+}/\text{Mg}^{2+}$ tolerances in *cax1* plants (Cheng et al., 2003).

In summary, CAXs seem to be used for loading or restoring Ca^{2+} (and probably other cations such as Mn^{2+} , Cd^{2+} , Zn^{2+}) into endomembrane compartments. Their

activities can be linked to nutritional supply, homeostasis of Ca^{2+} in signaling, and detoxification of heavy metals when plants are exposed to excess cations.

c. Ca^{2+} -pumping ATPases

Two groups of Ca^{2+} -ATPases have been identified in *Arabidopsis*: ACAs (Autoinhibitory Ca^{2+} -ATPase, 10 predicted) and ECAs (ER-type Ca^{2+} -ATPase, 4 as predicted) (Sze et al., 2000; Axelsen and Palmgren, 2001). An alignment of these pumps and other PM and ER-type Ca^{2+} pumps is shown in Chapter 2 (Fig. II-1). However, the *Arabidopsis* genome seems to lack a secretory pathway-type Ca^{2+} -ATPases (SPCA), which is found in yeast and mammals and loads $\text{Ca}^{2+}/\text{Mn}^{2+}$ into the Golgi lumen (Wuytack et al., 2002).

Autoinhibitory Ca^{2+} -ATPases (ACA). Plant ACAs resemble mammalian plasma membrane-type Ca^{2+} -ATPases (PMCA) in primary protein sequence and mode of regulation. ACA pumps have an N-terminal autoinhibitory domain, which constitutively deactivates the Ca^{2+} transport activity by 4-10 fold unless alleviated by CaM binding to an adjacent region (Hwang et al., 2000; Sze et al., 2000). However, the location of a similar autoinhibitory domain is at the C-terminus of animal PMCA (Harper et al., 1998). ACAs are not sensitive to either CPA (cyclopiazonic acid) or thapsigargin (TG). Members of ACA family have been localized to plasma membrane (ACA8, ACA9) (Bonza et al., 2000; Schiott et al., 2004), ER (ACA2) (Hong et al., 1999), small vacuoles (ACA4) (Geisler et al., 2000), and perhaps the plastid inner envelope membrane (ACA1) (Huang et al., 1993b). A plasma membrane-located Ca^{2+} pump, ACA9, is required for pollen tube growth and fertilization (Schiott et al., 2004). *Arabidopsis* knockout mutants of ACA9 showed a reduced migration distance of pollen tubes in the transmitting tract,

thus a reduced percentage of fertilized embryos in the siliques. The underlying mechanism is not clear yet. One interpretation is that the PM-located Ca^{2+} pumping by ACA9 is involved in exocytosis of wall-constructing materials and enzymes which are critically required to sustain the fast surface expansion of growing pollen tubes because yeast homolog of ACA9, PMC1, is inhibited by interaction with Nvy1p, a vacuolar v-SNARE protein (Takita et al., 2001).

The yeast version of PMCA, PMC1, is encoded by a single gene and located on vacuole membranes. Pmc1 can be transcriptionally activated when cytosolic Ca^{2+} is elevated. This activation depends on calcineurin, a $[\text{Ca}^{2+}]_{\text{cyt}}$ -dependent protein phosphatase (Cunningham and Fink, 1994). It is not clear whether PMC1 is also autoinhibited by its own terminal domain as is the case for both animal PMCA and plant ACAs.

Endomembrane Ca^{2+} -ATPases (ECA). In *Arabidopsis*, four members of the ECA family have been identified according to their homology to animal sarcoplasmic-/endoplasmic reticulum-type pump (SERCA) (Sze et al., 2000; Axelsen and Palmgren, 2001). The 4 genes are further clustered into 2 groups: AtECA3 as one group and ECA1, ECA2, and AtECA4 as another (Baxter et al., 2003). All ECA proteins are predicted to have 10 transmembrane domains, 2 Ca^{2+} -binding sites, 2 ATP binding sites, a large cytoplasmic third loop, and a short basic C-terminal domain which is thought to be involved in protein interactions. Only AtECA1 has been functionally characterized in yeast as a Ca^{2+} pump (Liang et al., 1997).

ECA1 is localized to the ER by membrane fractionation and immuno-staining (Liang et al., 1997), and is expressed ubiquitously in plants. AtECA1 is inhibited by

cyclopiazonic acid but not by thapsigargin, which is different from animal SERCA pumps. The K_m for Ca^{2+} transport is 30 nM while for ATP the K_m is 20 μ M (high affinity site), or 235 μ M (low affinity site), respectively (Liang and Sze, 1998). In addition, AtECA1 also has Mn^{2+} transport activity and doesn't interact with CaM directly. *Arabidopsis ecal-1* mutants show impaired growth of primary roots and root hairs in either high Mn^{2+} -supplemented media or low Ca^{2+} media, and the phenotypes can be reversed by overexpression of AtECA1 cDNA (Wu et al., 2002). ECA1, therefore, is likely to be used for loading Ca^{2+} and/or Mn^{2+} into endomembrane compartments and detoxification in case of high cytosolic ion concentration.

The functions of the other 3 ECAs are not known. AtECA4 shares the highest homology to AtECA1 (97 %), implying a recent genomic duplication event during evolution.

ECA3 (58 % to ECA1) is distantly related to the other 3 family members. However, the ion transport activity, the subcellular localization, and the physiological functions of ECA2, 3, and 4 remain to be determined.

The best understood Ca^{2+} -ATPase is the mammalian SERCA (Futai et al., 2004). There are three SERCA genes in human. These three genes differ in their tissue expression patterns and are alternatively spliced in different cell types. SERCA1 and SERCA2 have similar high-affinity Ca^{2+} transport activities and optimal pH requirements, usually with higher expression levels than SERCA3. SERCA1 is mainly found in skeletal muscle cells whose function is to rapidly sequester released Ca^{2+} back into the sarcoplasmic reticulum after muscle excitation. SERCA2 is the housekeeping gene found in most tissues whose function is to maintain Ca^{2+} homeostasis in the ER

lumen and help modulate $[Ca^{2+}]_{\text{cyt}}$ signature in signaling events. SERCA3 is more distantly related to SERCA1 (76%) and SERCA2 (77%) with 5-fold lower $[Ca^{2+}]_{\text{cyt}}$ affinity and a slightly higher pH optimum. SERCA3 is found in various tissues and often co-expressed with SERCA2b. SERCA3 is also a differentiation indicator whose expression is turned down if the cell loses differentiation identity such as in cancer cells (Wuytack et al., 2002).

Secretory Pathway Ca^{2+} ATPases (SPCA). The origin of SPCA began from a functional study of Pmr1, a single gene encoding a Ca^{2+} -ATPase in yeast. PMR1 is located on Golgi membranes and loads Ca^{2+} and Mn^{2+} into the Golgi lumen (Rudolph et al., 1989; Strayle et al., 1999). Unlike SERCA whose transport activity of Mn^{2+} is limited, PMR1 transports both Ca^{2+} and Mn^{2+} efficiently. It translocates only 1 Ca^{2+} per cycle instead of 2 per cycle for SERCA. Nevertheless, PMR1 is insensitive to all classical SERCA inhibitors, e.g. thapsigargin and cyclopiazonic acid (Wuytack et al., 2003).

Mammalian SPCA pumps Ca^{2+} and Mn^{2+} into Golgi or secretory compartments. Ca^{2+} is required in these compartments as some Golgi enzymes depend on millimolar levels of Ca^{2+} or Mn^{2+} for activity (Oda, 1992; Kaufman et al., 1994). In some tissues with intense secretion such as mammary gland, SPCA may be the major contributor to the observed 30-60 mM Ca^{2+} in the milk of mice and cows (Wuytack et al., 2003). Besides, Golgi-located enzymes also require high Ca^{2+} . For instance, proteolysis by furin, a member of proprotein convertase, is dependent on Golgi luminal Ca^{2+} (Seidah and Chretien, 1997; Bennett et al., 2000) and is associated with Alzheimer's disease, a neurodegenerative disorder (LaFerla, 2002).

In planta, a Ca^{2+} -ATPase activity was detected from a Golgi-enriched subcellular fraction of etiolated pea hypocotyls. This activity has a maximal Ca^{2+} uptake of $2.5 \text{ nmol mg}^{-1} \text{ min}^{-1}$ and an apparent K_m for Ca^{2+} of 209 nM (Ordenes et al., 2002). This activity is inhibited by vanadate, CPA, and thapsigargin. However, the molecular identity of this pump is unclear.

1.8. Research Questions: What are the biological roles of AtECAs?

It is not known how multicellular plants translocate Ca^{2+} and produce Ca^{2+} transients and oscillations in cells in response to chemical and environmental cues. Ca^{2+} pumps are likely to be involved, though only a few of the 14 Ca^{2+} -ATPases from *Arabidopsis* have been studied. What are the roles of multiple ECAs found in *Arabidopsis* and in rice? I hypothesized that multiple ECAs have differential expression patterns, subcellular locations and perhaps biological roles. Only one of four AtECAs has been functionally characterized, so the general goal is to understand the roles of three other ECAs.

2. STATEMENT OF RESEARCH GOALS

The main objectives of my dissertation research are to determine the biochemical functions and physiological roles of AtECA2, AtECA3 and AtECA4 genes, using a combination of molecular, biochemical, cell biological and genetic approaches. In the course of the study, I chose to focus on one gene AtECA3 that diverged from other ECAs. The specific questions and approaches are:

- 1. What is the tissue expression pattern and cellular membrane location of each AtECA gene?**
- 2. How is each AtECA distinct from each other in transport activity and sensitivity to inhibitors?**
- 3. What physiological roles do AtECAs play in plants? What processes are compromised if one AtECA is absent from the plants?**

In this dissertation, results and approaches used to address above questions are presented with a focus on AtECA3. The results are organized into chapters. Each chapter is written as an independent unit with its introduction, method, results and discussion. In a final chapter, I summarize and integrate the findings, reach conclusions and offer strategies for future directions.

II. BIOINFORMATIC ANALYSES AND TISSUE EXPRESSION PATTERNS OF *ARABIDOPSIS* ECAs

1. ABSTRACT

Multiple genes encode endomembrane P-type Ca^{2+} -ATPases (ECA or SERCA) in multicellular organisms of all kingdoms, including the higher plants *Arabidopsis thaliana* and rice. AtECA1 has been characterized as an endoplasmic reticulum (ER)-located $\text{Ca}^{2+}/\text{Mn}^{2+}$ -ATPase (Liang et al., 1997). However, the biological functions of the other 3 *Arabidopsis* ECAs are still unknown. In this study, a bioinformatic approach was used first to get clues to the structures, functions and expression patterns of a family of Ca^{2+} -ATPases (ECA) in *Arabidopsis*. The results of protein comparisons with metazoan Ca^{2+} pumps indicated that AtECAs are homologous to SERCA-type Ca^{2+} -ATPases. AtECA3 in particular shared 53% identity with animal SERCA1a pumps and only 45% with AtECA1 or AtECA2. The expression of AtECAs was unaffected by various stimuli, or during development, based on genome-wide microarray analyses. Differential tissue expression patterns among AtECAs were revealed by promoter-driven Gus activity and confirmed by RT-PCR. The results showed that most AtECAs are preferentially expressed in vascular tissues at different organs, except for AtECA1 which is highly expressed in all tissues examined. These differences imply that each AtECA plays different roles during the plant life cycle. To determine their biochemical and cellular roles, cDNAs of AtECA2-4 were cloned and sequenced.

2. INTRODUCTION

ECAs are plant SERCA-type pumps belonging to P2A subfamily of P-type ATPase family, where P stands for phosphorylated intermediate. Functional characterization of P2A family members in animals and plants has revealed that these ATPases use energy from the hydrolysis of ATP to load cytosolic Ca^{2+} into the ER (or sarcoplasmic reticulum, a specialized ER in muscle cells), and thus set the observed low $[\text{Ca}^{2+}]_{\text{cyt}}$ (Liang et al., 1997; Wuytack et al., 2002; Inesi and Toyoshima, 2004). SERCA-type pump genes are present in many organisms ranging from unicellular cyanobacteria and yeasts to multi-cellular insects, plants, and mammals (Fig. II-1). The genome of the model plant *Arabidopsis thaliana*, contains 4 genes encoding SERCA-type pumps, namely AtECA1-4 (Axelsen and Palmgren, 2001), whereas the rice genome has 3 OsECA genes (Baxter et al., 2003) implying a conserved requirement of ECA genes in monocots and dicots.

However, scrutiny of both *Arabidopsis* and rice genomes failed to reveal a secretory pathway Ca^{2+} ATPase (SPCA) gene that is mainly found in the Golgi. SPCA functions to supply $\text{Ca}^{+}/\text{Mn}^{2+}$ into the Golgi lumen and secretory vesicles derived from the Golgi in yeasts and mammals (Wuytack et al., 2002). An interesting question thus arises: is there an ECA gene in the plant genome that functions as SPCA? Sequence comparisons of SERCA and SPCA pumps from different organisms may provide clues to this question.

AtECA1 has been previously cloned and characterized as ER-located $\text{Ca}^{2+}/\text{Mn}^{2+}$ pump whose function is important for root growth under Ca^{2+} limiting / Mn^{2+} toxic conditions (Liang et al., 1997; Wu et al., 2002). However, a null mutant of AtECA1 was

viable, and the abnormality in root growth was conditional, which raised the question whether other AtECA2-4 genes could partially substitute for AtECA1 function. More importantly, why do plants like *Arabidopsis* have 4 ECA genes similar in number to mammals? I attempted to address this question first by molecular cloning the cDNAs of ECA2-ECA4. The sequences were used for bioinformatic analyses in this chapter and studies in chapter III and IV.

In this chapter, I show that AtECAs differ not only in their gene and protein structures, but also in their tissue expression patterns. AtECA3 is particularly interesting due to its close homology to mammalian SERCAs, so it was chosen for functional characterization (chapter III and IV).

3. RESULTS

3.1. Molecular cloning of At ECAs

To clone the cDNAs spanning full ORF of AtECA2-4, primers containing start or stop codon were designed based on genomic annotation of TAIR and the partial sequences of various EST results (Tab. II-3c). Complementary DNA templates were obtained by reverse transcription of RNA isolated from vegetative tissues of young *Arabidopsis* plants. The cDNA clones (App. 1) were verified by full-length sequencing and used for generating other molecular constructs. Complete and error-free clones have been successfully obtained for AtECA3 and AtECA4 and the complete sequence attached and submitted to Genbank with accession numbers AY650902 (AtECA3) and DQ989372 (AtECA4) (App. 1c-d). Each of these sequences contains an ORF that

Table II-1. *Arabidopsis* ECA/ACA Genomic DNA.

Gene Name	Locus	Accession Numbers		a.a.	Exons
		Genome (Protein)			
<i>P2A-type ATPase</i>					
AtECA1/ACA3	At1g07810	I	AC007583 (AAF75073)	1061	8
AtECA2/ACA5	At4g00900	IV	AF013294 (AAB62850)	1054	5
AtECA3/ACA6	At1g10130	I	AC004122 (AAC34328)	998	34
AtECA4	At1g07670	I	AC007583 (AAF75088)	1061	8
<i>P2B-type ATPase</i>					
AtACA1/PEA1	At1g27770	I	AC012375 (AAF24958)	1034	7
AtACA2	At4g37640	IV	AL035605 (CAB38303)	1014	7
AtACA4	At2g41560	II	AC002510 (AAB84338)	1030	7
AtACA7	At2g22950	II	AC004786 (AAM15005)	1015	7
AtACA8	At5g57110	V	AB023042 (BAA97361)	1099	34
AtACA9	At3g21180	III	AB023045 (BAB01709)	1073	32
AtACA10	At4g29900	IV	AL050352 (CAB43665)	1093	34
AtACA11	At3g57330	III	AL137080 (CAB68139)	1025	7
AtACA12	At3g63380	III	AL163818 (CAB87791)	1033	1
AtACA13	At3g22910	III	AP001300 (BAB03036)	1017	1
AtACA14 (?)	At5g53010	V	AB018116 (BAA97141)	1095	32

encodes a protein with a size as predicted by annotation but with variations at certain amino acid residue loci. However, only 2 partial clones of AtECA2 were obtained, ECA2-3 (lacking the first 843 bp of full ORF) and ECA2-9 (only the first 2677 bp of full ORF). Both contain no errors that disrupt ORF otherwise. The PCR product was of a similar size to prediction when the PCR primers were designed against the start and stop codons of predicted full length AtECA2 ORF. And the terminal sequences of PCR production were correct as verified by sequencing. It seems AtECA2 full length cDNA is somehow toxic in *E coli* since a complete error-free genomic clone of AtECA2 has been obtained from the BAC clone F18A10 that hosts AtECA2, the reason for this is not clear.

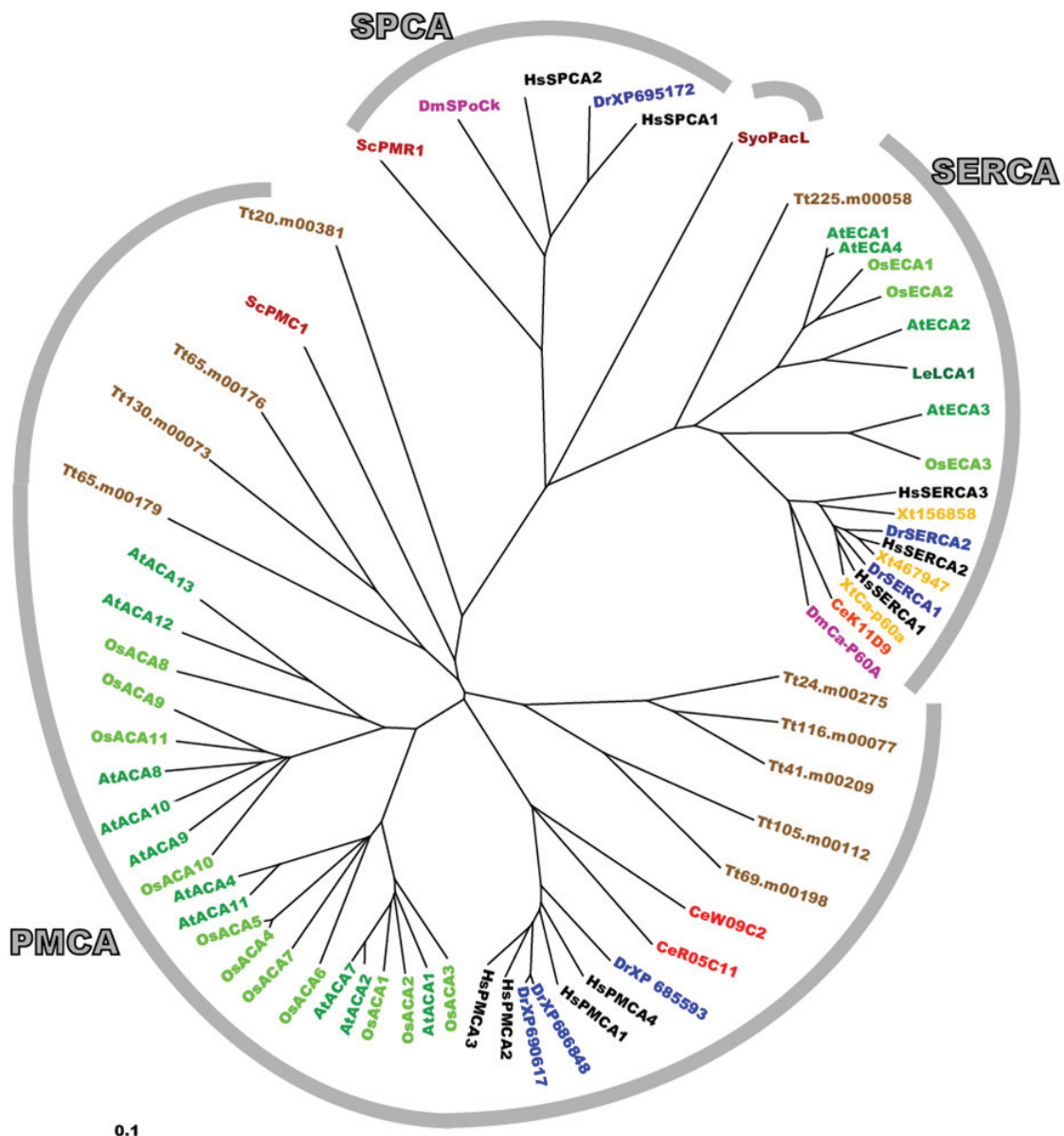
3.2. Bioinformatic analyses of AtECAs

a. Phylogenetic alignment of Ca²⁺-ATPases from different kingdoms

Sequence annotations of the dicot *Arabidopsis* and monocot rice (*Oryza sativa*) genomes revealed 14 P-type Ca²⁺-ATPases from *Arabidopsis* (4 ECA and 10 ACA) and 14 from rice (3 ECA and 11 ACA). The predicted proteins were aligned with P-type Ca²⁺-ATPases from other kingdoms using MUSCLE program (Edgar, 2004) (Fig. II-1). The phylogenetic tree showed that these proteins were divided into 4 main clades as PMCA, SERCA, SPCA and cyanobacteria Ca²⁺ pumps. Plant ECAs fell into SERCA group while ACAs into PMCA group. Both *Arabidopsis* and rice possessed multiple members in PMCA and in SERCA groups, suggesting that both of ACA and ECA subfamilies are needed for plants. Surprisingly, none of the *Arabidopsis* or rice genes was found in the SPCA group, whose function is to load Ca²⁺/Mn²⁺ into lumens of secretory compartments in yeast and animal.

Figure II-1. Phylogenetic tree of Ca²⁺-ATPases from cyanobacteria, yeast, protozoan, plants, nematode, insect, fish, amphibian, and mammal.

Values shown indicate the number of times (in percent) that each branch topology was found in 1000 reps of the performed bootstrap analysis, which utilized the tree-bisection-reconnection (TBR) branch-swapping algorithm. The analysis was performed upon the optimal tree found by PAUP* 4.0b10; the optimality criterion was set to distance (minimum evolution). *Arabidopsis* (*At*) and rice (*Os*) ECA and ACA sequences were obtained from PlantsT. Aligned also are *Synechococcus* SyoPacL, *Saccharomyces cerevisiae* (*Sc*) genes Pmr1 and Pmc1, 10 *Tetrahymena* (*Tt*) genes, tomato LeLCA1, 4 *C. elegans* (*Ce*) genes, 2 *Drosophila* (*Dm*) genes, 6 zebra fish (*Dn*) genes, 3 *Xenopus* (*Xt*) genes, human SERCA genes 1-3, PMCA genes 1-4, and SPCA1-2. Alignment was performed in the MUSCLE program.



SyoPacl: *synechococcus* **Tt:** *Tetrahymena* (10) **Ce:** *C. elegans* (3) **Dm:** *Drosophila* (2) **Xt:** *Xenopus* (3)

cyanobacteria yeast protozoan plant nematode insect fish amphibian human

Sc: *S. cerevisiae* (2) **At:** *Arabidopsis* (14) **Dr:** *Zebra fish* (6) **Hs:** *H. sapiens* (9)

Os: *rice* (14) **LeLCA1:** tomato

Within the PMCA group, there were 4 subclades of plant ACAs that were conserved between *Arabidopsis* and rice, implying conserved functions before the divergence of dicots and monocots. Within the SERCA group, AtECA3 proteins from both plants stood out from the branch of the remaining plant ECAs, raising the possibility that it has a distinct function. However, the role of AtECA3 from plant is unknown. One major goal here is to decipher the biological function of AtECA3.

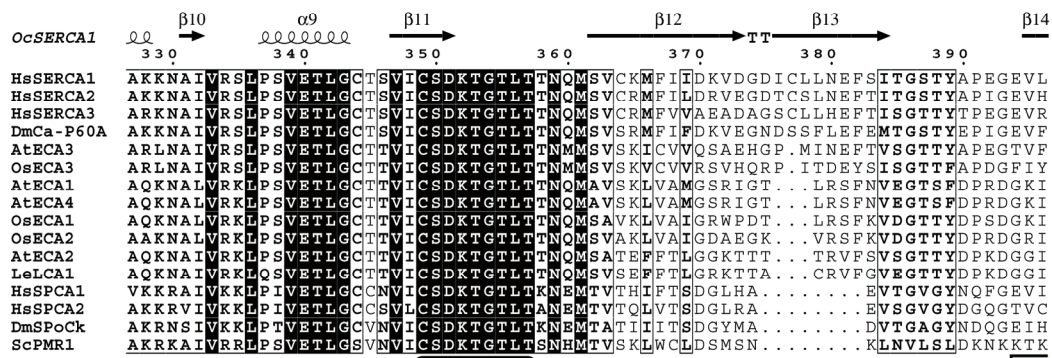
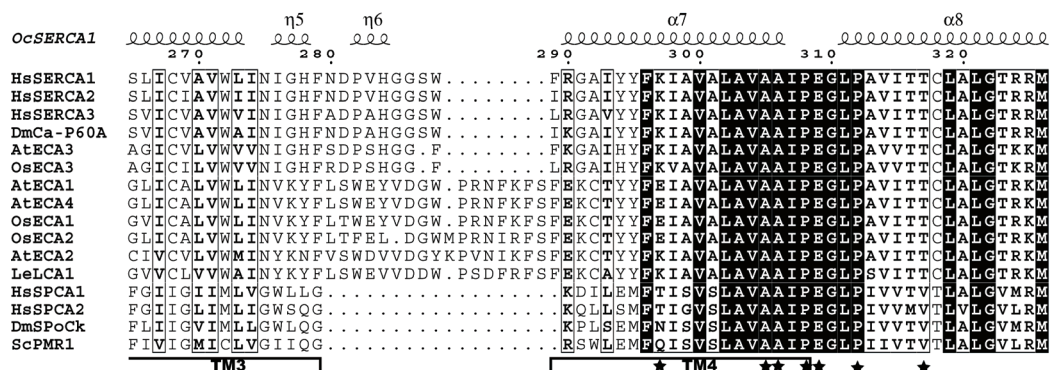
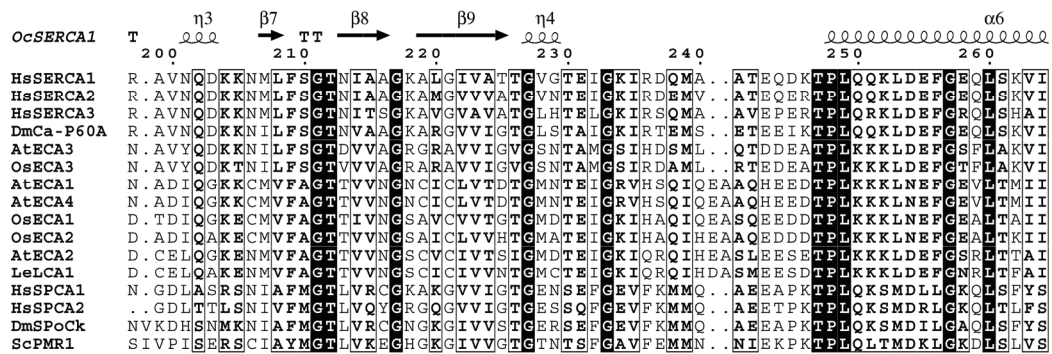
b. Comparisons of functional motifs and domains

Primary protein sequences of Ca²⁺-ATPase representatives were aligned and the residues important for function annotated (Fig. II-2). These included human (HsSERCA1-3), *Arabidopsis* (AtECA1-4), rice (OsECA1-3), tomato (LeLCA1), yeast (ScPmr1), rat (RnSPCA1), *Drosophila* (DmCa-P6A) and *Synechococcus* (SyoPacL). The alignment showed that in general AtECAs and OsECAs were more closely related to animal SERCA-type Ca²⁺ pumps than to SPCA-type pumps at the functionally conserved regions such as the phosphorylation site (P-site) and Ca²⁺ binding sites. Remarkably, AtECA3 shared higher (56%) similarity with either human or rabbit SERCA1a than with AtECA1 (44%) or AtECA2 (45%). The sequence similarity is also observed with rice ECA3. AtECA3 and OsECA3 shared identical residues with SERCA pump at several important loci including 122Y, 293K, 774C (based on HsSERCA1a), implying a close resemblance in biochemical properties between plant ECA3 to animal homologs.

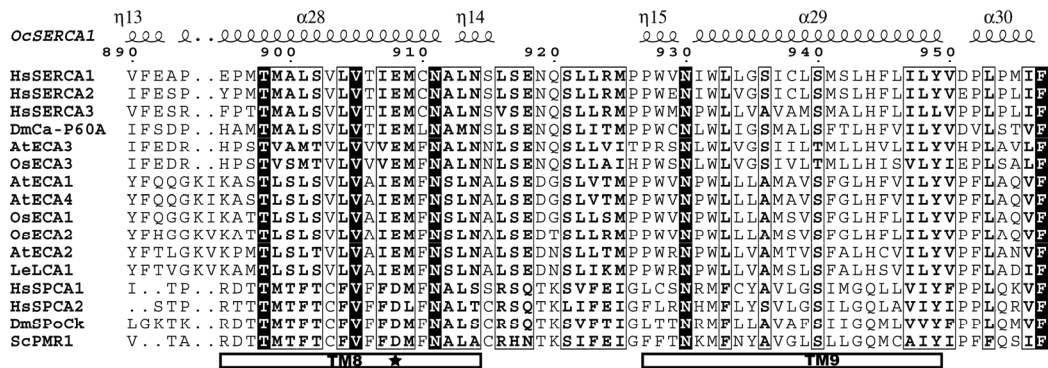
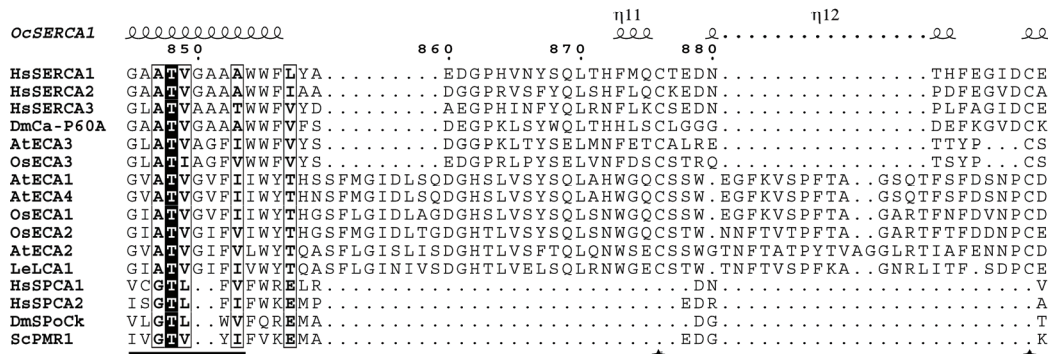
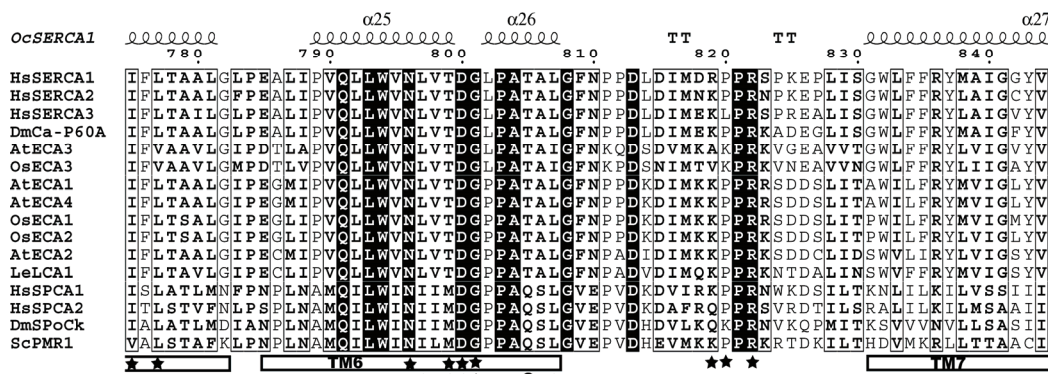
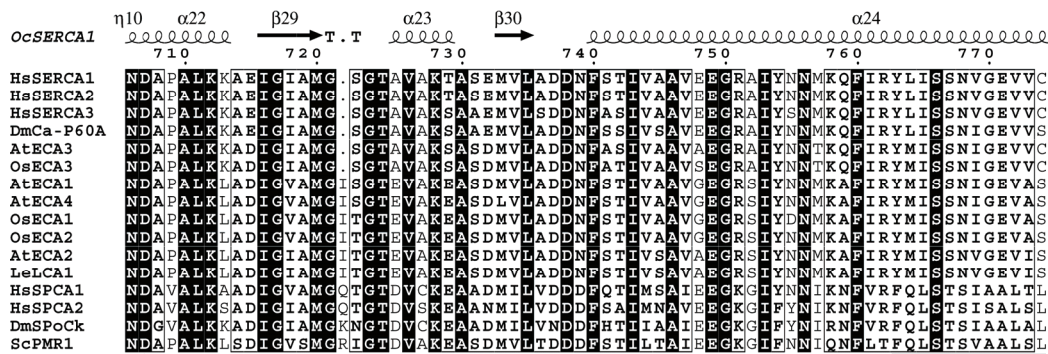
AtECA1 is insensitive to SERCA inhibitor thapsigargin (TG) (Liang and Sze, 1998). Although both TG binding sites are conserved between SERCA and plant ECA, the discrepancy between ECA1/ECA4 and SERCA lay at D254N around the first TG binding site F256, and L764M around second TG binding site I765, which could cause

Figure II-2. Primary sequence alignment of endomembrane-type Ca^{2+} -ATPases from eukaryote organisms human, *Arabidopsis*, rice, tomato, *Drosophila*, and yeast.

Primary sequences of Ca^{2+} -ATPase representatives from human (HsSERCA1, O14983; HsSERCA2, AAH35588; HsSERCA3, Q93084; HsSPCA1, AAH28139; HsSPCA2, AAV54193), *Arabidopsis* (AtECA1, AAC68819; AtECA2, CAA10659; AtECA3, AAT68271; AtECA4, AAD29957), rice (OsECA1, AAN64492; OsECA2, BAA90510; OsECA3, PlantsT_64539), tomato (LeLCA1, Q42883), yeast (ScPmr1, CAA96880), *Drosophila* (DmCa-P6A, P22700; DmSPoCk, NP_730745) were obtained from Genebank and aligned using T-COFFEE program. The resultant alignment file was processed in ESPript 2.2 in which the structure of *Oryctolagus cuniculus* (rabbit) OcSERCA1a (PDB_ID 1SU4) was used as the reference for secondary structure for this alignment. Some key features, in reference to HsSERCA1 sequence, were highlighted beneath aligned sequences: transmembrane domains (hollow square), thapsigargin binding site (solid hexagon), phosphorylation site (solid round square), Ca^{2+} , Mg^{2+} and Mn^{2+} binding site (solid triangle, hollow triangle and solid circle, respectively), and phospholamban binding site (grey solid square), are shown based on functional study summarized for SERCA and SPCA pump study (Wuytack et al., 2002; Inesi and Toyoshima, 2004). Functionally important residues that strongly abolish SERCA pump activity when mutated are also underlined with solid stars.



	TM domain		PLN binding site		Phosphorylation site
	Ca2+ binding		Mn2+ binding		Tg binding
	Ca2+ binding		Mn2+ binding		important residues



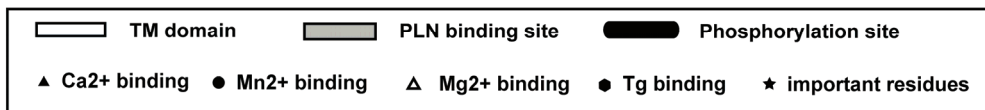
TM domain
 PLN binding site
 Phosphorylation site

▲ Ca²⁺ binding
 ● Mn²⁺ binding
 ▲ Mg²⁺ binding
 ● Tg binding
 ★ important residues

$\alpha 31$ $\alpha 32$
 O*cSERCA1* 960 970 980 990 1000
 H*sSERCA1* KLRALD^{*}LTQWLMVLIKISLPVIGLD^{*}EILK^{*}FVAR^{*}NYLED...PEDERRK...
 H*sSERCA2* QITPLNVTQWLMVLIKISLPVILMDE^{*}TLK^{*}FVAR^{*}NYLEP...GKECVQ^{*}PATK^{*}S^{*}C^{*}S^{*}F^{*}S^{*}A^{*}C^{*}T^{*}D^{*}G^{*}I^{*}S^{*}W...
 H*sSERCA3* QVTPLS^{*}GRQWV^{*}VVLQISLPV^{*}ILLDE^{*}ALK^{*}YLS^{*}R^{*}NHMA...CLYPGL^{*}LRT^{*}V^{*}S^{*}Q^{*}A^{*}W^{*}S^{*}R^{*}Q^{*}L^{*}T^{*}T^{*}S^{*}W^{*}T^{*}P^{*}D^{*}H^{*}T^{*}G^{*}R
 D*mCa-P60A* QVTPLS^{*}AEEW^{*}ITVMKFSIPV^{*}VLLDE^{*}TLK^{*}FVAR^{*}KIADG...ESPIYK...
 A*tECA3* SVTPLS^{*}WAEW^{*}TAVLYLSFPV^{*}IIIDE^{*}LK^{*}FLS^{*}RNTG.M...RF...
 O*sECA3* SVSPLS^{*}WAEW^{*}KVLYLSFPV^{*}ILIDE^{*}VLK^{*}FFS^{*}RSSRGR...RF...
 A*tECA1* GIVPLS^{*}LNEW^{*}LLVLAVSLPV^{*}ILIDE^{*}VLK^{*}FVGR^{*}CTSGYRYS^{*}PRTLSTK...
 A*tECA4* GIVPLS^{*}LNEW^{*}LLVLAVSLPV^{*}ILIDE^{*}VLK^{*}FVGR^{*}CTSGYRYS^{*}PRTPSAK...
 O*sECA1* GIVPLS^{*}FNEW^{*}LVI^{*}AVAF^{*}PV^{*}VLLIDE^{*}VLK^{*}FVGR^{*}CLTA...R.ARKQSGK...
 O*sECA2* GIVPLS^{*}LNEW^{*}LLVLVALPV^{*}VLLIDE^{*}VLK^{*}FVGR^{*}CTSS...SGPKRRTRK...
 A*tECA2* GIVPLS^{*}FREW^{*}FVVLVLSFPV^{*}ILIDE^{*}ALK^{*}FIGR^{*}CRRT...RI...
 L*eLCA1* GIVPLS^{*}LYEW^{*}LLVILL^{*}SAPV^{*}ILIDE^{*}VLK^{*}FVGR^{*}RRRR...TK...
 H*sSPCA1* QTESLS^{*}ILGLAL...GEEWTAAG...
 H*sSPCA2* QTENL^{*}GALD^{*}LLFLT^{*}G^{*}LASS^{*}VFILS^{*}E^{*}LK^{*}LCE^{*}KYCCSP...KRVQMHPEDV...
 D*mSPoCk* QTEAL^{*}TPYD^{*}IFFLVSLTSS^{*}VLVSE^{*}IKK^{*}WFER^{*}TMERK...MYSTRSELD^{*}FV...
 S*cPMR1* KTEK^{*}LG^{*}ISD^{*}IL^{*}LLLLISS^{*}W^{*}FIVD^{*}E^{*}L^{*}RK^{*}LWT^{*}RKKNEE...DSTYFSNV...
 TM10

O*cSERCA1*

H*sSERCA1*
 H*sSERCA2* ..PFVLLIMPLVIWVYSTDTNFSDMFWS...
 H*sSERCA3* NEPEVSAGNRVESPVCTSD.....
 D*mCa-P60A*MHGIVLMWAVFPGLLYAMML...
 A*tECA3* ..RFRLRKADLLPKDRRDK.....
 O*sECA3* ..PLRLRRREILPKESRDN.....
 A*tECA1*QKEE...
 A*tECA4*QKEE...
 O*sECA1*QKED...
 O*sECA2*QKGE...
 A*tECA2*KKKIKTM...
 L*eLCA1*LKAA...
 H*sSPCA1*
 H*sSPCA2*
 D*mSPoCk*
 S*cPMR1*



structural alteration that might abolish TG binding capability of the plant ECA. In contrast, this was not observed on AtECA3, suggesting AtECA3 may be TG sensitive. The potential important amino acid residues as well as conserved signature sequences of AtECA3 are summarized in Figure II-3. Like SERCA and AtECA1, AtECA3 is also predicted to possess 10 TM domains, with a large cytosolic loop between TM4 and TM5 and short cytosolic terminal domains at either end. TM domain 4, 5, 6, and 8 are particularly conserved with SERCA as are several residues in the loop.

c. 3-D structure simulation of AtECA3

The sequence of AtECA3, AtECA1, AtECA2, and OsECA3 were aligned with the 3-D-crystal structure of rabbit SERCA1a (Fig. II-4), whose structure was resolved at 2.6 Å (Toyoshima et al., 2000). Despite differences in primary amino acid sequences, plant ECAs aligned well with the human SERCA1-3 homolog (Fig. II-1). For example, the structures around 2 bound Ca^{2+} ions were conserved in all 4 plant ECA proteins, implying a conserved Ca^{2+} affinity tunnel. However, the nucleotide binding domain (N domain) varied between SERCA1a and plant ECAs. In addition, it seems AtECA1 and AtECA2 lost the structures around phospholamban binding site (K400) homologous to SERCA1a, whereas both AtECA3 and OsECA3 are conserved, which implies that ECA3 may be regulated by phospholamban, a small membrane protein that mediates protein kinase A-regulated Ca^{2+} pump activity in mammalian cells. Nevertheless, both ECA3s differed from SERCA1a at luminal loops, where stabilization of head-piece domains by H-bonding in Ca^{2+} free environment occurs. It is also where the counter-transport of H^+ , and probably H_2O as well, are thought to happen based on recent structural dissection of SERCA1a, whose structure is stabilized by dibutyldihydroxybenzene and thapsigargin

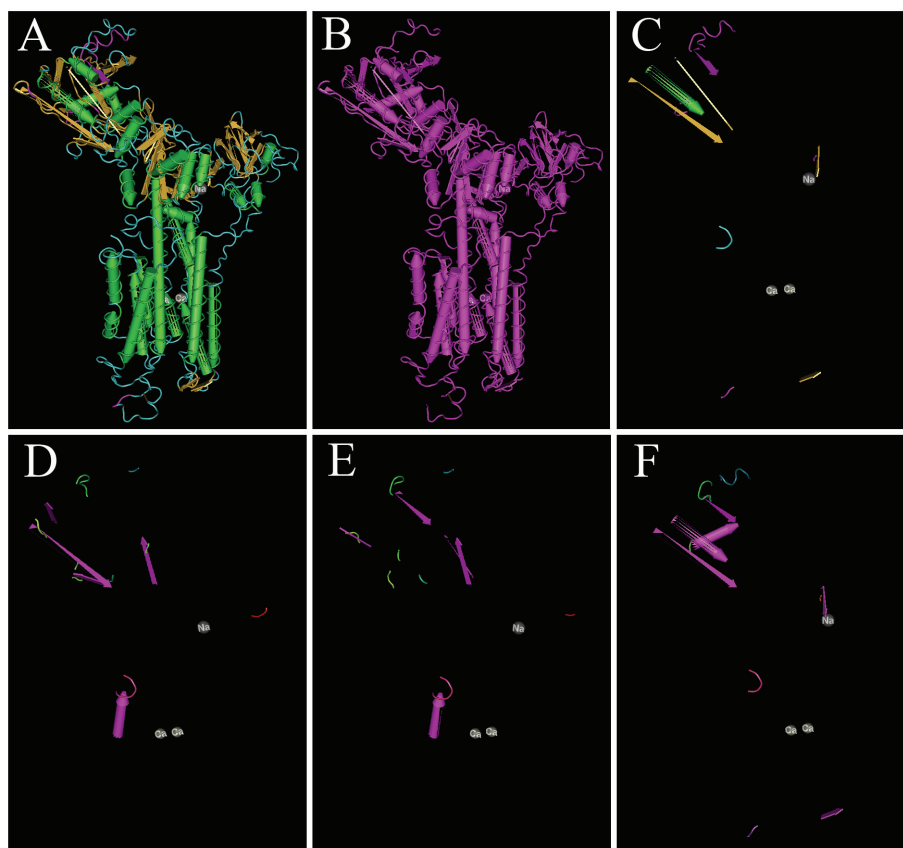


Figure II-4. Structural alignment of SERCA1a and plant ECAs.

A. Crystal structure of rabbit SERCA1a, as resolved by Toyoshima *et al.* (2000). B, Aligned residues between SERCA1a and AtECA3. C-F, unaligned residues between SERCA1a and AtECA3 (C), AtECA1 (D), AtECA2 (E), and OsECA3 (F). Pictures were generated in Cn3D 4.1 using BLAST Single algorithm. The protein domains are painted in magenta green, and ochre. Also showed in each picture are 2 bound Ca^{2+} and 1 Na^{+} present in the rabbit SERCA1a crystal structure as grey balls and used as coordinates.

(Obara et al., 2005). It is also noted that TM10 structure is conserved in both ECA3 proteins but not in AtECA1 or AtECA2 to SERCAs.

d. Structure of Arabidopsis Ca²⁺-ATPase genes

Gene structures of Arabidopsis Ca²⁺-ATPases. Members of the AtECA subfamily differ from one another in gene structure, for instance in the number of exons and introns (Fig. II-5). AtECA1 and AtECA4 are very likely generated by a recent segmental duplication based on the similarity in gene structures (number of 5-8 exons and intron positions) as well as coding sequences. In contrast, AtECA3 is distinct in the large number of exons (33) and the total length of coding region (11 kb instead of 3-5 kb for ECA1, 2, and 4). More interestingly, this gene structure is conserved in the rice ortholog OsECA3 (Baxter et al., 2003), strongly suggesting ECA3 function emerged earlier than the divergence of monocots and dicots. Based on gene structure, ACAs also cluster into several groups: intronless, AtACA12/13; 7-intron cluster, AtACA1/2/4/7/11; and multiple intron cluster, AtACA8/9/10. Genes within one cluster may be products of segmental duplication, as these differences roughly resemble the phylogenetic relationship (Fig. II-1), suggesting different gene clusters may have evolved independently to carry out distinct functions in plants.

Chromosome positions of Arabidopsis Ca²⁺-ATPases. AtECAs and AtACAs are scattered in all 5 chromosomes (Fig. II-6). AtECA1, AtECA3, and AtECA4 are very closely located on chromosome 1. There is no sign of chromosomal re-organization in ECA genesis, which implies the whole ECA subfamily is important for multicellular organisms and conserved during evolution except that AtECA1 and AtECA4 were possibly generated from a recent duplication event since rice has only 1 of these 2.

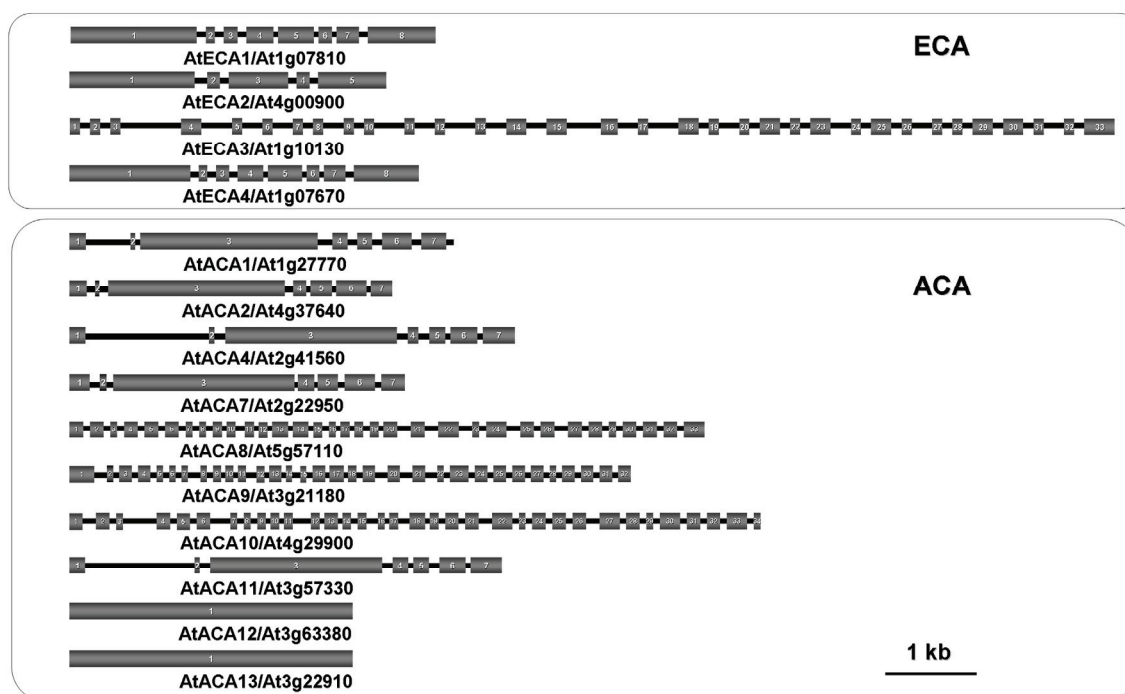


Figure II-5. Gene structures of *Arabidopsis* Ca²⁺-ATPases.

Sequences and exon/intron prediction were obtained from PlantsT. Grey boxes, exons. Scale bar = 1 kb. Exons and introns are drawn to scale according to the TAIR annotation of *Arabidopsis* genome. For AtECA2, a modified prediction from plantsT is used.

Several chromosomal segmental duplication events, on the other hand, gave rise to multiple ACAs such as AtACA2 (chrom IV) and AtACA7 (Chrom II), as well as ACA8 (chrom V) and ACA10 (chrom IV) (Fig. II-6).

e. Searching for Potential Regulators of AtECA activities

In animal cells, SERCA pumps are inhibited by a small integral membrane protein called phospholamban (PLN) or sarcolipin (SLN), depending on cell types. Both PLN and SLN inhibit pump activity by physically interacting with the transmembrane and the cytosolic domains of SERCA. PLN and SLN can be phosphorylated by protein kinase A (PKA), which disrupts the inhibitory interaction between PLN/SLN and SERCA pumps and thus restoring SERCA pumps to resting state after $[Ca^{2+}]_{\text{cyt}}$ surge (MacLennan and Kranias, 2003). I searched for potential PLN-like proteins in plants based on sequence homology. However, no PLN/SLN homologs were found in *Arabidopsis* genome mainly due to the lack of significant algorithm over a short polypeptide of merely 50 amino acid residues if normal setting of sequence alignment is used. In addition, the alignment of multiple SERCA/ECA proteins showed that the PLN binding domain is highly variable (Fig. II-2). Therefore, through modified BLASTP over *Arabidopsis*, one putative PLN homolog, AtPLN1 (At1g56060), was identified. AtPLN1 resembles other phospholambans at the cytoplasmic domain where PLN binds to SERCA (Fig. II-7). A transmembrane span of 22 amino acid residues was predicted and a strong ER location (certainty = 0.85 in PSORT) further implies it may be functionally linked to ER-located ECA pumps (Fig. II-8). The predicted TM of AtPLN1 also resembles that of human PLN and SLN which is the main binding site of PLN/SLN to SERCA pumps.

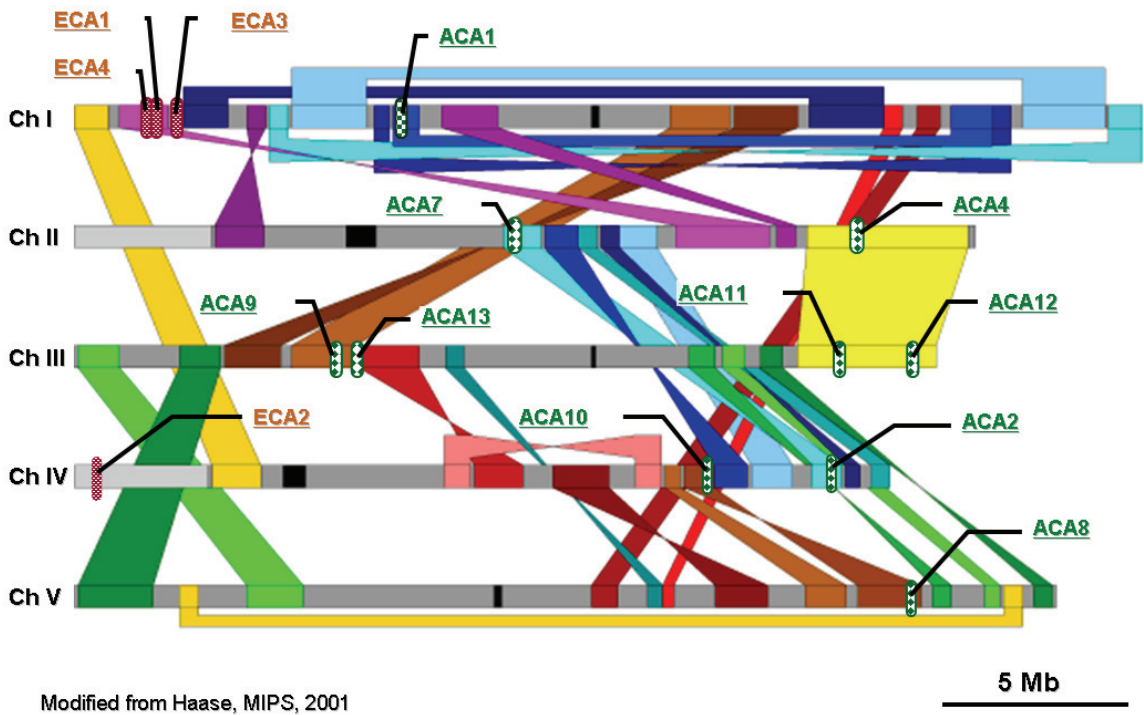


Figure II-6. Chromosome position of *Arabidopsis* Ca²⁺-ATPases.

AtECAs are labeled in red while AtACAs in green. Genome duplication scheme was from MIPS. Relative chromosomal positions were retrieved from TAIR.

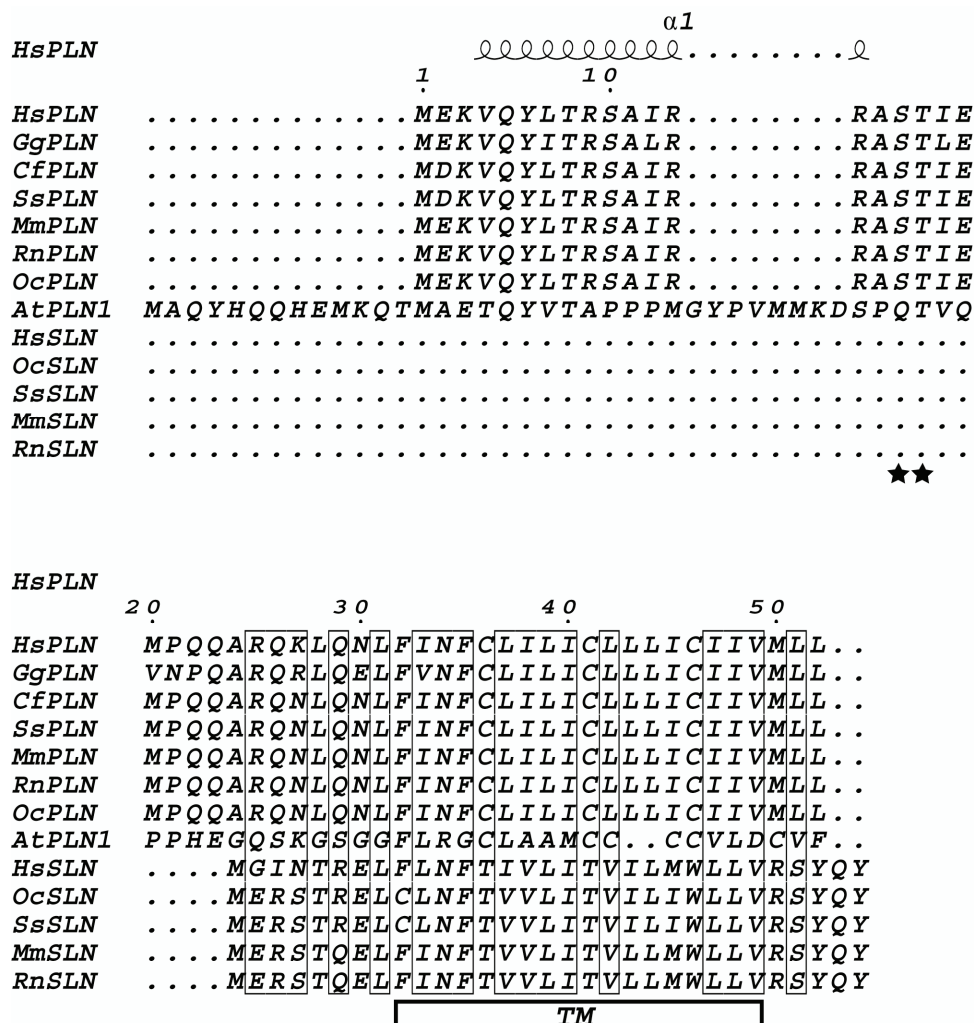


Figure II-7. Multiple sequence alignment of animal phospholambans (PLN) and sarcolipins (SLN) with putative plant phospholamban.

Proteins were obtained from Genebank. Hs, human; Oc, rabbit; Mm, mouse; Rn, rat; Gg, chicken; Cf, dog; Ss, pig; At, *Arabidopsis*. Multiple sequence alignment was generated in EXPRESSO (3Dcoffee) using reference structures of human PLN (1PLP), pig PLN (1FJP), and synthetic SLN (1JDM). The alignment was processed in ESPrpt 2.2. Also highlighted in the graph are phosphorylation sites of PLN (solid star), and the sole transmembrane domain for both PLN and SLN (open square).

Although PLN structure has been resolved, the small size greatly limits the use of analytic software to deduce the structure of AtPLN1. Microarray results collected from Genevestigator (Zimmermann et al., 2004), showed that AtPLN1 is also expressed in various tissues including roots, shoots and flowers (data not shown). Further experiments are needed to test if AtPLN1 is indeed the modulator of plant ECA pump activities.

3.3. Tissue expression of AtECA1-4

a. Promoter-Gus analyses

The spatio-temporal expression patterns of each ECA gene were determined by ECA promoter-driven GUS reporter activity. Intergenic sequences upstream to each AtECA gene were used to drive expression of Gus whose presence can be examined by histochemical staining. RT-PCR was also used to evaluate the transcripts of the ECAs in different plant body parts.

Based on promoter::GUS expression analyses, AtECA1 is ubiquitously expressed at all cell types of root system, hypocotyl, cotyledon/leaf, floral tissues and pollen (Fig. II-9), while the other 3 ECAs only drive restricted GUS expression at different locations. This staining pattern indicates that AtECA1 is the most abundant player of ECA family while other 3 ECAs are important in specific cell types. AtECA1 is localized to the ER (Liang et al., 1997), thus the expression patterns may also reflect the relative abundance of the ER to other subcellular membranes.

ECA2::GUS is restricted to vascular tissues at root, stem, and leaf as well as in developing guard cells, ovules, stigmas, styles, and young seeds (Fig. II-10). In general, AtECA2 is expressed strongly in differentiating cells like root cap, lateral root primordium, and young guard cells. Although ECA2::GUS is highly expressed in pollen

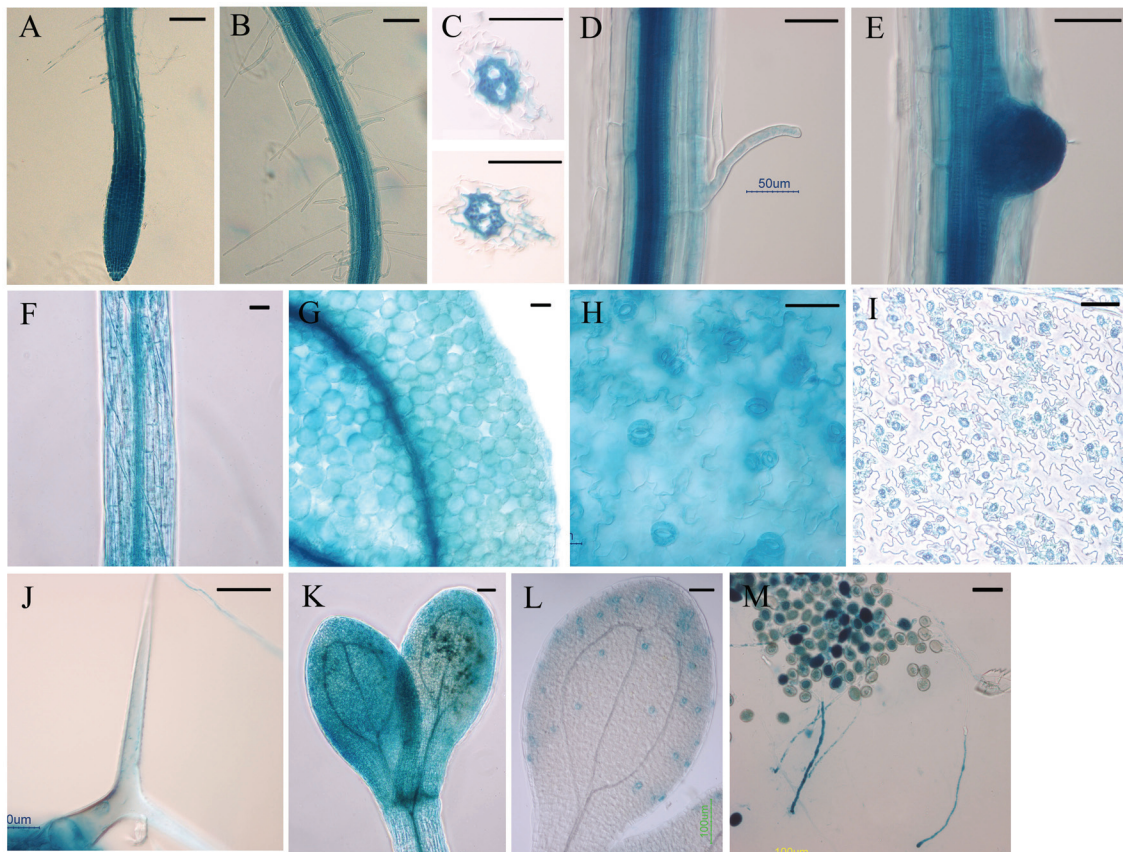


Figure II-9. ECA1::GUS expression in *Arabidopsis*.

GUS activity appears blue. For vegetative tissue staining, transgenic plants hosting the 3.2 kb AtECA1 promoter::GUS construct were grown on $\frac{1}{2}$ MS medium and stained as whole seedlings in X-Gluc for 3 h. Pollen was stained overnight after 6 h *in vitro* germination on agarose-based germination medium. The GUS staining was detected in all cell types at the primary root tip (A) and the differentiation zone (B). The same staining pattern is also shown in cross sections of primary roots in C. The staining was also found in a root hair (D), in a lateral root primordium (E), in all cell types at the hypocotyl (F), in the mesophyll cells and veins of a true leaf (G), in guard cells as on a leaf (H) or on an epidermal peel (I), in a leaf trichome (J), in all cell types of the cotyledons grown under light (K) but only in the guard cells of cotyledons grown in the dark (L), and in both pollen grains and germinating pollen tubes (M). Note the lighter grains are hollow inside because the plasma has moved out in the tube (I). Scale bar = 50 μm .

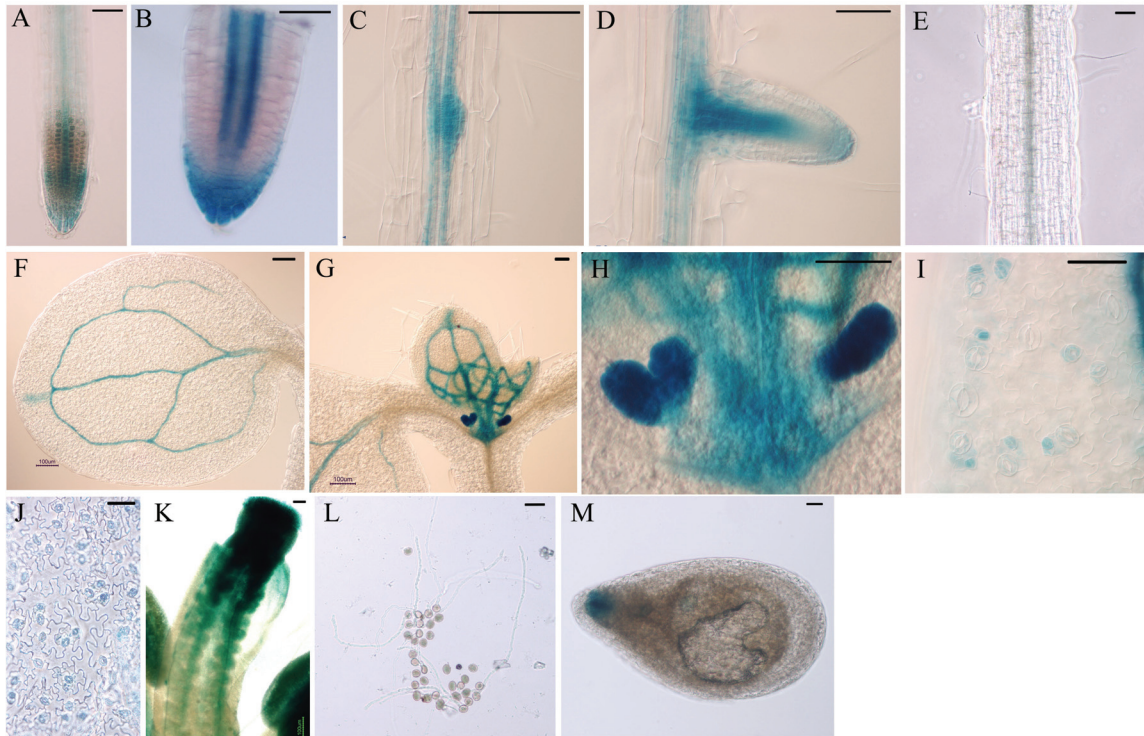


Figure II-10. ECA2::GUS expression in *Arabidopsis*.

GUS activity appears blue. For vegetative tissue staining, transgenic plants hosting the 3.1 kb AtECA2 promoter::GUS construct were grown on $\frac{1}{2}$ MS medium and stained as whole seedlings in X-Gluc for 3 h. Pollen was stained overnight after 6 h *in vitro* germination on agarose-based germination medium. Floral tissue and seed staining were performed on excised specimens for 3 h. The GUS staining was detected only at the cap and the vein of the primary root (A, B) and the lateral root (D), in lateral root primodium (C), not in the hypocotyl (E), in the veins of a cotyledon (F) and true leaves (G), in the stipules at the shoot apex (H), in the developing guard cells on a leaf (I) or on an epidermal peel, in the stigma, the style, ovule, and pollen (K), not in germinated pollen tubes (L), in the funiculus junction region of a young seed. Scale bar = 50 μ m.

grains when they are still in the anther (Fig. II-10K), the promoter activity decreased significantly in germinated pollen tube (Fig. II-10L).

ECA3::GUS activity is concentrated in the vascular tissue in roots and leaves, like ECA2, but only at early developmental stages (Fig. II-11). ECA3::GUS activity was also detected in sub-papillar region and receptacle vasculature at late stages of flower development (Fig. II-11J-K). Most interestingly, AtECA3-driven GUS expression diminished during microgametogenesis (Fig. II-11 I vs J-K). It is noteworthy that all the cell types where ECA3::GUS is detected are highly secretory, suggesting that AtECA3 might play a role in supporting secretory activities.

Despite a high similarity between AtECA1 and AtECA4 at the protein sequence level, the tissue expression pattern of AtECA4 is different from that of AtECA1 (Fig. II-12). Above the elongation zone in the root, AtECA4 is preferentially expressed in vascular tissue. The situation is similar in the leaf: AtECA4 is only found in the vein but not in the mesophyll, and only to a limited extent in guard cells and trichomes. AtECA4 is also expressed significantly in germinating pollen.

The relative strength of promoter activity as detected by GUS activity was also compared by the time it takes to stain using the substrate X-gluc and by the intensity of the blue stain. AtECA1, 2 and 4 were expressed at comparably high levels as GUS staining as dark blue was detectable within 3 h of staining. However AtECA3 expression was relatively weak, so 1-2 days of staining were needed.

b. RT-PCR

Direct evaluation of AtECA transcript presence was also carried out through RT-PCR using cDNA-specific primers (Fig. II-13). The results showed that all 4 AtECA

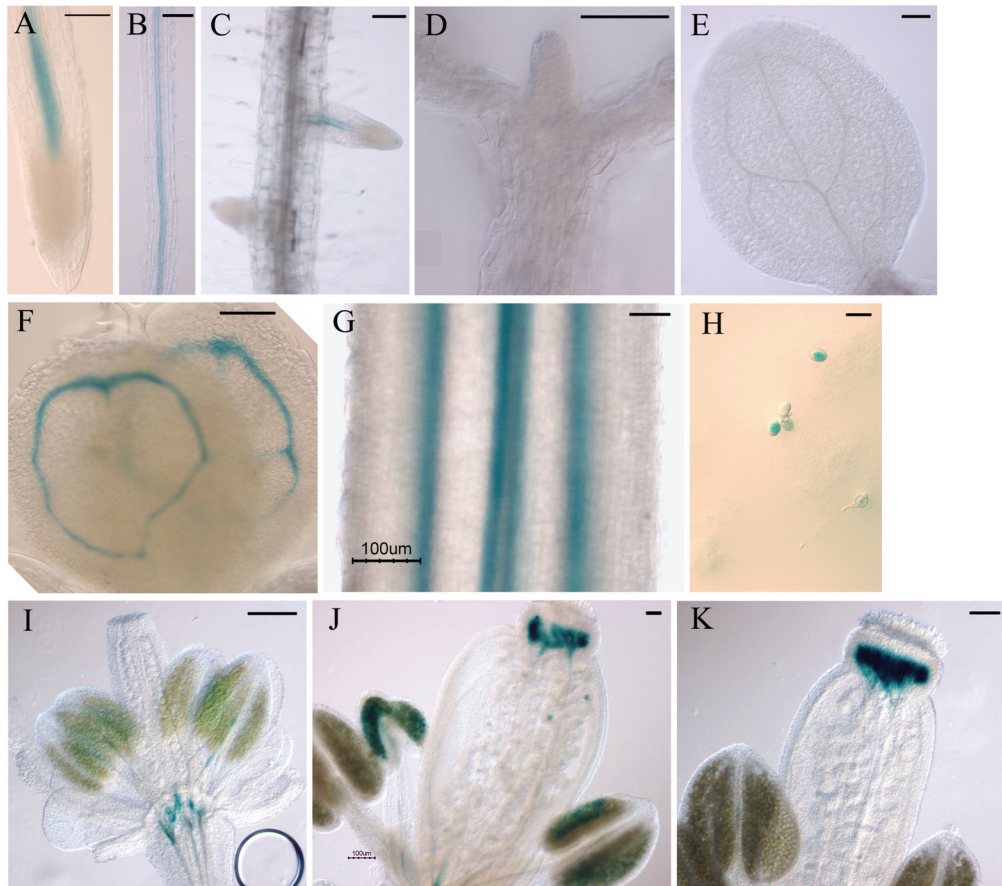


Figure II-11. ECA3::GUS expression in *Arabidopsis*.

GUS activity appears blue. For vegetative tissue staining, transgenic plants hosting the 5.2 kb AtECA3 promoter::GUS construct were grown on $\frac{1}{2}$ MS medium and stained as whole seedlings in X-Gluc for 2 days. Pollen was stained overnight after 6 h *in vitro* germination on agarose-based germination medium. Floral tissue staining was performed on excised specimens for 2 days. The GUS staining was detected only in the vascular tissues at the primary root (A, B), at the lateral root (C), and at the true leaves (F), not in the hypocotyl (D) or cotyledon (E). The staining was also found in the vascular strands of the floral stem (G), in pollen grains (H), in the mature style (J, K) but not in the immature style (I). Pollen staining as the anther is strong at floral stage 11 (I), but faded at later stages such as stage 12 (J) and 13 (K). Scale bar = 50 μ m.

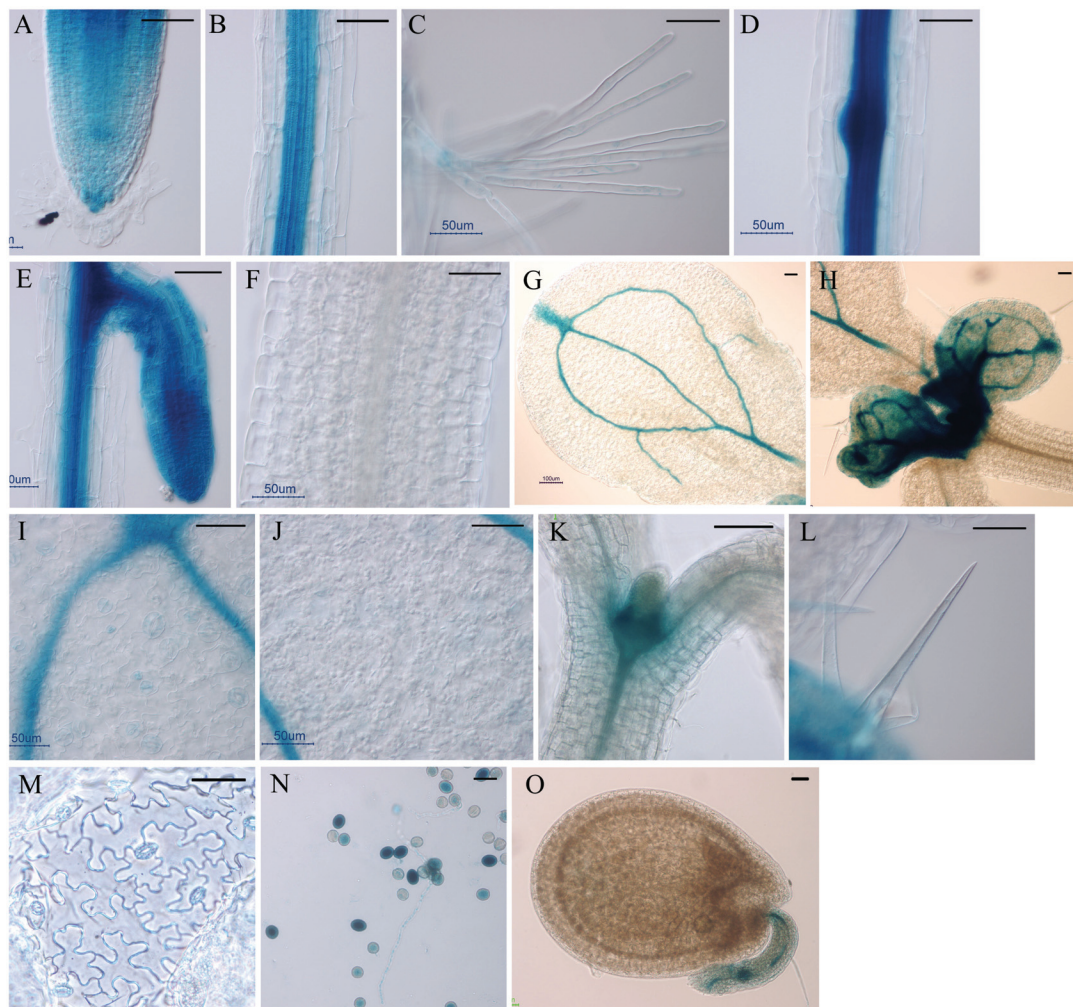


Figure II-12. ECA4::GUS expression in *Arabidopsis*.

GUS activity appears blue. For vegetative tissue staining, transgenic plants hosting the 1.9 kb AtECA4 promoter::GUS construct were grown on $\frac{1}{2}$ MS medium and stained as whole seedlings in X-Gluc for 3 h. Pollen was stained overnight after 6 h *in vitro* germination on agarose-based germination medium. Floral and seed staining was performed on excised specimens for 3 h. The GUS staining was detected in all cell types at the primary root tip, but only in the vascular tissues above the root elongation zone (B), in root hairs (C), in the lateral root primordium (D) and in all cell types of a young lateral root (E), not in the hypocotyl (F), in the veins both of a cotyledon (G) and of true leaves (H, I, J), not in the mesophyll cells (J), in stipules at the shoot apex (K), in a trichome (L), in guard cells on an epidermal peel with low levels (M), in pollen grains and pollen tubes (N), in the funiculus of a young seed (O). Scale bar = 50 μ m.

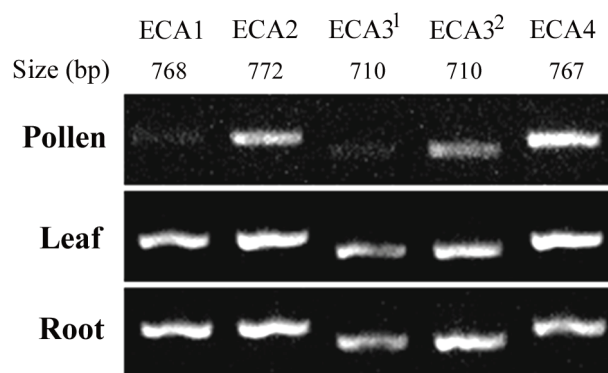


Figure II-13. Presence of AtECA transcripts in plant body parts.

First strand cDNA synthesized from total RNA in pollen, leaf and root of *Arabidopsis* (Col) was used as the template for 35 cycles of PCR amplification. Note 2 primer pairs, which are specific to 5'-half (ECA3¹) and 3'-half of AtECA3 (ECA3²), respectively, were used and amplified products showed variation. Product sizes are also labeled above each lane. The primer annealing regions to cDNAs were -67 to 701 bp, 1263 to 2035 bp, -19 to 691 bp, 2315 to 3025 bp, and 7 to 774 bp for ECA1, ECA2, ECA3¹, ECA3², ECA4 (Table II-3), respectively. Position 1 is A in start codon ATG.

transcripts were detected in root, leaf, and mature pollen. The variation in the PCR product quantity is also observed. For example, AtECA1 and AtECA3¹ in pollen are less than the other ECAs in pollen. However, it does not correlate with the transcript abundance in plant tissues since quantitative-PCR was not used. In stead, the variation could be accounted to the primer efficiency and the location of amplified regions on a complete cDNA as the primers used to amplify AtECA1 and AtECA3¹ both pick up 5'-untranslated region (UTR) of the target cDNA, which may be present in less amount than partial cDNA lacking 5'-UTR in the total 1st strand cDNA population (Fig. II-13).

The difference in tissue expression patterns based on promoter::GUS and RT-PCR analyses clearly indicate that each ECA gene is expressed in a distinct pattern, which means each cell type may be equipped with a combination of different ECA genes with variable transcription levels. The study of biological function of individual ECA genes is therefore needed.

c. Whole Genome Microarrays

I surveyed transcriptome data that are available to the public to determine the developmental and tissue expression patterns of *Arabidopsis* Ca²⁺ pumps. Genevestigator provides a collection of normalized microarray results which can be used to evaluate the relative abundance of specific gene transcripts in defined conditions (Zimmermann et al., 2004). Summaries are listed in Fig. II-14 to 16. AtECAs do not have a very distinct expression pattern in plant body parts (Fig. II-14), although the expression of one gene, such as AtECA3 in pollen, is higher than others in certain cases. During all developmental stages, AtECAs do not show significantly enhanced expression at different stages (Fig. II-15). The changes in expression of AtECAs in response to various

signals are also examined in Figure II-16. AtECA2 is the most responsive ECA gene. It is induced by the biotrophic pathogen (syringolin) but repressed by necrotropic pathogen (persicae), implying a role in pathogenesis. AtECA2 is also repressed by cellulose synthesis inhibitor isoxaben, implying a role in cell wall construction. Unfortunately, Affymetrix chip array cannot distinguish between AtECA1 and AtECA4 due to high sequence identity (Tab. II-2, Fig. II-1). Nevertheless, AtECA1/4 together have similar induction/repression patterns as AtECA2, but at lesser extents. In contrast, AtECA3 is the least responsive among ECAs. It is insensitive to almost all treatments reported.

The global expression profiles of transporter genes from a pollen transcriptome study in *Arabidopsis* (Bock et al., 2006) showed that the expression levels of all AtECAs tend to decrease from microspore to mature pollen (Fig. II-17). However, overall expression varies among AtACAs, in which AtACA9 is significantly higher than any other AtACAs, suggesting AtACA9 is important for late pollen development and germination. This observation is supported by the characterization of null mutants of AtACA9 (Schiott et al., 2004). All 3 ECA profiles showed a diminishing tendency along with pollen maturation. This suggests that ECA activities are required for pollen development at early stages, or that the protein may be stable and active throughout the life of the male gametophyte.

Table II-2. Similarity and identity of AtECA to mammalian SERCA pumps.

Sequences were aligned in pairs using AlignX of Vector NIT (Invitrogen, Carlsbad CA).

The sequence similarity (consensus) and identity are indicated. Protein accession numbers were AAT68271 (AtECA3), AAC68819 (AtECA1), CAA10659 (AtECA2), Q9XES1 (AtECA4), AAB53113 (HsSERCA1a), AAA31165 (OcSERCA1a).

	Similarity (%) / Identity (%)					
	AtECA3	AtECA1	AtECA2	AtECA4	HsSERCA1a	OcSERCA1a
AtECA3	--	--	--	--	--	--
AtECA1	58.0 / 45.1	--	--	--	--	--
AtECA2	56.8 / 44.6	72.5 / 62.8	--	--	--	--
AtECA4	57.7 / 44.7	97.3 / 97.8	72.5 / 62.6	--	--	--
HsSERCA1a	66.1 / 52.9	58.3 / 46.2	58.5 / 46.7	57.9 / 46.5	--	--
OcSERCA1a	65.8 / 52.6	58.6 / 46.3	58.6 / 47.0	58.0 / 46.1	98.5 / 96.7	--



Figure II-14. Summary of tissue expression patterns of AtECAs.

ATH1 22k chip data for wild-type were collected and graphed. AtECA1 and AtECA4 are not distinguishable on the chip. The number of chip experiments for each location is indicated. The values shown are normalized between experiments. Note the AtECA3 signal in pollen is even higher than combination of AtECA1 and AtECA4. Data were retrieved from Genevestigator.

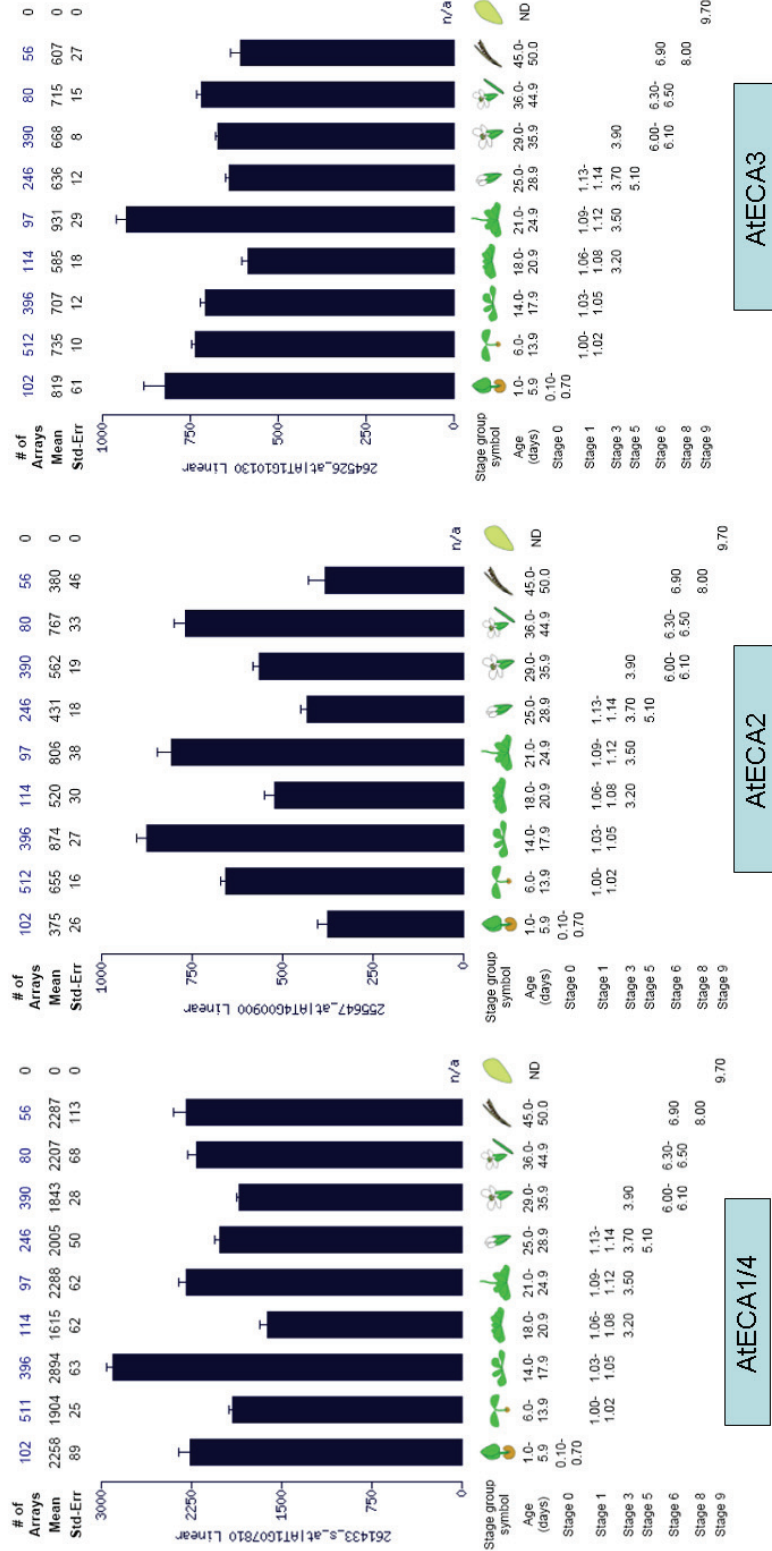


Figure II-15. Summary of expression of AtECAs over developmental stages.

ATH1 22k chip data for wild-type were collected and graphed. AtECA1 and AtECA4 are not distinguishable on the chip. The number of chip experiments for each location is indicated. The values shown are normalized between experiments. It seems ECA genes are not subject to developmental regulation at transcriptional level. Data were retrieved from Genevestigator.

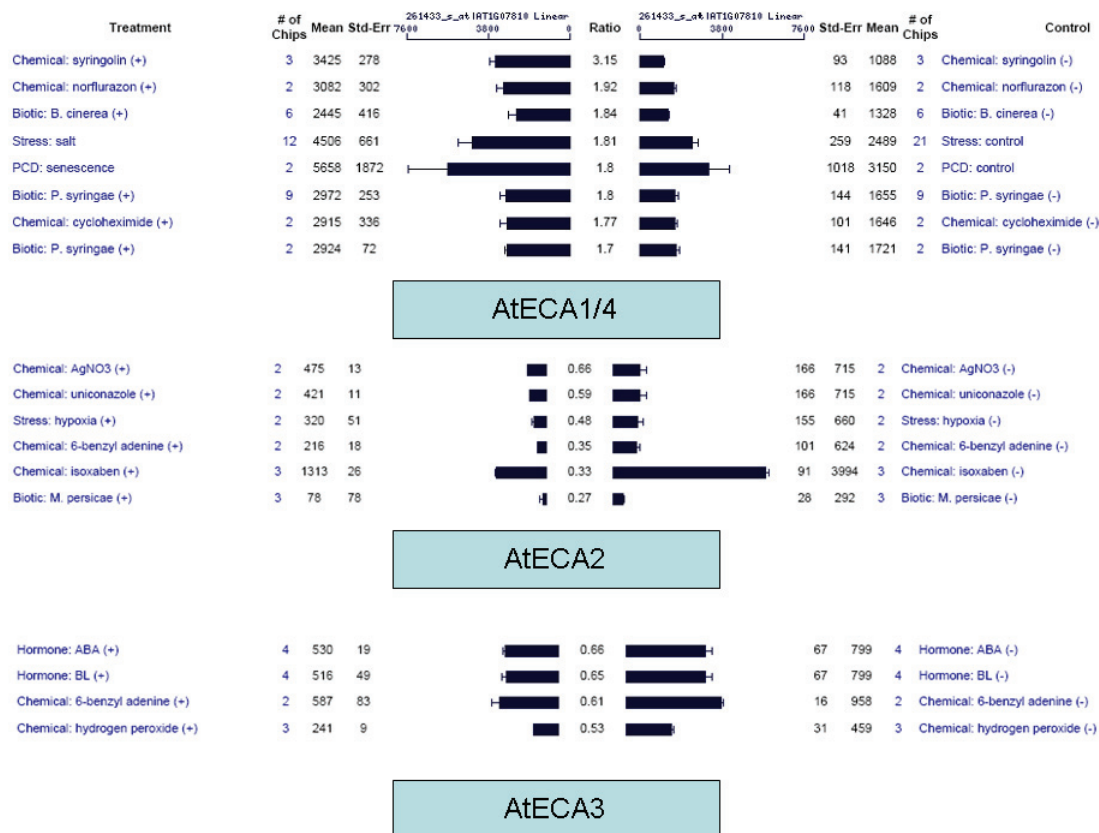


Figure II-16. Summary of expression of AtECAs responding to various signals.

ATH1 22k chip data for wild-type were collected and graphed. AtECA1 and AtECA4 are not distinguishable on the chip. The number of chip experiments for each location is indicated. The values shown are normalized between experiments. Only induction by >1.5 fold or repression by <0.66 fold are listed. Data were retrieved from Genevestigator.

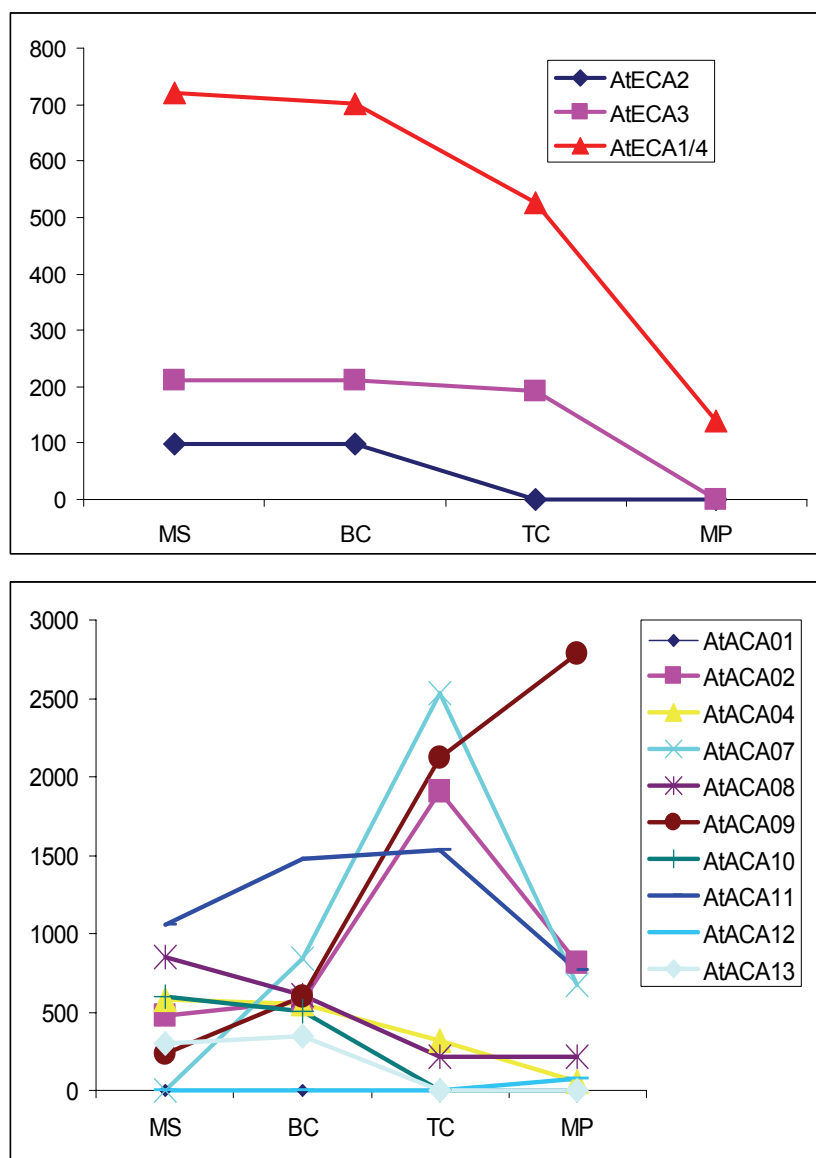


Figure II-17. Expression of AtECAs and AtACAs on different pollen developmental stages.

Data were collected from *in silico* transporter expression study in *Arabidopsis* pollen (Bock et al., 2006). X-axis indicates different stages of pollen development. MS, microspore; BC, bicellular pollen; TC, tricellular pollen; MP, mature pollen. Y-axis indicates normalized expression level in signal strength on microarray.

4. DISCUSSION

4.1. Divergent AtECA genes suggest functional diversity

Sequence comparison revealed 4 AtECA and 3 OsECA genes not only share high homology (>50%) with mammalian SERCA pumps (Fig. II-1), but also possess all the essential functional motifs and domains found in SERCA pumps, such as Ca²⁺-binding sites, P(phosphorylation)-site, ATP-binding site and transmembrane domains (Fig. II-2). The similarity in sequences was also reflected in 3-D structures because most parts of AtECA proteins were fit to the structure coordinates of mammalian SERCA1 without disrupting the biochemical properties (Fig. II-4). These observations are supported by functional characterization of AtECA1 as ER-located Ca²⁺-ATPase (Liang et al., 1997). The Ca²⁺ transport activity by AtECA1 resembles that of mammalian SERCA in its high Ca²⁺ affinity and sensitivity to inhibition of cyclopiazonic acid, but diverges in its insensitivity to thapsigargin (Liang and Sze, 1998). These results together suggested that AtECAs are plant SERCA pumps, although the functions of individuals among AtECA2-4 are still unknown.

The working hypothesis is that multiple ECAs are differentially regulated in time and in space in higher plants, and that they may differ in their transport affinities, cation specificities and inhibitor sensitivities. For example, the human genome has 3 SERCA genes, each distinct in their tissue expression locations, protein isoforms, transport kinetics and sensitivity to specific inhibitors (Wuytack et al., 2002). While AtECA4 may be indistinguishable from AtECA1 due to their extremely high identities of 96% at

nucleotide level and 97% at protein level, AtECA2 and AtECA3 deviate in structural features (Fig. II-4).

AtECA3 is of particular interest because of its higher sequence and structural similarity to mammalian SERCA than any other AtECAs (Fig. II-1, 2, 4). In addition, AtECA3 possesses 33 exons, which is much higher than any other ECA, but close to its mammalian homologs (Fig. II-7). These observations were also true for rice ECA3. Therefore, ECA3 may represent an ancient prototype Ca^{2+} -ATPase that evolved even before the divergence between metazoa and planta.

4.2. Differential gene expression of multiple *Arabidopsis* ECAs

AtECA1-4 also differ in their tissue expression patterns. The microarray results from various sources (Fig. II-14-17) indicated that transcripts of AtECA1-4 genes are present in all different plant body parts, although the expression level is relatively low (values below 1000 in general) compared to other highly expressed genes (in several 1000 at least). There seems to be no drastic up- or down-regulation of AtECA1-4 transcription during development (Fig. II-15) or at organ levels (Fig. II-14). AtECA1-4 also rarely respond to biotic, abiotic or chemical treatments by more than a 3-fold change (Fig. II-16). Nevertheless, AtECA1-4 genes each respond differentially. AtECA1/4 (undistinguishable in microarray chip) are most responsive to pathogen or environmental stresses. AtECA2 is mostly affected by cell wall synthesis or pathogens. AtECA3 is the least responsive among AtECA1-4, as only marginal induction was observed in hormone treatments of ABA and brassinolide, and in H_2O_2 treatment. In addition, the transcription of all AtECA1-4 genes was progressively repressed during microgametogenesis (Fig. II-17), suggesting they also participate in pollen development. However, in most cases

microarray results using whole plants or organs could not resolve the gene expression at tissue levels, not mentioning the inability to distinguish AtECA1 and AtECA4.

Promoter::GUS analyses were therefore used to overcome this disadvantage.

AtECA1-4 genes exhibited differential expression at the tissue level according to promoter::GUS analyses (Fig II-9 to II-12). Histochemical staining of GUS activity driven by the AtECA promoter gave more details at tissue levels of different developmental stages. For instance, the abundance of GUS activity driven by promoters of AtECA2, 3 and 4 in vascular tissues was first disclosed by this assay. However, caution needs to be taken, since the promoter used in this assay only covered cis-acting elements in intergenic regions and therefore was unable to reveal the effect of transcriptional elements in the coding region and 3'-untranslated region. One example was that AtECA3 promoter-driven GUS activity was lower than that reported from various microarray results. This could be due to the presence of intronic transcription enhancer in the 3rd intron (>1 kb), which was not included in promoter::GUS construct. Nevertheless, results from promoter::GUS transcriptional fusion not only disclosed differential expression patterns of AtECA1-4 genes, but also provided clues to the functional studies of each gene as seen in Chapter 3 and 4.

4.3. The multiplicity of AtECA genes may reflect the importance of their functional divergence in multicellular organisms

The multiplicity of AtECA genes may reflect the requirements of a complex multicellular organism. From an evolutionary aspect, P-type Ca²⁺-pumping ATPase was first seen in prokaryotic organism *Synechococcus* (Fig. II-1), which resembles the yeast PMR1 (plasma membrane ATPase-related 1) (Kanamaru et al., 1993). This scenario

became complicated when 2 genes, Pmr1 and Pmc1 (plasma membrane-type Ca^{2+} pump 1) appeared in the unicellular eukaryote yeast, and the number increased in higher organisms (Fig. II-1). The increased number and probable diversity of functional units implies that differentiated cells resulting from multi-cellularization tend to be equipped with different Ca^{2+} -pumping ATPases, probably for strengthened cellular processes such as signal response, muscle contraction, and cell secretion.

Interestingly, both *Arabidopsis* and rice have 14 genes coding Ca^{2+} pumps, which by far represent the largest number of such genes (both PMCA and SERCA groups) in single organisms in all kingdoms. There are two possible reasons for this: i) plants are sedentary, therefore they need multiple functions to adapt and survive changes in environmental conditions; ii) plants have about 35 cell types and may be the most complex in subcellular membranes, which may necessitate extra Ca^{2+} -pumping ATPases. Obviously, even though plant Ca^{2+} pumps may perform the same biochemical missions as their well studied animal mammalian counterparts, they participate in processes that sustain a completely different form of life strategy. Therefore, the biological function of each pump is needed to understand how Ca^{2+} fluxes and homeostasis are integrated from germination through reproduction in plant biology.

In summary, AtECA1-4 genes may play different roles based on their diversities in gene and protein sequences and locations of tissue expression, as suggested by bioinformatic analyses, promoter::GUS analyses, and microarray results. AtECA3 is of particular interest in its higher similarity to animal SERCA than the other 3 AtECAs in conserved functional regulatory motifs and complex gene structures, suggesting it may

represent a novel type of Ca^{2+} -ATPase with new features. Therefore, AtECA3 was chosen for further characterization (Chap 3, 4).

5. MATERIALS AND METHODS

5.1. Molecular cloning of AtECA cDNAs

AtECA1 has previously been cloned and characterized as an ER-located $\text{Ca}^{2+}/\text{Mn}^{2+}$ pump (Liang et al., 1997; Wu et al., 2002). Complementary DNA fragments of ECA2-4 were amplified by RT-PCR. Total RNA was extracted from 2.5-3.5 weeks old young rosette leaves of *Arabidopsis* (Columbia ecotype), reverse transcribed using SuperScript II reverse transcriptase (Invitrogen, Carlsbad CA) and oligo dT to yield cDNA. Proof-reading high fidelity Taq DNA polymerase Deep Vent (NEB, Boston MA) was used to generate the PCR fragments using the primers with start and stop codons underlined (Tab. II-3c). The PCR product was purified by gel extraction and ligated to an EcoRV-linearized vector pBlueScriptSK (Stratagene, La Jolla CA) or in the case of AtECA4 to a SmaI-linearized vector pGEM7z (Promega, Madison WI). The cloned sequences were verified by full length sequencing and used for all subsequent cDNA subcloning.

5.2. Bioinformatic analyses

The DNA and protein sequences used in this study were obtained from well-maintained databases available on Internet (Tab. II-4a). The analyses were performed using programs developed and published by individual groups available on Internet unless otherwise specified (Tab. II-4b).

Table II-3. PCR primers used in Chapter 2

- a. PCR primers used to clone promoter regions of AtECAs. Introduced restriction enzyme sites are underlined.
- b. RT-PCR primers used for examination of tissue expression of AtECAs. 2 pairs of primers were used for AtECA3 which pick up the 5' region or 3' region of AtECA3 cDNA, respectively.
- c. PCR primers used for cloning of ECA2-4 cDNA. Primers were designed to clone end-to-end of predicted ECA cDNA. All primers are 5'-phosphorylated for blunt-end cloning purposes.

Usage:	Primer name	Primer sequence
a. Promoter::GUS analyses		
AtECA1	pECA1-F	5'-CGGGATCCGAATTCTCACTCGTTGCAAAAC-3'
	pECA1-R	5'-CCGCTCGAGAGAGACCCGGTTAGGGTTTTT-3'
AtECA2	pECA2-F	5'-CCGCTCGAGATCACTTTCAATTACACATCG-3'
	pECA2-R	5'-CGGGATCCTGGTTCAAAGCTTTACTTTAA-3'
AtECA3	pECA3-F	5'-CCGCTCGAGTCCTCTGCTTCAACAACAACC-3'
	pECA3-R	5'-CATGCCATGGGTTGGAAAAGCCAAGGGTTT-3'
AtECA4	pECA4-F	5'-CCGCTCGAGGGGTCTAGAAAAGATGATTGA-3'
	pECA4-R	5'-CGGGATCCCTTCCACTGTCAAAGAGATCAA-3'

b. Tissue expression using RT-PCR

AtECA1	E1-F	5'-AAAACCGTAAGCTTTGGCGAGTTTCC-3'
	E1-R	5'-CCTGCAAACACCATGCATTTCTTTCC-3'
AtECA2	E2-F	5'-AGCTGAGCCAAGGCATAAGCAAGAAAT-3'
	E2-R	5'-CGATAGCCACAAGAACGGTGAGTGATAAT-3'
AtECA3	E3a-F	5'-AACCCCTGGCTTTTCCAACATGGAAGAC-3'
	E3a-R	5'-TACCCATTGCGGTGTTTGAACCAACT-3'

AtECA3	E3b-F	5'-CTGATACCTTGGCACCTGTTCAACTTCTG-3'
	E3b-R	-TGACGAAAAAGCCATCTCTTGCTTTC-3'
AtECA4	E4-F	5'-AAAGGAGGTGAAGATTGCGGGAATAAG-3'
	E4-R	5'-AACCTTCCAATCTCAGTATTCATCCCAG-3'

c. Molecular cloning of AtECAs

AtECA2	ECA2-F	5'- <u>ATGG</u> GAGGAGGAGAAGTCGTTCTCGG-3'
	ECA2-R	5'- <u>TTAC</u> ATTGTCTTGATCTTCTTCTTGATTC-3'
AtECA3	ECA3-F	5'- <u>ATGGA</u> AGACGCCTACGCCAGATCTGT-3'
	ECA3-R	5'- <u>CTA</u> CTTGTCACGCCGGTCCTTGGG GAGTAA-3'
AtECA4	ECA4-F	5'- <u>ATGGG</u> GAAAGGAGGTGAAGATTGCG-3'
	ECA4-R	5'- <u>TTA</u> CTCCTCCTTTTGCTTAGCTGAGGGA-3'

Table II-4. Web-based databases and software used in this research

A. Sequence information databases used in this study.

Name	Website
Genebank	www.ncbi.nlm.nih.gov/Genbank/
Genevestigator	www.genevestigator.ethz.ch/
MIPS	mips.gsf.de/projects/plants
PlantsT	plantst.genomics.purdue.edu/
TAIR	www.Arabidopsis.org/
The <i>Arabidopsis</i> Ionomics Database	hort.agriculture.purdue.edu/Ionomics/
TIGR	www.tigr.org/tdb/e2k1/osa1/index.shtml

B. Programs used for sequence analyses in this study.

Name	Website
BioEdit	www.mbio.ncsu.edu/BioEdit/bioedit.html
CN3D	130.14.29.110/Structure/CN3D/cn3d.shtml
MUSCLE	www.ebi.ac.uk/muscle/
PlantsT	plantst.genomics.purdue.edu/
SOSUI	www.proteome.bio.tuat.ac.jp/sosuiframe0.html
T-COFFEE	igs-server.cnrs-mrs.fr/Tcoffee/tcoffee_cgi/index.cgi
TMHMM	www.cbs.dtu.dk/services/TMHMM/
TOPO2	www.sacs.ucsf.edu/TOPO-run/wtopo.pl
ESPrIpt	espript.ibcp.fr/ESPrIpt/cgi-bin/ESPrIpt.cgi

5.3. Promoter::GUS constructs for tissue expression pattern of ECAs

a. DNA manipulation. Genomic DNA was isolated from 4 weeks old seedlings of *Arabidopsis* Col-0 using the CTAB method (Ausubel et al., 1988). The promoter of each ECA was determined as the intergenic region between start codon of ECA and its immediate ORF. The primers used with appended restriction enzyme sites are pECA1-F and pECA1-R (for ECA1), pECA2-F and pECA2-R (for ECA2), pECA3-F and pECA3-R (for ECA3), pECA4-F and pECA4-R (for ECA4), respectively (See Tab. II-3a).

PCR fragments of each ECA promoter were double digested with appended enzymes and cloned into a GUS ORF-containing vector pRITA to make a promoter::GUS construct ECA-RITA and verified by sequencing. This NotI-NotI fragment of ECA-RITA was ligated to a binary vector pMLBART via NotI. The resulting pECA-GUS-MLBART constructs were used for promoter::GUS analyses.

b. Agrobacterium-mediated plant transformation. The pECA-GUS-MLBART constructs were transformed into the *Agrobacterium* strain GV3101 via electroporation and selected on LB plates with gentamicin and spectinomycin. A floral dip method was used to transform *Arabidopsis* Col-0 with *Agrobacteria* hosting ECA promoter::GUS constructs (Clough and Bent, 1998). Plant transformants were selected on Basta-containing plates and at least 5 T3 lines of each were checked for consistent GUS-staining patterns.

c. Histochemical staining of GUS activity. The GUS staining was performed according to the protocol described previously (Lagarde et al., 1996). Samples were harvested in 90% acetone at various stages, rinsed once with staining buffer lacking 5-bromo-4-chloro-3-indolyl β -D-glucuronide (X-gluc; 50 mM sodium phosphate, pH 7.2,

0.5 mM $K_4Fe[CN]_6$, 0.5 mM $K_3Fe[CN]_6$), and then incubated for 16 h at 37°C in staining buffer containing 1 mM X-gluc. The staining reaction was stopped in 70% ethanol and chlorophyll cleared in 95% ethanol. GUS staining patterns were photographed using a Nikon Eclipse E600 microscope capable of differential interference contrast image capture (Nikon Instruments, Melville, NY). The data were summarized in Fig. II-9 to II-12.

5.4. RT-PCR for tissue expression of AtECAs

PCR primers were designed for ECA1-4 to pick up the relatively similar region located on each ECA cDNA. PCR reactions were performed using identical settings for all primer pairs. The first strand cDNA templates were prepared from total RNA isolated from root, leaf, and pollen of *Arabidopsis* Columbia ecotype (Gift from Dr. S. Padmanaban (Sze et al., 2004)). The primers used are listed in Table II-3b. Two primer pairs specific to N- or C-region were used for ECA3. The results were shown in Fig. II-13.

III. A THAPSIGARGIN-SENSITIVE $\text{Ca}^{2+}/\text{Mn}^{2+}$ PUMP

ATECA3, SUPPORTS POLLEN TUBE GROWTH AND

MALE FERTILITY

1. ABSTRACT

The temporal and spatial changes in cellular $[\text{Ca}^{2+}]$ are critical for plant growth, reproduction and survival, although the molecular bases of the transporters involved are not yet understood. One *Arabidopsis* endomembrane Ca^{2+} -ATPase, AtECA3, shares particularly high identity with animal SER Ca^{2+} -ATPases. Expression of AtECA3 cDNA in a yeast mutant defective in its endogenous Ca^{2+} pumps, conferred the ability to grow on Ca^{2+} -depleted medium and tolerance to toxic levels of Mn^{2+} . AtECA3-dependent yeast growth was sensitive to thapsigargin and to cyclopiazonic acid. A functional ECA3-GFP was localized to intracellular membranes of yeast, indicating that AtECA3 pumps Ca^{2+} and Mn^{2+} into the lumen. In *Arabidopsis*, AtECA3 was expressed in the vasculature of vegetative and floral organs, and in pollen grains according to promoter::Gus analyses. *In vitro* tube growth of wild-type pollen was enhanced by 10 mM Ca^{2+} , however, tube growth of T-DNA insertional *eca3* mutants was reduced 33% and failed to respond to Ca^{2+} . Significantly, thapsigargin inhibited growth of wild-type pollen tubes, phenocopying the *eca3* mutants. GFP-tagged AtECA3 was localized to punctate structures beneath the PM in the apical region of growing pollen tubes. These results demonstrate that sequestration of Ca^{2+} into secretory vesicles by a thapsigargin-sensitive AtECA3, is critical for pollen tube elongation and for male fertility.

2. INTRODUCTION

The role of Ca^{2+} as a macronutrient in plants (Marschner, 1986) depends on the ability to translocate this cation to the appropriate organs and cell-types, and the ability to regulate its cellular levels both spatially and temporally. In plant cells, the extracellular wall spaces and the lumen of organelles contain millimolar Ca^{2+} , in contrast to submicromolar Ca^{2+} in the cytosol of un-stimulated cells (Dauwalder et al., 1985; Sakai-Wada and Yagi, 1993). Plants have evolved the ability to respond to diverse environmental cues as they grow, and develop by producing Ca^{2+} oscillations and Ca^{2+} transients with distinct signatures that are transmitted and decoded to produce specific physiological responses (Sanders et al., 1999; Sanders et al., 2002; Hepler, 2005). This remarkable feat relies on the coordination of multiple Ca^{2+} channels, exchangers and pumps, though the molecular identity and functions of most Ca^{2+} transporters are still unknown (White and Broadley, 2003).

The role of Ca^{2+} in regulating growth is best exemplified by polar tip growth of pollen tubes. First, a massive Ca^{2+} entry at the extreme apex guides tube growth (Malho and Trewavas, 1996). Second, a tip-focused steep cytosolic Ca^{2+} gradient oscillates in phase with the tube growth rate (Holdaway-Clarke et al., 1997; Messerli and Robinson, 1997), and is essential for growing tubes (Obermeyer and Weisenseel, 1991; Rathore et al., 1991; Miller et al., 1992). These results remain valid during *in vivo* pollination, although with higher cytosolic Ca^{2+} levels and faster oscillations in growing tubes (Iwano et al., 2004). Ca^{2+} dynamics is also linked to vesicle exocytosis and pectin wall modification during fast tube growth (Hepler et al., 2001; Bosch et al., 2005). However, a molecular mechanism is still unclear relative to how the apical-oriented Ca^{2+} gradient is

generated and sustained, in particular how low cytosolic Ca^{2+} is achieved within 20 μm after massive Ca^{2+} influx from the tube apex. The oscillations and Ca^{2+} transients seen in cells are thought to be generated and maintained by Ca^{2+} channels, Ca^{2+} -pumping ATPases and $\text{Ca}^{2+}/\text{H}^+$ exchangers. Channels only allow Ca^{2+} entry into the cell down the Ca^{2+} electrochemical gradient from internal stores or from the extracellular medium, whereas pumps and exchangers load cytosolic Ca^{2+} into organellar lumens or remove excessive cytosolic Ca^{2+} following a signal-elicited $[\text{Ca}^{2+}]_{\text{cyt}}$ spike. Little is known about the molecular bases of Ca^{2+} permeable channels at the PM or intracellular membranes of pollen tube cells, though this area is attracting more attention (Sze et al., 2006).

Although Ca^{2+} pumps are better understood in plants, only a few of the 14 predicted Ca^{2+} pump genes in *Arabidopsis* have been functionally characterized (Sze et al., 2000; Sanders et al., 2002). P-type ATPases are divided into P2A-type which consists of ECA1-ECA4, and P2B-type with 10 ACA genes based on sequence homology to animal SERCA-type and PMCA-type pumps, respectively (Axelsen and Palmgren, 2001). ACA pumps, such as an ER-localized ACA2, have an auto-inhibitory domain at N-terminus which is activated through binding with calmodulin (Hwang et al., 2000; Sze et al., 2000). ACA9 is highly expressed on the PM of pollen and required for pollen tube elongation and discharge of sperm cells upon fertilization (Schlott et al., 2004). AtECA1 is the only well characterized ECA in plants. AtECA1 is a $\text{Ca}^{2+}/\text{Mn}^{2+}$ pump with high affinity for Ca^{2+} . *Arabidopsis* ECA1 knockout mutants grow poorly when there is insufficient Ca^{2+} or toxic levels of Mn^{2+} (Wu et al., 2002), suggesting that one role of this ER-localized pump is to load $\text{Ca}^{2+}/\text{Mn}^{2+}$ into the lumen of the ER for biochemical

activity, and to remove excess and toxic levels of divalent cations. However, the functions of other ECAs, are still not known.

Here I demonstrate that AtECA3 is also a $\text{Ca}^{2+}/\text{Mn}^{2+}$ pump. Unlike AtECA1, AtECA3 is sensitive to thapsigargin, a specific inhibitor of SER-type Ca^{2+} pumps from mammals. Three independent alleles of T-DNA mutants displayed 33% reduction in *in vitro* pollen tube growth that in wild-type is dependent on millimolar levels of Ca^{2+} . The defect in pollen tube growth of *eca3* mutants reduced seed set by 13%. GFP-tagged AtECA3 was located on punctate structures beneath the PM in the apical region of growing pollen tubes. These results demonstrate for the first time that an endomembrane $\text{Ca}^{2+}/\text{Mn}^{2+}$ pump supports pollen tube elongation and promotes seed set.

3. RESULTS

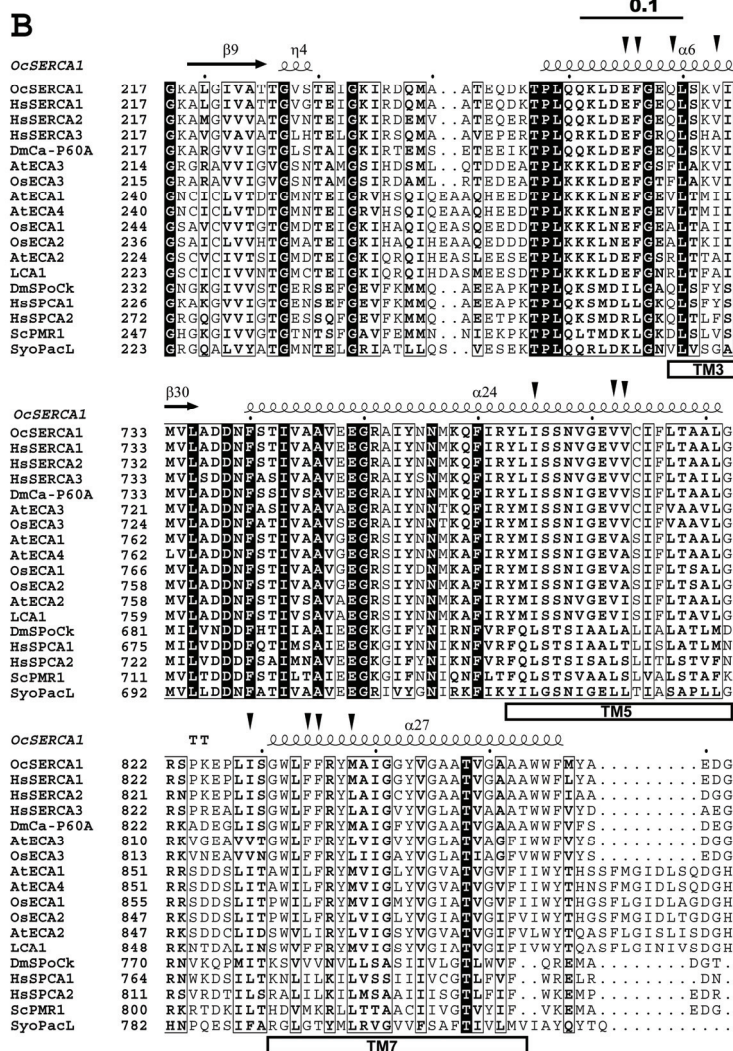
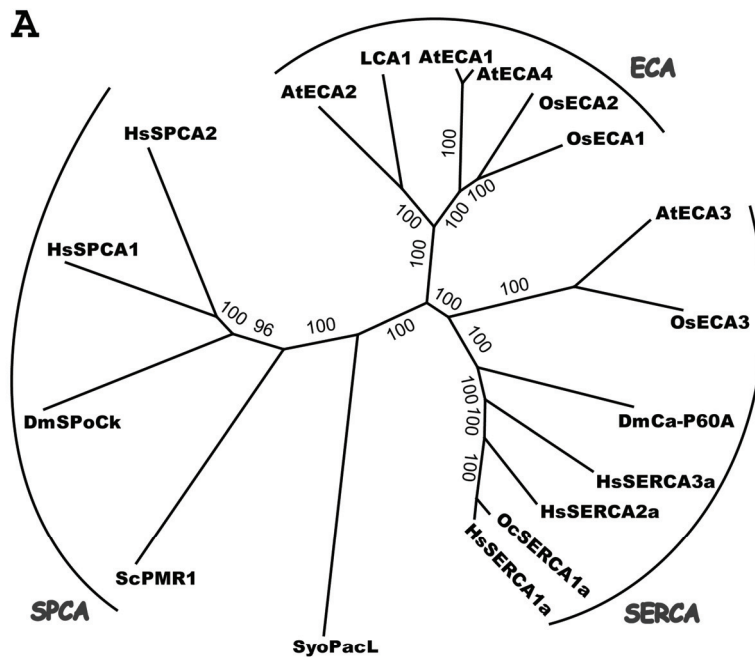
3.1. AtECA3 diverges from other *Arabidopsis* ECA and shares high identity with animal SERCAs

A sequence comparison of plant ECAs with other Ca^{2+} pumps was performed to get clues about functions of plant ECAs. The primary protein sequences of each pump were aligned using T-COFFEE to generate a phylogenetic tree (Fig. III-1A). Three observations emerged: 1), Plant AtECAs, from *Arabidopsis*, rice, and tomato, clustered with mammalian SERCA-type Ca^{2+} -ATPases; 2), both AtECA3 and OsECA3 diverged from other plant ECAs, and shared high identity (53%) with mammalian SERCA1a pumps, and 3). None of the plant ECAs clustered with SPCA, or secretory pathway Ca^{2+} -ATPases (Wuytack et al., 2002), which are found in fungi and metazoans (Fig. III-1A).

Figure III-1. AtECA3 shares high similarity with animal SERCA.

A. Phylogenetic relationship of type 2A Ca-ATPases from plant, bacteria, yeast and animal. *Arabidopsis* (At) and rice (Os) ECA protein accession numbers are shown in parenthesis: AtECA1 (AAC68819), AtECA2 (CAA10659), AtECA3 (AAT68271), AtECA4 (AAC68819), OsECA1 (ABF95313), OsECA2 (BAA90510), and OsECA3 (ABF98693). Other Ca pumps aligned are *Synechococcus* SyoPacL (BAA03906), *Saccharomyces cerevisiae* ScPmr1 (P13586) and ScPmc1 (P38929), tomato LCA1 (Q42883), human (Hs) SERCA1 (O14983), SERCA2 (P16615), SERCA3 (Q93084), and SPCA1 (AAH28139), SPCA2 (AAN12202), *Drosophila melanogaster* (Dm) Ca-P60A (P22700) and SPoCk (AAV54193), *Oryctolagus cuniculus* (rabbit, Oc) SERCA1a. Tree was aligned by T-coffee. Values shown indicate the number of times (in percent) that each branch topology was found in 1000 replicates of the performed bootstrap analysis using PAUP* 4.0b10.

B. Protein sequence alignment of plant ECAs and other Ca²⁺-ATPases with thapsigargin-interacting regions of animal SERCA. Residue numbers correspond to HsSERCA1. Black triangles indicated amino acid residues in direct contact with TG in the structure of a rabbit SERCA1a (1SU4_A) (Toyoshima and Nomura, 2002). Identical residues were shaded in black while similar residues are boxed. Transmembrane domains corresponding to HsSERCA1 were indicated as TM. Figure was generated in ESPript 2.2 (Gouet et al., 1999) using T-Coffee generated alignment.



Closer examination of AtECA3 with mammalian SERCA sequences suggested AtECA3 might differ from other AtECAs in their sensitivity to inhibitors. A unique feature of mammalian SERCA is their sensitivity to two specific inhibitors, thapsigargin (TG) and by cyclopiazonic acid (CPA) (Goeger et al., 1988; Seidler et al., 1989; Lytton et al., 1991; Sagara and Inesi, 1991; Soler et al., 1998). However, so far there is no molecular evidence for a plant S/ER-type Ca^{2+} -ATPase sensitive to TG. AtECA1 is inhibited by CPA only (Liang and Sze, 1998). TG binds to the cavity surrounded by the transmembrane region M3, M5 and M7 helices in E2 conformation state of rabbit skeletal muscle SERCA (Toyoshima and Nomura, 2002). Interestingly, among the hydrophobic residues complementary in shape to TG molecule, V263, V773 and F834 (as on HsSERCA1, O14983) are identical in AtECA3 and in OsECA3 and other TG-sensitive SERCAs. In contrast, these residues are not found in AtECA1 and SPCAs (Fig. III-1B) which are TG-insensitive Ca^{2+} pumps. In addition, an extra tripeptide of Q/HEA, corresponding to a region between residues 240-241 on HsSERCA1, was present in most plant ECAs except ECA3. These results suggest that the biochemical properties of AtECA3, may differ from AtECA1, and might be sensitive to TG.

3.2. AtECA3 confers tolerance to low Ca^{2+} / high Mn^{2+} in yeast

To determine the transport function of AtECA3, a cDNA containing the complete ORF (AY650902) was cloned and expressed in the yeast mutant strain K616. Yeast strain K616 lacks both Ca^{2+} -ATPase genes *Pmr1* and *Pmc1*, and thus fails to load Ca^{2+} and Mn^{2+} into endomembrane compartments (Cunningham and Fink, 1994). This strain can survive by *Vcx1* activity, a vacuolar $\text{Ca}^{2+}/\text{H}^{+}$ exchanger when Ca^{2+} is relatively high

(> μM) (Cunningham and Fink, 1996). However, growth is arrested when the media contains less than μM levels of Ca^{2+} , or when the media Mn^{2+} concentration is toxic at mM levels.

In normal media with sufficient Ca^{2+} at ~ 1 mM, AtECA3 did not affect K616 growth relative to strains harboring the empty yeast p426 vector only, (Fig. III-2A). However, in the presence of 5 mM EGTA, when free Ca^{2+} was ~ 0.8 μM (Portzehl et al., 1964), growth of K616 was severely curtailed. The expression of AtECA3 in K616 greatly improved yeast growth when Ca^{2+} is depleted (Fig. III-2A), suggesting AtECA3 is able to transport Ca^{2+} with relatively high affinity.

I also tested if AtECA3 might support yeast growth at high Mn^{2+} . AtECA3 expression under the Gal1 promoter on vector p426 failed to suppress the Mn^{2+} sensitivity of K616 strain (data not shown). Consequently, AtECA3 was expressed using pDR196 vector which contains a very strong constitutive promoter of the plasma membrane H^+ ATPase 1 (PMA1) (Rentsch et al., 1995). Under the PMA1 promoter, the resultant AtECA3 expression improved K616 growth on media containing 1 mM Mn^{2+} (Fig. III-2B). This observation suggested that AtECA3 may also function as a Mn^{2+} pump to remove excessive Mn^{2+} from the cytosol when the cell was faced with excess manganese.

However, under the same Gal1 promoter AtECA3 was less effective than AtECA1 and AtECA4 (Fig. III-2C) in restoring mutant growth on medium depleted of Ca^{2+} . AtECA1 was able to rescue K616 growth in medium with 10 mM EGTA (Liang et al., 1997), while AtECA3 was not as effective. As shown later, AtECA3 clearly restored mutant growth on a medium containing 1 mM EGTA.

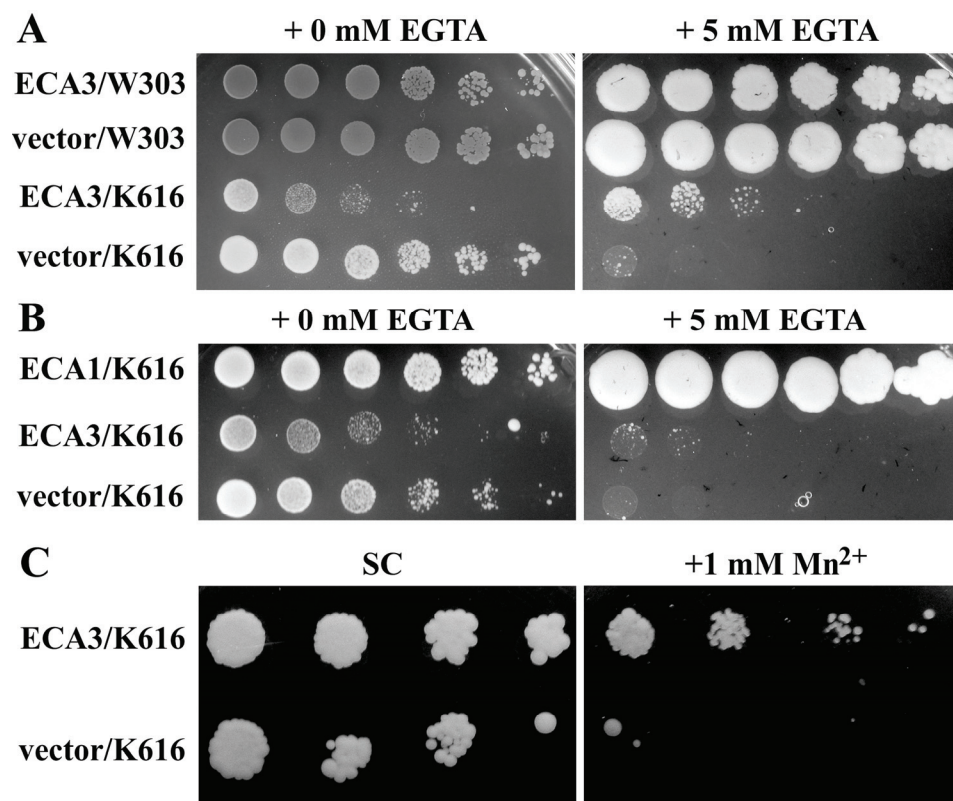


Figure III-2. AtECA3 confers tolerance of K616 yeast growing on medium depleted of Ca²⁺ or supplemented with high Mn²⁺.

A. Yeast growth on SC-URA medium with or without 5 mM EGTA. Seed culture was prepared in SC medium with 2% raffinose as carbon source. W303, *wildtype* or mutant K616 (*pmr1*, *pmc1*, *cnb1*) harboring either AtECA3 under the GAL1 promoter or an empty vector were normalized to 0.5 A₆₀₀. Cultures were serially diluted (5x) and 5 μ l was spotted on plates containing 2% galactose and 10 mM MES-K at pH 6.25 and incubated for 3.5 d.

B. ECA3 was less effective than ECA1 in promoting K616 yeast growth on medium depleted of Ca²⁺. Both ECA1 and ECA3 were subcloned in p426GAL1 vector. Method was as described in (A).

C. Yeast growth on SC-URA medium supplemented with 1 mM Mn²⁺. K616 mutant was transformed with an empty vector pDR196 or with AtECA3 under the control of the PMA1 promoter. Cells were serially diluted (10x) and 10 μ l was spotted on media containing 2% glucose and 10 mM MES-K at pH 6.25 alone (SC) or containing 1 mM Mn²⁺, and incubated for 7 d. Figure shows one representative experiment of three.

3.3. AtECA3-dependent yeast growth is inhibited by cyclopiazonic acid and thapsigargin

I tested if growth of AtECA3-expressing K616 was affected by CPA or TG (Tab. III-1). AtECA3 was not required for K616 growth in medium containing 1 mM Ca^{2+} (Fig. III-3A). However, when free Ca^{2+} in the media was lowered by adding 2 mM EGTA, AtECA3 expression greatly improved K616 growth which otherwise was greatly retarded (Fig. III-3B). Growth of K616 cells expressing AtECA3 was inhibited by 20% when the CPA concentration was increased from 0.2 μM to 2 μM (Tab. III-1). In contrast, the growth of K616 containing only the control vector, was almost unaffected by CPA at concentrations between 0.2 μM and 2 μM . Therefore, it is suggested that AtECA3-enhanced growth was blocked by CPA at effective levels.

Interestingly, TG also inhibited growth of AtECA3-expressing K616 by ~ 25% at 500 nM when compared to no or low TG (50 nM). No inhibition was observed for K616 containing the vector only under the above conditions (Tab. III-1). Thus only AtECA3-dependent growth is sensitive to the inhibitor, suggesting that AtECA3 activity was sensitive to TG. The concentration of 500 nM required for TG inhibition appears relatively high, probably because the growth assay utilized whole cells containing multiple subcellular membranes instead of isolated membranes used in *in vitro* assays. TG is soluble in DMSO and thus would partition into any membrane. Attempts to detect active $^{45}\text{Ca}^{2+}$ accumulation into isolated membranes have been unsuccessful.

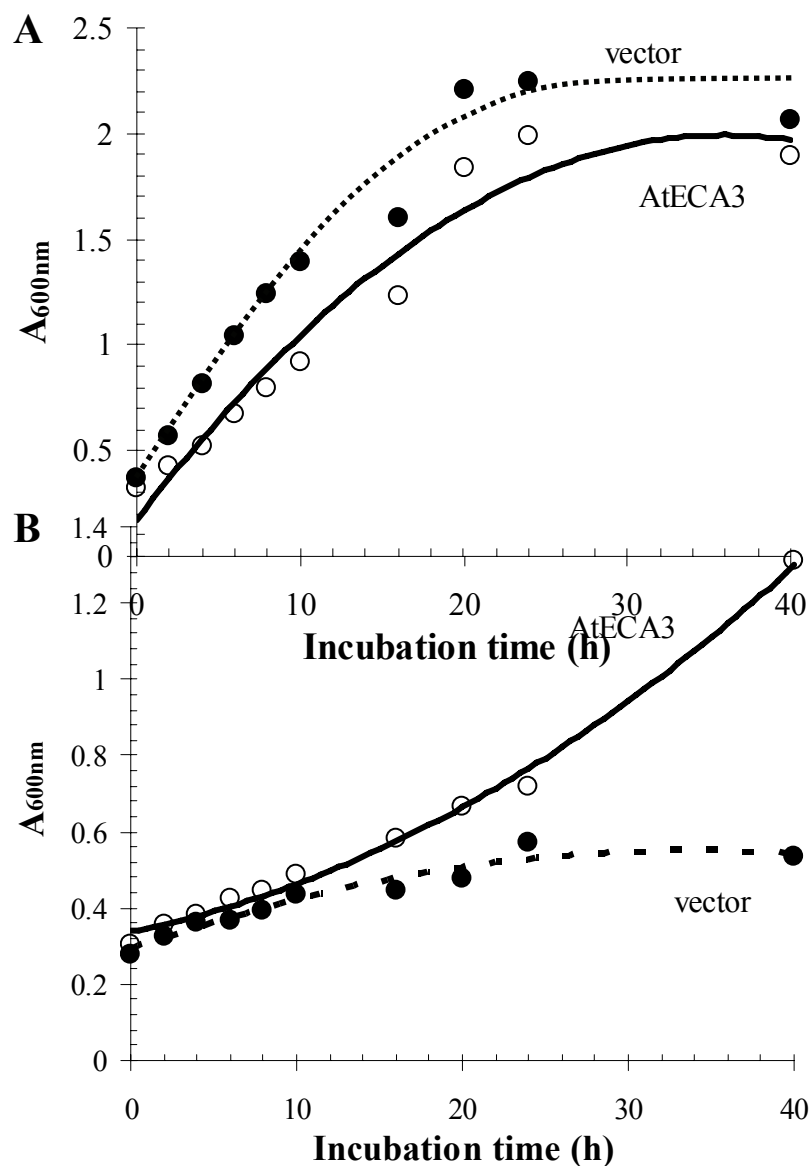


Figure. III-3. Growth of yeast mutants and *AtECA3* transformants in medium with or without EGTA.

K616 mutant carrying vector alone (pDR196) (●) or transformants expressing *ECA3* under the *PMA1* promoter (○) were suspended in SC-URA medium containing either (A) 1 mM Ca^{2+} [no EGTA] or (B) 0.001 mM Ca^{2+} [2 mM EGTA].

Table III-1. AtECA3-dependent yeast growth is sensitive to cyclopiazonic acid and to thapsigargin.

Yeast strain K616 harboring the empty vector pDR196 or AtECA3 under the PMA1 promoter was cultured in liquid SC-URA medium with 2% glucose. The cell density of each was adjusted to 0.1 OD₆₀₀. EGTA was added to a final concentration of 1 mM, and cells were incubated for 8 h. Then DMSO alone, CPA or TG in DMSO was added to give a final concentration as indicated. The final concentration of DMSO was 1%.

Inhibitor	Conc.	Cell Density (A _{600nm})			Growth (%)
		Vector	AtECA3	AtECA3-dep	
thapsigargin (nM)					
	0	0.5349	1.3117	0.7768	100
	50	0.5423	1.3939	0.8516	110
	500	0.5287	1.1882	0.6595	84.9
	5000	0.4104	0.9776	0.5672	73.0
cyclopiazonic acid (μM)					
	0	0.5349	1.3117	0.7768	100
	0.2	0.5335	1.3386	0.8051	104
	2	0.5513	1.1923	0.6410	82.5
	20	0.3692	0.9161	0.5469	70.4

3.4. AtECA3 confers hypersensitivity to high Ca²⁺ and toxic Mn²⁺ when expressed in K667

I also tested if AtECA3 interferes with endogenous Pmr1p in the yeast mutant strain K667. K667 lacks both of its active Ca²⁺ transporters Pmc1 and Vcx1 (Cunningham and Fink, 1996). Growth of K667 is arrested by high levels of Ca²⁺, Na⁺ and Mn²⁺, probably because of an inability to sequester high Ca²⁺ or high Mn²⁺ into the vacuole using VCX1.

Interestingly, when expressed in strain K667, AtECA3 exacerbates the hypersensitivity of K667 to 5mM Mn²⁺ or 150mM Ca²⁺ while AtECA1 did not seem to have this effect (Fig. III-4). Strain K667 possesses Pmr1p but lacks Pmc1p and Vcx1p, and thus is highly sensitive to high concentrations of Ca²⁺ and Mn²⁺. These results again underscore the distinct biological functions of AtECA3 and AtECA1 in yeast. Since Pmr1p is the only active Ca²⁺ transporter in K667, one possibility is that overproduction of heterologous AtECA3 caused attenuated Pmr1p function. This down-regulation of endogenous Pmr1 activity could arise from interference at the transcriptional or translational level. In either case, AtECA3 may have common features, such as mRNA, protein structure, subcellular location, regulating mechanism, with Pmr1p. In contrast, AtECA1 expression does not interfere with Pmr1 function because K667 transformants with AtECA1 expression grew similarly to vector-containing transformants in all conditions tested, suggesting that AtECA1 is sufficiently different from Pmr1. Further investigation of the differential regulation of endogenous Pmr1 in K667 yeast over-expressing plant AtECA3 or AtECA1 is needed to answer this question.

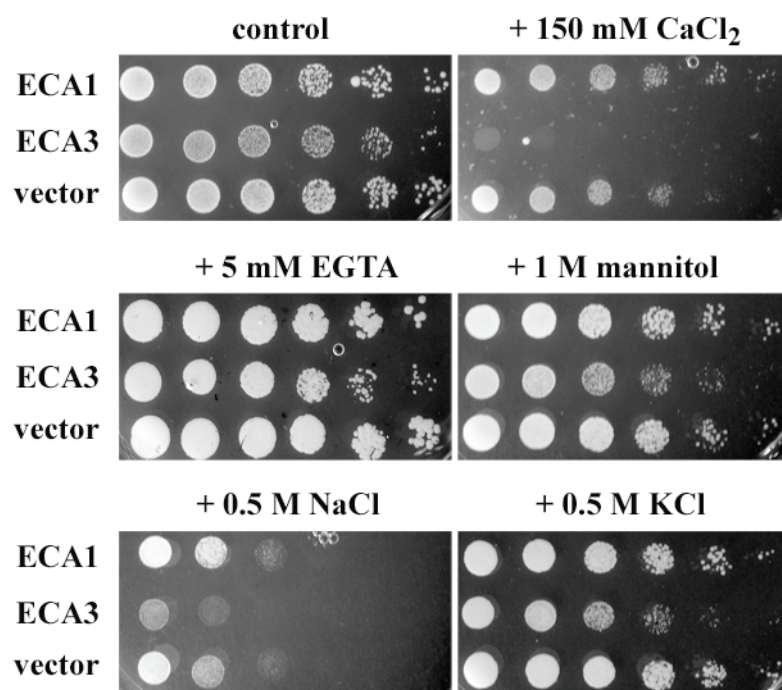


Figure III-4. Growth of K667 yeast expressing AtECA3 is hypersensitive to high Ca^{2+} .

K667 strain was transformed with p426 vector alone or with AtECA3 under the GAL1 promoter. Seed cultures were prepared in SC medium with 2% raffinose as carbon source. Yeast was then cultured in SC-URA medium containing 2% galactose (pH 5.5, 10 mM MES-K). Cultures were serially diluted (5x) and spotted on medium containing either no additions (control), or with 150 mM CaCl_2 , 5 mM EGTA, 1M Mannitol, 0.5 M NaCl or KCl. Pictures were taken 6 days after plating. W303, wild-type strain isogenic to mutant K667 (*vcx1*, *pmc1*, *cnb1*).

3.5. A functional GFP-tagged AtECA3 is localized to structures resembling ER-Golgi compartments in yeast

AtECA3 is the only member among four AtECAs that lacks an ER-retention motif KxKxx at its extreme C-terminus, in spite of a composition rich in basic amino acid residues (-KDRRDK). Therefore, a construct was made fusing GFP to the last amino acid of AtECA3 at its C-terminus, which is unlikely to disrupt a possible internal ER-retention signal. When expressed in yeast cells under the control of the PMA1 promoter (vector pDR196), ECA3-GFP fluorescence was observed in tubular and granular structures within the cells, which resembled Pmr1p-GFP whose location spreads from ER to Golgi (Fig. III-5A). Besides, the same GFP signal patterns were observed in both the W303 strain and the K616 strain. AtECA4, which shares 97% protein identity to ER-located AtECA1, was fused to GFP and expressed in yeast for comparison. The results showed that ECA3-GFP and ECA4-GFP were both possibly localized to Golgi-ER like structures, in yeast (Fig. III-5B).

I verified that the GFP-tagged AtECA3 retained its native activity. Expression of ECA3-GFP in K616 restored growth of the yeast transformant at 1 mM Mn^{2+} or 1 μM Ca^{2+} (Fig. III-5B). These results together indicate that the ECA3-GFP is functional and that it is localized to ER-Golgi membranes in yeast.

3.6. Inhibition of *Arabidopsis* pollen growth by cyclopiazonic acid and thapsigargin

Promoter-Gus reporter gene analysis showed that AtECA3 and other ECAs are expressed in pollen grains at different stages. I tested their role in *in vitro* pollen tube

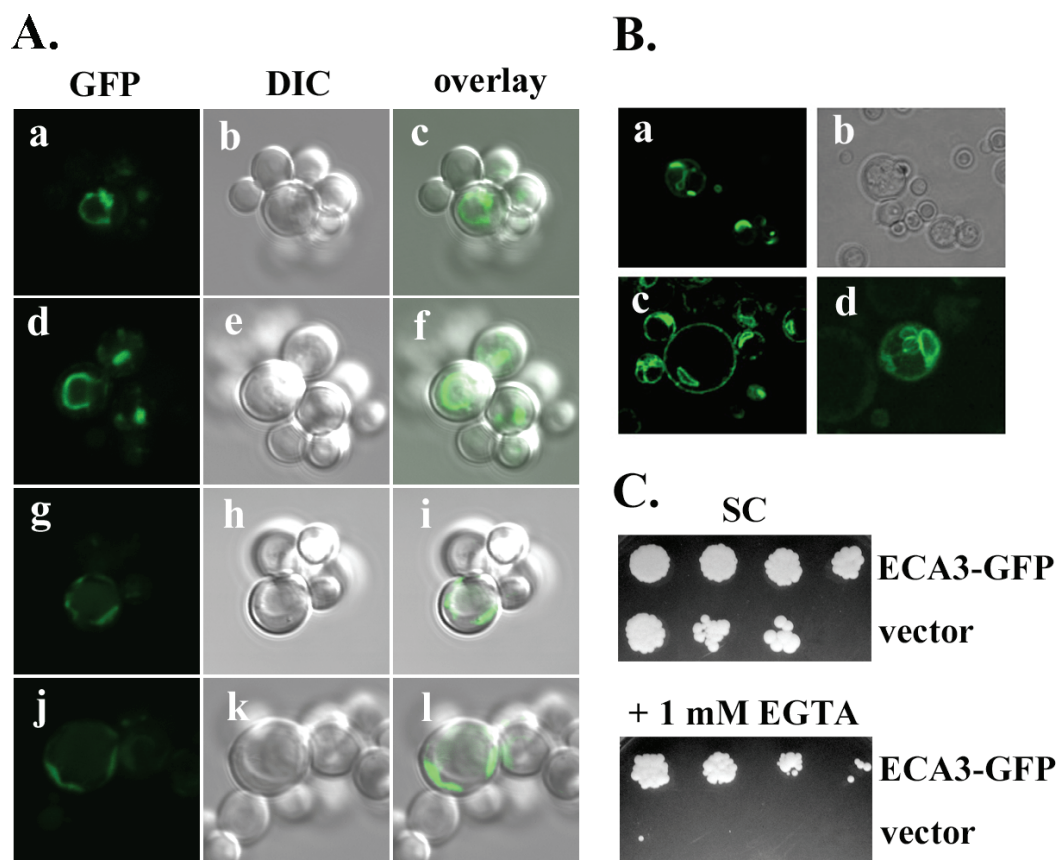


Figure III-5. AtECA3-GFP expressed in yeast exhibits an ER-Golgi pattern.

Yeast was transformed with pDR196 vector harboring AtECA3-GFP under the PMA1 promoter.

A), Subcellular location of AtECA3-GFP. a, d, g, j show green fluorescence of ECA3-GFP. b, e, h, k show the corresponding DIC pictures of the yeast cells; c, f, i, l, overlay of GFP and DIC. Yeast strain was either W303 (*wildtype*, a-f) or triple mutant K616 (g-l).

B), Localization of AtECA4-GFP in yeast strain W303. b, DIC picture of the cells in a.

C), ECA3-GFP expressed in K616 yeast retains activity. Yeast hosting vector alone or ECA3-GFP was cultured on SC-URA (pH 6.25, 10 mM MES-K) supplemented with 1 mM EGTA to deplete Ca^{2+} as described in Fig. III-2. Pictures were taken 6 days after plating.

growth and whether growth might be a TG- or CPA-sensitive. Pollen grains from freshly-opened flowers of *Arabidopsis* Col-0 were germinated on a solid agarose-based medium supplemented with CPA or TG for 6 hours and then tube length was measured. The results showed that pollen tube growth was sensitive to both inhibitors (Fig. III-6). Tube length under 1 nM TG was only ~60% of that with no inhibitor added (Fig. III-6A). CPA at 1 μ M also inhibited tube growth by ~40% (Fig. III-6B). The concentrations that affect tube growth were comparable to CPA levels that blocked AtECA1 and to TG concentrations that blocked SERCA activities (Seidler et al., 1989; Sagara and Inesi, 1991; Liang and Sze, 1998). These results clearly indicated that a CPA and TG-sensitive ECA activity is required for optimal pollen tube growth although the molecular identity is unclear.

3.7. Identification and analyses of T-DNA insertional mutants of AtECA3

To test the biological function of AtECA3 in whole plants, AtECA3 T-DNA insertional lines (*3-1*, *3-4*, and *3-5*) were collected from the Salk institute T-DNA collection or from the Syngenta T-DNA collection. Left border sequencing of the T-DNA insertion was used to verify its location in each allele (Fig. III-7A). The results showed that both *eca3-1* and *eca3-5* hosted a T-DNA insertion in an intron while *eca3-4* had an exonic insertion. Homozygous lines of each allele were screened by genotyping.

I tested for AtECA3 transcripts in the mutants by RT-PCR using T-DNA flanking primers and primers for upstream or downstream region of respective T-DNA insertion site. The cDNA template was made from total RNA extracted from 2 week old seedlings grown on $\frac{1}{2}$ MS medium (Fig. III-7B). A pair of AtECA1-specific primers, which gave rise to a PCR product of similar size, was used as the cDNA quality control. The results

showed that a full-length AtECA3 mRNA is not detected in all 3 alleles. No PCR product was amplified using primers specific to the regions flanking each T-DNA insertion or downstream of each T-DNA insertion (Fig. III-7B). However, the RT-PCR revealed partial transcripts specific to the region upstream of the T-DNA insertion in each 3 alleles, probably because of a polyadenylation sequence within the T-DNA region. Nevertheless, these partial transcripts are unlikely to produce a functional Ca^{2+} pump because several critical transmembrane domains (TM5-8) are missing. These mutant lines were used in experiments as non-functional AtECA3 mutants, though interference of a partial AtECA3 protein is not excluded. The sibling plants without a T-DNA insertion in AtECA3 from the same segregating population were used as wild-type controls. All mutant lines were viable and reproductive under normal conditions and no obvious defect was observed on the vegetative plant stages.

3.8. Pollen tube growth is impaired in *eca3* mutants

I tested pollen tube growth of *eca3* T-DNA alleles (Fig. III-8). Wild-type pollen failed to germinate when Ca^{2+} was absent in the medium (not shown). When Ca^{2+} was added at 1, 10, or 25 mM in an agarose-based medium, the pollen tube growth was optimal at 10 mM Ca^{2+} , suggesting that millimolar levels of Ca^{2+} are required for pollen germination and tube growth. Deficient, or excess, Ca^{2+} impaired tube growth (Fig. III-8B).

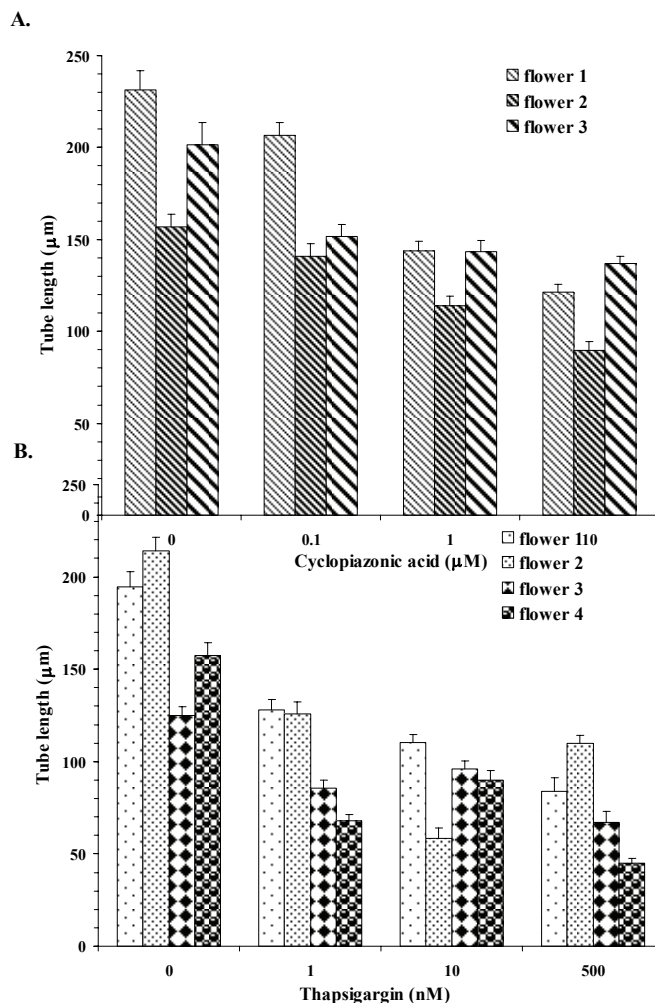


Figure III-6. *In vitro* Arabidopsis pollen tube growth is inhibited by cyclopiazonic acid (A) and by thapsigargin (B).

To control for variations, pollen from a single anther was tested for all treatments. Pollen grains from 3-4 flowers were used as replicates. Pollen was dabbed onto solid media contained either DMSO or inhibitors at the concentration indicated. After 6 h of *in vitro* tube growth at 25-27 °C under saturated humidity, pollen tubes were digitally recorded and tube lengths were measured. Each result was the mean of 50-150 pollen tubes. Error bar = S.E.

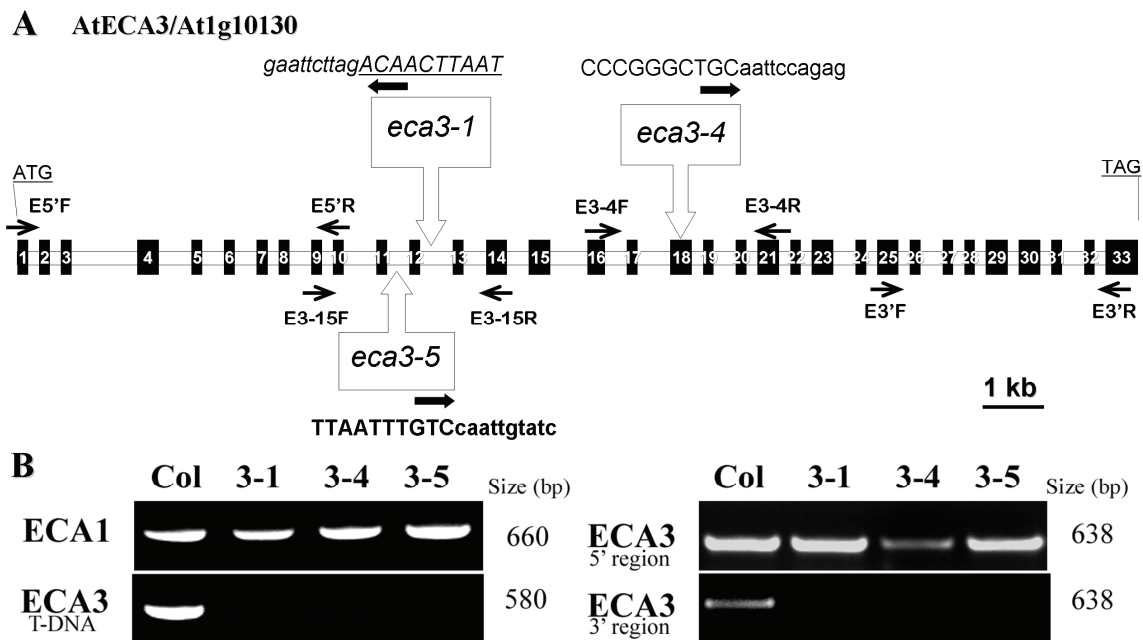


Figure III-7. Three alleles of AtECA3 mutants were identified.

A. Genomic structure of ECA3 showing location of T-DNA insertion sites of *eca3-1*, *eca3-4* and *eca3-5*. The insertions were verified by left border sequencing. Lower case letter indicates the genomic sequence of AtECA3, upper case corresponds to T-DNA sequence. The left borders of T-DNA were indicated in black block arrows. Primers used for RT-PCR are displayed as line arrows and listed in Table III-1.

B. RT-PCR shows absence of ECA3 transcripts in the mutants. Total RNA from 1.5 week-old seedlings of Columbia-0 and mutants were reverse transcribed. Primers were used to amplify either ECA1 (positive control) or ECA3 by 35 cycles of PCR. Col, the mixture of *wt* control lines for *eca3-1* and *3-4*. Three primer pairs were used to amplify the regions upstream (5' region, from E5'F and E5'R primers) or downstream (3' region, from E3'F and E3'R) of T-DNA insertion sites and T-DNA flanking region (T-DNA). The location of primer recognition sites were indicated as arrows in (A).

Figure III-8. Ca^{2+} -dependent pollen tube growth is impaired in *eca3* mutants.

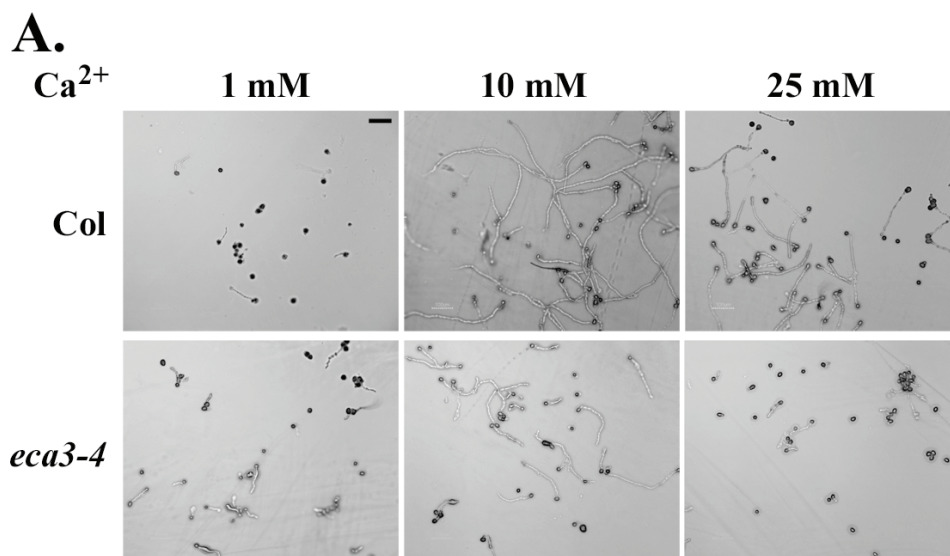
Pollen grains from newly dehisced flowers (stage 13-14) were collected from *wild-type* and *eca3* plants grown side by side. Grains were cultured in pollen germination medium containing CaCl_2 at 1, 10 or 25 mM. Photographs of pollen tubes were taken after 6 h germination. Data shown are representative of 3 experiments. Error bar = S.E.

A. Representative pictures of pollen germinated in vitro on solid medium. Col (wild-type) and *eca3-4* mutant. Scale bar = 100 μm .

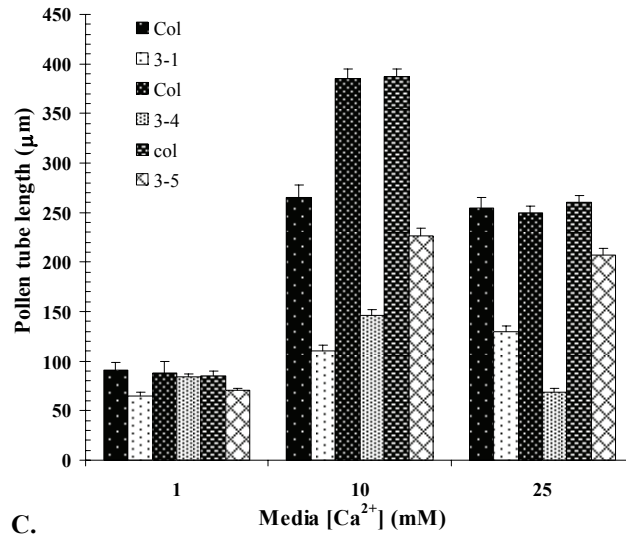
B. Wild-type pollen tubes show optimal growth at 10 mM Ca^{2+} . Each mutant allele was placed with their sibling wild-type pollen on the same plate. Length of mutant tubes was reduced at 10 and 25 mM Ca. 150-450 pollen tubes were measured for each treatment and presented as the mean value.

C. All three mutant alleles of *eca3* show decreased tube length. Pollen grains were germinated in liquid medium containing 10 mM Ca^{2+} . Tube length represents the mean of 50-150 pollen tubes from each treatment.

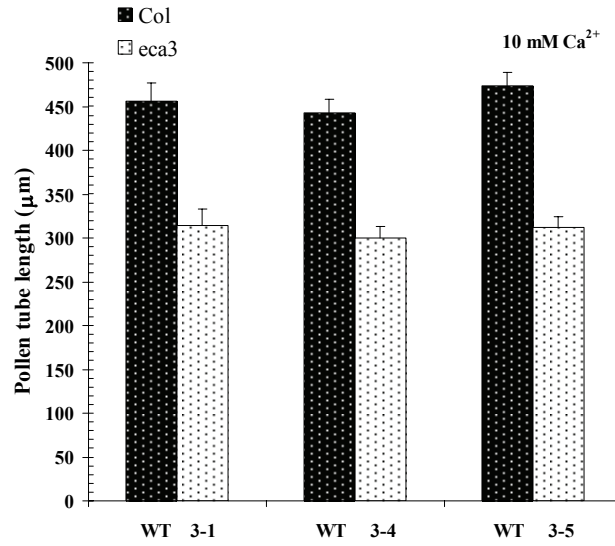
D), Pollen size was not altered in *Ateca3-4* mutants. Long axis of mature pollen grains was measured.



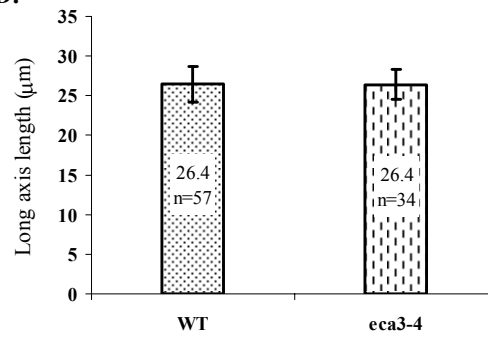
B.



C.



D.



Strikingly, all 3 alleles of *eca3* consistently displayed reduced tube growth under all Ca^{2+} concentrations tested (Fig. III-8B). The decrease by 33% was pronounced at 10 mM Ca^{2+} , at which the *wild-type* pollen grew the longest tubes. Similar results were also observed, but with better consistency, between different alleles when a PEG-based liquid medium was used (Fig. III-8C). The pollen tubes of *eca3*, however, looked similar to that of *wild-type* in morphology such as callose plug, tube width, and tight apex. Pollen germination percentage was also undistinguishable between *eca3* and wild-type germination ranged between 60-90% depending on medium Ca^{2+} (not shown). These results indicated AtECA3 activity is required to sustain fast tube growth.

The size of pollen grains was identical between *eca3* and *wild-type* (Fig. III-8D). Histochemical staining of pollen walls using fluorescent dyes tinopal for intine or DiOC₂ for exine (Regan and Moffatt, 1990), also failed to reveal any obvious differences between *wild-type* and *eca3* in the cell wall composition of mature pollen grains (not shown).

3.9. Pollen tube growth of *eca3-4* is insensitive to cyclopiazonic acid

If thapsigargin (TG) blocks AtECA3 activity exclusively, the pollen tube growth of *eca3* mutants would be insensitive to the inhibitor. So I tested if the pollen tube growth of *eca3* mutants was affected by cyclopiazonic acid (CPA) or TG. Pollen from wild-type or from *eca3-4* was collected in aqueous suspension and an aliquot of each was put into liquid germination media with or without inhibitors. In one preliminary experiment, wild-type pollen tube growth is inhibited only 7 % (P-value = 0.03, t-Test) by CPA level at 0.1 μM (Fig. III-9A). The pollen tube growth *eca3-4* was unaffected (P-value = 0.87, t-Test). The CPA sensitivity of wild-type tube growth is small compared

with results of Fig. III-6. The discrepancy may be due to liquid versus agarose-solidified germination medium.

Thapsigargin (TG) was also less effective in blocking pollen tube growth (inhibited by 8 % (P-value = 0.02, t-Test)) in liquid germination medium (Fig. III-9B). This small reduction would mask any inhibitory effect of TG on *eca3* pollen tube growth. An experiment to test tube growth on agarose medium is in progress.

3.10. AtECA3 T-DNA mutants have reduced seed set and male gamete transmission

Defects in pollen tube growth may cause a failure to reach the ovules and so reduce fertilization. The seed set in *eca3-4* was therefore examined to see if reduced pollen tube growth observed in *eca3* mutants affected fertilization and therefore seed setting. The results showed that the average number of seeds per silique was reduced by 23% in *eca3-4* (37 seeds / silique) than in *wild-type* (45 seeds / silique) (Fig. III-10A). In addition, more frequent unfertilized ovules were observed in *eca3-4* at 13.6% than in *wild-type* at 1.2% (Fig. III-10A). Close check of the siliques revealed that failed seed set occurred more often at the lower part of siliques in *eca3-4* (Fig. III-10B), suggesting that failure to elongate pollen tubes resulted in reduced fertilization.

The transmission of male gametes carrying an AtECA3 T-DNA allele in fertilization was also tested in a segregation assay. Segregating pollen grains of a heterozygous (+/-) T-DNA line were used to pollinate a *wild-type* (+/+) stigma. If pollen function and transmission of the *eca3* mutant and wild type are similar, the expected

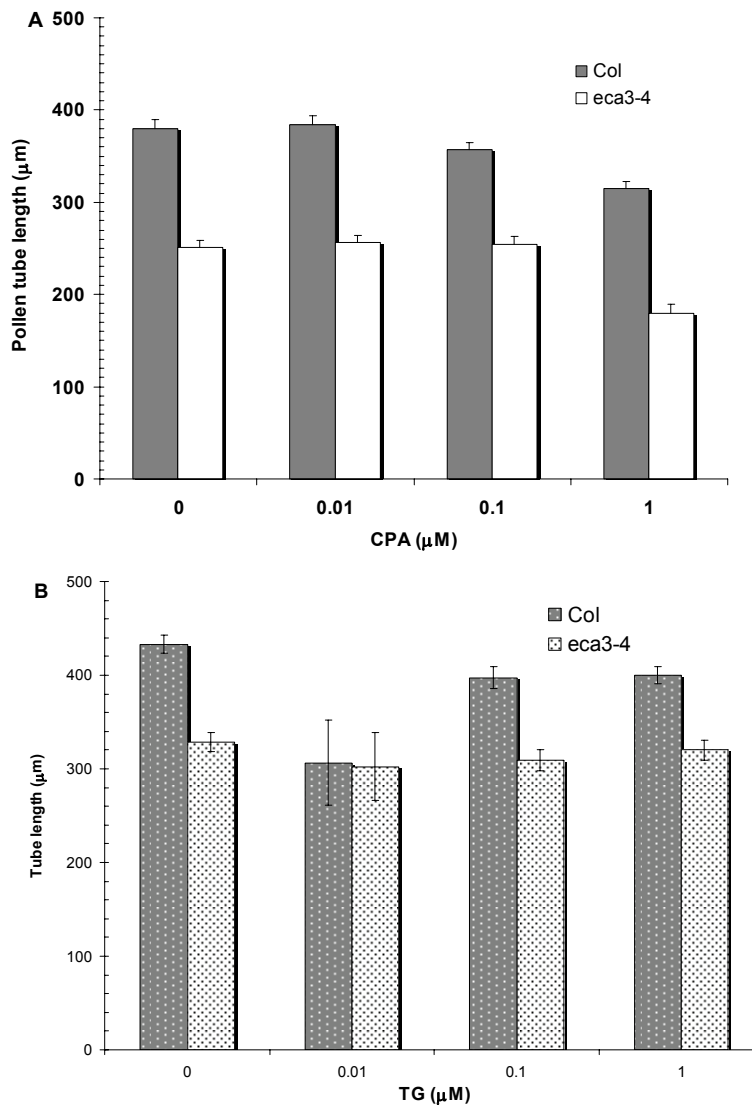


Fig. III-9. *In vitro* pollen tube growth of *eca3-4* is insensitive to inhibition by cyclopiazonic acid (A) and by thapsigargin (B).

Pollen from wild-type (Col-0) or mutant *eca3-4* was tested for all treatments. Pollen grains from 15-20 flowers were collected in suspension solution and aliquots were used under different inhibitor conditions. The germination was in liquid medium with DMSO or inhibitors at the concentration indicated. After 6 h of *in vitro* tube growth at 25-27 °C under saturated humidity, pollen tubes were digitally recorded and tube lengths were measured. Each result was the mean of 100-250 pollen tubes (1 experiment). Error bar = S.E.

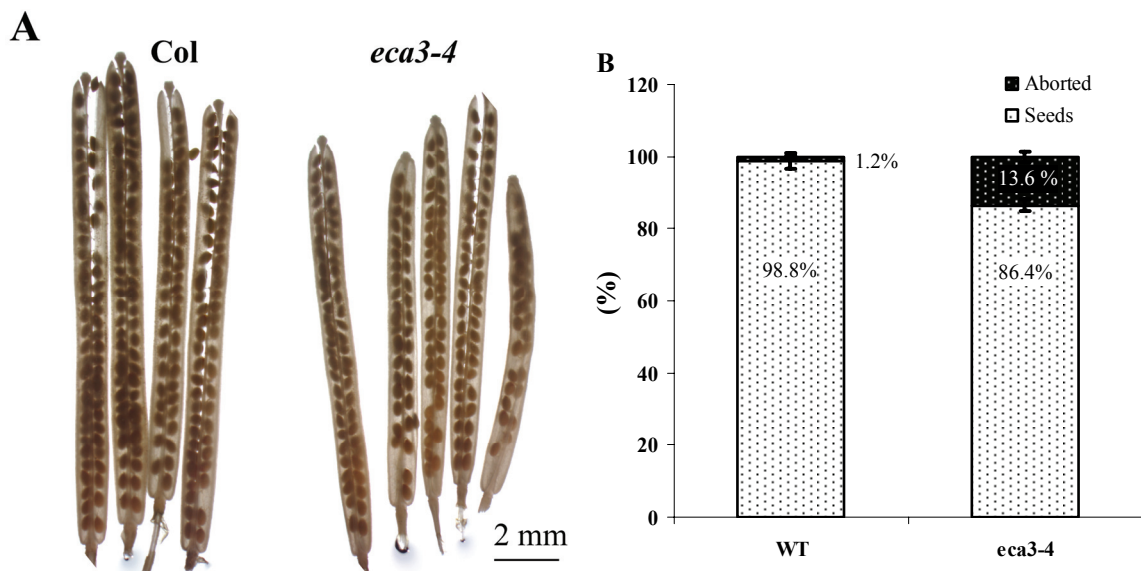


Figure III-10. AtECA3 T-DNA mutants show reduced seed set.

The first ten siliques on the primary floral stem were picked and opened under a dissecting microscope.

A), Seeds in silique from *Ateca3-4* and *wild-type* (Col.). Siliques were treated with 70% ethanol for 2 d to remove pigments. The aborted ovules are invisible because of their tiny sizes under the magnification used. Scale bar = 2 mm.

B) The siliques of *eca3* mutant contained more unfertilized ovules. Fresh green siliques (stage 16-17) were split open and the number of developed seeds per silique was determined. The small white and dried structures were scored as aborted ovules. Error bar = *S.E.*. N= 30. The P values of the paired two sample t-test are 4×10^{-7} and 1×10^{-10} for developed seeds and aborted ovules, respectively. Total seeds and ovules (100%) in wild-type and mutant are 45.9 and 42.7, respectively.

progeny would have a ratio of one heterozygous (+/-) for every one (++) wild type (50:50). Instead, the heterozygous progeny consisted of only 13% (ECA3/*eca3-1*) or 26% (ECA3/*eca3-5*), respectively, reflecting a severe segregation distortion for both T-DNA-inserted alleles of AtECA3. These results further support the evidence that AtECA3 activity is required for normal transmission of male gametes.

3.11. AtECA3-GFP exhibits tip-concentrated punctate locations in pollen tubes

I examined the subcellular location of AtECA3 by confocal microscopy of growing pollen tubes expressing the GFP-tagged AtECA3. Pollen grains of T1 transformants were germinated and observed using a filter set for GFP. The results showed that AtECA3-GFP displayed a punctate pattern dispersed in pollen grains (Fig. III-11B). Strikingly, AtECA3-GFP fluorescence in growing pollen tubes was concentrated in the 10-20 μm of the apical region (Fig. III-11C-E). Closer examination revealed the location of AtECA3-GFP in punctate structures, which were mostly lined beneath the PM (Fig. III-11D-E). Given the extensive exocytosis in this region, it is likely that AtECA3-GFP was located in secretory vesicles which deliver wall materials to the tube surface by fusion with the PM. It is also noteworthy that the AtECA3-GFP was functional as suggested by yeast growth assay (Fig. III-5). These data together suggested that AtECA3 resided on distinct secretory membranes of growing pollen tubes.

4. DISCUSSION

4.1. AtECA3 is a $\text{Ca}^{2+}/\text{Mn}^{2+}$ -ATPase on the endomembrane

Here I provide evidence for a novel plant $\text{Ca}^{2+}/\text{Mn}^{2+}$ pump that belongs to the ECA subfamily. Only one member of this subfamily, AtECA1, had been characterized

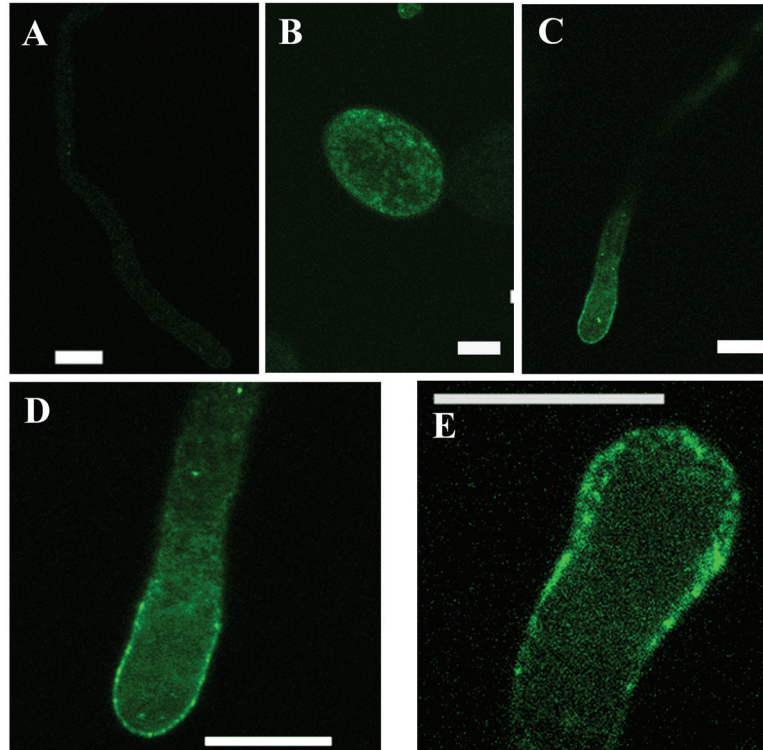


Figure III-11. AtECA3 fused to GFP show punctate fluorescence in pollen grains and tube tip.

Pollen was collected from T2 *Arabidopsis* (Col.) plants that carried an ECA3-GFP construct under a pollen-specific CHX08 promoter. Pollen grains were germinated on Whatman Nuclepore polycarbonate membranes soaked with liquid medium for 4 h and then examined by confocal microscopy. GFP was shown in green. Scale bar = 10 μ m.

A. A pollen tube from the same segregating pollen population as viewed by green fluorescence shows no signal.

B. Mature pollen grain expressing ECA3-GFP show green fluorescence.

C-E. Pollen tubes expressing ECA3-GFP show tip-rich signal in punctate structures.

The image in D represents the medial focal plane of the tip region of the tube in C. The punctate structures of ECA3-GFP location is shown in E, which is also the medial focal plane of a different tube.

previously and demonstrated to be a $\text{Ca}^{2+}/\text{Mn}^{2+}$ pump localized to the ER (Liang et al., 1997; Liang and Sze, 1998). The function of AtECA3 as a $\text{Ca}^{2+}/\text{Mn}^{2+}$ pump was inferred from its expression in K616. K616 yeast strain lacks both the Golgi Pmr1 and the vacuolar Pmc1 Ca^{2+} -ATPases and is sensitive to a medium depleted in Ca^{2+} or a medium supplemented with high Mn^{2+} (Cunningham and Fink, 1994). PMR1 pumps both Ca^{2+} and Mn^{2+} to the ER/Golgi of yeast. Expression of AtECA3 in K616 partially restored the ability to grow on medium containing 5 mM EGTA or 1 mM Mn^{2+} . A functional AtECA3 tagged with GFP was localized to the endomembrane system in yeast, the results (Fig. III-2) are consistent with the idea that AtECA3 loads Ca^{2+} into endomembrane compartments and the accumulated Ca^{2+} activates biochemical processes needed for growth. High levels of Mn^{2+} are toxic to cells lacking PMR1 (Lapinskas et al., 1995). I also showed that AtECA3 conferred tolerance to yeast growing on medium supplemented with high Mn^{2+} , suggesting that it is able to remove Mn^{2+} from the cytosol. Thus, biochemically, AtECA3 appears very similar to AtECA1 in being a Ca^{2+} pump with selectivity for other divalent cations, like Mn^{2+} .

However, several observations suggest AtECA3 differs in function from AtECA1. First, when expressed on the same yeast expression vector, p426, AtECA1 was much more effective than AtECA3 in promoting growth of the K616 mutant on medium depleted of Ca^{2+} (Fig. III-2C). The protein levels of AtECA1 and AtECA3 are likely close to each other in yeast cells since they are under the same promoter and possess similar protein sizes and membrane topology. This difference could be caused by different K_m or V_{max} of the two pumps. AtECA1 was demonstrated to have an unusually high-affinity for Ca^{2+} with a K_m of around 30 nM (Liang and Sze, 1998). As AtECA3

conferred on yeast a tolerance to grow on medium containing 1 mM EGTA, instead of 10 mM EGTA, it is possible that the affinity for Ca^{2+} of AtECA3 differs from that of ECA1. Second, AtECA3 expression in K667 strain caused a hypersensitive response to 150 mM Ca^{2+} , whereas AtECA1 expression in K667 had no detrimental effect compared to K667 harboring the empty vector. Thus, the activities of AtECA1 and AtECA3 appear to be different in yeast, although it is unclear at this time if the expressed protein levels of these two $\text{Ca}^{2+}/\text{Mn}^{2+}$ pumps differ, or if they are localized to functionally distinct endomembrane compartments, or both.

4.2. AtECA3 is a thapsigargin-sensitive Ca^{2+} pump that supports pollen tube growth

Several lines of evidence indicate that AtECA3 is a $\text{Ca}^{2+}/\text{Mn}^{2+}$ -ATPase with a distinct functional niche in plants. First, the genomic DNA sequence and the protein of AtECA3 differ from those of other ECAs. AtECA3 has more than 30 exons, a feature that is conserved in rice OsECA3 and that is similar to mammalian SERCA, (Baxter et al., 2003), suggesting AtECA3 is derived from a different ancestor gene because AtECA1, AtECA2 and AtECA4 genes consist of only 4-7 exons. Furthermore, the protein sequence comparison revealed that AtECA3 shares high identity with SERCAs, including several conserved residues that were shown to directly interact with thapsigargin (TG) (Xu et al., 2004).

So far, the only plant ECA characterized at the molecular level was shown to be insensitive to TG (Liang and Sze, 1998). Here I demonstrated that AtECA3-dependent growth of yeast on Ca^{2+} -depleted medium is sensitive to both TG and CPA. As the ability to grow on medium containing mM EGTA depends on a functionally active

AtECA3, the results suggest that AtECA3 activity is blocked by these inhibitors. The effective concentration required for inhibition of growth is slightly higher compared to studies measuring the activity of isolated membranes, probably because intact yeast cells are composed of different membranes. TG and CPA are soluble in DMSO and thus they will diffuse and partition into all membranes. CPA inhibited AtECA1 activity with a half-inhibition dosage (I50) of 3 nM/mg total protein, but thapsigargin had no effect on AtECA1 up to 3 μ M (Liang and Sze, 1998). Here, TG at 0.5 μ M blocked yeast growth on Ca^{2+} -depleted medium. To our knowledge, this is the first evidence for a thapsigargin-sensitive Ca^{2+} pump from plants. *In vitro* pollen tube growth was also inhibited by thapsigargin and by cyclopiazonic acid. Notably, the effective concentration for inhibition by 0.1-1 μ M CPA is similar to that seen with isolated membranes (Liang and Sze, 1998; Wu et al., 2002). The results would suggest that ECA1, or other related ECAs expressed in pollen, are possible targets of this inhibitor. Intriguingly, the effective concentration of 10 nM TG required for inhibition of pollen tube growth was lower than that needed to impair growth of K616 yeast expressing AtECA3. Assuming AtECA3 is the major target of thapsigargin, this result suggests that AtECA3 may be relatively abundant in membranes of the growing pollen tube.

Reduction of pollen tube growth of a single *eca3* mutant phenocopies the effect of TG on tube growth of wild type pollen. This genetic evidence clearly verifies that thapsigargin inhibition of wild type pollen is caused in large part by specific inhibition of AtECA3. Together, these results point to a critical role of AtECA3 in promoting pollen tube growth. CPA also retarded pollen tube growth though it is unclear whether other ECA activities participate in supporting tube growth. Nevertheless, the finding that a

single homozygous mutant of *eca3* effectively reduced pollen tube growth by 33% is a strong indication that the role of AtECA3 cannot be fully replaced by other ECAs.

4.3. Proposed roles of AtECA3 in pollen tube growth

It is well-known that pollen tube growth is guided by an extracellular Ca^{2+} influx at the tip, and sustained by an oscillating intracellular Ca^{2+} gradients beneath the extreme apex (Miller et al., 1992; Malho and Trewavas, 1996; Holdaway-Clarke et al., 1997); however the molecular bases for these Ca^{2+} dynamics are largely unknown. Asymmetrical Ca^{2+} channel activity on the PM, such as one gated by voltage, is responsible for apical Ca^{2+} influx to direct tube growth (Malho et al., 1995; Malho and Trewavas, 1996). The intracellular Ca^{2+} gradient is thought to establish the growth polarity and is linked to exocytosis, which delivers materials to the cell surface for PM and wall construction (Steer and Steer, 1989; Roy et al., 1999; Hepler et al., 2001). However, the roles of specific active pumps and/or exchangers that lower $[\text{Ca}^{2+}]_{\text{cyt}}$ to basal level are still not well understood. Multiple Ca^{2+} pumps, found in plant vegetative tissues, have been localized to the plasma membrane, and intracellular compartments like the vacuole and ER (Sze et al., 2000). ECA3-GFP is localized to endomembranes in yeast, and appears to be associated with secretory vesicles that fuse with the PM at the tip of growing pollen tubes. The tip of growing pollen tubes is filled with small secretory vesicles in the clear zone (Steer and Steer, 1989; Lancelle et al., 1997).

A Ca^{2+} pump, like AtECA3, located on these membranes could promote and guide tube growth in several ways. First, an active $\text{Ca}^{2+}/\text{Mn}^{2+}$ transporter on the secretory compartments could maintain sufficient levels of Ca^{2+} and Mn^{2+} needed to activate enzymes for wall synthesis and for proper protein folding, modification and

sorting. Pollen tube growth is largely dependent on efficient and directional delivery of materials to tube apex for construction of new membranes and walls (Roy et al., 1999; Holdaway-Clarke and Hepler, 2003). For instance, pectin, the major component of pollen tube wall, is synthesized in the Golgi (Buchanan et al., 2000) and secreted as soluble methyl esters to form a pliable and yielding wall at the tube tip. One approach to test this idea is to analyze the cell wall components of *eca3* mutants. Second, active Ca^{2+} pumping into endomembrane compartments would lower $[\text{Ca}^{2+}]_{\text{cyt}}$ and could contribute to Ca^{2+} gradients (Taylor and Hepler, 1997) and Ca^{2+} oscillations (Holdaway-Clarke et al., 1997; Messerli and Robinson, 1997) observed in the tip of growing pollen tubes. Thirdly, Ca^{2+} accumulated in secretory vesicles is a source of stored Ca^{2+} that could be released via gated cation channels in response to certain cues. If so, then Ca^{2+} oscillations seen at the pollen tip would be perturbed in *eca3* mutants.

Although multiple Ca^{2+} pumps and Ca^{2+} exchangers are expressed in mature pollen grains based on the whole genome transcriptome studies (Hony and Twell, 2004; Pina et al., 2005; Bock et al., 2006), genetic evidence for their function in pollen tube growth is available for only two pumps so far. Mutant pollen of ACA9 showed decreased tube growth, impaired fertilization and reduced seed set (Schiott et al., 2004). This pump is localized to the PM along the entire shank of the tube indicating that its function is to increase apoplastic $[\text{Ca}^{2+}]$ and to lower $[\text{Ca}^{2+}]_{\text{cyt}}$ along the length of the growing tube. In contrast, AtECA3 is predominantly localized in endomembranes at the tip of the tube and the fluorescent signals of the ECA3-GFP fusion protein are found at the tube periphery, which would suggest its association with secretory vesicles fusing with the PM. Thus these two Ca^{2+} pumps share similar functions in lowering $[\text{Ca}^{2+}]_{\text{cyt}}$.

However they are localized differentially, suggesting they participate in orchestrating the spatial and temporal dynamics of Ca^{2+} so critical to pollen tube growth and guidance. Furthermore, association of AtECA3 with secretory vesicles during tip growth suggests it may participate in other events, including membrane fusion and Ca^{2+} -dependent exocytosis (Roy et al., 1999; Hepler et al., 2001).

In summary, this study provides the first evidence for a plant Ca^{2+} pump that is sensitive to thapsigargin, a specific blocker of animal SER-type Ca^{2+} -ATPases. AtECA3 is an endomembrane- $\text{Ca}^{2+}/\text{Mn}^{2+}$ -ATPase involved in Ca^{2+} uptake and Mn^{2+} detoxification. Genetic evidence demonstrates AtECA3 activity at the growing pollen tip promotes tube growth and seed set. Our current model is that AtECA3 activity is needed to generate or maintain tip-focused Ca^{2+} -gradients and/or Ca^{2+} oscillations and nurture exocytosis in growing pollen tubes. These findings reveal a novel member of the ECA gene family with functions distinct from other plant Ca^{2+} -ATPases.

5. MATERIALS AND METHODS

5.1. Plant Growth, and Mutants

a. Plant material.

An *Arabidopsis thaliana* Columbia ecotype (Col-0) was used in this study.

For growth on plates, Arabidopsis seeds were surface sterilized by soaking in 20% (v/v) Clorox, 0.05% Tween 20 for 10 min followed by 5 times of rinsing in sterile DI water. The seeds were planted on 1/2 MS medium ((Murashige and Skoog, 1962) containing 0.1% agar and 15 mM MES-K at pH5.7, followed by stratification in dark at 4

°C for 3 days. The media plates were then positioned vertically in a Conviron growth chamber with a photoperiod 16 hr light/ 8 hr dark at temperature 22 °C in the day under an illumination of $150 \mu\text{E m}^{-2} \text{s}^{-1}$ and 20 °C at night.

For soil-grown plants, Arabidopsis seeds were planted on synthetic soil medium containing Miracle-Gro[®] potting mix and perlite, followed by 3 days of 4 °C stratification in the dark before taken to the growth chamber with a photoperiod of 16 h light at 22 °C under an illumination of $150 \mu\text{E m}^{-2} \text{s}^{-1}$ and 8 h dark at 20 °C and 60% relative humidity. Plants were watered twice a week or as needed. Flowers from unstressed plants that have flowered within 2 weeks were used for *in vitro* pollen germination assays. *Wild-type* and mutant plants were always grown side by side in the same tray for consistency.

b. Identification of homozygous T-DNA mutants.

The genetic background of all 3 lines is Col-0 ecotype. For each *eca3* line, a pair of AtECA3 primers flanking the site of T-DNA insertion was used to PCR-verify the homozygosity of a T-DNA insertion in AtECA3. This part was done in collaboration with Harper's lab at University of Nevada.

5.2. DNA manipulations

a. cDNA cloning & molecular constructs.

cDNA of AtECA3 was amplified by PCR from the total first strand cDNA. The template was reverse transcribed from total RNA from rosette leaves of 2.5-3.5 weeks old *Arabidopsis* (Col.) using the primers ECA3-f and ECA3-r with start and stop codons underlined (Tab. III-2). Proof-reading high fidelity Taq DNA polymerase Deep Vent (NEB, Boston MA) was used to generate the PCR fragments. The PCR product was purified by gel extraction and ligated to an EcoRV-linearized vector pBlueScriptSK

(Stratagene, La Jolla CA) or in the case of AtECA4 to a SmaI linearized vector pGEM7z (Promega, Madison WI). The cloned sequences were verified by full length sequencing and used for all subsequent cDNA subcloning.

b. Promoter::GUS constructs for tissue expression pattern of ECAs.

Genomic DNA was isolated from 4 weeks old seedlings of *Arabidopsis* Col-0 using the CTAB method (Ausubel et al., 1988). The promoter region of AtECA3 (~ 5kb) was determined as the intergenic region between the start codons of AtECA3 (At1g10130) and its adjacent ORF (At1g10120) on BAC clone the T27I1. The primers used with appended restriction enzyme sites were ECA3-pf and ECA3-pr (Tab. III-2), with appended restriction enzyme sites underlined.

The PCR-amplified product of the AtECA3 promoter was double digested with XhoI/NcoI and cloned into a GUS ORF-containing vector pRITA to make a promoter::GUS construct ECA-RITA and verified by sequencing. This NotI-NotI fragment of ECA-RITA was ligated to a binary vector pMLBART via NotI. The resulting pECA-GUS-MLBART constructs were used for promoter::GUS analyses of transgenic plants.

c. Pollen-specific GFP-tagged AtECA3.

The AtECA3 cDNA was amplified by PCR using Platinum Pfx DNA polymerase (Invitrogen, Carlsbad CA) and the primers ECA3-Gf and ECA3-Gr (Tab. III-2). The PCR -amplified product of AtECA3 (stop codon removed) was cloned into a Gateway vector pDONR221 (Invitrogen, Carlsbad CA) to give rise to an entry clone ECA3-DONR221. The sequence of the AtECA3 insert was verified by sequencing.

Table III-2. Primer sequences used in this study.

A. Cloning and subcloning AtECA3. ECA3-f and ECA3-r were used to blunt-end clone AtECA3 by RT-PCR into pBSK vector. Start and stop codons on primers were underlined. ECA3-Gf and ECA3-Gr were used to subclone AtECA3 into pDONR221 vector to generate Gateway compatible constructs. Appended Gateway AttB1 and AttB2 recombination sites are underlined.

B. Generation of AtECA3 promoter::GUS construct. ECA3-pf and ECA-pr primers were used to amplify the 5 kb promoter region of AtECA3 from genomic DNA. Appended Restriction enzymes XhoI and NcoI sites are underlined.

C. Verification of T-DNA alleles of AtECA3. E3-15F and E3-15R were used for alleles 3-1 and 3-5. E3-4F and E3-4R were used for 3-4. These primers were designed to flank the T-DNA insertion site on the cDNA. Primers were also designed to amplify the regions upstream or downstream of T-DNA insertions, including E3-5'F and E3-5'R (5' region) and E3-3'F and E3-3'R (3' region). E1-F and E1-R were used to amplify AtECA1 cDNA which serves as a positive control.

D. Test tissue expression of AtECAs. Two pairs of primers were used to amplify to 5' region (AtECA3^a) and 3' region (AtECA3^b) of its cDNA. Primers used are shown in Table I.

E. Generation of GFP-tagged AtECA4 for yeast expression. E4-XbaI and E4-XmaI were used to amplify AtECA4 cDNA and ligated through designated REN sites to a PCR product of eGFP using GFP-XmaI and GFP-XhoI primers. Appended enzyme sites in the primers are underlined.

F. Generation of yeast expression vectors for constitutive expression in yeast.

Gateway recombination cassettes AttB1-ccdB-CmR-AttB2 were amplified from Gateway destination vectors pYES-DR196, p2GWF7, p2FGW7 using primer pairs listed in the table. These fragments were ligated into yeast expression vector pDR196 via designated REN sites to give rise to pYESDR196, pGWFDR196 and pFGWDR196 vectors. Appended REN sites used are underlined on each primer.

Purpose	Primer Name	Primer Sequence
A. Clone cDNA and subclone of AtECA3		
cDNA clone	ECA3-f	<u>ATGGAAGACGCCTACGCCAGATCTGT</u>
	ECA3-r	<u>CTACTTGTCACGCCGGTCCTTGGG GAGTAA</u>
Subclone into Gateway vectors	ECA3-Gf	<u>GGGGACAAGTTTGTACAAAAAAGCAGGCTCGATGGAAGA</u> <u>CGCCTACGCC</u>
	ECA3-Gr	<u>GGGGACCACTTTGTACAAGAAAGCTGGGTACTTGTCACGC</u> <u>CGGTCC</u>
B. Amplify Promoter for GUS construct		
ECA3 promoter::Gus	ECA3-pf	<u>CCGCTCGAGTCCCTCTGCTTCAACAACAACC</u>
	ECA3-pr	<u>CATGCCATGGGTTGGAAAAGCCAAGGGTTT</u>
C. Verify transcript level of <i>eca3</i> mutants by RT-PCR		
AtECA1	E1-F	GTAAATCTCGTAACAGACGGTCCT
	E1-R	TCGTACACCTTCTACAAACTTGA
<i>eca3-1</i> & <i>eca3-5</i>	E3-15F	AACAACAAATGCTGTCTACCAAGA
	E3-15R	GTGCATAAGTTGTCCCACTAACAG
<i>eca3-4</i>	E3-4F	TAGCAAAGAGTGCTTCAGATATGG
	E3-4R	GATTGATTTTCGCTGAGGTTATTT
5' region	E3-5'F	ATGGAAGACGCCTACGCCAG
	E3-5'R	GCGACCACATCAGTTCCCGA
3' region	E3-3'F	AATCCCTGATACCTTGGCACCT
	E3-3'R	CTGAACCTGAATCTCATGCCTGTAT
D. Test expression in tissues using RT-PCR		
AtECA1	AtECA1-F	AAAACCGTAAGCTTTGGCGAGTTTCC
	AtECA1-R	CCTGCAAACACCATGCATTTCTTTCC
AtECA2	AtECA2-F	AGCTGAGCCAAGGCATAAGCAAGAAAT
	AtECA2-R	CGATAGCCACAAGAACGGTGAGTGATAAT
AtECA3 ^a 5' region	AtECA3a-F	AACCCTTGGCTTTTCCAACATGGAAGAC
	AtECA3a-R	TACCCATTGCGGTGTTTGAACCAACT
AtECA3 ^b 3' region	AtECA3b-F	CTGATACCTTGGCACCTGTTCAACTTCTG
	AtECA3b-R	TGACGAAAAAGCCATCTCTTGCTTTC
AtECA4	AtECA4-F	AAAGGAGGTGAAGATTGCGGGAATAAG
	AtECA4-R	AACCCTTCCAATCTCAGTATTCATCCCAG
E. GFP-tagged AtECA4 construct for yeast expression		
AtECA4	E4-XbaI	<u>GCTCTAGAATGGGGAAAGGAGGTGAAGATTGCG</u>
	E4-XmaI	<u>TCCCCCGGGCTCCTCCTTTTGCTTAGCTGAGGGA</u>
eGFP	GFP-XmaI	<u>TCCCCCGGGGATATAACAATGAGTAAAGGA</u>
	GFP-XhoI	<u>CCGCTCGAGCCCAGTCTAGTAACATAGATGA</u>
F. Generate yeast expression vectors hosting PMA1 promoter		
pYESDR196	YES196-F	<u>GGACTAGTAATACGACTCACTATAGGGAATATTAAGCTAT</u> <u>CA</u>
	YES196-R	<u>CCGCTCGAGCTTGCAAATTAAGCCTTCGAGCGTC</u>
pGWFD196	GWF196-F	<u>CCGCTCGAGGGTACTTGTACAGCTCGTCCATGCCGAGA</u>
	GWF196-R	<u>GGCCGCACTAGTGATATCACAAGTTTGTAC</u>
pFGWDR196	FGW196-F	<u>CCGCTCGAGGGATATCACCCTTTGTACAAGAAAG</u>
	FGW196-R	<u>CGCACTAGTATGGTGAGCAAGG</u>

The ECA3-DONR221 was recombined with two Gateway destination vectors pKPFWG2 and pKPWGF2 (Wang and Sze, unpublished), both hosting a pollen-specific AtCHX8 promoter-driven expression cassette (Sze et al., 2004). The resultant binary vectors, ECA3-PFGW (GFP-AtECA3) and ECA3-PGWF (AtECA3-GFP), were used to transform *Arabidopsis* (Col.) plants for visualization of AtECA3 in pollen tubes.

5.3. Bioinformatic analyses

Multiple protein sequence alignments were performed using T-COFFEE program (Poirot et al., 2003). A tree file was generated in Treeview (Page, 1996). Values shown indicate the number of times (in percent) that each branch topology was found in 1000 reps of the performed bootstrap analysis, which utilized the tree-bisection-reconnection branch-swapping algorithm. The analysis was performed upon the optimal tree found by PAUP* 4.0b10 (Swofford, 2003). The optimality criterion was set to distance (minimum evolution).

5.4. Agrobacterium-mediated plant transformation & Histochemical GUS staining

The binary vectors were transformed into the *Agrobacterium* strain GV3101 via electroporation and transformants were selected on LB plates with gentamicin and spectinomycin. A floral dip method was used to transform *Arabidopsis* Col-0 (Clough and Bent, 1998). Plant transformants were selected on Basta-containing plates and at least 5 T3 lines of each were checked for consistent GUS-staining patterns.

GUS staining was performed according to the protocol described previously (Lagarde et al., 1996). Samples were harvested in 90% acetone at various stages, rinsed once with staining buffer lacking the substrate containing 50 mM sodium phosphate, pH

7.2, 0.5 mM $K_4Fe[CN]_6$, 0.5 mM $K_3Fe[CN]_6$), and then incubated for 16 h at 37°C in staining buffer containing 1 mM X-gluc or 5-bromo-4-chloro-3-indolyl β -D-glucuronide. The staining reaction was stopped in 70% ethanol and chlorophyll was cleared in 95% ethanol. GUS staining patterns were photographed using a Nikon DXM1200 digital camera attached to a Nikon Eclipse E600 microscope (Nikon Instruments, Melville, NY) equipped with a differential interference contrast lens.

5.5. Expression analysis using RT-PCR

RT-PCR was used to detect mRNA levels of ECAs in all 3 mutant lines. The total RNA was isolated from 1.5 week old seedlings grown on 1/2 MS medium and reverse-transcribed into oligo dT-primed first strand cDNA. PCR was performed according to the Platinum Taq DNA polymerase user's manual (Invitrogen, Carlsbad CA) using the first strand cDNA as template. Primers used are listed in Table III-2.

To examine the specific expression of each AtECA gene, PCR primers were designed for ECA1-4 to pick up the relatively similar region located on each ECA cDNA. PCR reactions were performed using identical conditions for all primer pairs. The first strand cDNA templates were prepared from total RNA isolated from root, leaf, and pollen of *Arabidopsis* Col-0 ecotype (Sze et al., 2004). The primers used are listed in Table III-2.

5.6. Yeast strains, plasmids and transformation

Strains: The yeast Ca^{2+} -transporter strains used are W303-1A (*MATa, ade2-1 can1-100 his3-11,15 leu2-3,112 trp1-1 ura3-1*) and K616 (*Pmr1::HIS3 pmc1::TRP1*

cnb1::LEU2) (Cunningham and Fink, 1994, 1996). Yeast transformation was performed according to the manual for a yeast vector pYES-DEST52 (Invitrogen, Carlsbad, CA).

AtECA3 cDNA was subcloned into the yeast expression vector p426-Gal1 (Mumberg et al., 1994) by ternary ligation of 3 fragments: a 1.2 kb fragment of KpnI/HindIII-digested ECA3-BSK clone, a 1.6 kb fragment of SpeI/KpnI-digested ECA3-BSK, and a 6.3 kb fragment of SpeI/HindIII-digested p426-Gal1. The resultant clone p426-ECA3- was verified by enzyme digestion and hosts a GAL1 promoter::AtECA3 expression cassette. For Gateway cloning, the AtECA3 cDNA was amplified by PCR using Platinum Pfx DNA polymerase (Invitrogen, Carlsbad CA) and the primers are shown in Table III-2. The PCR fragment of AtECA3 (stop codon removed) was cloned into a Gateway vector pDONR221 (Invitrogen, Carlsbad CA) to give rise to an entry clone ECA3-DONR221. The AtECA3 insert was verified by sequencing. ECA3-DONR221 was recombined with 3 destination vectors pYES-DEST52 (Invitrogen, Carlsbad CA), pYESDR196 and pGWFDR196 (App. 3) to generate strong expression of AtECA3 constructs, GAL1::ECA3, PMA1::ECA3, and a GFP-tagged construct PMA1::ECA3-GFP, respectively.

To make an ECA4-GFP construct, ECA4-GEM was amplified using XbaI- and XmaI-appended primers E4-XbaI and E4-XmaI (Tab. III-2). A GFP PCR-amplified product was obtained using XmaI- and XhoI-appended primers GFP-XmaI and GFP-XhoI from pAVA393 (von Arnim et al., 1998) (Tab. III-2). The XbaI- and XmaI-digested AtECA4 fragment was then ligated with XmaI and XhoI-digested GFP fragments and a SpeI/XmaI-digested p426-Gal1 (Mumberg et al., 1994) in a tertiary ligation reaction, from which GAL1::ECA4-GFP was generated.

Another set of yeast expression Gateway destination vectors were also generated. In brief, the recombination cassettes of Gateway destination vectors pYES-DEST52 (Invitrogen, Carlsbad CA), p2GWF7, and p2FGW7 (Karimi et al., 2002) were amplified by PCR using the primers attached with enzyme sites (Tab. III-2). The PCR product of pYES-DEST, using primers YES196-F and YES196-R (Tab. III-2), was digested and ligated to the yeast expression vector pDR196 (Rentsch et al., 1995) via SpeI/BamHI sites to generate the vector pYESDR196. For PCR products of p2GWF7 and p2FGW7, SpeI/XhoI sites were used instead to generate vectors pGWFDR196 and pFGWDR196 (Appendix A5). This cloning was conducted in the *E. coli* strain DB3.1 (Invitrogen, Carlsbad CA).

5.7. Yeast growth assays

At least 3 independent transformants from each construct were inoculated in synthetic complete medium with glucose but omitting uracil (SC-URA/glu). The $A_{600\text{nm}}$ values of overnight cultures were adjusted to 0.5, washed twice and suspended in sterile water. A 6-step serial dilution of 5-fold was prepared in sterile water for each culture. Five microliters of each was spotted onto uracil dropout medium plates supplemented with different ions or EGTA. The yeast growth was photographed at various times after incubation at 30°C. The medium plates were supplemented with 10 mM MES-K (pH 5.5 or pH 6.4) to maintain the pH of the medium.

For growth assays using liquid culture, fresh single colonies were inoculated and grown in liquid medium overnight to an early stationary stage. The cells were then washed and suspended in SC-URA medium with 2 mM EGTA to obtain seed cultures with an $A_{600\text{nm}}$ of 0.1. The seed cultures were then inoculated for another 8 h before

addition of inhibitors, TG or CPA. The growth of yeast was monitored by absorption at 600nm for next 2 days.

5.8. Confocal microscopy

For confocal examination of yeast expressing GFP, liquid cultures at stationary phase were diluted to various folds into fresh medium and grown overnight. The culture with A_{600nm} between 0.2-0.4 was observed on a Zeiss LSM510 confocal microscope using Apochromat 63X water lens (Carl Zeiss, Germany). A filter set with 488 nm EX/BP510-550nm EM was used.

For the visualization of pollen-expressing AtECA3-GFP, pollen grains from transgenic *Arabidopsis* plants were germinated for 4 h on Nuclepore Track-Etch membranes (Whatman, Clifton NJ) placed on filter papers soaked with pollen germination medium (described below). The Nuclepore membranes were then mounted and observed under a Zeiss LSM510 confocal microscope using an Apochromat 63X water lens (Carl Zeiss, Germany). A filter set with 488 nm EX/BP510-550nm EM was used.

5.9. Analyses of plants

a. *In vitro* pollen germination. Newly dehisced flowers were excised and dried at ambient temperature for 1 h. The pollen grains were then directly applied onto the agarose-based medium surface by dabbing the anther with a tweezer. *Wild-type* and mutant were always dabbed on the same plate. The medium was adapted with modifications (Fan et al., 2001), containing 1 mM KCl, 0.8 mM MgSO₄, 1.5 mM H₃BO₃, 10 mM CaCl₂ (unless otherwise specified), 16.6% (w/v) sucrose, 1% (w/v) agarose, and 5

mM MES-Tris at pH 5.8). The germination was performed in an incubator with saturated humidity at 25-28 °C for 6 hours before being photographed under a Nikon Eclipse E600 light microscope using a 10x objective lens.

In some cases the pollen were germinated in liquid medium, which contains 1 mM KCl, 0.8 mM MgSO₄, 1.5 mM H₃BO₃, 10 mM CaCl₂, 5% (w/v) sucrose, 15% (w/v) PEG4000 (#95904, Fluka), 1% (w/v) agarose, and 5 mM MES-Tris at pH 5.8. Flowers collected and dried for 1 h at ambient temperature were put in germination medium omitting Ca²⁺ and on a vortex stiller at maximum speed for 2 min. The pollen were then pelleted by centrifugation at 500xg for 5 min and re-suspended in germination medium. Pollen suspension Aliquoting between treatments was also used as needed. The germination was performed under the same conditions as on solid medium except that saturated humidity was not used.

Tube measurement and data processing. Tube length of all germinated pollen was measured directly on photographs using ScionImage software (Scion Co., Fredrick MD). The data was evaluated using the statistical analysis software, R-package (www.r-project.org/). All datasets have passed a t-test for normal distribution, and the P values were less than 0.05 for the Student's two-sample t-Test.

b. Seed set analysis. The first 10 green siliques along the main floral stem were picked from each individual plant at flower stages 16-17 (Bowman, 1994). The siliques were then carefully opened under a dissecting microscope and seeds inside counted. Unfertilized ovules were scored based on pigmentation and size (Berg et al., 2005).

Siliques picked the same way were also bleached by 70% ethanol for 2 days and photographed under a Nikon MSZ1000 dissecting microscope with an attached Nikon DXM1200 digital camera (Nikon Instruments, Melville, NY).

IV. A GOLGI $\text{Ca}^{2+}/\text{Mn}^{2+}$ PUMP AFFECTS ROOT GROWTH THROUGH SECRETION

1. ABSTRACT

Ca^{2+} is required for protein processing and sorting in eukaryotic cells, although the identity of plant Ca^{2+} pumps and channels mediating the accumulation and release of Ca^{2+} in compartments of the secretory system are still obscure. I recently demonstrated the first thapsigargin-sensitive Ca^{2+} pump, AtECA3, in plants (Chap. III). One function of AtECA3 is to support pollen tube growth and enhance male fertility (see Chap. III), although the subcellular location and the bases of the growth defect were unclear. Here I show that Ca^{2+} -stimulated root growth is severely reduced in three independent alleles of *eca3* mutants. These results are consistent with the idea that Ca^{2+} pumping into an endomembrane compartment supports root growth. Mutant roots are also sensitive to 50 μM Mn^{2+} , a micronutrient required for growth at 3 μM , suggesting that AtECA3 catalyzes sequestration of excess divalent cations like Mn^{2+} into a compartment and aids in the detoxification of excess Mn^{2+} in plants as shown before in yeast (Chap. III). A functionally active AtECA3-tagged with GFP was colocalized with a cis- and a trans-Golgi marker after transient expression in mesophyll protoplasts. Promoter driven-GUS analyses showed AtECA3 was expressed in vascular tissues and in pollen grains, tissues that secrete large amounts of wall polysaccharides and proteins. Strangely, 60% more apoplastic peroxidase was secreted by roots of the *Ateca3* mutant relative to that of wild-type, suggesting that sorting, exocytosis, or both, were perturbed when the Golgi AtECA3 is incapacitated. Together these results demonstrate that a Golgi-localized Ca^{2+}

pump plays an essential role in supporting primary root growth, and that supplying sufficient levels of Ca^{2+} and Mn^{2+} into Golgi and secretory vesicles is critical for regulating plant secretory systems.

2. INTRODUCTION

Exocytosis, or secretion, is crucial for the growth and differentiation of plant cells for several reasons. First, non-cellulosic cell-wall precursors, are synthesized in the Golgi, and delivered in secretory vesicles to the outside of the cell (Buchanan et al., 2000). Second, new membranes are delivered to the PM to increase the surface area of biomembranes during cell growth. Biolipids are also brought to the cell surface via exocytosis. Third, cells respond and adapt to extracellular stimuli and environmental stresses by modifying the composition and structure of their walls and membranes. These processes are accomplished by precise control of many proteins and enzymes, though the molecular basis is still poorly understood (Battey and Blackbourn, 1993).

Ca^{2+} is well-recognized as being an important ion for secretion in two scenarios (Steer, 1988; Brandizzi and Hawes, 2004). First, membrane compartments forming the secretory pathway, such as the endoplasmic reticulum (ER) and Golgi apparatus, are filled with Ca^{2+} , usually at the mM levels, in contrast to submicromolar levels found in the cytosol (Dauwalder et al., 1985; Sakai-Wada and Yagi, 1993; Storey and Leigh, 2004). The mM Ca^{2+} concentrations maintained in secretory environment are required for functions of Ca^{2+} -dependent chaperones, such as calnexin (Wada et al., 1991; Huang et al., 1993a; Bergeron et al., 1994; Kwiatkowski et al., 1995) and calreticulin (Corbett et al., 2000; Johnson et al., 2001), both of which are fundamental to protein maturation and secretion. Second, an elevation of cytosolic free Ca^{2+} ($[\text{Ca}^{2+}]_{\text{cyt}}$) stimulates exocytosis

(Steer, 1988; Homann and Tester, 1997). In plants, polarized tip growth, for instance in the pollen tube or in the root hair, is thought to be the result of polarized secretion. Such tip growth is often accompanied by an high gradient in $[Ca^{2+}]_{cyt}$ at The tip as well as Ca^{2+} oscillations (Hepler et al., 2001). However, little is known about the biochemical relationship of these Ca^{2+} dynamics to plant growth.

Multiple Ca^{2+} channels, Ca^{2+} pumps and exchangers, identified from the *Arabidopsis* and rice genomes, are proposed to work together to regulate diverse Ca^{2+} transients and oscillations required for growth and development. Although 14 Ca^{2+} pumps have been reported, only a few have been functionally characterized at the molecular level. *Arabidopsis* Ca^{2+} pumps are localized to the PM (ACA8, ACA9), vacuole (ACA4), and ER (ECA1 and ACA2) of vegetative plant cells (Sze et al., 2000; Schiott et al., 2004)). Intriguingly, there is no secretory pathway-like Ca^{2+} pump (SPCA) gene in plants based on phylogenetic analyses of Ca^{2+} pumps from cyanobacteria, fungi, and animals (Chap II & III) (Baxter et al., 2003). SPCA Ca^{2+} pumps like the yeast PMR1 or human SPCA1 are localized to the Golgi and participate in protein modification, sorting and secretion (Durr et al., 1998; Wuytack et al., 2003). Could one or more of the Ca^{2+} pump(s) of the ECA and ACA families in *Arabidopsis* and rice, fill the role of an SPCA in plants? We have recently uncovered a novel Ca^{2+} -ATPase, AtECA3 (At1g10130), whose function resembles an SPCA in plants. AtECA3 is the first thapsigargin-sensitive Ca^{2+} -ATPase identified in plants. Mutants of *AtECA3* showed reduced pollen tube growth. The GFP-tagged protein was localized to endomembranes in yeast, and appeared to associate with secretory vesicles at the tip of growing pollen tubes. However, its subcellular functions and membrane location in plants are not clear.

In this study, I demonstrate molecular evidence for a Golgi-localized Ca^{2+} pump in higher plants. Mutants lacking this pump do not show Ca^{2+} -stimulated primary root growth seen in wild-type plants. The mutants were also sensitive to high levels of a micronutrient, Mn^{2+} , suggesting that in wild-type plants, AtECA3 is capable of detoxification. Furthermore, mutants showed enhanced secretion of apoplastic peroxidases, indicating that an adequate supply of Ca^{2+} and Mn^{2+} in the Golgi lumen is critical for regulated protein secretion. These results together show that a Golgi-bound $\text{Ca}^{2+}/\text{Mn}^{2+}$ pump supports root growth in part by affecting Golgi functions, including the secretory system of plant cells.

3. RESULTS

3.1. AtECA3 affects root growth

a. Ca^{2+} -stimulated root growth is reduced in *eca3* mutants.

Previously, I showed that *in vitro* pollen tube growth was retarded in T-DNA insertional lines of *eca3*, so I tested if root growth was also affected. Three alleles of *Arabidopsis eca3* mutant lines each contain a T-DNA insertion in the *AtECA3* gene (Chap. III). I first confirmed that optimal root growth in wild-type seedlings depends on ~ 3 mM external Ca^{2+} in a nutrient medium of $\frac{1}{2}$ strength MS (Murashige and Skoog, 1962). Reduced root growth at a Ca^{2+} concentration of 0.1 mM or less suggested that this nutrient was deficient. Similarly, root growth at a concentration of 20 mM Ca^{2+} was decreased suggesting that excess nutrients were stressful to the seedling (Fig. IV-1). Intriguingly, the Ca^{2+} stimulated root growth was not observed in *eca3* mutants (Fig. IV-1), suggesting that mutants were nearly insensitive to the beneficial effects of Ca^{2+} . At 3

mM Ca^{2+} , *eca3* mutant root length was inhibited by 28%. As 3 mM Ca^{2+} is optimal for plant growth and Ca^{2+} entry pathways are assumed to be fully functional in the *eca3* mutants, the results strongly indicate that reduced growth is due to defective sorting of Ca^{2+} within the cell into intracellular compartments.

b. Root growth of *eca3* mutants is sensitive to high Mn^{2+} .

Functional expression in the yeast mutant K616 indicated that AtECA3 also transports Mn^{2+} (Chap. III), so I examined the effect of Mn^{2+} on root growth. Plants were grown in liquid medium containing 3 μM up to 1 mM Mn^{2+} . Root lengths were indistinguishable between wild-type and mutant in medium containing Mn^{2+} at 3.5 μM (Fig. IV-2A). But root growth of *eca3* was reduced compared with that of wild-type when Mn^{2+} was elevated to 50 μM and 100 μM , as manifested as reduced initiation of lateral roots after 3 day growth (Fig. IV-2A). The compromised root growth also caused changes in shoot growth, such as reduced leaf expansion and rosette size (not shown). Therefore, AtECA3 appears to confer tolerance to high Mn^{2+} in plants.

High Mn^{2+} concentrations inhibited the primary root growth of the wild-type cultured on agar-solidified medium of 0.5x MS (Fig. IV-2B), which is probably the result of Mn^{2+} toxicity. Primary root growth of the wild-type was completely inhibited by 0.1 mM Mn^{2+} (Fig. IV-2B). It is noted that a concentration of 50 μM Mn^{2+} in MS medium is unusually high compared to, a recommended Mn^{2+} of less than 10 μM in Hoagland's nutrient medium (Hoagland and Arnon, 1950). Therefore, 50 μM probably imposes a Mn^{2+} stress on *wild-type* plants as well as to mutant *Arabidopsis* seedlings. In contrast, increasing Cu^{2+} inhibited root growth both of *wild-type* and *eca3-4* similarly (Fig. IV-

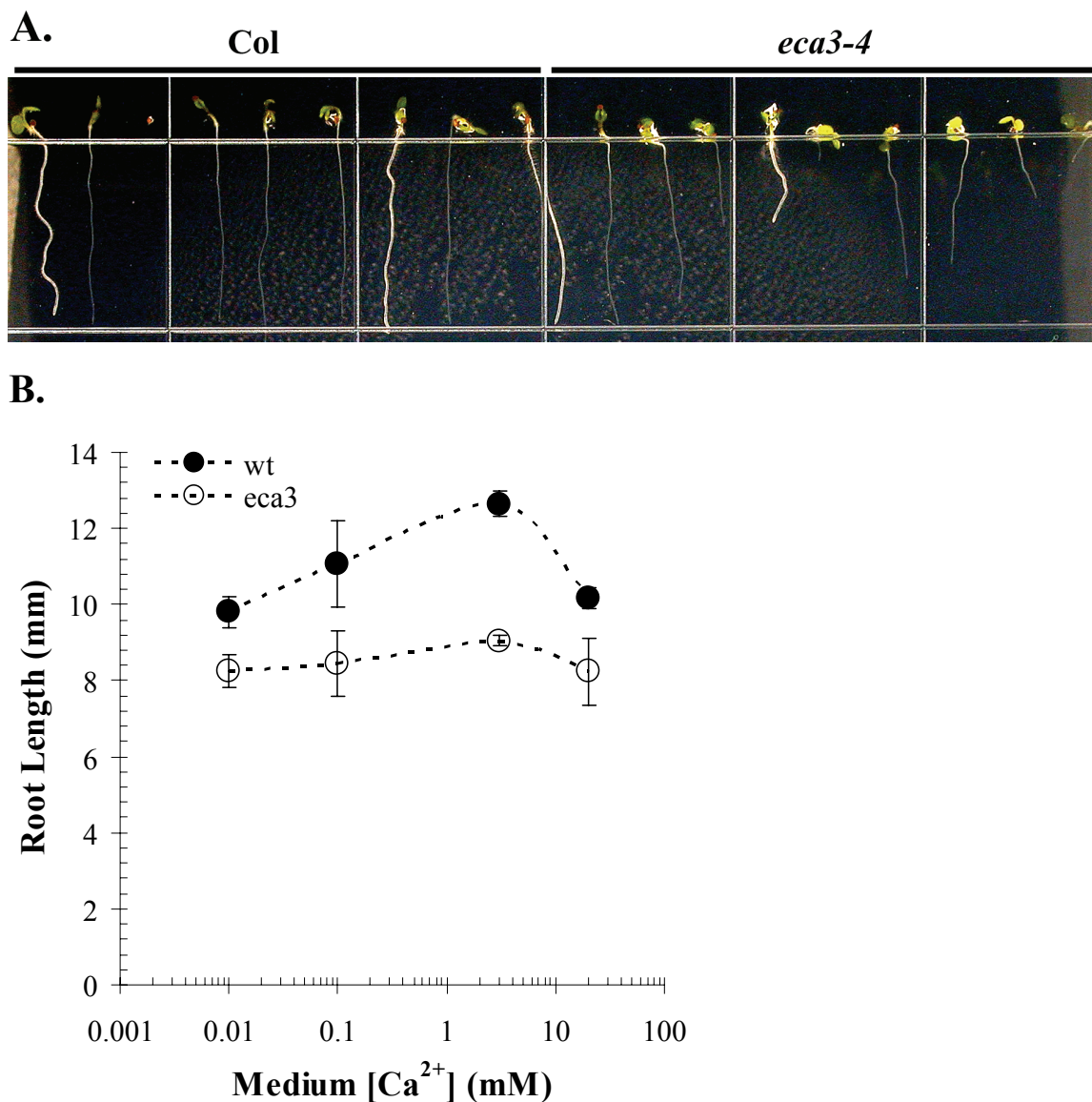


Figure IV-1. Ca^{2+} -stimulated root growth is inhibited in *Ateca3* mutants.

A. A representative picture of root growth of *ateca3-4* and its wild-type (Col-0) control. Wild-type and mutant seeds were germinated side by side on plates containing $\frac{1}{2}$ MS medium and 3 mM Ca^{2+} . Pictures were taken 3 days later.

B. Decreased growth of mutant roots at different Ca^{2+} concentrations. Seeds were germinated on plates containing $\frac{1}{2}$ MS with either no added Ca^{2+} (~ 0.01 mM) or supplemented with Ca^{2+} to give final concentrations of 0.1, 3, and 20 mM. Each experiment consisted of 20 seedlings per treatment. Data represent at least 3 independent experiments.

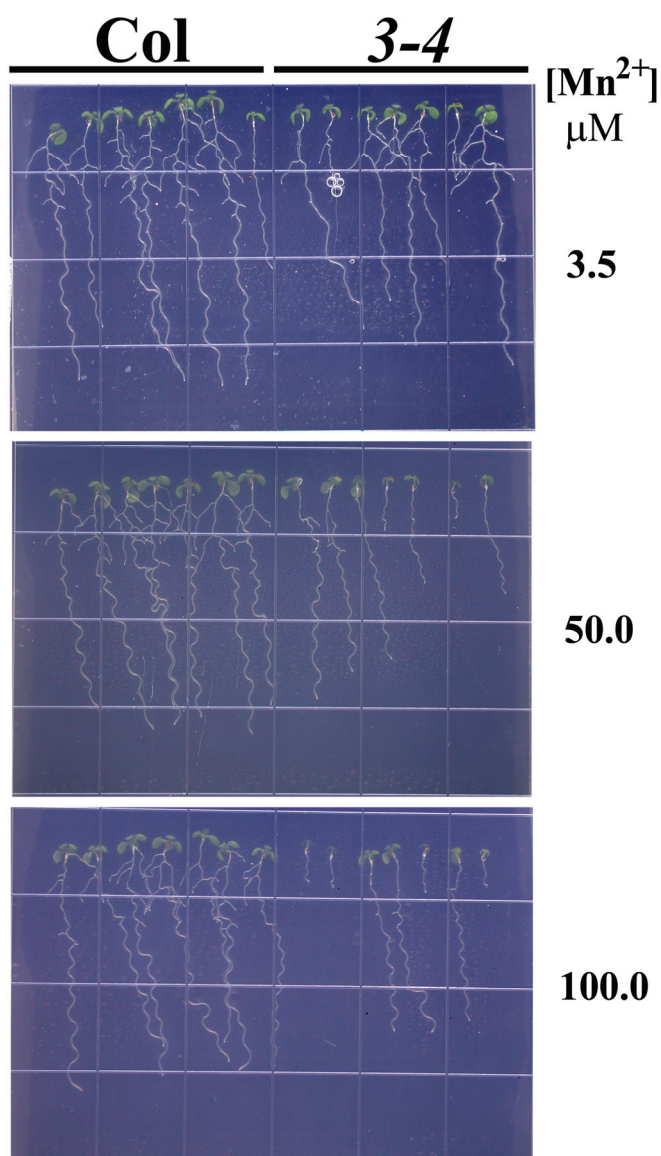
Figure IV-2. Root growth of mutants is sensitive to 50 μM Mn^{2+} .

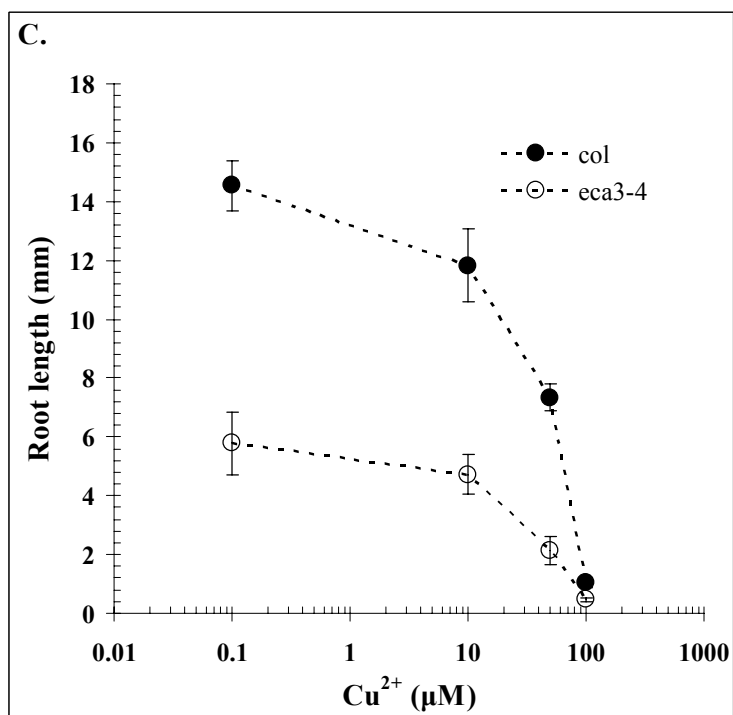
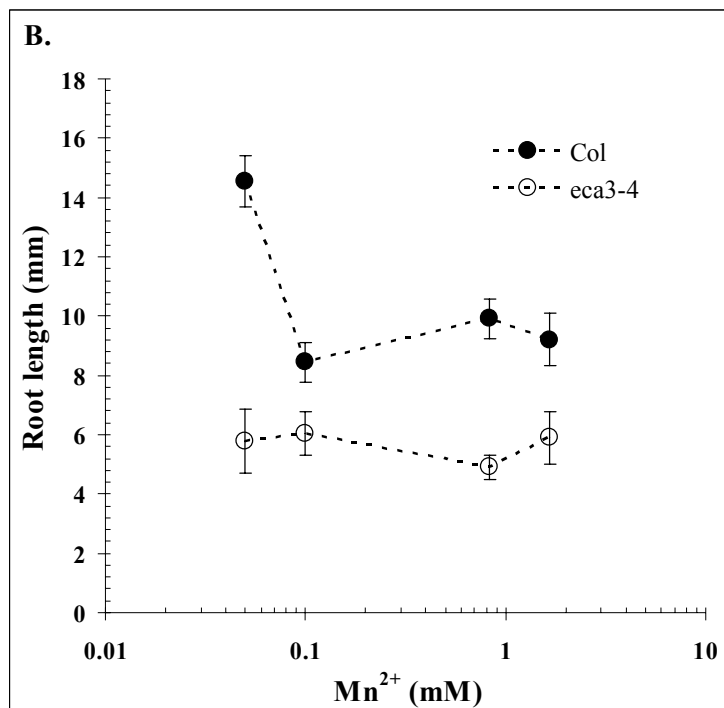
A, Root growth of seedlings transferred to a hydroponic solution of $\frac{1}{4}$ modified Hoagland's medium with 3.5 μM , 50 μM and 100 μM Mn^{2+} . *Arabidopsis* seeds were germinated on $\frac{1}{4}$ Hoagland's medium containing 2.5 mM Ca^{2+} (1 % agar, 10 mM MES- K^+ , pH5.7). Three day old seedlings were then transferred to the same medium, but supplemented with MnCl_2 to final concentrations of 3.5 (no added), 50 and 100 μM . Pictures were taken 3 days after transfer.

B, Root lengths of seedlings on medium with various Mn^{2+} concentrations. *Arabidopsis* seeds were germinated on $\frac{1}{2}$ MS medium containing 50 μM Mn^{2+} with 1% sucrose after 5 d of cold treatment. Seven day old seedlings were transferred to $\frac{1}{2}$ MS medium with 1% sucrose containing ~ 50 μM (no added), 0.1 mM, 0.8 mM, or 1.6 mM Mn^{2+} . Root length was scored 3 days after transfer. Six to ten seedlings were measured in each treatment. Results represent 3 independent experiments. Bar = *S.E.*.

C, Root lengths of seedlings on medium with various Cu^{2+} concentrations. Seed germination and seedling transfer were identical to that described in B except the seedlings were transferred to medium containing ~ 0.1 μM (no added) 10 μM , 50 μM , or 100 μM Cu^{2+} . Root lengths were scored 3 days after transfer. Six to ten seedlings were measured in each treatment. Results represent 3 independent experiments. Bar = *S.E.*.

A.





2C). The results indicate that AtECA3 was not involved in transporting Cu^{2+} ; therefore, it cannot alleviate toxicity from excess Cu^{2+} .

3.2. AtECA3 is expressed in vascular tissues of *Arabidopsis* root and leaf

The tissue location of AtECA3 expression was examined by GUS activity, driven by a 5 kb regulatory region upstream of the AtECA3 open reading frame (Chap. II). I previously showed that AtECA3 is expressed in pollen and vascular tissues in the floral receptacle (Chap. II). In vegetative tissues, AtECA3::GUS activity was particularly high in vascular tissues of primary roots (Fig. IV-3A,B), lateral roots (Fig. IV-3C) and young expanding leaves (Fig. IV-3F). At the root tip, AtECA3 promoter-driven GUS activity first appeared in the differentiation zone (Fig. IV-3A,C), but was not detected in the cell division zone or root cap under the conditions tested. No GUS activity was detected in the shoot apical meristem region (Fig. IV-3D) or in fully expanded cotyledons (Fig. IV-3E). Expression of AtECA3 in other cells is not excluded because the GUS gene was transcriptionally fused to the 5'-regulatory region only, so that any transcriptional regulation by cis-acting elements within introns would be missed. These results together demonstrated that AtECA3 was expressed in developing vascular tissues of young organs.

3.3. AtECA3 localized to Golgi membranes in plant cells

According to the promoter-driven GUS activity, AtECA3 expression was weak relative to ECA1, so I determined the membrane location of AtECA3 by transient overexpression using S35 CaMV promoter in *Arabidopsis* mesophyll protoplasts. This type of approach is now widely used for such purposes and several membrane markers are also available

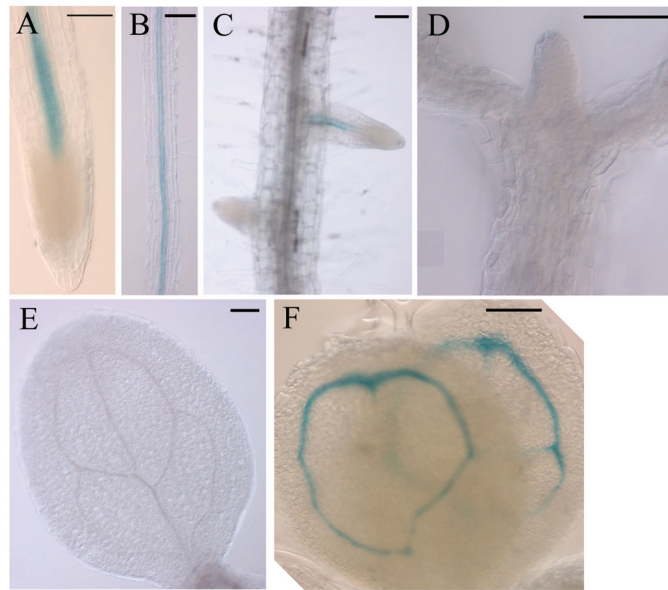


Figure IV-3. Expression pattern of AtECA3 promoter::GUS in root and leaf.

GUS activity is stained in blue. Transgenic plants hosting the 5.2 kb AtECA3 promoter::GUS construct were grown on $\frac{1}{2}$ MS medium and stained as whole seedlings in X-Gluc for 2 days. The GUS staining was detected only in the vascular tissues at the primary root (A, B), at the lateral root (C), and at the true leaves (F), not in the hypocotyl (D) or cotyledon (E). Scale bar = 50 μ m.

(Jin et al., 2001; Kim et al., 2001; Lee et al., 2002). I previously demonstrated that the GFP fused at the C-terminus of AtECA3 restored the tolerance of yeast mutant growth on Ca^{2+} -depleted medium (see Chap. III). Here I show that ECA3-GFP fusion protein also conferred tolerance to 1 mM Mn^{2+} in yeast K616 (Fig. IV-4). GFP fused to AtECA3 at either the N or C-terminus was expressed in protoplasts and their signals were compared with the location of several GFP-fused proteins of membrane markers. The results showed that cells expressing either AtECA3-GFP or GFP-AtECA3 exhibited distinct green fluorescence dots of 1-2 μm (Fig. IV-5A). This pattern differed from the reticulate structures of the ER marker, GFP-HDEL, as well as other membrane markers residing on the plasma membrane GFP-CPK9 (Harper JF, unpublished) and the vacuole (Jauh et al., 1998) (Fig. IV-5A). Instead, similar punctate structures were seen in cells expressing the Golgi membrane marker sialyltransferase (ST) (Wee et al., 1998) and a peroxisome marker (Mullen and Trelease, 2000).

To further clarify the membrane location of AtECA3, ECA3-GFP was co-expressed with two red fluorescent protein-tagged Golgi membrane markers using the same approach. The fluorescence signals were carefully collected using different filter settings on a confocal microscope. I found that ECA3-GFP co-localized in large part with a trans-Golgi-marker ST-RFP (Wee et al., 1998) and with a cis-Golgi-marker, GmMan1-tdTomato (Nebenfuhr et al., 1999) which are shown as yellow structures in the overlay images in Fig. IV-5B. A higher percentage of overlap was also observed between ECA3-GFP and ST-RFP than between AtECA3 and GmMan1-tdTomato, suggesting AtECA3 is localized within the Golgi apparatus with a preference toward the trans-Golgi membrane.

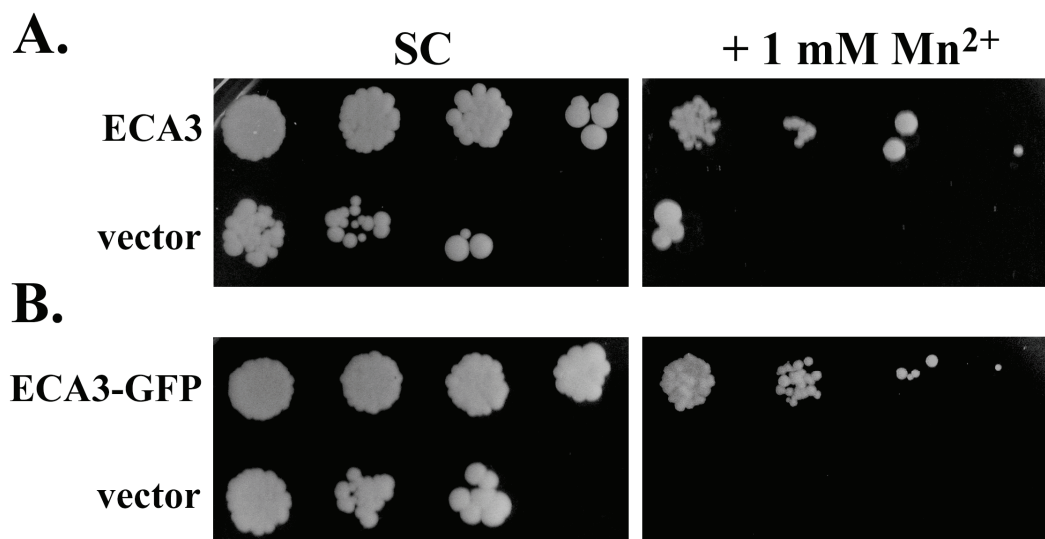


Figure IV-4. Free AtECA3 or ECA3-GFP fusion protein confers tolerance to toxic levels of Mn²⁺ in K616 yeast.

Expression was driven by a constitutive PMA1 promoter. Yeast strains transformed with empty vector were used as negative control. Basal Mn²⁺ concentration is estimated as 2.6 μ M in SC medium.

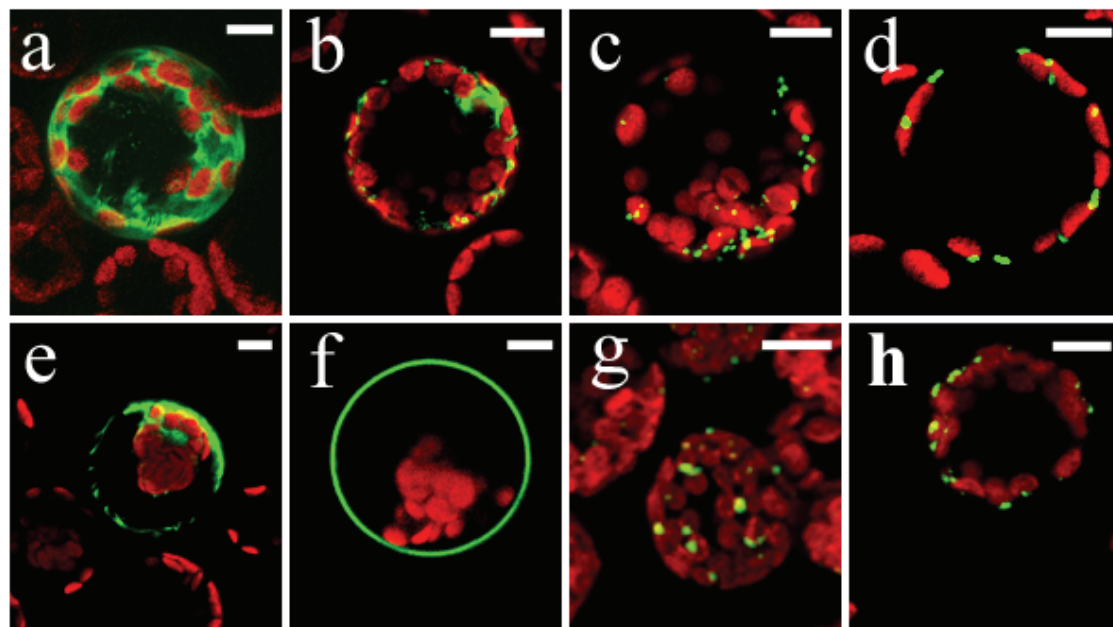
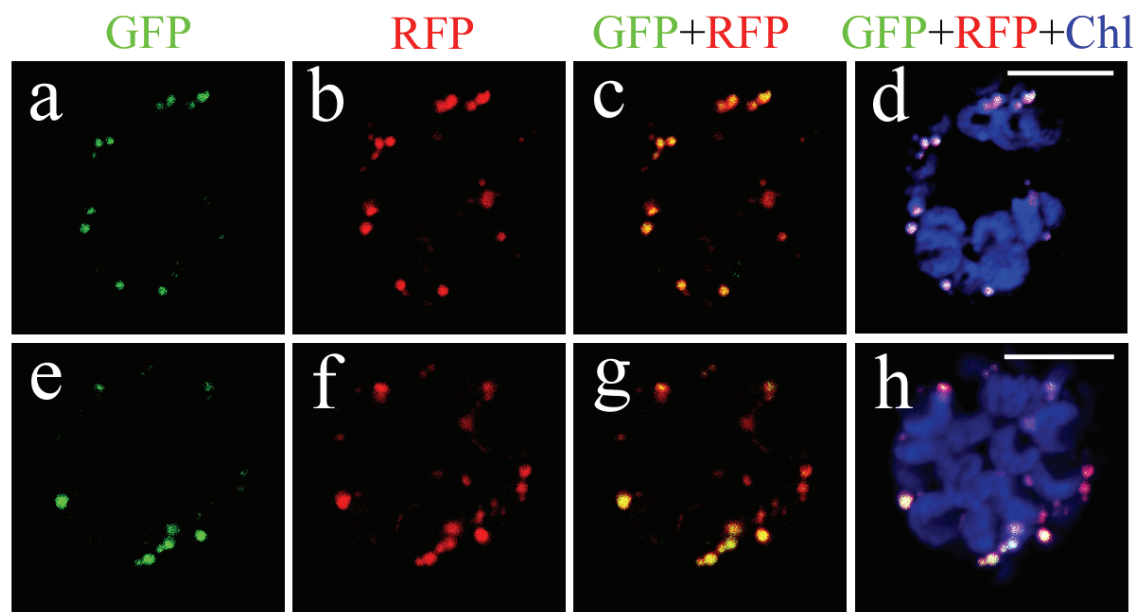
A. AtECA3 improves yeast mutant K616 growth on medium containing 1 mM Mn²⁺.

B. GFP-tagged AtECA3 also improves K616 growth in medium containing 1 mM Mn²⁺.

Figure IV-5. AtECA3 is localized to Golgi membranes in *Arabidopsis* mesophyll protoplasts.

A. Distribution pattern of GFP fused to AtECA3 and to marker proteins. All constructs were driven by CaMV 35S promoter. The GFP signal appears green while autofluorescence of chlorophyll is shown in red: **a**, free eGFP; **b**, GFP-HDEL, an ER marker; **c**, rat ST-GFP, a Golgi membrane marker; **d**, GFP-36 amino acids at C-terminus of APX, a peroxisome marker; **e**, GFP-TIP, a tonoplast membrane marker; **f**, GFP-CPK9, a plasma membrane marker. **g**, AtECA3-eGFP. **h**, eGFP-AtECA3. Scale bar = 10 μ m.

B. AtECA3 colocalized with cis and trans-Golgi membrane markers. All proteins were transiently expressed under CaMV 35S promoter in *Arabidopsis* mesophyll protoplasts. GFP-tagged AtECA3 (green) was co-transfected with either ST-RFP (trans-Golgi) (top panels) or tdTomato- α -1,2 mannosidase (cis-Golgi) markers (bottom panels). Blue, pseudo-colored autofluorescence of chlorophyll. Top panel shows signals from cell 1 where **a**, **b**, **c** and **d** refer to AtECA3-GFP, ST-RFP, overlay of **a** and **b**, and overlay of **a**, **b** and chlorophyll, respectively. Bottom panel shows signals from cell 2, **e-h** refer to ECA3-GFP, α -1,2 mannosidase-tdTomato, overlay of **e** and **f**, and overlay of **e**, **f** and chlorophyll, respectively. Scale bar = 10 μ m.

A.**B.**

3.4. Enhanced apoplastic peroxidase (APX) activity and protein secretion in *eca3* mutants

Since plant Golgi apparatuses are involved in the synthesis of non-cellulosic wall components and in the processing, sorting and exocytosis of proteins, I wondered if secretory activities might be compromised in *eca3* mutants. To determine whether secretion was impaired in *eca3* mutants, the activities of secreted apoplastic peroxidases (APXs), were examined in roots from hydroponically-grown plants. Plants produce a group of class III peroxidases that are secreted and are involved in diverse processes throughout the life cycle (Welinder, 1992; Passardi et al., 2005). Apoplastic wall fluid or AFW was extracted from roots by vacuum-infiltration and centrifugation. Guaiacol-dependent peroxidase activity was then monitored spectrophotometrically by following the oxidation of guaiacol by H_2O_2 to form tetraguaiacol.

I first established that the enzyme reaction, monitored by the appearance of tetraguaiacol, was linear for 2 min (Fig. IV-6A). The initial rate of the reaction was then estimated from the slope. Increasing aliquots of apoplastic wall fluid from *wild-type* roots produced enhanced rate of guaiacol oxidation, indicating that *Arabidopsis* roots contained extracellular peroxidase activity (Fig. IV-6B). Based on 3-4 independent experiments, the extracellular peroxidase activity of *wild-type* roots was estimated to be $\sim 70 \text{ nmole}\cdot\text{min}^{-1}\cdot\text{gm}^{-1}$ fresh weight root. When apoplastic wall fluid of mutants was analyzed, I consistently noticed an increase in peroxidase when activity is expressed per gram fresh weight of roots. The APX activity of *eca3-4* mutants was $\sim 120 \text{ nmole min}^{-1}\cdot\text{gm}^{-1}$ fresh weight root which is about 84 % higher in 3 independent experiments, compared with wild-type controls (Table IV-1). Using nitroblue tetrazolium chloride as a

histochemical stain, there was no obvious difference in the abundance of apoplastic reactive oxygen intermediates such as O_2^- formation between *wildtype* and *eca3-4* mutants (data not shown). When total protein was determined using the Bradford reagent (Bradford, 1976), mutant roots consistently showed more protein per fresh weight of tissue. Thus mutants showed increased secretory activity based on protein levels and peroxidase activity.

4. DISCUSSION

4.1. AtECA3 the first plant gene encoding a Golgi-bound Ca^{2+}/Mn^{2+} pump

Here, I provide evidence that AtECA3 is a plant Golgi-bound Ca^{2+}/Mn^{2+} pump. I have shown that AtECA3 fused to either GFP at the N or C terminus maintained activity as a Ca^{2+} pump as well as a Mn^{2+} pump (Chap. III, Fig. IV-4). AtECA3-GFP, expressed transiently in mesophyll protoplasts, emitted similar punctate fluorescent patterns as two markers of Golgi membranes, rat sialyltransferase-fused RFP or soybean α -mannosidase-fused RFP variant tdTomato (Fig. IV-5A). The same cauliflower mosaic virus 35S promoter was used to drive the expression of AtECA3 as well as the known Golgi markers, thus in some cases overexpression does not necessarily lead to aberrant localization. GFP fused to either the N-terminus or the C-terminus of AtECA3 exhibited the same pattern (Fig. IV-5B), suggesting the membrane targeting signal for the Golgi is located internal to the AtECA3 molecule. This conclusion agrees with the notion that the Golgi membrane localization signal is probably within its transmembrane span (Machamer, 1993; van Vliet et al., 2003). In growing pollen tubes, the AtECA3-GFP fusion protein is localized to cortical structures at the tip of pollen tubes (Chap. III). This

Figure IV-6. Apoplastic peroxidase (APX) activity and general protein secretion were enhanced in *Ateca3* mutant.

A. Time-course of guaiacol oxidation by root AWF. The reaction was started by adding guaiacol to a reaction mixture containing different aliquots of AWF from mutant or *wildtype*. Data represent the change in absorption at 470 nm due to tetraguaiacol formation time from a single experiment (Exp. 1 in Tab. IV-1). The volume of AWF was indicated. Solid symbols and solid trend lines represent *wildtype* (Col.) while open symbols and dotted trend lines represent *Ateca3-4*.

B. Rate of guaiacol oxidation as a function of AWF volume is linear. The slopes calculated from A (= rate of reaction) were plotted as a function of the AWF volumes. A regression equation describing the linear relation was shown. The slopes were used to calculate guaiacol-dependent APX activity. Open diamond symbols and dotted lines, *Ateca3-4*; solid diamond symbols and solid lines, *wildtype* (Col.). The linear regression equations and R square values for each series were also shown.

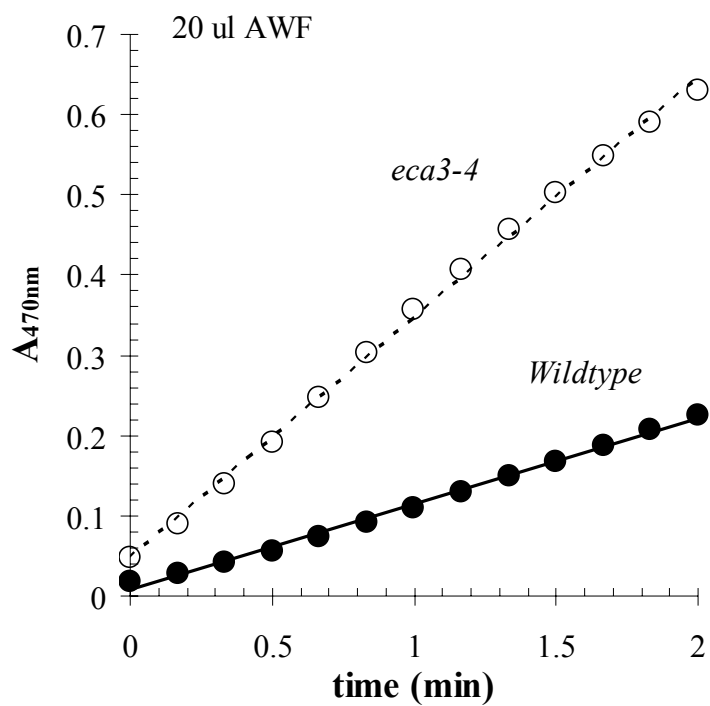
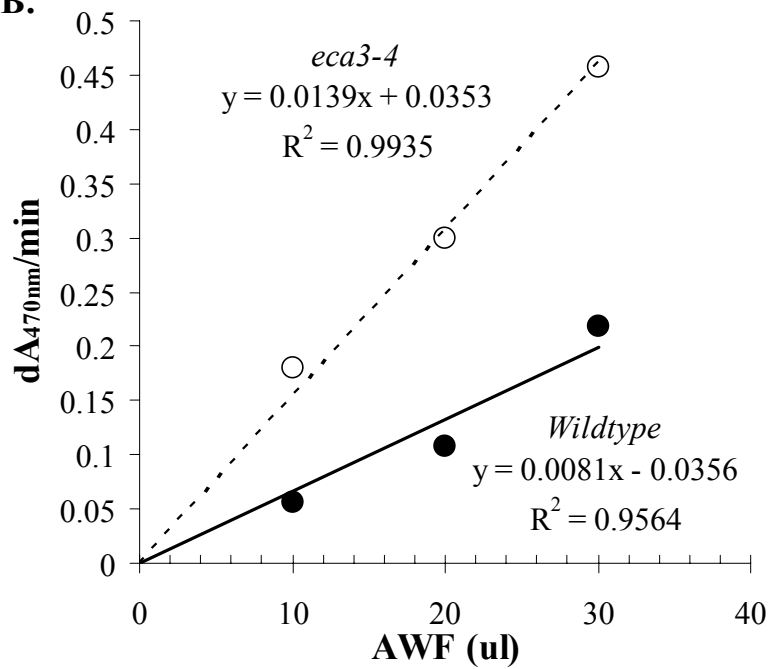
A.**B.**

Table IV-1. The summary of 3 experiments measuring APX activity and total apoplasic protein.

For each experiment, samples from *wildtype* and mutants were always treated under identical conditions. An extinction coefficient of $26.6 \text{ mM}^{-1} \text{ cm}^{-1}$ was used to convert the absorbance changes to enzyme activities. Root fresh weight (Root Fw) was determined after daubing dry on filter paper. Protein concentration was quantified by Bradford method (micro assay). A standard curve was developed using known amounts of BSA in the same buffer and likewise mixed with Bradford's reagent.

	Root Fw	AWF	Total Protein	Protein Yield		Peroxidase Activity	
	mg	μl	μg	$\mu\text{g/gm Fw}$	$A_{470}/\text{min}/\mu\text{l AWF}$	$\text{nmol}/\text{min}/\text{gm Fw}$	$\text{nmol}/\text{min}/\mu\text{g protein}$
Exp. 1							
Col	546	228	8.515	15.60	0.0081	89.97	5.77
<i>eca3-4</i>	449	204	11.23	25.01	0.0139	167.99	6.72
% mt/wt				160		187	116
Exp. 2							
Col	382	98	8.01	20.97	0.0046	31.39	1.50
<i>eca3-4</i>	771	239	31.61	41.00	0.0071	58.54	1.43
% mt/wt				196		186	95
Col	95	21	4.52	47.57	0.0081	47.63	1.00
<i>eca3-4</i>	98	28	6.48	66.16	0.0113	85.88	1.30
% mt/wt				139		180	130
Summary:							
Ave. % mt/wt				165		184	114
$\pm S.E.$				± 20.4		± 2.7	± 12.5

distribution pattern resembles that of secretory vesicles, and Golgi-derived endomembrane compartments that readily fuse with the plasma membrane during fast pollen tube growth. These results together support the idea that AtECA3 is located on Golgi membranes in plant cells. To my knowledge, this is the first Golgi Ca^{2+} pump identified in plants at the molecular level.

The Golgi-localized AtECA3 is also likely the only Ca^{2+} pump that is sensitive to thapsigargin in *Arabidopsis* (Chap. III). ECA1, was shown to be insensitive to TG (Liang and Sze, 1998), and ECA4, an almost identical protein to ECA1, is expected to share that property. AtECA2 has not been functionally characterized yet, though it shares more sequence similarity to AtECA1 (65% identity and 79% positive) than to AtECA3 (46% identity and 62% positive). Significantly, the molecular characterization of a Golgi Ca^{2+} -ATPase AtECA3 confirms and extends an earlier biochemical study where a Ca^{2+} pump activity of a Golgi-purified fraction from pea was inhibited by thapsigargin with an apparent I_{50} of 88 nM (Ordenes et al., 2002). So, it is possible that in all higher plants, a Golgi Ca -ATPase will be TG sensitive. For instance, I predict that OsECA3 (Os03g52090) is a TG-sensitive Ca^{2+} pump localized to the Golgi and possibly to secretory vesicles in rice.

4.2. Functions of a Golgi Ca^{2+} pump in plants

Golgi-located Ca^{2+} pumps in yeast and mammals support protein glycosylation and secretion. I showed before that Ca^{2+} -stimulated pollen tube growth is inhibited in *eca3* mutants (Chap. III). Here I show that Ca^{2+} -stimulated root growth is also inhibited in the mutants (Fig. IV-1). Importantly, root growth is stimulated optimally by 3 mM Ca^{2+} consistent with previous physiological studies (Marschner, 1995). At this high

concentration, Ca^{2+} entry is not impaired in these mutants, thus the requirement for millimolar levels of Ca^{2+} indicate that Ca^{2+} loading into certain endomembrane lumina is limiting growth. High level of Ca^{2+} was observed before in the Golgi lumen (Dauwalder et al., 1985; Sakai-Wada and Yagi, 1993), though the function was unclear. We suggest that AtECA3 promotes growth by loading an adequate level of Ca^{2+} into Golgi compartments. The sequestered Ca^{2+} could perform at least three major functions: (i) to activate enzyme or protein activities in the lumen; (ii) to fill Ca^{2+} stores that can be released via gated- Ca^{2+} channels to enhance local $[\text{Ca}^{2+}]_{\text{cyt}}$ in a temporal manner; and (iii) to supply Ca^{2+} to the extra-cellular medium for biochemical or signaling purposes. Golgi $[\text{Ca}^{2+}]_{\text{lum}}$ might activate protein and enzyme activities that are responsible for the synthesis and modification of polysaccharides and proteins. An induced local rise in $[\text{Ca}^{2+}]_{\text{cyt}}$ may aid (i) in directing the movement of secretory vesicles via the cytoskeleton to their destination, and (ii) to modulate exocytosis, including membrane docking and fusion events, and perhaps subsequent endocytosis to recycle essential components of secretory pathways. These ideas are consistent with the general functions of animal and yeast Golgi in protein processing, sorting, glycosylation and secretion (Robinson, 2003), and possibly in Ca^{2+} signaling (Van Baelen et al., 2004).

A Golgi Ca^{2+} pump is expected to be important for all cell types; however analyses of its promoter activity show it is highly expressed in vascular tissues of developing roots and in pollen grains (Fig. IV-3, Chap. III). These tissues are known to secrete large amounts of polysaccharides and wall proteins; thus the results suggest that Ca^{2+} pumping into the Golgi lumen and secretory vesicles are especially critical in cells with active secretory systems. Fully differentiated tissues that are no longer highly

secretory may not have as many Golgi apparatuses or need not expend energy to fill Ca^{2+} stores.

4.3. Role of Mn^{2+} in the Golgi

Mn^{2+} is a micro nutrient required mostly for photosynthesis and oligosaccharide transferases in protein glycosylation. While micromolar levels of Mn^{2+} in the soil is sufficient to sustain plant growth (Marschner, 1995), excess Mn^{2+} is detrimental, probably by affecting apoplastic redox status (Fecht-Christoffers et al., 2006). Besides transporting Ca^{2+} , AtECA3 can also pump Mn^{2+} into the Golgi lumen. This was demonstrated in both yeast and *Arabidopsis* seedlings, which became sensitive to excess Mn^{2+} when AtECA3 function was deficient (Chap. III; Fig. IV-2). The results suggest high $[\text{Mn}^{2+}]_{\text{cyt}}$ is toxic to cells; though its role in the Golgi lumen is unclear. Roots of *eca3* mutants grew as well as wild-type plants when Mn^{2+} was supplied at $\sim 3 \mu\text{M}$ levels (Fig. IV-6), indicating that a lack of AtECA3 did not interfere with root growth and that Mn^{2+} uptake and sorting is mediated by other transporters. Surprisingly, other divalent cation transporters, like ECA1, are apparently inadequate to remove excess $[\text{Mn}^{2+}]_{\text{cyt}}$ when the external Mn^{2+} is 1 mM. This observation suggests a potential role for Mn^{2+} in the Golgi. Many glycosyltransferases, such as galactosyl transferase require Mn^{2+} as a cofactor (White et al., 1993; Sterling et al., 2005), and are localized in the lumen of Golgi and secretory membranes. These enzymes play important roles in polysaccharide genesis and modification for complex cell wall construction (Delmer, 1987; Hayashi, 1989; Ridley et al., 2001). It is possible that some of the glycosyl transferases in the *Arabidopsis* genome have a role in the synthesis and modification of cell wall polysaccharides and proteins.

4.4. Possible roles of Golgi Ca²⁺ in secretion and wall remodeling

I found that *eca3* mutants secreted more total protein and peroxidase activity than *wildtype* plants (Fig. IV-6, Tab. IV-1), suggesting that a perturbation of Ca²⁺ homeostasis in the Golgi affects secretion. Coincidentally, the yeast mutants lacking *Pmr1* gene also secrete more proteins than wild-type (Smith et al., 1985; Rudolph et al., 1989), although the mechanism is still not clear. To my knowledge, this is the first genetic evidence linking a relationship of Golgi Ca²⁺ homeostasis to the secretory system in plants. It is not yet understood why a defect in *AtECA3* function would increase secretion of peroxidase, though several possibilities are considered.

Secreted peroxidases (class III) or apoplastic peroxidases include many isoforms, and are involved in diverse functions, such as generating reactive oxygen species, polymerize cell wall compounds and regulating hydrogen peroxide levels. They modify cell wall properties, such as loosening walls during growth, and cross-linking walls to form a barrier in response to wounding, biotic and abiotic stress. Interestingly, peroxidases and phenolic compounds are induced by heavy metals and appear to protect plants from heavy metal toxicity (Passardi et al. 2005). Increased peroxidase could result from (i) deregulated secretion of *eca3* mutants that are unable to adjust their intracellular Ca²⁺ and Mn²⁺ levels; and (ii) up-regulation of wall peroxidases in response to stress from an imbalance in intracellular ions or metal toxicity. Increased peroxidases might aid in cross-linking cell walls and thus reduce or arrest wall growth. Deregulated secretion might lead to altered cell wall composition in *eca3* mutants. Analyzing the quality and quantity of cell wall structure and chemical composition might provide clues to these ideas.

This study provides evidence for the first Golgi $\text{Ca}^{2+}/\text{Mn}^{2+}$ pump in plants, and genetic evidence that it plays a significant role in Ca^{2+} -dependent root growth. Ca^{2+} and Mn^{2+} in the Golgi lumen are proposed to affect the synthesis and modification of cell wall polysaccharides and secreted wall proteins. This idea is supported by the enhanced secretion of apoplastic peroxidase in mutants unable to load Ca^{2+} into the lumen of Golgi and secretory vesicles. Peroxidases might reduce root growth due to increased cross-linking of wall materials in *eca3* mutants.

5. MATERIALS AND METHODS

5.1. Plant Growth

a. Plant materials.

Wildtype and *eca3* mutants of *Arabidopsis thaliana* Columbia ecotype were used in this study.

b. Plant growth conditions.

For growth on plates, *Arabidopsis* seeds were surface sterilized by soaking in 20% (v/v) Clorox, 0.05% Tween 20 for 10 min followed by 5 times of rinsing in sterile DI water. The seeds were planted on $\frac{1}{2}$ MS medium ((Murashige and Skoog, 1962) containing 0.1% agar and 15 mM MES-K at pH5.7, followed by stratification in the dark at 4 °C for 3 days. The media plates were then positioned vertically in Conviron growth chamber with a photoperiod of 16 h light under an illumination of 120-180 $\mu\text{E m}^{-2} \text{s}^{-1}$ and 8 h dark. The temperature was set at 22 °C in the day and 20 °C at night.

For soil-grown plants, *Arabidopsis* seeds were planted on synthetic soil medium containing Miracle-Gro[®] potting mix and perlite, followed by 3 day of 4 °C stratification

in dark before taken to growth chamber with a photoperiod of 16 h light of 120-180 $\mu\text{E m}^{-2} \text{s}^{-1}$ at 22 °C and 8 h dark at 20 °C and 60% relative humidity, or with a short day photoperiod of 10-12 h light of 120 $\mu\text{E m}^{-2} \text{s}^{-1}$. Plants were watered twice a week or as needed. *Wildtype* and mutant plants were always grown side by side in the same tray for consistency.

Root growth measurement of root growth on medium plates. Three days after germination on square plates containing standard 1/2 MS medium, the seedlings were transferred onto 1/2 MS medium plates with Ca^{2+} or Mn^{2+} concentrations specified in results section. The plates were then positioned in an inverted orientation for another few days before photographs were taken by scanning of the plates using a Umax Astra 1200S scanner. Root measurement was conducted using ScionImage software (Scion Co., Frederick MD). The *wildtype* and mutant plants were always planted side by side on the same plate.

Hydroponic growth root AWF extraction. *Arabidopsis* seeds were dispersed on 1/2 x Hoagland medium (Hoagland and Arnon, 1950), solidified with 0.5% agar on the bottom of a 1 ml tip box (~0.5 cm depth). After germination, the tip boxes were floated on 1/2 Hoagland medium (pH5.5, 10 mM MES-K) which was aerated by a fish tank air pump. Medium was replaced twice a week to prevent algae contamination. Roots penetrating the medium were excised after 3-4 weeks.

5.2. DNA manipulations.

GFP-tagged AtECA3. Conventional cloning and Gateway cloning methods were used for GFP-tagged AtECA3 expression. For conventional cloning, AtECA3 cDNA (Chap. III) was amplified by PCR using platinum Pfx DNA polymerase (Invitrogen,

Carlsbad CA) and the primer pairs: a), 5'-CATGTCATGAATGGAAGACGCCTACGCC AGATCTGTCT-3' and 5'-CATGTCATGAACTTGTCACGCCGGTCCTTGGGGAGT AAAT-3' (for ECA3-GFP); and b), 5'-CGGGATCCATGGAAGACGCCTACGCCAGA TCTGTCT-3' and 5'-GGACTAGTCTACTTGTCACGCCGGTCCTTGGGGAGTAAAT -3' (for GFP-ECA3). The resultant PCR-amplified product for the C-tail fused GFP was digested with BspHI (from primer pair 1) and ligated to NcoI-cut vector pAVA393(von Arnim et al., 1998). The PCR-amplified product for GFP-fusion at the N terminus was digested with BamHI/SpeI (from primer pair 2) and ligated to BglII/XbaI-linearized vector pAVA393. The resultant constructs ECA3-GFP-393 and GFP-ECA3-393 were verified by sequencing of the AtECA3 coding region. Both constructs contain CaMV 35S-promoter.

For Gateway cloning, the AtECA3 cDNA was amplified by PCR using Platinum Pfx DNA polymerase (Invitrogen, Carlsbad CA) and the primers 5'-GGGGACAAGTTT GTACAAAAAAGCAGGCTCGATGGAAGACGCCTACGCC-3' and 5'-GGGGACCA CTTTGTACAAGAAAGCTGGGTACTTGTCACGCCGGTCC-3'. The PCR-amplified fragment of AtECA3 (stop codon removed) was cloned into a Gateway vector pDONR221 (Invitrogen, Carlsbad CA) to give rise to an entry clone ECA3-DONR221 using BP recombination cloning strategy. Sequence of AtECA3 insert was verified. The clone ECA3-DONR221 was then cloned into Gateway destination binary vectors pK7WGF2 and pK7FWG2 by LR recombination, respectively (Karimi et al., 2002). The resultant constructs ECA3-WGF and ECA3-FWG contain an expression cassette of CaMV P35S-eGFP-ECA3-T35S and CaMV P35S-ECA3-eGFP-T35S, respectively. Both conventional clones and gateway clones were used in localization experiments.

Promoter::GUS analyses. Promoter::GUS constructs, transgenic plant generation, and GUS staining were performed as previously described (Chap. III).

5.3. Transient expression in *Arabidopsis* mesophyll protoplast.

PEG-mediated protoplast transfection. Transient expression was conducted according to published protocols with modification (Jin et al., 2001; Sheen, 2001). Fully expanded young leaves of 3.5-4.5 weeks old *Arabidopsis* plants grown under short day condition were cut into small strips and digested under dark in enzyme digestion solution at 22-25 °C for 3 h. The enzyme digestion solution contains 1.5% (w/v) cellulase R10 and 0.2-0.4% (w/v) macerozyme R100 (Yakult, Tokyo, Japan) in 0.4 M mannitol, 20 mM KCl, 20 mM MES at pH5.7, 1-, 10 mM CaCl₂, 5 mM β-mercaptoethanol and 0.1% (v/v) fetal bovine serum (Sigma F6178, St. Louis MO). The released protoplasts were then filtered through 35-75 μm nylon mesh and centrifuged at 100 x g for 1.5 min. The pellet was carefully resuspended and washed in W5 solution containing 154 mM NaCl, 125 mM CaCl₂, 5 mM KCl and 2 mM MES at pH5.7. Fresh protoplasts were suspended in MMg solution (0.4 M mannitol, 15 mM MgCl₂ and 4 mM MES at pH5.7) before transfection. The plasmids were purified on Qiagen MidiPrep columns (Qiagen, Valencia CA). For each transfection, 400 μl protoplast suspension (10⁵ cells) was mixed with 20-40 pmole plasmids and equal volume of PEG solution (40% w/v PEG4000 (Fluka #81240), 0.2 M mannitol, 0.1 M CaCl₂) and the mixture was incubated at 22-25 °C for 30 min. The cells were then recovered by centrifugation at 100 x g for 1 min. The pellet was suspended in WI solution (0.5 M mannitol, 20 mM KCl and 4 mM MES at pH5.7) and kept in dark at 22-25 °C until confocal observation. For co-localization, two constructs with equal molarity of 10-20 pmole were mixed to transfect the same batch of

protoplasts. Fluorescent signals were examined 20-24 h after transfection on a Zeiss LSM510 confocal microscope (Carl-Zeiss, Germany). The filter sets used are: GFP, 488nm (Ex)/BP510-30 (EM); RFP and tdTomato, 543nm (EX)/BP560-615 (EM); Chlorophyll, 488nm (EX)/LP650nm (EM). Signals were captured in multi-channel mode. Pictures were processed in Adobe Photoshop (Adobe systems, San Jose, CA).

5.4. Extraction of wall fluid and measurement of Apoplastic peroxidase activity.

Apoplastic wall fluid (AWF) preparation. Root AWF was prepared from roots of *Arabidopsis* grown hydroponically in modified $\frac{1}{4}$ Hoagland medium (5 mM MES-K, pH5.7) (Hoagland and Arnon, 1950). The extraction was modified from a method used to extract apoplastic wall fluid from plant leaves (Rathmell and Sequeira, 1974; Fecht-Christoffers et al., 2006). In brief, *Arabidopsis* roots were rinsed in DI water and soaked in 10 mM Na⁺-phosphate buffer (pH 6.0) after excision, followed by vacuum infiltration (< -35kPa) for 5 min. The roots were then carefully dabbed dry on filter papers, weighed, and put into 5 ml syringe barrel. The barrel was placed in a 15 ml Falcon tube and the whole ensemble was centrifuged at 3,000 x g for 20 min. The AWF was collected from the bottom of the Falcon tube. I have assumed that the % recovery of apoplastic proteins from wild-type (Col.) and mutant plants was similar.

Total protein concentration in AWF. The total protein in AWF was determined using a Bio-Rad Protein Assay dye reagent (Bio-Rad lab, Hercules CA) (Bradford, 1976).

Peroxidase activity assay. Peroxidase activity of the AWF fraction was determined by measuring the rate of the oxidation of guaiacol to tetraguaiacol (Chance and Maehly, 1955; Cordoba-Pedregosa et al., 1996). In the presence of peroxidases, the artificial substrate guaiacol was oxidized by H₂O₂ to tetraguaiacol, whose absorption at

470 nm was converted using a molecular extinction co-efficient $26.6 \text{ mM}^{-1} \text{ cm}^{-1}$. Briefly, 10, 20, and 30 μl AWF sample containing 0.1-2 μg total protein was added to 1 ml reaction mixture containing 0.3% (v/v) H_2O_2 , 0.1% (v/v) guaiacol in 10 mM sodium-phosphate at pH 6.0. The reaction was started by adding guaiacol and monitored by increase in absorption at 470 nm for initial 2 min using a Beckman DU 640 spectrophotometer at ambient temperature. The rate of $A_{470\text{nm}}$ change was deduced as peroxidase activity, and expressed as relative activity per min per gm tissue (fresh weight).

V. CONCLUSIONS AND FUTURE PROSPECTS

1. CONCLUSIONS

This dissertation presents an extensive functional characterization of a P-type *Arabidopsis* Ca²⁺-ATPase, AtECA3, in its tissue expression, subcellular membrane location, transport activity, and biological functions in root growth and pollen tube elongation.

1.1. *Arabidopsis* ECA3 is a plant P-type ATPase transporting Ca²⁺ and Mn²⁺

Evolutionarily, multi-cellularity is accompanied by the increase in P-type Ca²⁺-ATPase genes, as in higher plants. The multiplicity of ECA genes (>50% similarity and > 45% identity to one another) in the model plant *Arabidopsis thaliana* and rice underscores the importance of their functions. When I started this project, only AtECA1 had been cloned and functionally characterized, whereas AtECA2-ECA4 were still unknown. The Ca²⁺/Mn²⁺ transport activity of AtECA1 was studied using a heterologous expression system in yeast (Liang et al., 1997). AtECA1 greatly improved growth of K616, a yeast strain lacking both of its Ca²⁺ pumps, in media depleted of Ca²⁺ or containing toxic Mn²⁺ by efficiently loading of Ca²⁺ into the ER lumen or removing excess Mn²⁺, respectively. Similarly, the expression of AtECA3 also improves the growth of K616 in media containing 0.8 μM free Ca²⁺ or 1 mM Mn²⁺. A GFP-fused AtECA3 is found on endomembranes when expressed in yeast, suggesting the function of AtECA3 is to load Ca²⁺/Mn²⁺ into the lumen of endomembranes. The GFP fusion does not disrupt AtECA3 function because AtECA3-GFP also improves K616 growth in similar conditions to AtECA3 alone. In addition, this growth improvement by AtECA3

expression is sensitive to 2 μM cyclopiazonic acid (CPA), a SERCA pump-specific inhibitor that also efficiently inactivates AtECA1 by half at 3 nmol/mg protein (Liang and Sze, 1998), suggesting AtECA3 shares biochemical features with AtECA1 and SERCA. These results, together with the high sequence similarity (58%) between AtECA1 and AtECA3, suggest that AtECA3 transports Ca^{2+} and Mn^{2+} . The kinetics of transport activity by AtECA3, such as affinity to $\text{Ca}^{2+}/\text{Mn}^{2+}$ and maximal velocity, were not determined in this study.

1.2. AtECA3 is the first plant Ca^{2+} pump localized to Golgi membrane

AtECA3 is localized on Golgi membranes as shown by confocal examination of GFP fused to AtECA3 when transiently expressed in *Arabidopsis* mesophyll protoplasts. A functional construct AtECA3-GFP, as shown in yeast growth assays (above), exhibit green fluorescence in punctate structures dispersed in plant cells, which is consistent with GFP-AtECA3, another construct of AtECA3 with GFP fused to its N-terminus. Furthermore, the fluorescence of AtECA3-GFP occurs in structures largely overlapping with either of 2 known Golgi membrane markers, ST-RFP (trans-) and GmMan1-tdTomato (cis-), when co-expressed within the same cell. AtECA3-GFP is also found in secretory vesicles beneath the PM of the apex of growing pollen tubes, suggesting the AtECA3 may also reside on vesicle membranes derived from the Golgi apparatus along the secretory pathway. These results demonstrated that AtECA3 is located on Golgi membranes. Given the absence of a Golgi/secretory pathway-type Ca^{2+} pump in higher plants, it is likely that independent strategies of the Ca^{2+} pump inventory have evolved between metazoan and planta. To my knowledge, AtECA3 is the first plant Ca^{2+} pump that is localized to the Golgi.

1.3. AtECA3 function is important for root growth and male sterility

The expression pattern of AtECA3 is high in the vascular tissues of root, leaf and stem, and in pollen grains, as revealed by promoter::GUS, RT-PCR, and microarray results. Therefore, root growth and pollen germination were focused on to disclose the roles of AtECA3 in *Arabidopsis*.

To study the biological functions of AtECA3, three *Arabidopsis* (Col.) lines each hosting an independent ~12 kb T-DNA insertion in AtECA3 were collected in collaboration with J.F. Harper's laboratory at the University of Nevada, Reno. The plants homozygous for all 3 alleles, namely *eca3-1*, *3-4* and *3-5*, completed their life cycle from germination to seed set. However, mRNA translatable for a full AtECA3 protein was not detected by RT-PCR from all 3 T-DNA lines, indicating these mutants were deficient in AtECA3 function.

The primary root growth of wild-type *Arabidopsis* seedlings is promoted by sufficient media Ca^{2+} concentrations of 3 mM compared to 1 mM or 25 mM, suggesting proper uptake and internal partitioning of Ca^{2+} are both critical for optimal root growth. However, 3 mM Ca^{2+} fails to promote root growth in all 3 mutant lines, when compared with their respective wild-type controls, suggesting AtECA3 is important for root growth by controlling intracellular Ca^{2+} distribution and dynamics.

AtECA3 also transports Mn^{2+} , an essential nutrient normally required at only micromolar levels. High media Mn^{2+} inhibits the root growth of *Arabidopsis* plants. This inhibition is tolerated in wild-type *Arabidopsis* plants, probably by removing excess Mn^{2+} from the cytosol to endomembrane compartments via Mn^{2+} transporters AtECA1 and AtECA3. Therefore, root growth may be compromised when AtECA3 function is

deficient. This turns out to be the case because one allele of the AtECA3 mutants, *Ateca3-4*, exhibits impaired root growth when Mn^{2+} is at 50 μM compared with the *wildtype*, suggesting Mn^{2+} detoxification is compromised in the *eca3* mutant.

AtECA3 is also required for optimal pollen tube growth *in vitro*. Extracellular Ca^{2+} is critical for pollen tube elongation, as media Ca^{2+} at low or high levels retards the polar growth of pollen tubes. However, even in media containing 10 mM Ca^{2+} , which is optimal for *wildtype* tube growth, the pollen tube length is consistently reduced by 33% from all 3 T-DNA lines of AtECA3. The defect in pollen tube growth also causes problems *in vivo*, as both seed set and ovule fertilization are reduced in *Ateca3-4* mutants. Transmission of *eca3-1* and *eca3-5* pollen is also less competent than *wildtype*. These results together suggest that AtECA3 function is critical for sustaining pollen tube growth by controlling intracellular Ca^{2+} distribution and dynamics.

1.4. AtECA3 is the first plant Ca^{2+} pump inhibited by thapsigargin

AtECA3-promoted K616 growth in media depleted in Ca^{2+} is inhibited by 20% in the presence of 0.5 μM thapsigargin (TG), a specific potent inhibitor of mammalian SERCA pumps. In contrast, AtECA1, another ECA, is insensitive to TG up to 3 μM (Liang and Sze, 1998). Coincidentally, *in vitro* pollen tube growth is also inhibited by CPA and TG, both at comparable concentrations to those inhibit AtECA1 or animal SERCAs. Since AtECA3 is the only known plant Ca^{2+} pump that is sensitive to TG, the inhibition of pollen tube growth by TG may actually reflect the role of TG-sensitive AtECA3, which also phenocopies genetic studies on AtECA3 mutants. In addition, a Ca^{2+} pumping activity was found from the Golgi membrane fraction in pea, which is sensitive to TG (Ordenes et al., 2002), also supporting AtECA3 as a TG-sensitive Golgi

Ca²⁺ pump. To my knowledge, AtECA3 is the first plant Ca²⁺ pump that is sensitive to thapsigargin. This discovery could aid dissecting the roles of Ca²⁺ in plant cells by pharmaceutical manipulation.

1.5. Protein secretion is affected by a Golgi Ca²⁺ pump, AtECA3

Golgi luminal Ca²⁺, maintained at millimolar levels by transporters like AtECA3, could function as releasable store during signaling events, and nurture protein processing, sorting and secretion. Insufficient Ca²⁺ loading capability on Golgi membranes could therefore compromise exocytosis. Surprisingly, a significant enhancement in protein secretion was observed in *Ateca3* roots by monitoring the total protein and peroxidase activities in root apoplasts. Given the dual roles of AtECA3 in maintaining low [Ca²⁺]_{cyt} and high [Ca²⁺]_{lum}, this enhancement could indicate either the [Ca]_{cyt}-elicited vesicle fusion during exocytosis is deregulated, or protein modification and sorting is impaired, or both in the AtECA3 mutants. Coincidentally, AtECA3 is highly expressed in cell types like vascular tissues and pollen grains, all with extensive secretion activities. These results suggest that AtECA3 function is irreplaceable in regulating protein processing, sorting and secretion, consistent with the roles of animal Golgi Ca²⁺ pumps in similar processes.

2. FUTURE DIRECTIONS

With the extensive characterization of AtECA3 functions in this study and AtECA1 in previous studies, it is now becoming clear that each ECA gene may carry out a distinct spectrum of cellular functions depending on their tissue expression, membrane location, biochemical properties, and interacting partners, which coincides with the

diverse roles of Ca^{2+} found in plant cells. However, several questions still remain. First, does the Golgi Ca^{2+} pump, AtECA3, alter the shape or frequency of cytosolic Ca^{2+} dynamics in plant cells? Why did multiple ECA/SERCA genes evolve in multicellular organisms, like higher plants? And how is each individual ECA gene placed in its tissue, cellular, and subcellular contexts?

2.1. To study how Ca^{2+} dynamics are controlled by AtECA3

AtECA3 function is irreplaceable in pollen tube growth, in which the progress of the Ca^{2+} dynamics plays an essential role. Therefore, the pollen tube is a good system to test how Ca^{2+} dynamics are controlled by AtECA3 by using genetic and pharmaceutical approaches. For example, pollen tube growth of *Arabidopsis* mutants, either defective in or overexpressing AtECA3, can be compared with that of the *wildtype* to understand how Ca^{2+} dynamics are affected by AtECA3 function. Thapsigargin (TG) is also a good inhibitor to dissect the contribution of AtECA3 function to tube growth from CPA-sensitive Ca^{2+} pump activities.

2.2. To study the significance of multiple ECA/SERCA in multicellular organisms

With the recent technical advances and progress in genome sequencing and transcriptome profiling, it is now amenable to study why multiple ECA/SERCA Ca^{2+} ATPases have invariably evolved with such complexity in cell differentiation in different organisms. Tissue expression, membrane location, transport activity, and regulation have been profiled experimentally for Ca^{2+} pumps of this type in plants (from this study, e.g.), animal and yeast. These discriminative features among these known pumps can be ascribed to their homologs in other organisms by bioinformatic analyses and

transcriptome profiling. Conclusions from these studies will help understand what strategies of Ca^{2+} control on endomembranes have been used in life to cope with respective programs of growth, development and adaptation.

2.3. To identify the regulators of ECA pumps

Mammalian SERCA activity is regulated by a small membrane protein phospholamban (PLN). This mechanism could be conserved in plants because the high similarity of AtECA3 and SERCA in sequence and transport activity suggest this type of Ca^{2+} pump may have evolved before the divergence of metazoan and planta. However, it is difficult to identify the plant homologs of animal PLN by bioinformatic approaches even after annotation of the complete *Arabidopsis* genome, partly because of the poor conservation and high variability of animal PLN. An attempt in this study identified an expressed gene in *Arabidopsis* genome akin to animal PLN, which may serve as a putative regulator of AtECA pumps, in particular AtECA3. This hypothesis could be tested in yeast because the functional study of AtECAs has well established in a heterologous expression system in yeast.

A different approach is equally amenable. By expressing of the full or partial protein of one AtECA as bait (the loop between TM4 and 5, for example), cDNA libraries prepared from the tissues where the AtECA is expressed, can be used as prey to fish out the physical interaction partners. The yeast two-hybrid systems have been developed successfully for studying interactions between both soluble protein and membrane protein.

2.4. To determine the biological functions of AtECA2

AtECA2 is the least known ECA in *Arabidopsis*. In this study, I have demonstrated that AtECA2 expression is rich in vascular tissues only at various body parts by promoter::GUS. The AtECA2 cDNA could not be cloned, probably because it is toxic to *E. coli*. However, several interesting features can be inferred from results in this dissertation and previous studies. AtECA2 expression is highly sensitive and the most responsive among the 4 AtECAs to various stimuli, such as the inhibitor of cellulose synthesis. A tomato homolog of AtECA2, LCA1, has 2 alternatively spliced transcripts and two proteins that are located on the vacuole and the PM membrane, respectively (Wimmers et al., 1992; Ferrol and Bennett, 1996). In addition, a nuclear-localization signal was also found on AtECA2, although uncommon for proteins with multiple transmembrane spans, suggesting AtECA2 may be associated with nuclear membranes. These data suggest that AtECA2 may represent another interesting Ca^{2+} pump with novel features. To understand the biological functions of AtECA2, similar approaches used in this dissertation, can be applied to determine its membrane location, transport activity, and the roles in whole plants.

2.5. To identify Ca^{2+} -permeable channels in higher plants

The molecular identity of Ca^{2+} channels is least understood. Many genes encoding putative Ca^{2+} channels in *Arabidopsis* are predicted by sequence similarity to animal homologs. However, few have been characterized as bona fide channels mediating Ca^{2+} because functional evidence of Ca^{2+} conductance is lacking. Because Ca^{2+} channels are likely to be gated by chemical and physical stimuli, their recessive alleles may not be identified through genetic approaches. On the other hand,

constitutively active Ca^{2+} -conducting channels will be detrimental to plant cells. Here I propose 2 approaches.

To identify a constitutively active Ca^{2+} -permeable channel, a transgenic *Arabidopsis* line hosting a luminescent $[\text{Ca}^{2+}]_{\text{cyt}}$ reporter, such as the aequorin variants (Gao et al., 2004), may be used to generate ethylmethanesulfonate-mutagenized seeds. The mutant seeds can then be screened on medium containing low Ca^{2+} (0.01 mM) and normal Ca^{2+} (3 mM). The root growth of desired mutants can be scored as normal or better on low Ca^{2+} but impaired on normal Ca^{2+} . The desired impairment in Ca^{2+} homeostasis of the mutants can be verified by observing the signal luminescence of $[\text{Ca}^{2+}]_{\text{cyt}}$ reporter. Other phenotypes, such as constantly closed stomata (elevation of $[\text{Ca}^{2+}]_{\text{cyt}}$ in guard cells), can also be scored and verified in this assay.

Confirmation of Ca^{2+} conductance is challenging for channels because channels are strictly gated and may form complexes with other proteins to be functional. To circumvent this situation, electrophysiology can be done using cells from aforementioned *Arabidopsis* constitutively active mutants.

2.6. To identify the processed apoplastic protein that mediate intercellular communication

Protein processing and sorting are important for plant growth and reproduction by affecting protein export under various conditions, as suggested in this dissertation and previous studies. In particular, small peptide ligands encoded by the nuclear genome and processed by proteolysis in secretory compartments, are crucial components in intercellular communication and involved in neuron functions that cause human disease (LaFerla, 2002) or in plant meristem maintenance (Ito et al., 2006; Kondo et al., 2006).

These ligands may play important roles in pollen tube guidance, cell differentiation, and cell identity maintenance. However, it is hard to identify the genes encoding such ligands because of high sequence variability and probably extensive posttranslational modification.

To approach this question, *Arabidopsis* pollen of high homogeneity can be used for proteomic analyses of the small peptides present in the wall space (Holmes-Davis et al., 2005). Once identified, the genes encoding these peptides can be studied by genetic approaches, such as phenotyping the mutants deficient and excessive of their functions. In addition, these peptides can be easily synthesized, and applied to a pollen germination system for their effects on pollen germination, tube elongation, tube guidance, and discharge of sperm cells. The targets of these ligands can be identified by searching for genetic enhancer or suppressor of the mutants, or by yeast two-hybrid split ubiquitin systems using a cDNA library prepared from carpels or pollen grains.

In conclusion, I have demonstrated that plants have a Golgi Ca^{2+} -ATPase whose function is irreplaceable for vegetative growth and male fertility. The study in this dissertation not only contributes to our understanding of the importance of Golgi Ca^{2+} control in the secretory pathway in higher plants, but also opens the possibility that Golgi Ca^{2+} serves as a releasable store to shape Ca^{2+} signals that regulate other cellular processes in higher plants.

APPENDICES

A. RESULTS

1. Sequences of cloned ECA cDNA

Fig. App-1a. Sequence of partial cDNA clone ECA2-3 (Accession No. DQ989373).

The clone lacks 843 b encoding the N terminal region. The first ATG corresponds to bases 844-46 of the predicted full length cDNA. No. on right refers to residue number. Nucleotide position is numbered at left.

```

      M I N Y K N F V S W D V V D G Y K P V N      20
1  ATGA T A A A C T A C A A G A A C T T T G T T T C T T G G G A T G T T G T G G A T G G C T A T A A A C C T G T G A A T
      I K F S F E K C T Y Y F K I A V A L A V      40
61 A T C A A G T T T T C A T T C G A G A A A T G T A C T T A C T A C T T C A A A A T C G C T G T T G C T C T C G C A G T G
      A A I P E G L P A V I T T C L A L G T R      60
121 G C A G C G A T A C C C G A G G G T T T A C C C G C T G T G A T C A C G A C A T G T T T A G C T T T A G G G A C G A G G
      K M A Q K N A I V R K L P S V E T L G C      80
181 A A A A T G G C G C A G A A G A A C G C G A T A G T G A G G A A G C T C C C G A G T G T A G A G A C A C T C G G T T G C
      T T V I C S D K T G T L T T N Q M S A T      100
241 A C A A C T G T G A T C T G T T C A G A T A A A A C C G G G A C T T T A A C A A C A A A C C A G A T G T C T G C A A C C
      E F F T L G G K T T T T R V F S V S G T      120
301 G A A T T C T T C A C A T T A G G C G G T A A A A C A A C G A C T A C T C G A G T G T T T T C A G T C A G T G G T A C G
      T Y D P K D G G I V D W G C N N M D A N      140
361 A C T T A T G A T C C T A A A G A T G G T G G A A T T G T G G A T T G G G G C T G C A A C A A T A T G G A T G C T A A C
      L Q A V A E I C S I C N D A G V F Y E G      160
421 T T G C A A G C T G T T G C T G A G A T A T G T T C A A T T T G T A A T G A T G C T G G A G T G T T C A T G A A G G G
      K L F R A T G L P T E A A L K V L V E K      180
481 A A G T T G T T T A G A G C A A C A G G T T T G C C T A C A G A A G C A G C A T T G A A A G T T C T T G T T G A G A A G
      M G I P E K K N S E N I E E V T N F S D      200
541 A T G G T A T C C C G G A G A A G A A C A G A C A T T G A G A A C T C G A G G A A G T T A C A A A C T T T T C A G A C
      N G S S V K L A C C D W W N K R S K K V      220
601 A A T G G T A G C T C A G T G A A G C T A G C T T G T T G C G A T T G G T G G A A C A A A A G A T C G A A A A A G G T A
      A T L E F D R V R K S M S V I V S E P N      240
661 G C G A C A T T A G A G T T T G A T C G C G T T C G T A A G T C C A T G A G T G T T A T T G T G A G C G A A C C A A A T
      G Q N R L L V K G A A E S I L E R S S F      260
721 G G A C A A A A C C G G C T T C T C G T T A A G G G T G C T G C T G A G A G T A T A C T T G A G A G A A G T T C T T T T
      A Q L A D G S L V A L D E S S R E V I L      280
781 G C A C A G C T T G C T G A T G G A T C T C T T G T A G C T T T A G A T G A A T C T A G C A G A G A A G T A A T C C T T
      K K H S E M T S K G L R C L G L A Y K D      300
841 A A G A A A C A T T C T G A A A T G A C T T C A A A A G G A T T A A G A T G T T T A G G A T T A G C T T A C A A A G A C
      E L G E F S D Y S S E E H P S H K K L L      320
901 G A A T T A G G A G A G T T T T C G G A T T A C T C T T C C G A A G A A C A T C C T T C A C A C A A G A A G C T T T T G
      D P S S Y S N I E T N L I F V G V V G L      340
961 G A C C C T T C T A G C T A T T C G A A C A T C G A A A C A A A T C T A A T C T T T G T T G G A G T T G T T G G T C T A
      R D P P R E E V G R A I E D C R D A G I      360
1021 A G G G A T C C T C C G C G T G A A G A A G T T G G A A G A G C A A T T G A A G A T T G C A G A G A C G C A G G G A T A
      R V M V I T G D N K S T A E A I C C E I      380

```

1081 AGAGTAATGGTTATAACTGGAGATAACAAATCAACAGCTGAAGCTATTTGTTGTGAAATT
 R L F S E N E D L S Q S S F T G K E F M 400
 1141 AGATTGTTTTTCGGAGAATGAAGATCTTTCGCAGAGTAGCTTCACTGGTAAAGAGTTTATG
 S L P A S R R S E I L S K S G G K V F S 420
 1201 TCTCTTCCGGCTTCACGGAGATCCGAGATTCTGTCAAAAATCTGGAGGGAAAAGTGTCTCT
 R A E P R H K Q E I V R M L K E M G E I 440
 1261 CGAGCTGAGCCAAGGCATAAGCAAGAAATCGTTAGGATGCTTAAGGAAAATGGGAGAAAATA
 V A M T G D G V N D A P A L K L A D I G 460
 1321 GTTGCCATGACAGGTGATGGTGTGAATGATGCTCCTGCTTTGAAACTTGCTGACATTGGT
 I A M G I T G T E V A K E A S D M V L A 480
 1381 ATCGCCATGGGAATCACTGGAAGTGGCAAAAGAAGCTTCGGATATGGTTCTTGCA
 D D N F S T I V S A V A E G R S I Y N N 500
 1441 GATGATAATTTTCAGTACTATAGTATCAGCTGTAGCAGAAGGTCGGTCCATTTACAACAAT
 M K A F I R Y M I S S N V G E V I S I F 520
 1501 ATGAAAAGCTTTTATCAGGTATATGATATCATCAAACGTTGGAGAAGTAATCTCCATCTTC
 L T A A L G I P E C M I P V Q L L W V N 540
 561 TTAACCGCGGCATTGGGGATACCGGAATGTATGATAACCGGTTTCAGCTTCTTTGGGTTAAT
 L V T D G P P A T A L G F N P A D I D I 560
 1621 CTTGTAAGTATGATGGTCTCCTGCTACTGCGTTAGGCTTCAATCCAGCTGATATTGATATC
 M K K P P R K S D D C L I D S W V L I R 580
 1681 ATGAAGAAGCCACCCCGAAAAGCGATGATTGTCTCATTGATTGATGGGTTCTTATTTCGA
 Y L V I G S Y V G V A T V G I F V L W Y 600
 1741 TATCTAGTGATTGGTTCTTATGTTGGAGTTGCAACTGTTGGAATCTTTGTCTTGTGGTAC
 T Q A S F L G I S L I S D G H T L V S F 620
 1801 ACACAAGCTTCATTCCCTTGGGATTAGCCTAATCTCAGATGGACACACATTGGTTAGCTTC
 T Q L Q N W S E C S S W G T N F T A T P 640
 1861 ACTCAGCTTCAGAAGTGGTCAGAGTGTCTTCGTGGGGAACGAACTTCACGGCGACTCCT
 Y T V A G G L R T I A F E N N P C D Y F 660
 1921 TACACAGTCGCAGGTGGTCTTAGGACCATCGCGTTTGAGAACAATCCTTGCATTACTTC
 T L G K V K P M T L S L T V L V A I E M 680
 1981 ACTCTCGGGAAAGTCAAGCCAATGACATTATCACTCACCGTTCTTGTGGCTATCGAAATG
 F N S L N A L S E D N S L L T M P P W R 700
 2041 TTTAACTCGCTGAACCGGTTGTCTGAAGACAACAGTCTCTTAACGATGCCACCATGGAGA
 N P W L L V A M T V S F A L H C V I L Y 720
 2101 AACCCCTGGCTACTAGTGGCCATGACTGTCTCCTTTGCGCTACACTGTGTCATCCTCTAT
 V P F L A N V F G I V P L S F R E W F V 740
 2161 GTTCTTTCTTAGCTAATGTGTTGGGATTGTGCCTTTGAGTTTCAGGGAATGGTTTGTG
 V I L V S F P V I L I D E A L K F I G R 760
 2221 GTTATTCTTGTTCCTTCCCTGTGATTCTGATCGATGAAGCTCTCAAGTTCATTGGGAGA
 C R R T R I K K K I K T M * 780
 2281 TGCAGAAGGACAAGAATCAAGAAGAAGATCAAGACAATGTAA

Fig. App-1b. Sequence of partial cDNA clone ECA2-9 (Accession No. DQ989374).

TCT corresponds to position 2675-77 of predicted full length cDNA. Predicted protein is missing the C terminus. No. on right refers to residue number. Nucleotide position is numbered at left.

```

      M E E E K S F S A W S W S V E Q C L K E      20
1  ATGGAGGAGGAGAAGTCGTTCTCGGCCTGGTCTTGGTCTGTTGAGCAATGTTTGAAAGAG
      Y K T R L D K G L T S E D V Q I R R Q K      40
61 TACAAGACAAGATTAGACAAGGGTTTAACTAGCGAAGATGTCCAAATCCGCCGTCAAAG
      Y G F N E L A K E K G K P L W H L V L E      60
121 TACGGTTTTTAACGAGCTTGCTAAGGAGAAAGGCAAGCCTTTATGGCATCTTGTATTGGAA
      Q F D D T L V K I L L G A A F I S F V L      80
181 CAATTCGACGATACGCTTGTGAAGATTCTTCTCGGTGCTGCGTTTATCTCTTTTCGTTTTA
      A F L G E E H G S G S G F E A F V E P F      100
241 GCCTTTTTTAGGTGAGGAACACGGCTCAGGTTTCAGGGTTCGAGGCCTTTGTTGAGCCTTTT
      V I V L I L I L N A V V G V W Q E S N A      120
301 GTGATTGTTTTGATTCTGATTTTAAACGCTGTGGTGGTGTGTGGCAAGAGAGTAATGCT
      E K A L E A L K E M Q C E S A K V L R D      140
361 GAGAAAGCACTTGAGGCTCTTAAAGAGATGCAATGTGAATCTGCAAAGTTTTGAGAGAT
      G N V L P N L P A R E L V P G D I V E L      160
421 GGGAAATGTGTTGCCTAATTTGCCTGCTAGAGAGCTTGTTCAGGGGATATTGTGGAGTTA
      N V G D K V P A D M R V S G L K T S T L      180
481 AATGTAGGAGATAAAGTCCCTGCTGATATGAGAGTTTCCGGTTTTGAAAACATCCACTTTA
      R V E Q S S L T G E A M P V L K G A N L      200
541 AGAGTCGAGCAAAGCTCGTTAACCGGTGAAGCAATGCCGGTTTTGAAAGGAGCGAATCTT
      V V M D D C E L Q G K E N M V F A G T T      220
601 GTAGTCATGGATGATTGTGAAGTGAAGGAAAATATGGTTTTTCGCTGGAACAACG
      V V N G S C V C I V T S I G M D T E I G      240
661 GTTGTTAACGGAAGCTGCGTTTGCATTGTGACAAGTATAGGTATGGATACGGAGATCGGG
      K I Q R Q I H E A S L E E S E T P L K K      260
721 AAAATCCAGAGACAGATTCACGAGGCGTCGCTTGAAGAGAGCGAGACTCCGTTAAAGAAG
      K L D E F G S R L T T A I C I V C V L V      280
781 AAGCTAGACGAGTTTGGGAGTAGATTGACTACAGCTATTTGCATTGTCTGTGTTCTTGTG
      W M I N Y K N F V S W D V V D G Y K P V      300
841 TGGATGATAAACTACAAGAACTTTGTTTCTTGGGATGTTGTGGATGGCTATAAACCTGTG
      N I K F S F E K C T Y Y F K I A V A L A      320
901 AATATCAAGTTTTTCATTTCGAGAAATGTACTTACTACTTCAAATCGCTGTTGCTCTCGCA
      V A A I P E G L P A V I T T C L A L G T      340
961 GTGGCAGCGATACCCGAGGGTTTACCCGCTGTGATCACGACATGTTTAGCTTTAGGGACG
      R K M A Q K N A I V R K L P S V E T L G      360
1021 AGGAAAATGGCGCAGAAGAACGCGATAGTGAGGAAGCTCCCGAGTGTAGAGACACTCGGT
      C T T V I C S D K T G T L T T N Q M S A      380
1081 TGCACAACGTGATCTGTTTCAGATAAAACCGGGACTTTAACAACAACAGATGTCTGCA
      T E F F T L G G K T T T T R V F S V S G      400
1141 ACCGAATTCCTCACATTAGGCGGTAACAACGACTACTCGAGTGTTCAGTCAGTGGT
      T Y D P K D G G I M D W G C N N M D A      420
1201 ACGACTTATGATCCTAAAGATGGTGAATTATGGATTGGGGCTGCAACAATATGGATGCT
      N L Q A V A E I C S I C N D A G V F Y E      440
1261 AACTTGCAAGCTGTTGCTGAGATATGTTCAATTTGTAATGATGCTGGAGTGTTCATGAA
      G K L F R A T G L P T E A A L K V L V E      460
1321 GGGAAAGTTGTTTAGAGCAACAGTTTTGCCTACAGAAGCAGCATTGAAAGTTCTTGTGAG
      K M G I P E K K N S E N I E E V T N F S      480
1381 AAGATGGGTATCCCGGAGAAGAAGAACAGTGAGAACATCGAGGAAGTTACAACTTTTCA

```

D N G S S V K L A C C D W W N K R S K K 500
 1441 GACAATGGTAGCTCAGTGAAGCTAGCTTGTTCGATTGGTGGAAACAAAAGATCGAAAAAG
 V A T L E F D R V R K S M S V I V S E P 520
 1501 GTAGCGACATTAGAGTTTTGATCGCGTTTCGTAAGTCCATGAGTGTTATTGTGAGCGAACCA
 N G Q N R L L V K G A A E S I L E R S S 540
 1561 AATGGACAAAACCGGCTTCTCGTTAAGGGTGCTGCTGAGAGTATACTTGAGAGAAGTTCT
 F A Q L A D G S L V A L D E S S R E V I 560
 1621 TTTGCACAGCTTGCTGATGGATCTCTTGTAGCTTTAGATGAATCTAGCAGAGAAGTAATC
 L K K H S E M T S K G L R C L G L A Y K 580
 1681 CTTAAGAAACATTCTGAAATGACTTCAAAGGATTAAGATGTTTAGGATTAGCTTACAAA
 D E L G E F S D Y S S E E H P S H K K L 600
 1741 GACGAATTAGGAGAGTTTTTCGGATTACTCTTCCGAAGAACATCCTTCACACAAGAAGCTT
 L D P S S Y S N I E T N L I F V G V V G 620
 1801 TTGGACCTTCTAGCTATTTCGAACATCGAAACAAATCTAATCTTTGTTGGAGTTGTTGGT
 L R D P P R E E V G R A I E D C R D A G 640
 1861 CTAAGAGATCCTCCGCGTGAAGAAGTTGGAAGAGCAATTGAAGATTGCAGAGACGCAGGG
 I R V M V I T G D N K S T A E A I C C E 660
 1921 ATAAGAGTAATGGTTATAACTGGAGATAACAAATCAACAGCTGAAGCTATTTGTTGTGAA
 I R L F S E N E D L S Q S S F T G K E F 680
 1981 ATTAGATTGTTTTTCGGAGAATGAAGATCTTTCGCAGAGTAGCTTCACTGGTAAAGAGTTT
 M S L P A S R R S E I L S K S G G K V F 700
 2041 ATGTCTCTTCCGGCTTCACGGAGATCCGAGATTCTGTCAAATCTGGAGGGAAAGTGTTTC
 S R A E P R H K Q E I V R M L K E M G E 720
 2101 TCTCGAGCTGAGCCAAGGCATAAGCAAGAAATCGTTAGGATGCTTAAGGAAATGGGAGAA
 I V A M T G D G V N D A P A L K L A D I 740
 2161 ATAGTTGCCATGACAGGTGATGGTGTGAATGATGCTCCTGCTTTGAAACTTGCTGACATT
 G I A M G I T G T E V A K E A S D M V L 760
 2221 GGTATCGCCATGGGAATCACTGGAAGTGGAGTTGCCAAAGAAGCTTCGGATATGGTTCTT
 A D D N F S T I V S A V A E G R S I Y N 780
 2281 GCAGATGATAATTTTCAGTACTATAGTATCAGCTGTAGCAGAAGGTTCGGTCCATTTACAAC
 N M K A F I R Y M I S S N V G E V I S I 800
 2341 AATATGAAAGCTTTTTATCAGGTATATGATATCATCAAACGTTGGAGAAGTAATCTCCATC
 F L T A A L G I P E C M I P V Q L L W V 820
 2401 TTCTTAACCGCGCATTGGGGATACCGGAATGTATGATACCGGTTTCAGCTTCTTTGGGTT
 N L V T D G P P A T A L G F N P A D I D 840
 2461 AATCTTGTAAGTATGATGGTCTCCTGCTACTGCGTTAGGCTTCAATCCAGCTGATATTGAT
 I M K K P P R K S D D C L I D S W V L I 860
 2521 ATCATGAAGAAGCCACCCCGCAAAGCGATGATTGTCTCATTGATTCATGGGTTCTTATT
 R Y L V I G S Y V G V A T V G I F V L W 880
 2581 CGATATCTAGTGATTGGTTCTTATGTTGGAGTTGCAACTGTTGGAATCTTTGTCTTGTGG
 Y T Q A S F L G I S L I 900
 2641 TACACACAAGCTTCATTCCTTGGGATTAGCCTAATCT

Fig. App-1c. Full-length cDNA sequence of AtECA3 (clone name: ECA3-12-1, Accession No. AY650902). No. on right refers to residue number. Nucleotide position is numbered at left.

```

M E D A Y A R S V S E V L D F F G V D P 20
1 ATGGAAGACGCCTACGCCAGATCTGTCTCAGAGGTGCTTGATTTCTTTGGGGTAGACCCA
  T K G L S D S Q V V H H S R L Y G R N V 40
61 ACAAAGGGTCTTTCTGATTCTCAGGTTGTTTCATCATTCCAGGCTTTATGGCAGGAATGTA
  L P E E K R T P F W K L V L K Q F D D L 60
121 CTGCCTGAAGAGAAAAGAACGCCATTCTGGAAACTGGTTCTGAAACAGTTTGATGATTTA
  L V K I L I V A A I V S F V L A L A N G 80
181 CTTGTCAAGATATTGATTGTGGCTGCAATTGTTTCTTTTCGTATTGGCTTTGGCTAATGGA
  E T G L T A F L E P F V I L L I L A A N 100
241 GAGACTGGTTTAAACAGCATTCTGGAGCCTTTTGTCACTCTGCTGATATTGGCTGCAAAT
  A A V G V I T E T N A E K A L E E L R A 120
301 GCGGCAGTGGGGGTGATCACGGAGACTAATGCTGAGAAGGCTCTTGAGGAGCTACGTGCC
  Y Q A N I A T A V L R N G G C F S I L P A T 140
361 TACCAQACAAATATAGCTACAGTGTGCGAAATGGGTGCTTCTCTATCCTACCAGCAACA
  E L V P G D I V E V A T V G C K I P A D L 160
421 GAGCTGGTTCCAGGCGACATTGTTGAAGTTACTGTGGGATGTAAGATTCCAGCTGACCTG
  R M I E M S S N T F R V D Q A I L T G E 180
481 AGGATGATTGAGATGTCTAGCAATACGTTTCGAGTTGATCAAGCCATTCTAACTGGTGAA
  S C S V E K D V D C T L T T N A V Y Q D 200
541 AGCTGTTCCGTGGAAAAAGATGTTGACTGTACTTTAACAACAAATGCTGTCTACCAAGAC
  K K N I L F S G T D V V A G R G R A V V 220
601 AAGAAAAATATTTTTATTTTCGGGAAGTGTGGTTCGCGGGTAGGGGAAGGGCTGTTGTC
  I G V G S N T A M G S I H D S M L Q T D 240
661 ATTGAGTTGGTTCAAACACCGCAATGGGTAGCATAACGATTCTATGTTGCAGACAGAT
  D E A T P L K K K L D E F G S F L A K V 260
721 GATGAGGCAACTCCATTGAAAAAGAAGCTGGACGAGTTTGGCAGCTTTTTGGCTAAGGTA
  I A G I C V L V W V V N I G H F S D P S 280
781 ATTGCGGGTATTTGTGTACTTGTGTGGGTTGTCAACATTGGTCACCTCAGTGACCCTTCT
  H G G F F K G A I H Y F K I A V A L A V 300
841 CATGGTGGATTTTTTAAAGGCGCAATTCACTATTTTAAAGATTGCAGTTGCCCTTGCTGTT
  A A I P E G L P A V V T T C L A L G T K 320
901 GCAGTATTCCTGAAGGACTTCCTGTCTGTGACAACTGTTTAGCTTTGGAACAAA
  K M A R L N A I V R S L P S V E T L G C 340
961 AAAATGGCTCGTTTGAATGCTATTGTACGGTCATTACCATCTGTGAGACGCTTGGGTGC
  T T V I C S D K T G T L T T N M M S V S 360
1021 ACTACTGTAATTTGCAGTGACAAGACTGGAACATTGACAACCAATATGATGTCGGTGTCT
  K I C V V Q S A E H G P M I N E F T V S 380
1081 AAGATATGTGTAGTCCAATCTGCAGAGCATGGTCCTATGATTAATGAATTCAGTGTAGT
  G T T Y A P E G T V F D S N G M Q L D L 400
1141 GGGACAACCTTATGCACCAGAAGGTACCGTCTTTGACAGCAATGGGATGCAGCTTGACTTA
  P A Q S P C L H H L A M C S S L C N D S 420
1201 CCTGCTCAGTCACCTTGCCTTCATCATTTAGCAATGTGTTTCATCACTCTGCAATGACTCC
  I L Q Y N P D K D S Y E K I G E S T E V 440
1261 ATCTTGCAATACAATCCAGATAAGGATTCTTATGAAAAAATTGGAGAGTCAACTGAAGTT
  A L R V L A E K V G L P G F D S M P S A 460
1321 GCTCTTCGAGTTCTTGAGAAAAGGTTGGGCTCCCTGGTTTTGATTCAATGCCTTCTGCT
  L N M L S K H E R A S Y C N H Y W E N Q 480
1381 CTAACATGTTGAGCAAGCATGAACGTGCATCATATTGCAACCATTATTGGGAAAACCAA
  F K K V Y V L E F T R D R K M M S V L C 500
1441 TTCAAAAAGGTTTATGTTTTGGAGTTTACTCGTGACCGAAAAATGATGAGCGTCCCTATGT
  S H K Q M D V M F S K G A P E S I I A R 520

```

1501 AGCCATAAGCAAATGGATGTTATGTTCTCAAAGGGTGCTCCAGAGAGTATAATAGCTAGG
C N K I L C N G D G S V V P L T A A G R 540
1561 TGTAATAAAATTTCTCTGCAACGGTGATGGTTCTGTTGTTCCCTCTAACTGCTGCTGGCCGT
A E L E S R F Y S F G D E T L R C L A L 560
1621 GCAGAGCTTGAGTCGAGGTTTTACAGTTTTGGCGATGAAACATTGAGATGCTTAGCATT
A F K T V P H G Q Q T I S Y D N E N D L 580
1681 GCATTTAAGACCGTGCCCCACGGTCAACAACTATTTCCCTATGATAATGAGAACGACCTG
T F I G L G M L D P P R E E V R D A M L 600
1741 ACGTTTATTGGGTTGGGAATGCTTGATCCACCAAGAGAAGAAGTGAGAGATGCTATGCTT
A C M T A G I R V I V V T G D N K S T A 620
1801 GCGTGTATGACTGCTGGGATACGTGTTATAGTTGTTACTGGGGATAACAAGTCCACAGCA
E S L C R K I G A F D N L V D F S G M S 640
1861 GAGTCACTATGTAGAAAAATAGGGGCTTTTTGACAATCTGGTAGACTTTTTCTGGTATGTCC
Y T A S E F E R L P A V Q Q T L A L R R 660
1921 TACACCGCTTCTGAATTTGAACGGCTTCCAGCAGTGCAGCAAACCTCTAGCATTGCGACGG
M T L F S R V E P S H K R M L V E A L Q 680
1981 ATGACACTTTTTTCCAGGGTTGAACCTTCCCACAAAAGGATGCTTGTGGAAGCCCTACAG
K Q N E V V A M T G D G V N D A P A L K 700
2041 AAACAAAACGAAGTGGTGGCAATGACTGGTGTATGGCGTTAATGATGCCCTGCATTGAAG
K A D I G I A M G S G T A V A K S A S D 720
2101 AAAGCTGACATTGGGATTGCCATGGGTTCTGGAACAGCTGTAGCAAAGAGTGCCTCAGAT
M V L A D D N F A S I V A A V A E G R A 740
2161 ATGGTTTTGGCTGATGATAATTTTTGCTTCAATAGTTGCGGCTGTTGCAGAAGGAAGGGCT
I Y N N T K Q F I R Y M I S S N I G E V 760
2221 ATATATAATAACACAAAGCAATTCATTAGATACATGATTTCTTCAAATATAGGGGAAGTG
V C I F V A A V L G I P D T L A P V Q L 780
2281 GTCTGTATATTTGTTGCAGCTGTACTGGGAATCCCTGATACCTTGGCACCTGTTCAACTT
L W V N L V T D G L P A T A I G F N K Q 800
2341 CTGTGGTCAATTTGGTAACAGATGGATTGCCACTGCCATTGGCTTTAATAAACA
D S D V M K A K P R K V G E A V V T G W 820
2401 GATTCGATGTTATGAAGGCAAAACCCCGAAAGGTTGGTGAAGCAGTGGTCACTGGGTGG
L F F R Y L V I G V Y V G L A T V A G F 840
2461 TTATTCTTCCGCTATTTGGTTATCGGAGTTTATGTGCGCCTGGCCACTGTTGCTGGCTTT
I W W F V Y S D G G P K L T Y S E L M N 860
2521 ATATGGTGGTTTGTTTACTCTGATGGTGGTCCTAACTTACTTACAGTGAAGTGAAC
F E T C A L R E T T Y P C S I F E D R H 880
2581 TTTGAACTTGGCACTTAGAGAGACAACCTATCCCTGCAGCATATTTGAGGATCGGCAC
P S T V A M T V L V V V E M F N A L N N 900
2641 CCATCTACTGTGGCTATGACAGTACTTGTGTTGTGTCGAGATGTTAATGCTCTAAATAAC
L S E N Q S L L V I T P R S N L W L V G 970
2701 CTCAGCGAAAATCAATCCCTTCTGGTTATAACCCCAAGGAGTAACTTATGGCTTGTGGT
S I I L T M L L H V L I L Y V H P L A V 940
2761 TCAATTATCCTGACGATGCTTCTGCACGTGCTAATATTATATGTTTCCACTGGCAGTC
L F S V T P L S W A E W T A V L Y L S F 960
2821 TTATTTTCTGTACGCCATTATCCTGGGCCGAGTGGACTGCTGTTCTGTATCTTTCTGTTT
P V I I I D E L L K F L S R N T G M R F 980
2881 CCAGTTATCATCATCGATGAGCTTCTGAAGTTCCCTCTCTAGAAATACAGGCATGAGATTC
R F R L R K A D L P K D R R D K * 1000
2941 AGGTTCAGATTGAGGAAGGCTGATTTACTCCCAAGGACCGGCGTGACAAGTAG

Fig. App-1d. Full-length cDNA sequence of AtECA4 (clone ECA4-4 Acc. No. DQ989372). No. on right refers to residue number. Nucleotide position is numbered at left.

```

      M G K G G E D C G N K Q T N S S E L V K      20
1  ATGGGGAAAGGAGGTGAAGATTGCGGGAATAAGCAAAC TAATAGTTCTGAATTGGTCAAG
      S D T F P A W G K D V S E C E E K F G V      40
61 TCTGATACTTTTCTGCTTGGGGTAAAGATGTGTGCGGAATGCGAAGAGAAGTTTGGTGTT
      S R E K G L S T D E V L K R H Q I Y G L      60
121 AGTCGTGAGAAAGGTTTGAGCACTGATGAGGTGTTGAAACGGCATCAGATCTATGGTTTG
      N E L E K P E G T S I F K L I L E Q F N      80
181 AATGAATTAGAGAAGCCTGAGGGTACTTCTATTTTTAAGCTGATTTTGGAACAGTTTAAT
      D T L V R I L L A A A V I S F V L A F F      100
241 GATACATTGGTTCGTATTCTTTTGGCGGCTGCTGTTATTTCCCTTTGTCTTAGCCTTCTTT
      D G D E G G E M G I T A F V E P L V I F      120
301 GATGGCGACGAAGGTGGTGGATGGGTATCACCGCATTGTTGAGCCGCTTGTATTTTT
      L I L I V N A I V G I W Q E T N A E K A      140
361 CTCATCTTGATTGTTAATGCCATTGTTGGCATCTGGCAAGAACTAATGCTGAGAAGGCG
      L E A L K E I Q S Q Q A T V M R D G T K      160
421 TTGGAAGCTTTGAAAGAGATTCAGTCTCAGCAAGCTACCGTCATGCGTGATGGGACTAAG
      V S S F P A K E L V P G D I V E L R V G      180
481 GTTTCCAGTTTCCCTGCAAAGGAGCTTGTTCCTGGTGATATTGTGGAAGTGGGGTTGGT
      D K V P A D M R V V A L I S S T L R V E      200
541 GATAAGGTGCCTGCTGATATGCGTGTGGTTGCTTTGATCAGTTCAACTTTGAGAGTCGAG
      Q G S L T G E S E A V S K T T K H V D E      220
601 CAGGGGTCCTTAACAGGAGAGAGTGAGGCAGTGAGCAAAACCACCAAGCACGTGGATGAG
      N A D I Q G K K C M V F A G T T V V N G      240
661 AATGCTGATATTCAAGGAAAGAAATGCATGGTGTGTTGCAGGAACCACTGTCGTGAATGGG
      N C I C L V T D T G M N T E I G R V H S      260
721 AACTGCATATGTTTAGTTACAGATACTGGGATGAATACTGAGATTGGAAGGGTTCAC TCA
      Q I Q E A A Q H E E D T P L K K K L V E      280
781 CAGATCCAGGAAGCTGCACAACACGAGGAAGATACCCCTCTGAAGAAAAA ACTTAAACGAG
      F G E V L T M I I G L I C A L V W L I N      300
841 TTTGGGGAAGTTCTGACTATGATCATTGGGTTAATTTGTGCGTTAGTGTGGCTCATCAAT
      V K Y F L S W E Y V D G W P R N F K F S      320
901 GTCAAATACTTTCTGTCTATGGGAGTATGTTGATGGCTGGCCCAGAACTTTAAGTTCTCC
      F E K C T Y Y F E I A V A L A V A A I P      340
961 TTCGAGAAGTGCACATATTACTTTGAGATTGCTGTTGCACTGGCGGTTGCTGCAATTCCA
      E G L P A V I T T C L A L G T R K M A Q      360
1021 GAAGGTCTGCCAGCAGTTATTACCACATGTTTGGCTCTTGGCACTAGGAAGATGGCTCAG
      K N A L V R K L P S V E T L G C T T V I      380
1081 AAGAATGCTCTGGTTAGGAAGCTACCCAGTGTGGAGACTCTTGGATGCACCACCGTGATA
      C S D K T G T L T T N Q M A V S K L V A      400
1141 TGCTCTGACAAA ACTGGA ACTCTTACAACCAATCAGATGGCTGTTTCAAAGCTCGTTGCT
      M G S R I G T L R S F N V E G T S F D P      420
1201 ATGGGTTTCGAGGATCGGAACTCTTCGATCTTTCAATGTTGAGGGGACCTCGTTTGATCCT
      R D G K I E D W P T G R M D A N L Q M I      440
1261 CGAGATGGAAAGATTGAAGATTGGCCAACGGGTCGGATGGATGCAAATCTTCAGATGATT
      A K I A A I C N D A N V E K S D Q Q F V      460
1321 GCAAAAATTGCTGCCATTTGCAACGATGCTAANTGTTGAGAAATCTGATCAGCAATTTGTG
      S R G M P T E A A L K V L V E K M G F P      480
1381 TCTAGGGGCATGCCTACTGAGGCAGCTTTGAAGGTTTTGGTTGAGAAAATGGGATTTCCC
      E G L N E A S S D G N V L R C C R L W S      500

```


1441 GAAGGATTGAATGAAGCTTCATCCGATGGCAATGTCTTACGTTGTTGTCGGCTATGGAGT
E L E Q R I A T L E F D R D R K S M G V 520

1501 GAACTAGAACAACGGATTGCCACCCTTGAGTTTGACCGTGACCGGAAATCAATGGGAGTT
M V D S S S G K K L L L V K G A V K N V 540

1561 ATGGTGGATTCCAGCTCAGGAAAGAACTGCTACTGGTCAAGGGTGCCGTAATAAATGTA
L E R S T H I Q L L D G S T R E L D Q Y 560

1621 TTGAAAGGAGTACCCATATTCAGCTACTTGATGGTTCCACTCGAGAGCTTGACCAATAC
S R D L I L Q S L H D M S L S A L R C L 580

1681 TCAAGGGATCTTATTTTACAAAGCCTACATGATATGTCCTTGAGTGCATTAAGATGTCTC
G F A Y S D V P S D F A T Y D G S E D H 600

1741 GGATTGCATACTCAGATGTTCCATCAGATTTTGCCACTTATGATGGCAGTGAAGACCAT
P A H Q Q L L N P S N Y S S I E S N L V 620

1801 CCTGCTCATCAGCAACTTCTCAACCCATCCAATTATTCATCAATTGAGTCCAATCTAGTA
F V G F V G L R D P P R K E V R Q A I A 640

1861 TTTGTTGGATTTGTTGGTTTAAAGGATCCTCCAAGGAAAGAGGTGCGTCAAGCCATTGCA
D C R T A G I R V M V I T G D N K S T A 660

1921 GACTGCAGAACAGCAGGTATTCGGGTCTGTTTATCACC GGAGACAACAAGAGCACAGCG
E A I C R E I G V F E A D E D I S S R S 680

1981 GAAGCAATCTGCCGTGAAATTGGCGTATTTGAAGCAGATGAAGATATCTCCTCGAGAAGC
L T G K E F M D V K D Q K N H L R Q T G 700

2041 TTGACAGGAAAAGAATTTATGGATGTTAAAGATCAGAAGAATCATCTAAGACAGACAGGA
G L L F S R A E P K H K Q E I V R L L K 720

2101 GGGCTCCTGTTCTCAAGGGCTGAACAAAACACAAACAAGAGATTGTCAGGTTACTGAAA
E D G E V V A M T G D G V N D A P A L K 740

2161 GAAGATGGAGAAGTGGTTGCCATGACTGGAGATGGAGTCAATGATGCTCCTGCCCTGAAG
L V D I G V A M G I S G T E V A K E A S 760

2221 TTGGTTGATATTGGTGTGGCTATGGGCATTTCCGGGACAGAGGTAGCAAAGGAGGCATCT
D L V L A D D N F S T I V A A V G E G R 780

2281 GACTTGGTGTGGCAGATGATAATTTTCAGCACCATTGTTGCAGCTGTTGGTGAAGCAGG
S I Y N N M K A F I R Y M I S S N I G E 800

2341 TCCATCTATAACAACATGAAGGCCTTCATCAGGTACATGATCTCTTCCAACATCGGTGAG
V A S I F L T A A L G I P E G M I P V Q 820

2401 GTTGCATCGATATTCTTGACAGCTGCTCTTGGAAATCCCAGAAGGCATGATACCCGTTCAA
L L W V N L V T D G P P A T A L G F N P 840

2461 CTTCTGTGGGTGAATCTCGTAACAGATGGTCCCTCCAGCTACTGCTTTGGGATTCAACCCC
P D K D I M K K P P R R S D D S L I T A 860

2521 CCTGACAAGGATATTATGAAAAAGCCTCCTCGTAGGAGCGATGACTCTCTTACTACTGCG
W I L F R Y M V I G L Y V G V A T V G V 880

2581 TGGATCCTCTTCCGCTATATGGTGATTGGTTTGTATGTGGGAGTAGCAACGGTGGGAGTA
F I I W Y T H N S F M G I D L S Q D G H 900

2641 TTCATCATATGGTACACACAACAGCTTTATGGGCATAGACCTGAGCCAAGACGGTCAC
S L V S Y S Q L A H W G Q C S S W E G F 970

2701 AGCCTTGTGAGCTATTCACAGCTCGCACATTGGGGCCAATGCTCTTCATGGGAAGGCTTC
K V S P F T A G S Q T F S F D S N P C D 940

2761 AAAGTGTCTCCTTTACAGCAGGCTCTCAGACTTTCTCGTTCGACTCAAACCCTTGCGAC
Y F Q Q G K I K A S T L S L S V L V A I 960

2821 TATTTTCAGCAGGGTAAAATCAAGGCATCCACACTCTCCCTCTCGGTGTTGGTGGCCATT
E M F N S L N A L S E D G S L V T M P P 980

2881 GAAATGTTCAACTCTCTGAATGCACTCTCAGAAGATGGCAGCCTGGTGACGATGCCACCC
W V N P W L L L A M A V S F G L H F V I 1000

2941 TGGGTTAACCCGTGGCTGCTCCTGGCAATGGCTGTCTCATTTGGACTCCACTTTGTGATA
L Y V P F L A Q V F G I V P L S L N E W 1020

3001 TTGTACGTCCCATTCTTGGCTCAGGTGTTTGGTATTGTGCCACTGAGCTTGAACGAGTGG
L L V L A V S L P V I L I D E V L K F V 1040

3061 CTGCTAGTGTGGCTGTGTGCTGCCGTAATTTTGATAGACGAAGTGCTCAAGTTTGTA
G R C T S G Y R Y S P R T P S A K Q K E 1060

3121 GGAAGGTGCACGAGTGGCTACCGCTACTCACCTCGCACTCCCTCAGCTAAGCAAAAGGAG

3181 E *
GAGTAA

2. Ion content in Mutants of AtECA

Since ECA genes are predicted to be cation transporters involved in ion uptake or detoxification, a global change in ion contents may occur when one ECA gene is disrupted. In collaboration with Harper's lab at University of Nevada at Reno, we have obtained T-DNA mutants of all AtECAs and submitted to Ionomics facility for a global examination of ion contents in aboveground parts. The results are summarized in Figure App-2.

The ion contents between different T-DNA lines of the same gene are often inconsistent mainly because the experimental conditions (plant growing conditions, etc.) are highly variable and only a global examination was conducted while most ions are compartmentalized at cellular and tissue levels. In addition, the nature of each of most mutant alleles caused by T-DNA insertion has not been experimentally clarified. Nevertheless, these results may also provide some clues to unravel the phenotypic features of AtECA mutants. For example, Ca^{2+} , Mn^{2+} , Zn^{2+} and Cu^{2+} contents are altered in all 3 AtECA3 mutant alleles when compared with those in *wildtype* grown side by side in soil.

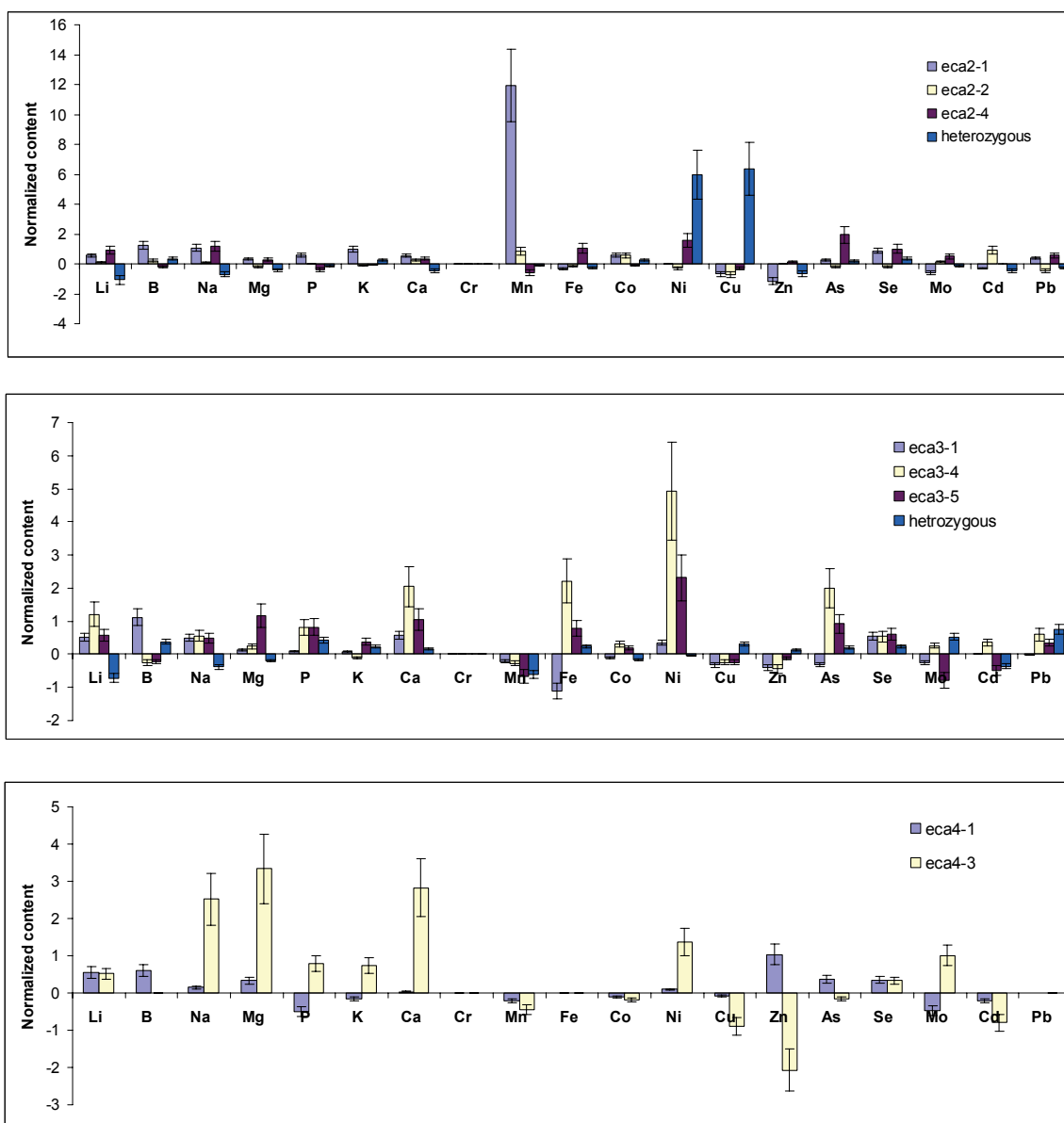
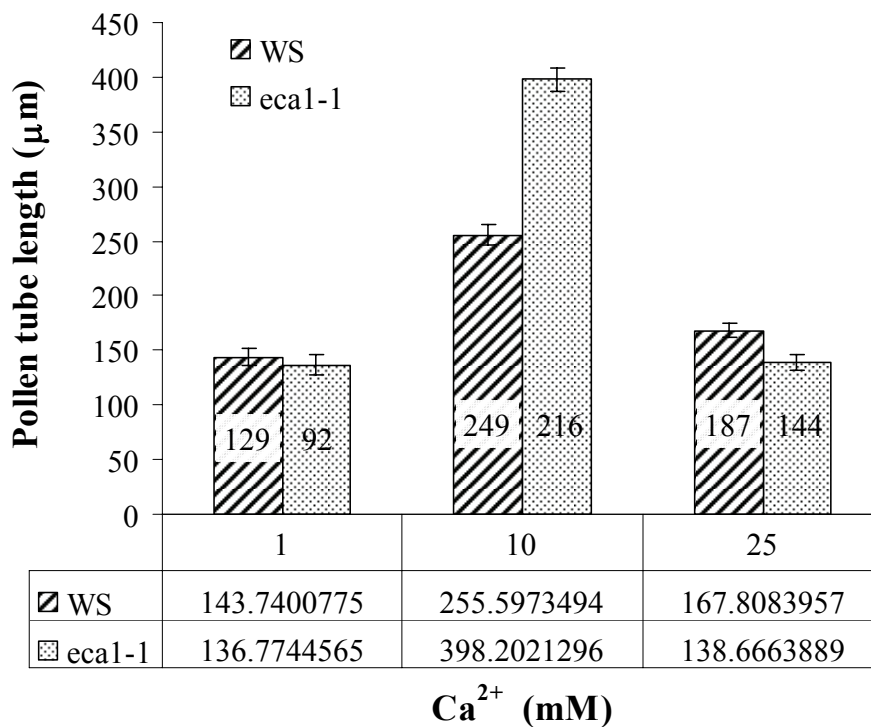


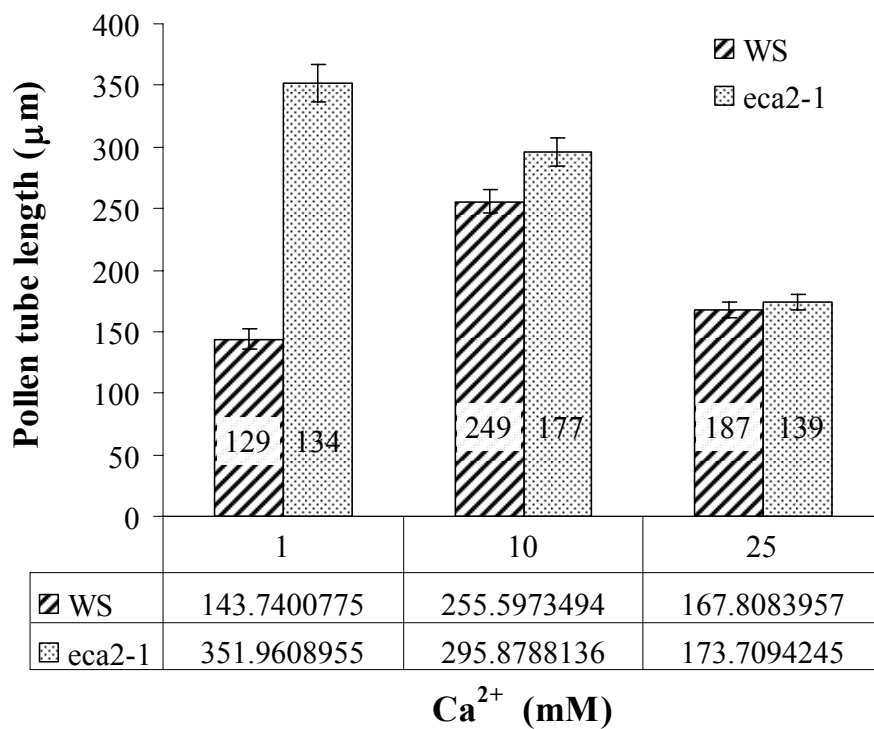
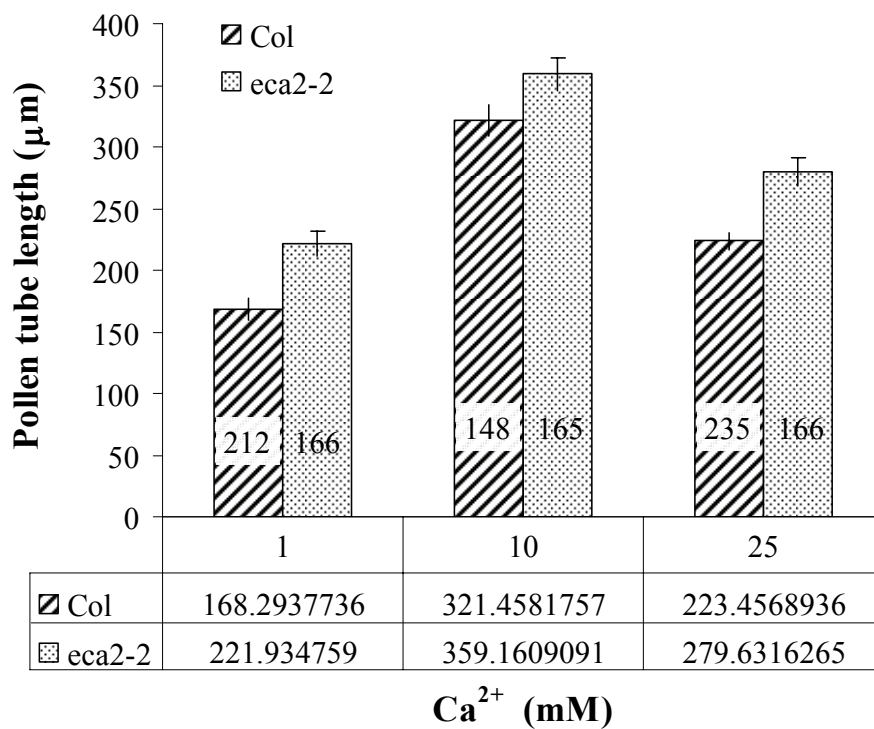
Fig. App-2. Summary of ion contents in the T-DNA mutants of *Arabidopsis* ECA genes. Data were retrieved from the *Arabidopsis* Ionomics Database. Value is the average of all available readings, error bar = *S.E.*. Ion content has been normalized to *wildtype* control.

3. Pollen germination of *eca1* and *eca2* mutants.

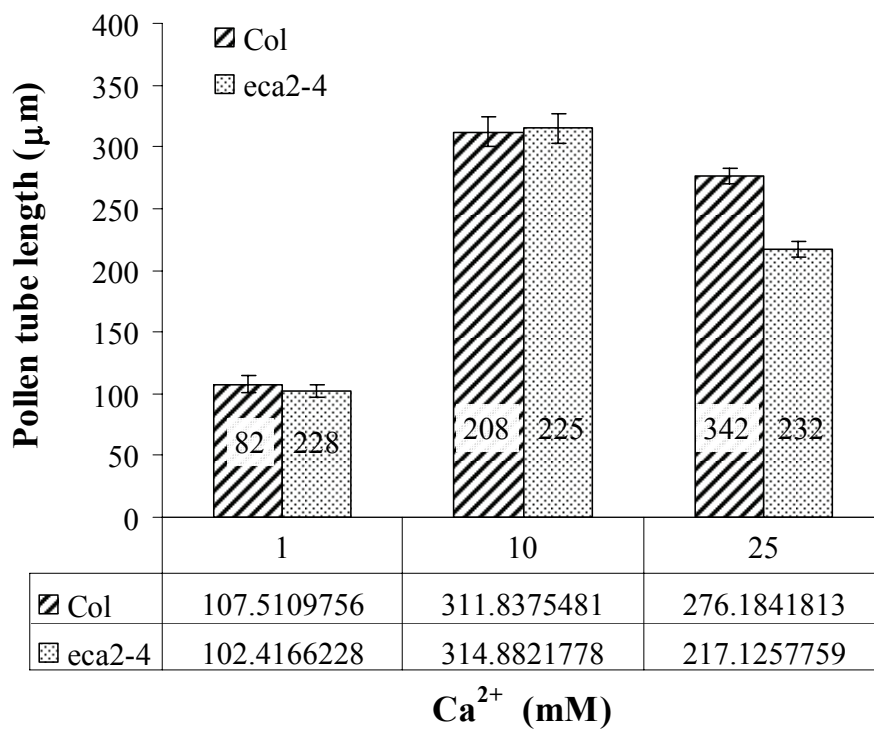
Pollen germination was performed as described for *eca3* mutants on agarose-based solid medium. Data processing was also similar. The *wildtype* control for *eca1-1* and *eca2-1* was WS ecotype originally for *eca2-1*. Both *eca2-2* and *eca2-4* have respective Columbia lines as *wildtype* control. Results represent 1 experiment. The number of measured pollen tubes was also indicated on each column. A, *eca1-1*; B, *eca2-1*; C, *eca2-2*; D, *eca2-4*.

A.



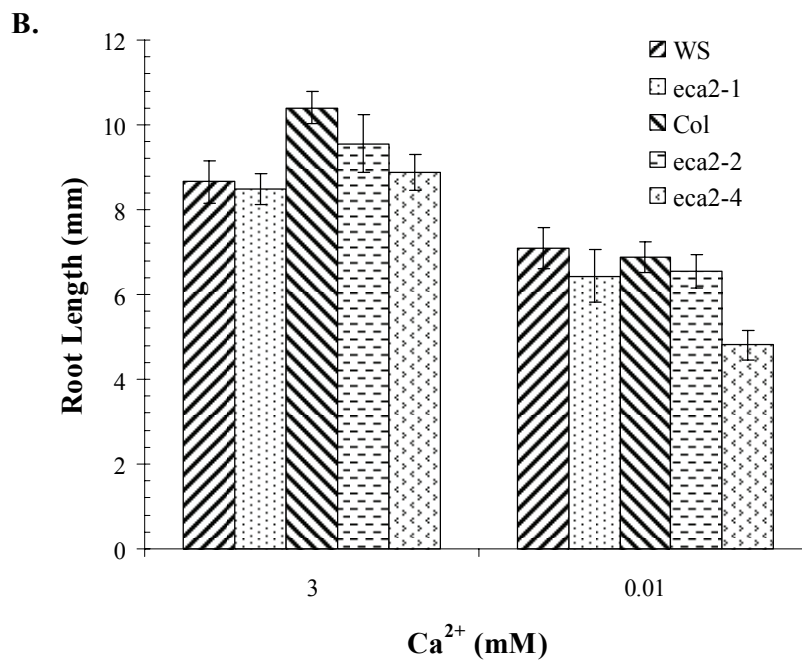
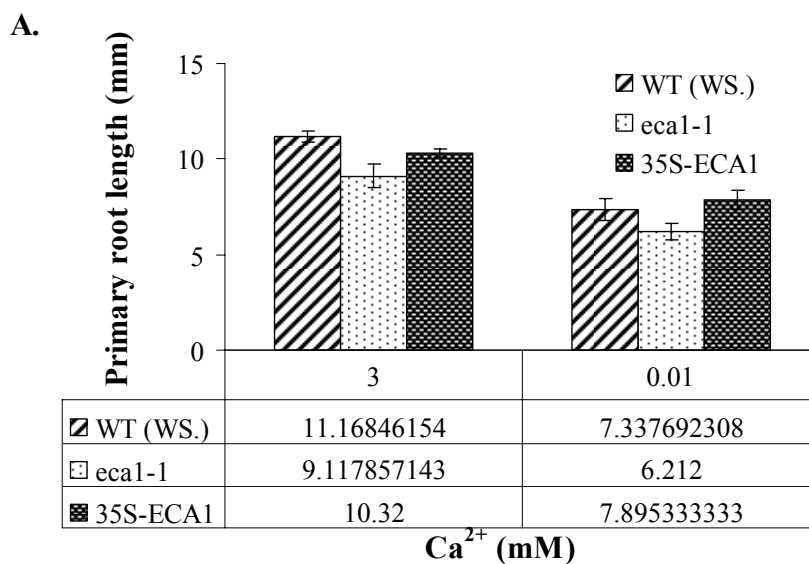
B.**C.**

D.



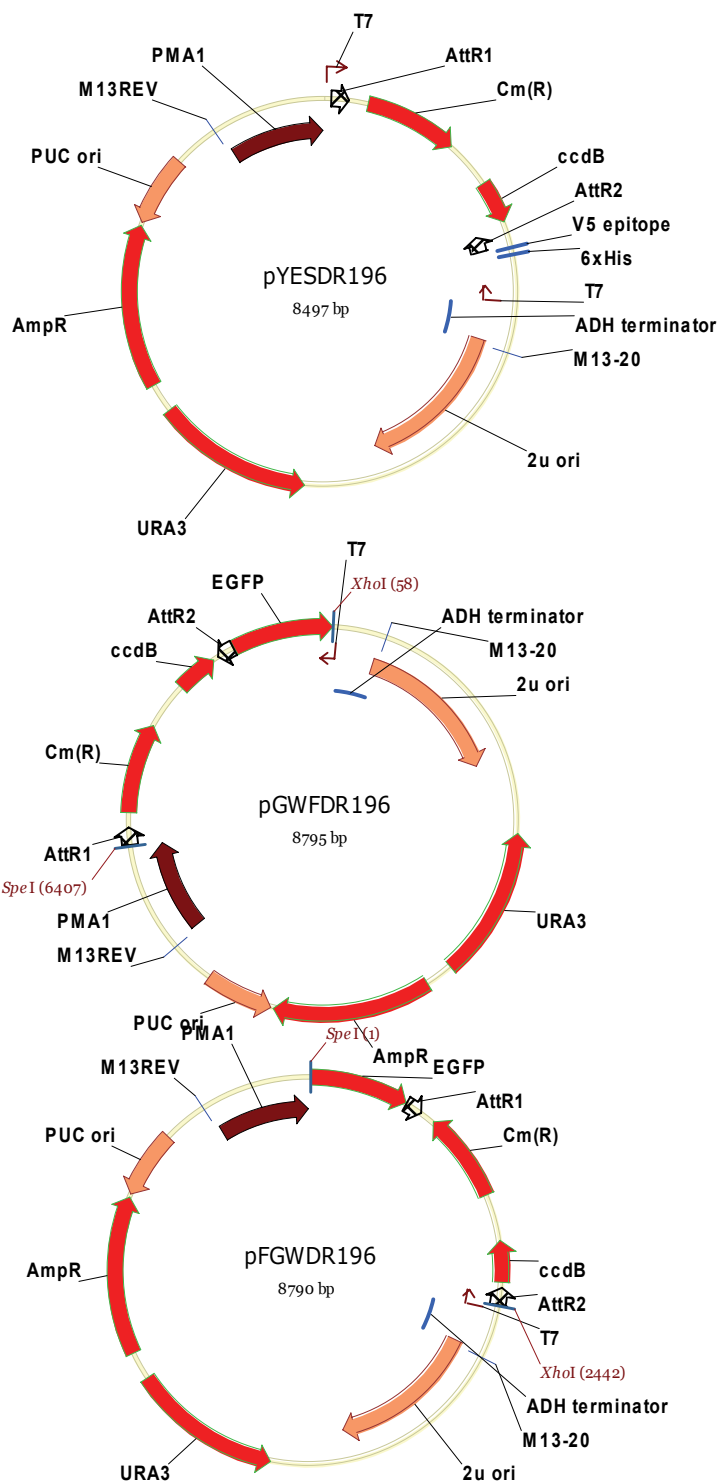
4. Root growth of *eca1* and *eca2* mutants.

Arabidopsis seeds were germinated on ½ MS medium containing 3 mM Ca²⁺ or no added Ca²⁺ (~ 0.01 mM). Root length was measured 3 days after germination. Each experiment represents a duplicate in which 12-14 seedlings were used. A. *eca1-1* and *wildtype* control (WS). B. *eca2* and *wildtype* controls (WS for *eca2-1*; Col for *eca2-2* and *eca2-4*).



5. Generation of Gateway destination vectors for heterologous expression in yeast.

Vectors were generated as described in Materials and Methods section Chapter 3. **Top**, pYESDR196 hosts ScPMA1::AttR1-ccdB-CmR-AttR2-V5 epitope-6xHis-T_{ADH} expression cassette. **Middle**, pGWFDR196 hosts ScPMA1::AttR1-ccdB-CmR-AttR2-eGFP-T_{ADH} expression cassette. **Bottom**, pFGWDR196 hosts ScPMA1:: eGFP-AttR1-ccdB-CmR-AttR2 -T_{ADH} cassette. Plasmids can be propagated in *E. coli* strain DB3.1 only. All three plasmids carry a URA gene for yeast autotrophic selection and ampicillin resistance gene for *E. coli* selection. Universal sequencing primers M13REV and M13-20 were indicated if present.



B. METHODS

1. Home-made Murashige and Skoog medium for *Arabidopsis* plants under different $\text{Ca}^{2+}/\text{Mn}^{2+}$ conditions

(ref: Murashige T. & Skoog F., *Physiol Plant* 15, 473-97 1962)

Stock solutions:

1. Macronutrients (10x)

mM (1x MS)	Salt	10x stock (g/l)
41.2	NH_4NO_3	16.5
18.8	KNO_3	19
3.0	CaCl_2 anhydrous *	3.3
1.5	$\text{MgSO}_4 \cdot 7\text{H}_2\text{O}$	3.7
1.25	KH_2PO_4	1.7

* CaCl_2 is dropped out for Ca^{2+} related medium.

2. Fe-EDTA (100x)

		100x stock (g/L)
Na 0.2	Na_2EDTA	3.73
Fe 0.1	$\text{FeSO}_4 \cdot 7\text{H}_2\text{O}$	2.78

3. Micronutrients (100x)

μM (1x MS)	Salt	100x stock (g/L)
100.0	H_3BO_3	0.62
100.0	$\text{MnSO}_4 \cdot \text{H}_2\text{O}$	1.69
30.0	$\text{ZnSO}_4 \cdot 7\text{H}_2\text{O}$	0.86
5.0	KI	0.083
1.0	$\text{Na}_2\text{MoO}_4 \cdot 2\text{H}_2\text{O}$	0.025
0.1	$\text{CuSO}_4 \cdot 5\text{H}_2\text{O}$	0.0025
0.1	$\text{CoCl}_2 \cdot 6\text{H}_2\text{O}$	0.0025

4. CaCl_2 0.5 M

5. MnCl_2 0.5 M

Make the Media: For ½ MS 1 L, add:

50 ml macronutrient 10x stock
 5ml Fe-EDTA 100x stock
 5ml micronutrient 100x stock
 proper CaCl_2 0.5M (add KCl to $-\text{Ca}^{2+}$ medium as control for Cl)
 0.5g MES (Sigma M-2933, always use 0.5g for 1 liter medium regardless of MS strength)

adjust pH to 5.7
 add agar to 1% all 0.8%
 autoclave for 20-30 min

Comparison of plant Media (mg/L, 1x)

Component	Gamborg's B5	Murashige and Skoog
Total Weight	3,300	4,620
Anorganic Salts		
CaCl ₂ anhydrous	113.23	332.16
CoCl ₂ ·6H ₂ O	0.025	0.025
CuSO ₄ ·5H ₂ O	0.025	0.025
FeSO ₄ ·7H ₂ O	27.8	27.8
H ₃ BO ₃	3	6.2
KH ₂ PO ₄		170
KI	0.75	0.83
KNO ₃	2,500	1,900
MgSO ₄ ·7H ₂ O	246	370
MnSO ₄ ·H ₂ O	10	16.9
NaH ₂ PO ₄ ·H ₂ O	150	
Na ₂ ·EDTA		37.3
Na ₂ MoO ₄ ·2H ₂ O	0.25	0.25
NH ₄ NO ₃		1,650
(NH ₄) ₂ SO ₄	134	
ZnSO ₄ ·7H ₂ O	2	8.6
Vitamins		
i-Inositol	10	100
Nicotinic acid	1	
Pantothenic acid·Ca ²⁺ -salt	0.874	
Pyridoxine·HCl	1	
Riboflavine	0.015	
Thiamine·HCl	10	0.4 *

* The original formulation contains 0.1 mg/l thiamine HCl.

2. Modified ¼ Hoagland medium for *Arabidopsis* growth

¼ Strength Hoagland's solution (used to water *Arabidopsis* plant).

1. Macros:

chemical	FW	Stock	g/250ml stock	Final conc.	ml stock/4L final
KNO ₃	101.1	2 M	50.6	1.25 mM	2.5 ml
FeNa-EDTA	367.1	20 mM	1.8355	12.5 uM	2.5 ml
KH ₂ PO ₄	136.1	1 M	34.0	0.5 mM	2.0 ml
MgSO ₄	120.4	2 M	60.2	0.5 mM	1.0 ml
*Ca(NO ₃) ₂ ·4H ₂ O	236.2	2 M	118.1	0.5 mM	1.0 ml

*:add last when volume is almost full.

2. Minors

Chemical	FW	Stock	final	g/100ml stock	1.0ml
H ₃ BO ₃	61.83	70 mM	17.5 µM	0.43	
MnCl ₂	197.9	14 mM	3.5 µM	0.28	
CuSO ₄	159.6	0.5 mM	0.125 µM	0.08	
ZnSO ₄	287.5	1 mM	0.25 µM	0.03	
Na ₂ MoO ₄ ·2H ₂ O	241.9	0.2 mM	0.05 µM	0.005	

Note: start from >3.9L water, then add every thing and stir thoroughly.
Ca²⁺ may precipitate with SO₄²⁻.

Reference:

Hoagland, D.R., and D.I. Arnon. 1950. The water-culture for growing plants without soil. Calif. Agric. Exp. Stn. Circ. 347 (Rev.).

3. GUS staining protocol (fool-proof version)

(Kirsten Bomblies, adapted from François Parcy's protocol)

A. Sample preparation and Staining

1. Harvest tissue and place in cold 90% Acetone on ice. This should stay on ice until all samples are harvested. For sample containers, eppendorf tubes and glass scintillation vials work well. Microtiter plates are useful for large numbers of samples, but these have to be polystyrene, NOT polypropylene.

2. When all samples are harvested, place at room temperature for 20 minutes and in the mean time make up staining buffer without X-Gluc (see below for recipe) on ice with cold solutions.
3. Remove acetone from the samples, and add staining buffer on ice.
4. Add X- Gluc to the staining buffer to a final concentration of 2mM - from a 100mM stock solution of X-Gluc in DMF- this must be kept in the dark at -20°C.
5. Remove staining buffer from samples and add staining buffer with X-Gluc on ice. Infiltrate the samples under vacuum, on ice, for 15 to 20 minutes. Release the vacuum slowly and verify that all the samples sink. If they don't, infiltrate again until they all sink to the bottom when the vacuum is released.
6. Incubate at 37°C (I usually do it overnight, but it depends on transgene strength. It is not advisable from my experience to go to long (over two days) as the tissue seems to begin deteriorating during long incubations.
7. Remove samples from incubator and remove staining buffer. Go through an Ethanol series in which samples are incubated successively in 20%, 35% and 50% ethanol at room temperature for 30 minutes each.
8. Incubate in FAA (recipe below) for 30 minutes at room temperature to fix the tissue.
9. Remove FAA and add 70% ethanol. At this point the tissue can be stored at 4°C for long periods, or examined under the microscope. if the tissue is to be sectioned, leave in 70% ethanol for 30 minutes and continue below.

Staining buffer

Chemical	final concentrations
Triton X-100	0.2%
Na-HPO ₄ Buffer (pH7.2)	50mM
Potassium Ferrocyanide	2mM
Potassium Ferricyanide	2mM
Water to volume	

make at time of use, do not prepare ahead of time.

note: higher ferri and ferrocyanide concentrations give lower overall staining level, but more specificity. 2mM works well for most

applications, but the concentrations may need to be adjusted for certain needs.

Stock solutions (can be made ahead of time)

Chemical	Concentration
Triton X-100	10%
Na-HPO ₄ Buffer (pH 7.2)	0.5 M
Potassium Ferrocyanide	100 mM (Store in the dark at 4°C)
Potassium Ferricyanide	100 mM (Store in the dark at 4°C)
X-Gluc (5-bromo-4-chloro-3-indolyl β-D-glucuronide cyclohexamine salt)	100mM (in DMF)

FAA (can be made ahead and stored at room temperature)

Chemical	Final concentration
Ethanol	50%
Formaldehyde	5%
acetic acid	10%
water to volume	

B. Embedding for sectioning

It is best to do the following series of steps in glass scintillation vials. Eppendorf tubes are too small for the paraplast changes.

1. Continue with an ethanol series by incubating in 80% and 90% ethanol for 30 minutes each at room temperature. Remove 90% ethanol and incubate overnight in 95% ethanol with 0.1-0.5% Eosin-Y.
2. Remove 95% ethanol the next day and incubate in 100% ethanol, shaking gently for 15 minutes at room temperature. Change the ethanol and incubate again for about 30 minutes.
3. Remove ethanol and add 25% tert-butanol in ethanol and incubate at room temperature for 30 minutes. Repeat with 50% tert-butanol. Remove this and add 100% tert-butanol and incubate at 60°C 6 hours or overnight. At this time, prepare 50%

paraplast in tert-butanol by filling a bottle half-way with the tert-butanol and then doubling the liquid volume by adding paraplast chips. Place in a 58-60°C incubator to melt.

4. Pour out the tert-butanol and add 50% paraplast, filling the vial almost to the top. Incubate overnight at 60°C. At this time melt 100% paraplast chips in a new bottle (not the one that had tert-butanol in it).
5. Pour off the 50% paraplast the next day and add 100% paraplast. Incubate several hours at 60°C.
6. Swirl the vials and let the samples settle. It is easier to pour off the paraplast if the samples are sealed into the bottom by putting your hand against the bottom of the vial to let a thin layer solidify and seal the samples in. Then pour off the melted paraplast quickly. Add more melted paraplast and incubate overnight at 60°C.
7. The next day, do another paraplast change as described above and incubate for one or a few hours. Set up a water-ice slurry, boats for pouring samples (weigh boats work well, or containers can be constructed from foil), and a hot plate with a temperature gradient.
8. After the paraplast has melted again, swirl the vials to suspend the samples and pour quickly into boats on the hot end of a heat block. Adjust the samples quickly with a wooden stick and move the boats as quickly as possible to a cooler temperature to do fine adjustments as the paraplast hardens. Leaving the paraplast too long on the hot end causes bubbles to form on the tissue, which will cause problems during sectioning. Once the paraplast hardens around the base of the tissue, stop moving it and move the boat to a cool surface without agitating it too much. Once it solidifies a bit, move the boat to the water-ice slurry bath to solidify the rest of the way. Store the tissue at 4°C until sectioning.

C. Sectioning

1. Mount the individual samples by cutting them from the blocks with a razor blade by first making a groove, and then breaking the block along the groove. Shave away extra paraplast and melt it on a spatula to mount the sample on a stub.
2. Adjust the angle of the sample and trim away excess paraplast with the microtome on trim. Then start sectioning. For GUS, 8 or 10 microns tends to give good results, but a

variety of thicknesses should be OK. Help the ribbons along with a small paint brush so they don't curl up on themselves.

3. Place the ribbons on a slide loosely and examine under a dissecting scope or inverted scope to choose the sections you want to keep. Put these on black paper so they are easy to see and cut to size with a clean razor blade. Pipette water onto the slide on which you would like to mount the tissue (We use Fisherbrand Superfrost /Plus precleaned microscope slides) and pick up the ribbons gently with a wooden stick with the end slightly moistened with water by touching the ribbons lightly. Place ribbons on the water with the shiny side DOWN (if you look closely, the ribbons come off the microtome with the dull side up and shiny side down, this is the way they should be mounted, otherwise, air bubbles get trapped under them). Place the slide with the water and ribbons on a 42°C slide warmer. Allow them to sit for about ten minutes and then remove excess water by tilting the slide to one corner and removing the drop with a pipette or a kimwipe, being careful not to touch any ribbons.
4. Leave the slides on the slide warmer at 42°C overnight.
5. If the slides are to be stored before they are deparafinized, they should be stored over drierite in a sealed container (but not touching the drierite).

D. Mounting

1. To deparafinize the slides, place them in a slide rack and put the whole rack into a glass container with Xylene and soak for 10 minutes (The xylene can be re-used several times if left in a closed container). Move to another container with xylene for another 10 minutes. This container should have fresher xylenes in it.
2. After the second incubation is over, take the slides out one at a time and drop a large drop of mounting media on each (We use DPX mounting media). Place an appropriately sized cover slip on it and squeeze gently to remove any small bubbles. Let the slides dry overnight on toothpicks or glass pipettes over foil so that both the top and bottom dry well (alternatively, the slides can be dried on foil on a 42°C slide warmer for several hours or overnight). Once dry, excess mounting media is scraped off with a clean razor blade. The samples are now ready to be looked at under a microscope with bright field or dark field illumination.

4. *Arabidopsis* pollen tube germination protocol

Adapted by Xiyan Li September 2006

1. Plant growth

a. Surface-sterilized seeds are stratified on 1X Johnson's medium at 4°C for at least 3 days to synchronize the flowering time. Transfer the plates to growth chamber with sufficient illumination (e.g. 12-16h light/day, growth chamber on the 2nd or 3rd floor is OK).

b. One week old seedlings are transferred to soil pot. I usually grow up to 8 seedlings per standard pot. Mutant and wild-type should be put side by side to avoid position effect in the growth chamber.

c. Water the plants twice a week (Tuesday and Friday, for example), and apply 0.5X Johnson's medium once every other week. The plants may begin to flower 3-4 weeks after transferring. The freshly flowers on the first inflorescence will be good for pollen germination experiments.

(Note: the time to pick flowers is very critical).

2. Preparation of germination plates

Prepare germination medium plates as following (from Fan et al. 2001)

Note: a. Mix well when add MgSO₄ and CaCl₂ to avoid precipitation.

b. According to Zhenbiao Yang's data, 5mM Ca might be better than 10mM.

c. You can make pollen germination medium without Ca²⁺, use it to prepare the pollen resuspension. The unwanted germination before time 0 can be avoided this way.

3. Collect pollens (modified from Honys and Twell, Plant Physiol, 2003)

a. Collect 20-50 freshly opened flowers (stage 13-15, in which the long filaments just level with stigma and petals) in 1.5ml tube, let dry on RT for 0.5 hour (tube cap opened).

Note: You can remove all open flowers from the Plant 16-24 hr before the pollen experiment. By this way just simply pick all flowers without spending time on identifying right stage (warning: wounding response may happen).
(from Yongxian Lu, 05/2006): flowers picked in the morning are better than in afternoon.

- b. Add 1ml germination medium to submerge the flowers. Vortex at maximal speed for 1 min
- c. Concentrate the pollens by 500g 5 min RT centrifuge (3,000rpm on mini-centrifuge).
- d. carefully remove the supernatant and floating flower residues, resuspend the pollen pellet in 1 ml germination medium (with Ca if you used –Ca PGM previously) by vortex. Use 10 ul suspension for pollen amount estimation and purity check under light microscope (typical yield of 10 μ l from 20 flowers is somewhere 2000-5000 grains).

3. Pollen germination

- a. Germinate the pollens at 25-28C for 6 hours or over night in the chambers of a chambered coverlip (200 μ l pollen suspension/ 8-well chamber, Lab-Tek 155411 or VWR 43300-774). No agitation.
- b. Take photos of the germinated tubes using 10X lens on Nikon microscope (inverted is better). Since the tube is transparent, phase contrast will give good pictures.
- c. Analyze the tube germination (rate and length) using Scion Image (free download from NCBI website). A normal distribution is expected for each population of pollen tube length, the P value should be less than 0.05 for student's test.

References:

Fan, L-M, Wang, Y-F, Wang, H, and Wu, W-H. 2001 In vitro *Arabidopsis* Pollen Germination and Characterization of the Inward Potassium Currents in *Arabidopsis* Pollen Grain Protoplasts. J Exp. Bot. 52(361): p1603-1614

- Lalanne E, Honys D, Johnson A, Borner GHH, Lilley KS, Dupree P, Grossniklaus U, and Twell D. 2004 SETH1 and SETH2, Two Components of the Glycosylphosphatidylinositol Anchor Biosynthetic Pathway, Are Required for Pollen Germination and Tube Growth in *Arabidopsis*. *Plant Cell* 16: p229-240.
- Mouline, K, Very, A-A, Gaymard, F, Boucherez, J, Pilot G, Devic, M, Bouchez, D, Thibaud, J-B, and Sentenac, H. 2002 Pollen Tube Development and Competitive Ability Are Impaired by Disruption of a Shaker K⁺ Channel in *Arabidopsis*. *Genes Dev.* 16:p339-350
- Thorsness, MK, Kandasamy, MK, Nasrallah, ME, and Thibaud, J-B. 1993 Genetic Ablation of Floral Cells in *Arabidopsis*. *Plant Cell* 5: p253-261

Pollen Germination Medium (solid)			
Chemical	Stock	Final Conc.	V stock/40ml
MES-Tris (pH5.8 adjusted with Tris base)	200mM	5mM	1ml
KCl	1 M	1 mM	40 µl
MgSO ₄	0.5 M	0.8 mM	64 µl
Boric acid	100 mM	1.5 mM	600 µl
CaCl ₂	0.5 M	10 mM	800 µl
Sucrose		16.6% w/v	6.64 g
Agarose		1% w/v	0.4 g

Pollen Germination Medium (liquid)			
Chemical	Stock	Final Conc.	V stock/40ml
MES-Tris (pH5.8 adjusted with Tris base)	200mM	5mM	1ml
KCl	1M	1mM	40µl
MgSO ₄	0.5M	0.8mM	64µl
Boric acid	100mM	1.5mM	600 µl
CaCl ₂	0.5M	10mM	800 µl
Sucrose		5% w/v	2g
PEG4000		15% w/v	6g

5. Transient expression in *Arabidopsis* mesophyll protoplasts

Latest modified on 2006-03-27.

This protocol is consolidated from Jen Sheen's protocol and Inhwan Hwang's protocol. For references please go to the following websites for their publication lists:

<http://genetics.mgh.harvard.edu/sheenweb/>

<http://www.postech.ac.kr/center/cpit/professor.html>

A. Protoplast Isolation

Plant Materials:

Arabidopsis Columbia plants are planted on soil, cold treated for 3 d, and then transferred to growth chamber (10h L/14h D, 22°C day/ 20°C night, 80-100 μ E). Well expanded leaves from 3.5-4.5 weeks old plants (6-8 leaves with elongated petiole) are used to prepare protoplasts.

B. Protoplast Isolation Procedure:

1. Make 10ml enzyme solution. This is enough for more than 10 standard transfections. Pour solution into 15cm petri plate.
2. Cut 0.5-1 mm leaf strips with fresh razor blades without wounding. Use 2-4 young leaves per plant. Put strips in enzyme solution immediately after cut. 10ml enzyme solution can hold 40-60 such leaves.
3. Put the plate into to a vacuum desiccator and apply vacuum for 30 min. Continue the digestion for about 3 h without shaking in the dark (wrapped in Al foil) at room temperature 22-25°C.
4. Use a round-bottom tube (like the one used for *E. coli* culture), filter the enzyme solution containing protoplasts with a 35-75 μ m nylon mesh by slowly releasing the cell-containing solution from a 10ml transfer pipette. Rinse the plate once with 4 ml W5 solution. Combine the filter-through and spin at 100 x g to pellet the protoplasts 1.5 min (speed 3 with an IEC clinical centrifuge).
5. Resuspend protoplasts once in 10ml W5 solution. Spin at speed 3 for 1.5min, and resuspend in 2ml W5 solution. Count the cell using a chamber counter. Add more W5 to a cell density of 2.5×10^5 /ml.

6. Keep the protoplasts on ice (30 min) in W5 solution.
7. Spin down protoplasts (speed 3 for 1 min) and resuspend in MMg solution (2.5×10^5 /ml) before PEG transfection.

C. PEG Transfection

All steps are carried out at room temperature (e.g. 23°C)

1. Coat the 15ml conical bottom tube with 5% fetal bovine serum (FBS) for 1 sec. Spin for 1min and remove the leftover.
2. Add 60 μ l DNA (60-120 μ g of plasmid DNA of 5 kb in size. For co-transfection, use each with equal moles, the total remains the same).
3. Add 400 μ l protoplasts to a microfuge tube (1×10^5 protoplasts), mix well gently with a 2ml plastic transfer pipet.
4. Add 460 μ l of PEG/Ca solution, mix well (handle 6-10 samples each time) gently with a 2ml plastic transfer pipet. Incubate at 23°C for 5-30 min.
5. Dilute with 3 ml W5 solution and mix well gently with a 2ml plastic transfer pipet.
6. Spin at speed 3 in a Clinical centrifuge for 1 min, remove supernatant. Resuspend protoplasts gently in 200 μ l WI solution by a 2ml plastic transfer pipet.
7. Wrap the tubes with Al foil and keep at ~ 23 °C until microscopic observation.
8. Check the cells for fluorescence under microscope. Most cells should be round with flashy red chloroplast (auto fluorescence) dispersed evenly throughout the cell.

D. Confocal microscope

Cells can be observed 3 h to 20 h after transfection, dependent on the nature of proteins. Soluble proteins take less time to fluoresce.

Common filter settings (on Zeiss LSM510)

Fluorophore	Excitation (nm)	Emission (nm)
GFP	488	BP505-530
RFP	543	BP560-615
Chlorophyll	488	LP650

E. Solutions**a. Enzyme solution (10ml)**

Stock	volume	final conc.
1 M mannitol	4 ml	0.4 M
1 M KCl	0.2 ml	20 mM
0.5 M MES pH5.7	0.4 ml	20 mM
cellulase R10	100-150 mg	1-1.5 %
macerozyme R10	20-40 mg	0.2-0.4 %

Heat the enzyme solution at 55°C for 10 min (to inactivate proteases and enhance enzyme solubility) and cool it to room temperature before adding

1M CaCl ₂	0.1 ml	10 mM
β-mercaptoethanol	4 μl	5 mM
10% FBS (Sigma F6178)	0.1 ml	0.1 %

The enzyme solution is light brown but clear (passed through a 0.45 μm filter).

b. PEG solution (40%, w/v) 10ml

PEG4000 (Fluka, #81240) **Very Important!!	4 g	40% w/v
1 M mannitol	2 ml	200 mM
1 M CaCl ₂	1 ml	100 mM
H ₂ O	3.5 ml	

c. W5 solution (50ml)

1 M NaCl	7.7 ml	154 mM
1 M CaCl ₂	6.25 ml	125 mM
1 M KCl	0.25 ml	5 mM
0.5 M MES-K (pH5.7)	0.2 ml	2 mM

d. MMg solution (5ml)

1 M mannitol	2 ml	0.4 M
0.3 M MgCl ₂	0.25 ml	15 mM
0.5 M MES-K (pH5.7)	40 μL	4 mM

Washing and incubation solution (WI) (10ml)

1 M mannitol	5 ml	0.5 M
0.5 M MES, pH 5.7	80 μL	4 mM
1 M KCl	0.2ml	20 mM

F. Material provider info.**a. Enzymes**

The Cellulase and macerozyme are purchased from

<http://www.yakult.co.jp/yipi/english/frame03.html>

CELLULASE "ONOZUKA" R-10

MACEROZYME R-10

Yakult Pharmaceutical IND. CO., LTD.

Shinbashi MCV Building

5-13-5 Shinbashi Minato-Ku

Tokyo, Japan

Tel 03-5470-9811

Fax 03-5470-8921

The purchasing process can take up to a few weeks.

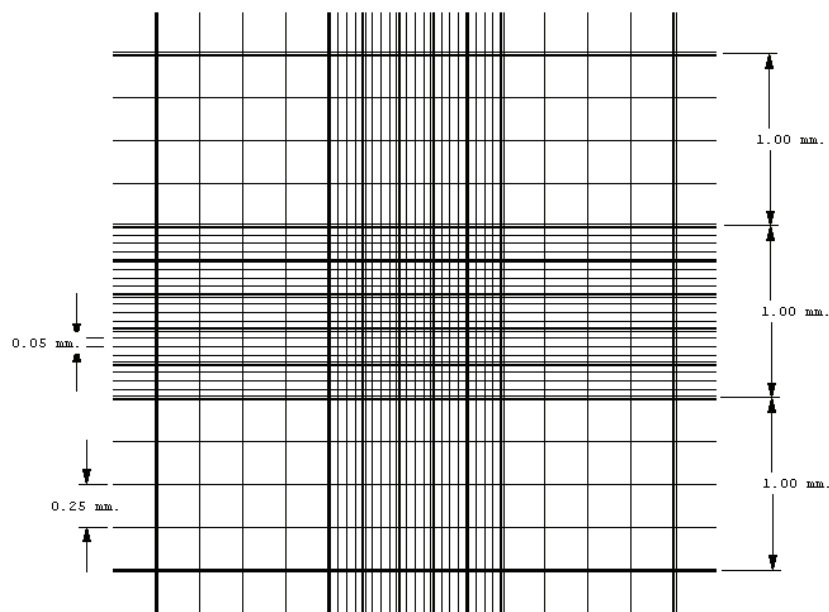
b. The Nylon filters (35-75 μm) can be purchased from Carolina Biological Supplies (65-2222N)

c. Directions for Chamber Counter

<http://www.hausserscientific.com/>

Bright-Line / Dark-Line Counting Chambers

The number of cells per milliliter = Number of cells counted per square millimeter X dilution (if used) X 10,000



Neubauer Ruling

G. Plasmid preparation for transient expression in *Arabidopsis* protoplast

Xiyan Li, Nov. 2005

Comments: If possible, use CsCl gradient for plasmid isolation. This gives maximal transfect efficiency.

I am using Qiagen Plasmid Midi Kit (Cat. No.12143) to prepare ultrapure plasmid DNA. It works efficiently. Due to the cost concern, I may use home-made solutions (instruction on the manual, easy to make), and recycle the Qiagen-tip 100 (4 times sterile DI water wash). For high-copy plasmids use 25ml culture/isolation, and 100ml/isolation for low-copy plasmids.

Miniprep kit like Qiagen kit may also be used, but I don't feel comfortable since it elutes plasmid DNA in 10mM Tris 8.0 in stead of water.

6. Extraction of apoplastic wall fluid for apoplastic peroxidase activity assay.

1. Plant growth

Surface-sterilized *Arabidopsis* seeds are planted on $\frac{1}{4}$ modified Hoagland medium (1 % agar, 5 mM MES-K, pH 6.0) solidified on 1 ml pipette tip box insert (the part with holes). After germination for 2-3 days under light, the boxes with young seedlings are floated in $\frac{1}{4}$ modified Hoagland liquid medium with 5 mM MES-K at pH 6.0, aerated by a fishtank water pump.

2. Extraction of apoplastic wall fluid (AWF)

- Roots of Col seedlings (2.5 weeks old) are rinsed in dI water and cut into 10 mM
- Na⁺-PO₄ pH 6.0.
 - Vacuum for 5 min on ice, followed by slow release for infiltration.
 - The roots are then daubed onto filter paper to dry, measured on balance and recorded as fresh weight.
 - The roots are then put to the plunger barrel of a 5 ml syringe. The syringe barrel is placed in a 15 ml Falcon tube and centrifuged at 3000xg for 15 min at 4 °C.
 - The apoplastic wall fluid (AWF) is rescued from the tube bottom. Total volume is measured by pipetting. AWF is kept on ice.

3. Total protein quantification

Protein concentration measurement (Bradford micro assay) is done according to Bio-Rad reagent instruction.

4. Apoplastic peroxidase (APX) activity assay

To set up a reaction, mix the following:

Chemical	Volume	FW	Stock conc.
Guaiacol	880 μ l	124.14; D=1.112 g/ml	20 mM in 10 mM Na-PO ₄ pH 6.0
AWF	x μ l		
Start the reaction by adding:			
H ₂ O ₂	100 μ l	34.01; 31.4 %	0.3 % (v/v)

Total volume is adjusted to 1 ml.

Reactions are followed spectrophotometrically at 470 nm for 2 min at room temperature. Extinction coefficient = $26.6 \text{ mM}^{-1} \text{ cm}^{-1}$

C. Materials used in this study.

1. Plant Materials

Table 1-I. Collection of ECA T-DNA knockout mutants and transgenic plants from various sources

Line	Homozygous	Ecotype	Marker	Source	Insertion site	Intron/Exon
Wild-type		Col				
		WS				
Knockout						
eca1-1	Yes	WS	Kan	Wisconsin	C-term	exon
eca2-1	Yes	WS	Basta	Wisconsin	C-term	exon
eca2-2	Yes	Col	Basta	SAIL 1167_B11	N-term	exon
eca2-4	Yes	Col	Kan	SALK_039146	Middle	exon
eca3-1	Yes	Col	Basta	SAIL 557_C07	N-term	intron
eca3-4	Yes	Col	Kan	SALK_032802	C-term	exon
eca3-5	Yes	Col	Kan	SALK_045567	N-term	intron
eca4-1	Yes	Col	Kan	SALK_013398	N-term	exon
eca4-3	Yes	Col	Kan	SALK_048468	Middle	exon
Overexpression						
ECA1-1296	Yes	WS	Basta	Harper	Overexpression on eca1-1 background	
ECA1-1297	Yes	WS	Basta	Harper	background	
Col-ECA3	No	Col	Basta	Wild-type	Overexpression on Col	
eca3-4-ECA3	No	Col	Basta	SALK_032802	Overexpression on eca3-4	

The mutants of eca2, eca3, and eca4 are homozygous-DNA insertions as verified with PCR by S. Romanowsky from J.F. Harper's lab at Scripps and X. Li at H. Sze's lab.

Table 1-II. The transgenic *Arabidopsis* plants generated or obtained in this study

Line	Homozygous	Ecotype	Marker	Construct	Source
Promoter::GUS					
ECA1	ECA1GUS1-5	Yes	Col	Basta	P(ECA1)::GUS::T(nos) X Li
	ECA1GUS8-1	Yes	Col	Basta	P(ECA1)::GUS::T(nos) X Li

	ECA1GUS12-5	Yes	Col	Basta	P(ECA1)::GUS::T(nos)	X Li
ECA2	ECA2GUS2-4	Yes	Col	Basta	P(ECA2)::GUS::T(nos)	X Li
	ECA2GUS3-5	Yes	Col	Basta	P(ECA2)::GUS::T(nos)	X Li
	ECA2GUS4-5	Yes	Col	Basta	P(ECA2)::GUS::T(nos)	X Li
	ECA2GUS5-3	Yes	Col	Basta	P(ECA2)::GUS::T(nos)	X Li
	ECA2GUS7-4	Yes	Col	Basta	P(ECA2)::GUS::T(nos)	X Li
	ECA2GUS10-4	Yes	Col	Basta	P(ECA2)::GUS::T(nos)	X Li
	ECA2GUS15-1	Yes	Col	Basta	P(ECA2)::GUS::T(nos)	X Li
ECA3	ECA3GUS5-3	Yes	Col	Basta	P(ECA3)::GUS::T(nos)	X Li
	ECA3GUS6-4	Yes	Col	Basta	P(ECA3)::GUS::T(nos)	X Li
ECA4	ECA4GUS2-4	Yes	Col	Basta	P(ECA4)::GUS::T(nos)	X Li
	ECA4GUS3-4	Yes	Col	Basta	P(ECA4)::GUS::T(nos)	X Li
	ECA4GUS7-5	Yes	Col	Basta	P(ECA4)::GUS::T(nos)	X Li
	ECA4GUS13-3	Yes	Col	Basta	P(ECA4)::GUS::T(nos)	X Li
GFP lines						
ECA3	GE3strong	No	Col	Basta	P(35S)::GFP5-ECA3::T	X Li
	GE3weak	No	Col	Basta	P(35S)::GFP5-ECA3::T	X Li
	E3G	No	Col	Basta	P(35S)::ECA3-GFP5::T	X Li
	PE3G-3	No	Col	Kan	P(Chx08)::ECA3- eGFP::T35S	X Li
	PE3G-5	No	Col	Kan	P(Chx08)::ECA3- eGFP::T35S	X Li
	PE3G-8	No	Col	Kan	P(Chx08)::ECA3- eGFP::T35S	X Li
	E3-PWGF	No	Col	Kan	P(Chx08)::eGFP- ECA3::T35S	X Li
GFP	35S-GFP(1)	No	Col	Basta	P(35S)::GFP5::T	X Li
	35S-GFP(2)	No	Col	Basta	P(35S)::GFP5::T	X Li
	35S-GFP(3)	No	Col	Basta	P(35S)::GFP5::T	X Li
	Lat52-GFP	No	Col	Kan	P(Lat52)::GFP::T(nos)	A Cheung
GFP- ADF	Lat52-GFP-ADF (99-3)	No	Col	Kan	P(Lat52)::GFP-NtADF1 ::T(nos)	A Cheung
	Lat52-GFP-ADF (99-7)	No	Col	Kan	P(Lat52)::GFP::T(nos)	A Cheung

Table 1-III. Plants obtained from other sources

	Sources	Usage
<i>Nicotiana benthamiana</i>	Seeds (from J. Culver's lab)	Transient expression
imp-1	<i>A. thaliana</i> seeds (from Z. Liu's lab)	Male sterility test

2. Yeast Strains and Transformants

Table 2-I. Yeast strains used in this study

Yeast Strain	Genotype	Functional genes
W303-1A	<i>MATa, ade2-1 can1-100 his3-11,15 leu2-3,112 trp1-1 ura3-1</i>	<i>PMR1 PMC1 VCX1 CNB1</i>
K616	<i>Pmr1::HIS3 pmc1::TRP1 cnb1::LEU2</i>	<i>VCX1</i>
K667	<i>Pmc1::TRP1 vcx1Δ cnb1::LEU2</i>	<i>PMR1</i>

Table 2-II. Yeast transformants

Strain name	Yeast strain	Plasmid	Selection	Expression
P426/W303	W303-1A	P426-Gal1	-ura	-
ECA3/W303	W303-1A	pECA3-426	-ura	Gal-induced
P426/K616	K616	P426-Gal1	-ura	-
ECA3/K616	K616	pECA3-426	-ura	Gal-induced
P426/K667	K667	P426-Gal1	-ura	-
ECA3/K667	K667	pECA3-426	-ura	Gal-induced
pDR196/K616	K616	pDR196	-ura	-
ECA3-YESDR196/K616	K616	ECA3-YESTDR196	-ura	Constitutive (PMA1)
ECA3-GWFDR196/K616	K616	ECA3-GWFDR196	-ura	Constitutive (PMA1)
ECA3-FGWDR196/K616	K616	ECA3-FGWDR196	-ura	Constitutive (PMA1)
ECA3-GWFDR196/W303	W303-1A	ECA3-GWFDR196	-ura	Constitutive (PMA1)
pECA3-YES/K616	K616	pECA3-YES	-ura	Gal-induced
pYES/K616	K616	pYES-DEST52	-ura	Gal-induced
pECA3-YES/W303-1A	W303-1A	pECA3-YES	-ura	Gal-induced
pYES/W303-1A	W303-1A	pYES-DEST52	-ura	Gal-induced

3. Vectors used in this study

vectors	Description	Source
Conventional cloning		
p426-Gal1		K Cunningham

p426-ECA3	Gal1-driven ECA3 expression in yeast	X Li
ECA3-GFP-393	Using pAVA393, under CAMV 35S promoter 35S::ECA3-GFP	Von Arnim; see ch. 4 Li X
GFP-ECA3-393	35S::GFP-ECA3	X Li
ECA4-GEM	ECA4 full-length ORF on pGEM7z (Promega)	X Li
pAVA393	35S-driven GFP fusion vector	Von Arnim
ECA3-pMLBart	35S-driven ECA3 expression in plant	X Li
PGal1-ECA4-GFP	GAL1::ECA4-GFP	X Li
GFP-tagged membrane markers		
GFP-CPK9	PM marker, P(35S)::TAP-GFP-CPK9	J-Y Lee & JF Harper
GFP-TIP	Vacuole marker, P(35S)::TAP-GFP-TIP	J-Y Lee & JF Harper
GFP-APX	Peroxisome marker, P(35S)::TAP-GFP-APX36aa	J-Y Lee & JF Harper
GFPper	ER marker, P(35S)::spGFP-HDEL	I Hara-Nishimura
ST-GFP	trans-Golgi marker, P(35S)::ST-GFP	I Hwang
ST-RFP	trans-Golgi marker, P(35S)::ST-RFP	I Hwang
pAN459	cis-Golgi marker, P(35S)::GmMan1-tdTomato	A Nebenfuhr
Gateway cloning		
Entry		
pDONR221	Empty entry vector	Invitrogen
ECA3-DONR221		X Li
Destination Vector		
pYES-DEST52	Empty with Gal1 promoter	Invitrogen
pYES-DR196	Destination pYES-DEST with pDR196 promoter	X Li, see ch III
Destination-GFP		
pKWGF2	Binary with CaMV 35S::eGFP-insert-T35S	D Inze
pKFWG2	Binary CaMVp35S::insert-eGFP-T35S	D Inze
pGWFD196	Destination p2GWF7 with pDR196 promoter	X Li
pFGWDR196	Destination p2FWG7 with pDR196 promoter	X Li
pKPFWG2	Destination vector with pollen-sp promoter CHX08	C Wang
pKPWGF2	Destination vector with pollen-sp promoter CHX08	C Wang
Destination vec + insert		
ECA3-YES-DEST52	GAL1::ECA3	X Li
pYES-DR196-ECA3	PMA1::ECA3	X Li
pGWFD196-ECA3	PMA1::ECA3-GFP	X Li
ECA3-pFGW	Binary vector From pKPFWG2:CHX08::GFP-AtECA3	X Li
ECA3-pGWF	Binary vector from pKPWGF2: CHX08::AtECA3-GFP used in stable transformation to see pollen expression	X Li

REFERENCES

- Ales, E., Tabares, L., Poyato, J.M., Valero, V., Lindau, M., and Alvarez de Toledo, G.** (1999). High calcium concentrations shift the mode of exocytosis to the kiss-and-run mechanism. *Nat Cell Biol* **1**, 40-44.
- Assmann, S.M., and Wang, X.Q.** (2001). From milliseconds to millions of years: guard cells and environmental responses. *Curr Opin Plant Biol* **4**, 421-428.
- Ausubel, F.M., Brent, R., Kingston, R.E., Moore, D., Seidman, J.G., Smith, J.A., and Struhl, K.** (1988). *Current protocols in molecular biology*. (New York: Published by Greene Pub. Associates and Wiley-Interscience : J. Wiley).
- Axelsen, K.B., and Palmgren, M.G.** (2001). Inventory of the Superfamily of P-Type Ion Pumps in Arabidopsis. *Plant Physiol.* **126**, 696-706.
- Battey, N.H., and Blackbourn, H.D.** (1993). The control of exocytosis in plant cells. *New Phytologist* **125**, 307-338.
- Battey, N.H., James, N.C., Greenland, A.J., and Brownlee, C.** (1999). Exocytosis and endocytosis. *Plant Cell* **11**, 643-660.
- Baxter, I., Tchieu, J., Sussman, M.R., Boutry, M., Palmgren, M.G., Gribskov, M., Harper, J.F., and Axelsen, K.B.** (2003). Genomic Comparison of P-Type ATPase Ion Pumps in Arabidopsis and Rice. *Plant Physiol.* **132**, 618-628.
- Bennett, B.D., Denis, P., Haniu, M., Teplow, D.B., Kahn, S., Louis, J.C., Citron, M., and Vassar, R.** (2000). A furin-like convertase mediates propeptide cleavage of BACE, the Alzheimer's beta -secretase. *J Biol Chem* **275**, 37712-37717.
- Berg, M., Rogers, R., Muralla, R., and Meinke, D.** (2005). Requirement of aminoacyl-tRNA synthetases for gametogenesis and embryo development in Arabidopsis. *Plant J* **44**, 866-878.
- Bergeron, J.J.M., Brenner, M.B., Thomas, D.Y., and Williams, D.B.** (1994). Calnexin: a membrane-bound chaperone of the endoplasmic reticulum. *Trends in Biochemical Sciences* **19**, 124-128.
- Bock, K.W., Honys, D., Ward, J.M., Padmanaban, S., Nawrocki, E.P., Hirschi, K.D., Twell, D., and Sze, H.** (2006). Integrating Membrane Transport with Male Gametophyte Development and Function through Transcriptomics. *Plant Physiol.* **140**, 1151-1168.

- Bonza, M.C., Morandini, P., Luoni, L., Geisler, M., Palmgren, M.G., and De Michelis, M.I.** (2000). At-ACA8 Encodes a Plasma Membrane-Localized Calcium-ATPase of Arabidopsis with a Calmodulin-Binding Domain at the N Terminus. *Plant Physiol.* **123**, 1495-1506.
- Borisjuk, N., Sitailo, L., Adler, K., Malysheva, L., Tewes, A., Borisjuk, L., and Manteuffel, R.** (1998). Calreticulin expression in plant cells: developmental regulation, tissue specificity and intracellular distribution. *Planta* **206**, 504-514.
- Bosch, M., Cheung, A.Y., and Hepler, P.K.** (2005). Pectin methylesterase, a regulator of pollen tube growth. *Plant Physiol* **138**, 1334-1346.
- Bowman, J.L.** (1994). *Arabidopsis : an atlas of morphology and development.* (New York: Springer-Verlag).
- Bradford, M.M.** (1976). A rapid and sensitive method for the quantitation of microgram quantities of protein utilizing the principle of protein-dye binding. *Anal Biochem* **72**, 248-254.
- Brandizzi, F., and Hawes, C.** (2004). A long and winding road: symposium on membrane trafficking in plants. *EMBO Rep* **5**, 245-249.
- Brewbaker, J., and Kwack, B.** (1963). The essential role of calcium ion in pollen germination and pollen tube growth. *Am J Bot* **50**, 859-865.
- Buchanan, B.B., Gruissem, W., and Jones, R.L.** (2000). *Biochemistry and molecular biology of plants.* (Rockville, Md.: American Society of Plant Physiologists).
- Carol, R.J., and Dolan, L.** (2002). Building a hair: tip growth in *Arabidopsis thaliana* root hairs. *Philos Trans R Soc Lond B Biol Sci* **357**, 815-821.
- Cassab, G.I.** (1998). Plant Cell Wall Proteins. *Annu Rev Plant Physiol Plant Mol Biol* **49**, 281-309.
- Catala, R., Santos, E., Alonso, J.M., Ecker, J.R., Martinez-Zapater, J.M., and Salinas, J.** (2003). Mutations in the Ca²⁺/H⁺ transporter CAX1 increase CBF/DREB1 expression and the cold-acclimation response in Arabidopsis. *Plant Cell* **15**, 2940-2951.
- Chanat, E., and Huttner, W.B.** (1991). Milieu-induced, selective aggregation of regulated secretory proteins in the trans-Golgi network. *J Cell Biol* **115**, 1505-1519.
- Chance, B., and Maehly, A.C.** (1955). *Assay of Catalases and Peroxidases.* (New York: Academic Press).

- Chang, R.** (2005). Physical chemistry for the biosciences. (Sausalito, Calif.: University Science Books).
- Cheng, N.H., Pittman, J.K., Shigaki, T., and Hirschi, K.D.** (2002). Characterization of CAX4, an Arabidopsis H(+)/cation antiporter. *Plant Physiol* **128**, 1245-1254.
- Cheng, N.H., Pittman, J.K., Barkla, B.J., Shigaki, T., and Hirschi, K.D.** (2003). The Arabidopsis cax1 mutant exhibits impaired ion homeostasis, development, and hormonal responses and reveals interplay among vacuolar transporters. *Plant Cell* **15**, 347-364.
- Cheng, N.H., Pittman, J.K., Shigaki, T., Lachmansingh, J., LeClere, S., Lahner, B., Salt, D.E., and Hirschi, K.D.** (2005). Functional association of Arabidopsis CAX1 and CAX3 is required for normal growth and ion homeostasis. *Plant Physiol* **138**, 2048-2060.
- Clough, S.J., and Bent, A.F.** (1998). Floral dip: a simplified method for *Agrobacterium*-mediated transformation of *Arabidopsis thaliana*. *The Plant Journal* **16**, 735-743.
- Corbett, E.F., Michalak, K.M., Oikawa, K., Johnson, S., Campbell, I.D., Eggleton, P., Kay, C., and Michalak, M.** (2000). The conformation of calreticulin is influenced by the endoplasmic reticulum luminal environment. *J Biol Chem* **275**, 27177-27185.
- Cordoba-Pedregosa, M., Gonzalez-Reyes, J.A., Canadillas, M., Navas, P., and Cordoba, F.** (1996). Role of Apoplastic and Cell-Wall Peroxidases on the Stimulation of Root Elongation by Ascorbate. *Plant Physiol* **112**, 1119-1125.
- Cosgrove, D.J.** (1997). Assembly and enlargement of the primary cell wall in plants. *Annu Rev Cell Dev Biol* **13**, 171-201.
- Cosgrove, D.J.** (2005). Growth of the plant cell wall. *Nature Reviews Molecular Cell Biology* **6**, 850-861.
- Cunningham, K., and Fink, G.** (1994). Calcineurin-dependent growth control in *Saccharomyces cerevisiae* mutants lacking PMC1, a homolog of plasma membrane Ca²⁺ ATPases. *J. Cell Biol.* **124**, 351-363.
- Cunningham, K., and Fink, G.** (1996). Calcineurin inhibits VCX1-dependent H⁺/Ca²⁺ exchange and induces Ca²⁺ ATPases in *Saccharomyces cerevisiae*. *Mol. Cell Biol.* **16**, 2226-2237.
- Dauwalder, M., Roux, S.J., and Rabenberg, L.K.** (1985). Cellular and subcellular localization of calcium in gravistimulated corn roots. *Protoplasma* **129**, 137-148.

- Delmer, D.P.** (1987). Cellulose Biosynthesis. Annual Review of Plant Physiology **38**, 259-290.
- Doblin, M.S., Kurek, I., Jacob-Wilk, D., and Delmer, D.P.** (2002). Cellulose biosynthesis in plants: from genes to rosettes. Plant Cell Physiol **43**, 1407-1420.
- Durr, G., Strayle, J., Plemper, R., Elbs, S., Klee, S.K., Catty, P., Wolf, D.H., and Rudolph, H.K.** (1998). The medial-Golgi Ion Pump Pmr1 Supplies the Yeast Secretory Pathway with Ca^{2+} and Mn^{2+} Required for Glycosylation, Sorting, and Endoplasmic Reticulum-Associated Protein Degradation. Mol. Biol. Cell **9**, 1149-1162.
- Edgar, R.C.** (2004). MUSCLE: multiple sequence alignment with high accuracy and high throughput. Nucleic Acids Research **32**, 1792-1797.
- Fan, L.-M., Wang, Y.-F., Wang, H., and Wu, W.-H.** (2001). In vitro Arabidopsis pollen germination and characterization of the inward potassium currents in Arabidopsis pollen grain protoplasts. J. Exp. Bot. **52**, 1603-1614.
- Faure, J.E., Rotman, N., Fortune, P., and Dumas, C.** (2002). Fertilization in *Arabidopsis thaliana* wild type: developmental stages and time course. Plant J **30**, 481-488.
- Fecht-Christoffers, M.M., Fuhrs, H., Braun, H.-P., and Horst, W.J.** (2006). The Role of Hydrogen Peroxide-Producing and Hydrogen Peroxide-Consuming Peroxidases in the Leaf Apoplast of Cowpea in Manganese Tolerance. PLANT PHYSIOLOGY **140**, 1451-1463.
- Ferrol, N., and Bennett, A.B.** (1996). A Single Gene May Encode Differentially Localized Ca^{2+} -ATPases in Tomato. Plant Cell **8**, 1159-1169.
- Finkelstein, R.R., Gampala, S.S., and Rock, C.D.** (2002). Abscisic acid signaling in seeds and seedlings. Plant Cell **14 Suppl**, S15-45.
- Furuichi, T., Cunningham, K.W., and Muto, S.** (2001). A putative two pore channel AtTPC1 mediates Ca^{2+} flux in *Arabidopsis* leaf cells. Plant Cell Physiol **42**, 900-905.
- Futai, M., Wada, Y., and Kaplan, J.H.** (2004). Handbook of ATPases : biochemistry, cell biology, pathophysiology. (Weinheim: Wiley-VCH.).
- Gao, D., Knight, M.R., Trewavas, A.J., Sattelmacher, B., and Plieth, C.** (2004). Self-reporting Arabidopsis expressing pH and $[\text{Ca}^{2+}]$ indicators unveil ion dynamics in the cytoplasm and in the apoplast under abiotic stress. Plant Physiol **134**, 898-908.

- Gardiner, J.C., Taylor, N.G., and Turner, S.R.** (2003). Control of cellulose synthase complex localization in developing xylem. *Plant Cell* **15**, 1740-1748.
- Geisler, M., Frangne, N., Gomes, E., Martinoia, E., and Palmgren, M.G.** (2000). The ACA4 Gene of Arabidopsis Encodes a Vacuolar Membrane Calcium Pump That Improves Salt Tolerance in Yeast. *Plant Physiol.* **124**, 1814-1827.
- Goda, Y., and Sudhof, T.C.** (1997). Calcium regulation of neurotransmitter release: reliably unreliable? *Curr Opin Cell Biol* **9**, 513-518.
- Goeger, D.E., Riley, R.T., Dorner, J.W., and Cole, R.J.** (1988). Cyclopiazonic acid inhibition of the Ca²⁺-transport ATPase in rat skeletal muscle sarcoplasmic reticulum vesicles. *Biochem Pharmacol* **37**, 978-981.
- Goldraij, A., Kondo, K., Lee, C.B., Hancock, C.N., Sivaguru, M., Vazquez-Santana, S., Kim, S., Phillips, T.E., Cruz-Garcia, F., and McClure, B.** (2006). Compartmentalization of S-RNase and HT-B degradation in self-incompatible Nicotiana. *Nature* **439**, 805-810.
- Gouet, P., Courcelle, E., Stuart, D.I., and Metz, F.** (1999). ESPript: analysis of multiple sequence alignments in PostScript. *Bioinformatics* **15**, 305-308.
- Harper, J.F., Hong, B., Hwang, I., Guo, H.Q., Stoddard, R., Huang, J.F., Palmgren, M.G., and Sze, H.** (1998). A novel calmodulin-regulated Ca²⁺-ATPase (ACA2) from *Arabidopsis* with an N-terminal autoinhibitory domain. *J Biol Chem* **273**, 1099-1106.
- Hawes, C.** (2005). Cell biology of the plant Golgi apparatus. *New Phytol* **165**, 29-44.
- Hayashi, T.** (1989). Xyloglucans in the Primary Cell Wall. *Annual Review of Plant Physiology and Plant Molecular Biology* **40**, 139-168.
- Hepler, P.K.** (2005). Calcium: a central regulator of plant growth and development. *Plant Cell* **17**, 2142-2155.
- Hepler, P.K., Vidali, L., and Cheung, A.Y.** (2001). Polarized cell growth in higher plants. *Annu Rev Cell Dev Biol* **17**, 159-187.
- Higo, T., Hattori, M., Nakamura, T., Natsume, T., Michikawa, T., and Mikoshiba, K.** (2005). Subtype-specific and ER lumenal environment-dependent regulation of inositol 1,4,5-trisphosphate receptor type 1 by ERp44. *Cell* **120**, 85-98.
- Hirschi, K.** (2001). Vacuolar H⁺/Ca²⁺ transport: who's directing the traffic? *Trends Plant Sci* **6**, 100-104.

- Hirschi, K.D.** (1999). Expression of *Arabidopsis* CAX1 in tobacco: altered calcium homeostasis and increased stress sensitivity. *Plant Cell* **11**, 2113-2122.
- Hirschi, K.D., Zhen, R.-G., Cunningham, K.W., Rea, P.A., and Fink, G.R.** (1996). CAX1, an H⁺/Ca²⁺ antiporter from *Arabidopsis*. *PNAS* **93**, 8782-8786.
- Hoagland, D.R., and Arnon, D.I.** (1950). The water-culture for growing plants without soil. *Univ Calif Coll Agric Exp Stn Circ* **347**.
- Holdaway-Clarke, T.L., and Hepler, P.K.** (2003). Control of pollen tube growth: role of ion gradients and fluxes. *New Phytologist* **159**, 539-563.
- Holdaway-Clarke, T.L., Feijo, J.A., Hackett, G.R., Kunkel, J.G., and Hepler, P.K.** (1997). Pollen Tube Growth and the Intracellular Cytosolic Calcium Gradient Oscillate in Phase while Extracellular Calcium Influx Is Delayed. *Plant Cell* **9**, 1999-2010.
- Holmes-Davis, R., Tanaka, C.K., Vensel, W.H., Hurkman, W.J., and McCormick, S.** (2005). Proteome mapping of mature pollen of *Arabidopsis thaliana*. *Proteomics* **5**, 4864-4884.
- Homann, U.** (1998). Fusion and fission of plasma-membrane material accommodates for osmotically induced changes in the surface area of guard-cell protoplasts. *Planta* **206**, 329-333.
- Homann, U., and Tester, M.** (1997). Ca²⁺-independent and Ca²⁺/GTP-binding protein-controlled exocytosis in a plant cell. *Proc Natl Acad Sci U S A* **94**, 6565-6570.
- Hong, B., Ichida, A., Wang, Y., Gens, J.S., Pickard, B.G., and Harper, J.F.** (1999). Identification of a calmodulin-regulated Ca²⁺-ATPase in the endoplasmic reticulum. *Plant Physiol* **119**, 1165-1176.
- Honys, D., and Twell, D.** (2004). Transcriptome analysis of haploid male gametophyte development in *Arabidopsis*. *Genome Biol* **5**, R85.
- Houston, N.L., Fan, C., Xiang, J.Q., Schulze, J.M., Jung, R., and Boston, R.S.** (2005). Phylogenetic analyses identify 10 classes of the protein disulfide isomerase family in plants, including single-domain protein disulfide isomerase-related proteins. *Plant Physiol* **137**, 762-778.
- Huang, L., Franklin, A.E., and Hoffman, N.E.** (1993a). Primary structure and characterization of an *Arabidopsis thaliana* calnexin-like protein. *Journal of Biological Chemistry* **268**, 6560-6566.

- Huang, L., Berkelman, T., Franklin, A.E., and Hoffman, N.E.** (1993b). Characterization of a Gene Encoding a Ca²⁺-ATPase-Like Protein in the Plastid Envelope. *Proceedings of the National Academy of Sciences* **90**, 10066-10070.
- Hwang, I., Harper, J.F., Liang, F., and Sze, H.** (2000). Calmodulin Activation of an Endoplasmic Reticulum-Located Calcium Pump Involves an Interaction with the N-Terminal Autoinhibitory Domain. *Plant Physiol.* **122**, 157-168.
- Inesi, G., and Toyoshima, C.** (2004). Catalytic and Transport Mechanism of the Sarco-(Endo)Plasmic Reticulum Ca²⁺-ATPase (SERCA). In *Handbook of ATPases : biochemistry, cell biology, pathophysiology*, M. Futai, Y. Wada, and J.H. Kaplan, eds (Weinheim: Wiley-VCH.), pp. 63-87.
- Ishitani, M., Liu, J., Halfter, U., Kim, C.S., Shi, W., and Zhu, J.K.** (2000). SOS3 function in plant salt tolerance requires N-myristoylation and calcium binding. *Plant Cell* **12**, 1667-1678.
- Ito, Y., Nakanomyo, I., Motose, H., Iwamoto, K., Sawa, S., Dohmae, N., and Fukuda, H.** (2006). Dodeca-CLE peptides as suppressors of plant stem cell differentiation. *Science* **313**, 842-845.
- Ivessa, N.E., De Lemos-Chiarandini, C., Gravotta, D., Sabatini, D.D., and Kreibich, G.** (1995). The Brefeldin A-induced retrograde transport from the Golgi apparatus to the endoplasmic reticulum depends on calcium sequestered to intracellular stores. *J Biol Chem* **270**, 25960-25967.
- Iwano, M., Shiba, H., Miwa, T., Che, F.S., Takayama, S., Nagai, T., Miyawaki, A., and Isogai, A.** (2004). Ca²⁺ dynamics in a pollen grain and papilla cell during pollination of *Arabidopsis*. *Plant Physiol* **136**, 3562-3571.
- Jaffe, L.A., Weisenseel, M.H., and Jaffe, L.F.** (1975). Calcium accumulations within the growing tips of pollen tubes. *J Cell Biol* **67**, 488-492.
- Jauh, G.Y., Fischer, A.M., Grimes, H.D., Ryan, C.A., Jr., and Rogers, J.C.** (1998). delta-Tonoplast intrinsic protein defines unique plant vacuole functions. *Proc Natl Acad Sci U S A* **95**, 12995-12999.
- Jiang, L., Yang, S.-L., Xie, L.-F., Puah, C.S., Zhang, X.-Q., Yang, W.-C., Sundaresan, V., and Ye, D.** (2005). VANGUARD1 Encodes a Pectin Methylesterase That Enhances Pollen Tube Growth in the Arabidopsis Style and Transmitting Tract. *Plant Cell* **17**, 584-596.
- Jin, J.B., Kim, Y.A., Kim, S.J., Lee, S.H., Kim, D.H., Cheong, G.-W., and Hwang, I.** (2001). A New Dynamin-Like Protein, ADL6, Is Involved in Trafficking from the trans-Golgi Network to the Central Vacuole in Arabidopsis. *Plant Cell* **13**, 1511-1526.

- Johnson, S., Michalak, M., Opas, M., and Eggleton, P.** (2001). The ins and outs of calreticulin: from the ER lumen to the extracellular space. *Trends in Cell Biology* **11**, 122-129.
- Kanamaru, K., Kashiwagi, S., and Mizuno, T.** (1993). The cyanobacterium, *Synechococcus* sp. PCC7942, possesses two distinct genes encoding cation-transporting P-type ATPases. *FEBS Letters* **330**, 99-104.
- Karimi, M., Inze, D., and Depicker, A.** (2002). GATEWAY vectors for Agrobacterium-mediated plant transformation. *Trends Plant Sci* **7**, 193-195.
- Kaufman, R.J., Swaroop, M., and Murtha-Riel, P.** (1994). Depletion of manganese within the secretory pathway inhibits O-linked glycosylation in mammalian cells. *Biochemistry* **33**, 9813-9819.
- Kim, D.H., Eu, Y.J., Yoo, C.M., Kim, Y.W., Pih, K.T., Jin, J.B., Kim, S.J., Stenmark, H., and Hwang, I.** (2001). Trafficking of phosphatidylinositol 3-phosphate from the trans-Golgi network to the lumen of the central vacuole in plant cells. *Plant Cell* **13**, 287-301.
- Kondo, T., Sawa, S., Kinoshita, A., Mizuno, S., Kakimoto, T., Fukuda, H., and Sakagami, Y.** (2006). A plant peptide encoded by CLV3 identified by in situ MALDI-TOF MS analysis. *Science* **313**, 845-848.
- Koren'kov, V., Park, S., Cheng, N.H., Sreevidya, C., Lachmansingh, J., Morris, J., Hirschi, K., and Wagner, G.J.** (2006). Enhanced Cd(2+)-selective root-tonoplast-transport in tobaccos expressing Arabidopsis cation exchangers. *Planta*.
- Kwiatkowski, B.A., Zielinska-Kwiatkowska, A.G., Migdalski, A., Kleczkowski, L.A., and Wasilewska, L.D.** (1995). Cloning of two cDNAs encoding calnexin-like and calreticulin-like proteins from maize (*Zea mays*) leaves: identification of potential calcium-binding domains. *Gene* **165**, 219-222.
- LaFerla, F.M.** (2002). Calcium dyshomeostasis and intracellular signalling in Alzheimer's disease. *Nat Rev Neurosci* **3**, 862-872.
- Lagarde, D., Basset, M., Lepetit, M., Conejero, G., Gaymard, F., Astruc, S., and Grignon, C.** (1996). Tissue-specific expression of Arabidopsis AKT1 gene is consistent with a role in K⁺ nutrition. *The Plant Journal* **9**, 195-203.
- Lancelle, S.A., Cresti, M., and Hepler, P.K.** (1997). Growth inhibition and recovery in freeze-substituted *Lilium longiflorum* pollen tubes: structural effects of caffeine. *Protoplasma* **196**, 21-33.

- Lapinskas, P.J., Cunningham, K.W., Liu, X.F., Fink, G.R., and Culotta, V.C.** (1995). Mutations in PMR1 suppress oxidative damage in yeast cells lacking superoxide dismutase. *Mol Cell Biol* **15**, 1382-1388.
- Lee, M.H., Min, M.K., Lee, Y.J., Jin, J.B., Shin, D.H., Kim, D.H., Lee, K.-H., and Hwang, I.** (2002). ADP-Ribosylation Factor 1 of Arabidopsis Plays a Critical Role in Intracellular Trafficking and Maintenance of Endoplasmic Reticulum Morphology in Arabidopsis. *Plant Physiol.* **129**, 1507-1520.
- Liang, F., and Sze, H.** (1998). A High-Affinity Ca²⁺ Pump, ECA1, from the Endoplasmic Reticulum Is Inhibited by Cyclopiazonic Acid but Not by Thapsigargin. *Plant Physiol.* **118**, 817-825.
- Liang, F., Cunningham, K.W., Harper, J.F., and Sze, H.** (1997). ECA1 complements yeast mutants defective in Ca²⁺ pumps and encodes an endoplasmic reticulum-type Ca²⁺-ATPase in Arabidopsis thaliana. *PNAS* **94**, 8579-8584.
- Lutgens, F.K., and Tarbuck, E.J.** (1995). *Essentials of geology.* (Englewood Cliffs, NJ: Prentice-Hall).
- Lytton, J., Westlin, M., and Hanley, M.R.** (1991). Thapsigargin inhibits the sarcoplasmic or endoplasmic reticulum Ca-ATPase family of calcium pumps. *J Biol Chem* **266**, 17067-17071.
- Machamer, C.E.** (1993). Targeting and retention of Golgi membrane proteins. *Current Opinion in Cell Biology* **5**, 606-612.
- MacLennan, D.H., and Kranias, E.G.** (2003). Phospholamban: a crucial regulator of cardiac contractility. *Nat Rev Mol Cell Biol* **4**, 566-577.
- Malho, R., and Trewavas, A.J.** (1996). Localized Apical Increases of Cytosolic Free Calcium Control Pollen Tube Orientation. *Plant Cell* **8**, 1935-1949.
- Malho, R., Read, N.D., Trewavas, A.J., and Pais, M.S.** (1995). Calcium Channel Activity during Pollen Tube Growth and Reorientation. *Plant Cell* **7**, 1173-1184.
- Marschner, H.** (1986). *Mineral nutrition in higher plants.* (Academic Press Inc.).
- Marschner, H.** (1995). *Mineral nutrition of higher plants.* (London ; San Diego: Academic Press).
- Martin, T.F.J.** (1997). Stages of regulated exocytosis. *Trends in Cell Biology* **7**, 271-276.
- Maser, P., Thomine, S., Schroeder, J.I., Ward, J.M., Hirschi, K., Sze, H., Talke, I.N., Amtmann, A., Maathuis, F.J., Sanders, D., Harper, J.F., Tchieu, J.,**

- Gribskov, M., Persans, M.W., Salt, D.E., Kim, S.A., and Guerinot, M.L.** (2001). Phylogenetic relationships within cation transporter families of *Arabidopsis*. *Plant Physiol* **126**, 1646-1667.
- Massa, G.D., Fasano, J.M., and Gilroy, S.** (2003). Ionic signaling in plant gravity and touch responses. *Gravit Space Biol Bull* **16**, 71-82.
- Matsushima, R., Hayashi, Y., Yamada, K., Shimada, T., Nishimura, M., and Hara-Nishimura, I.** (2003). The ER Body, a Novel Endoplasmic Reticulum-Derived Structure in *Arabidopsis*. *Plant and Cell Physiology* **44**, 661-666.
- Maurer, P., and Hohenester, E.** (1997). Structural and functional aspects of calcium binding in extracellular matrix proteins. *Matrix Biol* **15**, 569-580; discussion 581.
- Meckel, T., Hurst, A.C., Thiel, G., and Homann, U.** (2005). Guard cells undergo constitutive and pressure-driven membrane turnover. *Protoplasma* **226**, 23-29.
- Messerli, M., and Robinson, K.R.** (1997). Tip localized Ca^{2+} pulses are coincident with peak pulsatile growth rates in pollen tubes of *Lilium longiflorum*. *J Cell Sci* **110**, 1269-1278.
- Miller, D.D., Callahan, D.A., Gross, D.J., and Hepler, P.K.** (1992). Free Ca^{2+} Gradient in Growing Pollen Tubes of *Lilium*. *J Cell Sci* **101**, 7-12.
- Mullen, R.T., and Trelease, R.N.** (2000). The sorting signals for peroxisomal membrane-bound ascorbate peroxidase are within its C-terminal tail. *J Biol Chem* **275**, 16337-16344.
- Mumberg, D., Muller, R., and Funk, M.** (1994). Regulatable promoters of *Saccharomyces cerevisiae*: comparison of transcriptional activity and their use for heterologous expression. *Nucleic Acids Res* **22**, 5767-5768.
- Murashige, T., and Skoog, F.** (1962). A revised medium for rapid growth and bio assays with tobacco tissue cultures. *Physiologia Plantarum* **15**, 473-497.
- Nash, P.D., Opas, M., and Michalak, M.** (1994). Calreticulin: not just another calcium-binding protein. *Molecular and Cellular Biochemistry* **135**, 71-78.
- Navazio, L., Bewell, M.A., Siddiqua, A., Dickinson, G.D., Galione, A., and Sanders, D.** (2000). Calcium release from the endoplasmic reticulum of higher plants elicited by the NADP metabolite nicotinic acid adenine dinucleotide phosphate. *Proc Natl Acad Sci U S A* **97**, 8693-8698.
- Nebenfuhr, A., Gallagher, L.A., Dunahay, T.G., Frohlick, J.A., Mazurkiewicz, A.M., Meehl, J.B., and Staehelin, L.A.** (1999). Stop-and-go movements of plant Golgi stacks are mediated by the acto-myosin system. *Plant Physiol* **121**, 1127-1142.

- Obara, K., Miyashita, N., Xu, C., Toyoshima, I., Sugita, Y., Inesi, G., and Toyoshima, C.** (2005). Inaugural Article: Structural role of countertransport revealed in Ca^{2+} pump crystal structure in the absence of Ca^{2+} . *PNAS* **102**, 14489-14496.
- Obermeyer, G., and Weisenseel, M.H.** (1991). Calcium channel blocker and calmodulin antagonists affect the gradient of free calcium ions in lily pollen tubes. *Eur J Cell Biol* **56**, 319-327.
- Oda, K.** (1992). Calcium depletion blocks proteolytic cleavages of plasma protein precursors which occur at the Golgi and/or trans-Golgi network. Possible involvement of Ca^{2+} -dependent Golgi endoproteases. *Journal of Biological Chemistry* **267**, 17465-17471.
- Ordenes, V.R., Reyes, F.C., Wolff, D., and Orellana, A.** (2002). A Thapsigargin-Sensitive Ca^{2+} Pump Is Present in the Pea Golgi Apparatus Membrane. *Plant Physiol.* **129**, 1820-1828.
- Page, R.D.** (1996). TreeView: an application to display phylogenetic trees on personal computers. *Comput Appl Biosci* **12**, 357-358.
- Passardi, F., Cosio, C., Penel, C., and Dunand, C.** (2005). Peroxidases have more functions than a Swiss army knife. *Plant Cell Reports* **24**, 255-265.
- Peiter, E., Maathuis, F.J.M., Mills, L.N., Knight, H., Pelloux, J., Hetherington, A.M., and Sanders, D.** (2005). The vacuolar Ca^{2+} -activated channel TPC1 regulates germination and stomatal movement. *Nature* **434**, 404-408.
- Periz, G., and Fortini, M.E.** (1999). Ca^{2+} -ATPase function is required for intracellular trafficking of the Notch receptor in *Drosophila*. *Embo J* **18**, 5983-5993.
- Pierson, E.S., Miller, D.D., Callaham, D.A., Shipley, A.M., Rivers, B.A., Cresti, M., and Hepler, P.K.** (1994). Pollen tube growth is coupled to the extracellular calcium ion flux and the intracellular calcium gradient: effect of BAPTA-type buffers and hypertonic media. *Plant Cell* **6**, 1815-1828.
- Pina, C., Pinto, F., Feijo, J.A., and Becker, J.D.** (2005). Gene family analysis of the *Arabidopsis* pollen transcriptome reveals biological implications for cell growth, division control, and gene expression regulation. *Plant Physiol* **138**, 744-756.
- Plieth, C.** (2005). Calcium: Just Another Regulator in the Machinery of Life? *Ann Bot* **96**, 1-8.
- Poirot, O., O'Toole, E., and Notredame, C.** (2003). Tcoffee@igs: a web server for computing, evaluating and combining multiple sequence alignments. *Nucleic Acids Research* **31**, 3503-3506.

- Portzehl, H., Caldwell, P.C., and Rueegg, J.C.** (1964). The Dependence of Contraction and Relaxation of Muscle Fibres from the Crab *Maia Squinado* on the Internal Concentration of Free Calcium Ions. *Biochim Biophys Acta* **79**, 581-591.
- Rathmell, W.G., and Sequeira, L.** (1974). Soluble Peroxidase in Fluid from the Intercellular Spaces of Tobacco Leaves. *Plant Physiol.* **53**, 317-318.
- Rathore, K.S., Cork, R.J., and Robinson, K.R.** (1991). A cytoplasmic gradient of Ca^{2+} is correlated with the growth of lily pollen tubes. *Dev Biol* **148**, 612-619.
- Raven, J.A.** (1986). Long Distance Transport of Calcium. (New York: Plenum Press).
- Regan, S.M., and Moffatt, B.A.** (1990). Cytochemical Analysis of Pollen Development in Wild-Type *Arabidopsis* and a Male-Sterile Mutant. *Plant Cell* **2**, 877-889.
- Rentsch, D., Laloi, M., Rouhara, I., Schmelzer, E., Delrot, S., and Frommer, W.B.** (1995). NTR1 encodes a high affinity oligopeptide transporter in *Arabidopsis*. *FEBS Letters* **370**, 264-268.
- Ridley, B.L., O'Neill, M.A., and Mohnen, D.** (2001). Pectins: structure, biosynthesis, and oligogalacturonide-related signaling. *Phytochemistry* **57**, 929-967.
- Robert, S., Bichet, A., Grandjean, O., Kierzkowski, D., Satiat-Jeunemaitre, B., Pelletier, S., Hauser, M.T., Hofte, H., and Vernhettes, S.** (2005). An *Arabidopsis* endo-1,4-beta-D-glucanase involved in cellulose synthesis undergoes regulated intracellular cycling. *Plant Cell* **17**, 3378-3389.
- Robinson, D.G.** (2003). The Golgi apparatus and the plant secretory pathway. (Oxford, UK; Boca Raton, FL: Blackwell Pub.;CRC Press).
- Robinson, K.R.** (1977). Reduced external calcium or sodium stimulates calcium influx in *Pelvetia* eggs. *Planta* **136**, 153-158.
- Roy, S.J., Holdaway-Clarke, T.L., Hackett, G.R., Kunkel, J.G., Lord, E.M., and Hepler, P.K.** (1999). Uncoupling secretion and tip growth in lily pollen tubes: evidence for the role of calcium in exocytosis. *Plant J* **19**, 379-386.
- Rudolph, H.K., Antebi, A., Fink, G.R., Buckley, C.M., Dorman, T.E., LeVitre, J., Davidow, L.S., Mao, J.I., and Moir, D.T.** (1989). The yeast secretory pathway is perturbed by mutations in PMR1, a member of a Ca^{2+} ATPase family. *Cell* **58**, 133-145.
- Sagara, Y., and Inesi, G.** (1991). Inhibition of the sarcoplasmic reticulum Ca^{2+} transport ATPase by thapsigargin at subnanomolar concentrations. *J Biol Chem* **266**, 13503-13506.

- Sakai-Wada, A., and Yagi, S.** (1993). Ultrastructural studies on the Ca^{2+} localization in the dividing cells of the maize root tip. *Cell Struct Funct* **18**, 389-397.
- Salnikov, V.V., Grimson, M.J., Delmer, D.P., and Haigler, C.H.** (2001). Sucrose synthase localizes to cellulose synthesis sites in tracheary elements. *Phytochemistry* **57**, 823-833.
- Sanders, D., Brownlee, C., and Harper, J.F.** (1999). Communicating with Calcium. *THE PLANT CELL* **11**, 691-706.
- Sanders, D., Pelloux, J., Brownlee, C., and Harper, J.F.** (2002). Calcium at the Crossroads of Signaling. *Plant Cell* **14**, S401-417.
- Schiott, M., Romanowsky, S.M., Baekgaard, L., Jakobsen, M.K., Palmgren, M.G., and Harper, J.F.** (2004). A plant plasma membrane Ca^{2+} pump is required for normal pollen tube growth and fertilization. *PNAS* **101**, 9502-9507.
- Seidah, N.G., and Chretien, M.** (1997). Eukaryotic protein processing: endoproteolysis of precursor proteins. *Current Opinion in Biotechnology* **8**, 602-607.
- Seidler, N.W., Jona, I., Vegh, M., and Martonosi, A.** (1989). Cyclopiazonic acid is a specific inhibitor of the Ca^{2+} -ATPase of sarcoplasmic reticulum. *J Biol Chem* **264**, 17816-17823.
- Sheen, J.** (2001). Signal transduction in maize and Arabidopsis mesophyll protoplasts. *Plant Physiol* **127**, 1466-1475.
- Shigaki, T., and Hirschi, K.** (2000). Characterization of CAX-like genes in plants: implications for functional diversity. *Gene* **257**, 291-298.
- Shigaki, T., and Hirschi, K.D.** (2006). Diverse functions and molecular properties emerging for CAX cation/ H^+ exchangers in plants. *Plant Biol (Stuttg)* **8**, 419-429.
- Showalter, A.M.** (2001). Arabinogalactan-proteins: structure, expression and function. *Cell Mol Life Sci* **58**, 1399-1417.
- Sijacic, P., Wang, X., Skirpan, A.L., Wang, Y., Dowd, P.E., McCubbin, A.G., Huang, S., and Kao, T.H.** (2004). Identification of the pollen determinant of S-RNase-mediated self-incompatibility. *Nature* **429**, 302-305.
- Smith, R.A., Duncan, M.J., and Moir, D.T.** (1985). Heterologous protein secretion from yeast. *Science* **229**, 1219-1224.
- Sogo, A., and Tobe, H.** (2005). Intermittent pollen-tube growth in pistils of alders (*Alnus*). *Proc Natl Acad Sci U S A* **102**, 8770-8775.

- Soler, F., Plenge-Tellechea, F., Fortea, I., and Fernandez-Belda, F.** (1998). Cyclopiazonic acid effect on Ca²⁺-dependent conformational states of the sarcoplasmic reticulum ATPase. Implication for the enzyme turnover. *Biochemistry* **37**, 4266-4274.
- Steer, M.W.** (1988). The role of calcium in exocytosis and endocytosis in plant cells. *Physiologia Plantarum* **72**, 213-220.
- Steer, M.W., and Steer, J.M.** (1989). Pollen tube tip growth. *New Phytologist* **111**, 323-358.
- Sterling, J.D., Lemons, J.A., Forkner, I.F., and Mohnen, D.** (2005). Development of a filter assay for measuring homogalacturonan: alpha-(1,4)-Galacturonosyltransferase activity. *Anal Biochem* **343**, 231-236.
- Storey, R., and Leigh, R.A.** (2004). Processes modulating calcium distribution in citrus leaves. An investigation using x-ray microanalysis with strontium as a tracer. *Plant Physiol* **136**, 3838-3848.
- Strayle, J., Pozzan, T., and Rudolph, H.K.** (1999). Steady-state free Ca²⁺ in the yeast endoplasmic reticulum reaches only 10 microM and is mainly controlled by the secretory pathway pump pmr1. *Embo J* **18**, 4733-4743.
- Swofford, D.L.** (2003). PAUP*. Phylogenetic Analysis Using Parsimony (*and Other Methods). (Sunderland, Massachusetts: Sinauer Associates).
- Sze, H., Liang, F., Hwang, I., Curran, A.C., and Harper, J.F.** (2000). DIVERSITY AND REGULATION OF PLANT Ca²⁺ PUMPS: Insights from Expression in Yeast. *Annu Rev Plant Physiol Plant Mol Biol* **51**, 433-462.
- Sze, H., Frietsch, S., Li, X., Bock, K.W., and Harper, J.F.** (2006). Genomic and molecular analyses of transporters in the male gametophyte. In *The pollen tube : a cellular and molecular perspective*, R. Malho, ed (Berlin ; New York: Springer), pp. x, 295.
- Sze, H., Padmanaban, S., Cellier, F., Honys, D., Cheng, N.H., Bock, K.W., Conejero, G., Li, X., Twell, D., Ward, J.M., and Hirschi, K.D.** (2004). Expression patterns of a novel AtCHX gene family highlight potential roles in osmotic adjustment and K⁺ homeostasis in pollen development. *Plant Physiol* **136**, 2532-2547.
- Taiz, L., and Zeiger, E.** (2002). *Plant physiology*. (Sunderland, Mass.: Sinauer Associates Inc. Publishers).

- Takita, Y., Engstrom, L., Ungermann, C., and Cunningham, K.W.** (2001). Inhibition of the Ca²⁺-ATPase Pmc1p by the v-SNARE Protein Nyv1p. *Journal of Biological Chemistry* **276**, 6200-6206.
- Taylor, L.P., and Hepler, P.K.** (1997). Pollen Germination and Tube Growth. *Annu Rev Plant Physiol Plant Mol Biol* **48**, 461-491.
- Toyoshima, C., and Nomura, H.** (2002). Structural changes in the calcium pump accompanying the dissociation of calcium. *Nature* **418**, 605-611.
- Toyoshima, C., Nakasako, M., Nomura, H., and Ogawa, H.** (2000). Crystal structure of the calcium pump of sarcoplasmic reticulum at 2.6 Å resolution. *Nature* **405**, 647-655.
- Van Baelen, K., Dode, L., Vanoevelen, J., Callewaert, G., De Smedt, H., Missiaen, L., Parys, J.B., Raeymaekers, L., and Wuytack, F.** (2004). The Ca²⁺/Mn²⁺ pumps in the Golgi apparatus. *Biochim Biophys Acta* **1742**, 103-112.
- van Vliet, C., Thomas, E.C., Merino-Trigo, A., Teasdale, R.D., and Gleeson, P.A.** (2003). Intracellular sorting and transport of proteins. *Progress in Biophysics and Molecular Biology* **83**, 1-45.
- von Arnim, A.G., Deng, X.W., and Stacey, M.G.** (1998). Cloning vectors for the expression of green fluorescent protein fusion proteins in transgenic plants. *Gene* **221**, 35-43.
- Wada, I., Rindress, D., Cameron, P.H., Ou, W.J., Doherty, J.J., 2nd, Louvard, D., Bell, A.W., Dignard, D., Thomas, D.Y., and Bergeron, J.J.** (1991). SSR alpha and associated calnexin are major calcium binding proteins of the endoplasmic reticulum membrane. *J Biol Chem* **266**, 19599-19610.
- Wee, E.G.-T., Sherrier, D.J., Prime, T.A., and Dupree, P.** (1998). Targeting of Active Sialyltransferase to the Plant Golgi Apparatus. *Plant Cell* **10**, 1759-1768.
- Weisenseel, M.H., and Jaffe, L.F.** (1976). The major growth current through lily pollen tubes enters as K⁺ and leaves as H⁺. *Planta* **133**, 1-7.
- Welinder, K.G.** (1992). Superfamily of plant, fungal and bacterial peroxidases. *Current Opinion in Structural Biology* **2**, 388-393.
- White, A.R., Xin, Y., and Pezeshk, V.** (1993). Xyloglucan glucosyltransferase in Golgi membranes from *Pisum sativum* (pea). *Biochem J* **294** (Pt 1), 231-238.
- White, P.J.** (2001). The pathways of calcium movement to the xylem. *J. Exp. Bot.* **52**, 891-899.

- White, P.J., and Broadley, M.R.** (2003). Calcium in Plants. *Ann Bot* **92**, 487-511.
- Willats, W.G., McCartney, L., Mackie, W., and Knox, J.P.** (2001). Pectin: cell biology and prospects for functional analysis. *Plant Mol Biol* **47**, 9-27.
- Wimmers, L.E., Ewing, N.N., and Bennett, A.B.** (1992). Higher Plant Ca²⁺-ATPase: Primary Structure and Regulation of mRNA Abundance by Salt. *Proceedings of the National Academy of Sciences* **89**, 9205-9209.
- Wu, Z., Liang, F., Hong, B., Young, J.C., Sussman, M.R., Harper, J.F., and Sze, H.** (2002). An Endoplasmic Reticulum-Bound Ca²⁺/Mn²⁺ Pump, ECA1, Supports Plant Growth and Confers Tolerance to Mn²⁺ Stress. *Plant Physiol.* **130**, 128-137.
- Wuytack, F., Raeymaekers, L., and Missiaen, L.** (2002). Molecular physiology of the SERCA and SPCA pumps. *Cell Calcium* **32**, 279-305.
- Wuytack, F., Raeymaekers, L., and Missiaen, L.** (2003). PMR1/SPCA Ca²⁺ pumps and the role of the Golgi apparatus as a Ca²⁺ store. *Pflugers Arch* **446**, 148-153.
- Xu, C., Ma, H., Inesi, G., Al-Shawi, M.K., and Toyoshima, C.** (2004). Specific Structural Requirements for the Inhibitory Effect of Thapsigargin on the Ca²⁺ ATPase SERCA. *Journal of Biological Chemistry* **279**, 17973-17979.
- Zimmermann, P., Hirsch-Hoffmann, M., Hennig, L., and Gruissem, W.** (2004). GENEVESTIGATOR. Arabidopsis microarray database and analysis toolbox. *Plant Physiol* **136**, 2621-2632.

CURRICULUM VITAE**Xiyan Li****Addresses:**

<i>Home Address:</i>	<i>Work Address:</i>	<i>Emails:</i>
3312 Marlborough Way College Park, MD 20740	H J Patterson Hall Rm3232 University of Maryland College Park, MD 20742	xyli@umd.edu lixian@hotmail.com lixian@gmail.com
<i>Phone number:</i>	301-405-8496	

Education background:

2000-2006	University of Maryland	Ph.D.	Cell Biology & Molecular Genetics
1997-2000	China Agricultural University	M.S.	Plant Physiology
1992-1997	Peking University	B.S.	Biochemistry & Molecular Biology

Research Experiences:*Doctoral dissertation:*

“The importance of sorting calcium in plant cells: uncovering the roles of a sarcoplasmic/endoplasmic reticulum-type calcium ATPase”.
Advisor: Dr. Heven Sze. University of Maryland, College Park, US

M.S. thesis:

“Functional characterization of an abscisic acid-binding protein from *Vicia Fava*”.
Advisor: Dr. Zhang, Da-Peng. China Agricultural University, Beijing, China

B.S. Thesis:

“An improved method of RNA isolation from hardy tissues of grape leaves”.
Advisor: Dr. Zhang, Da-Peng. Peking University, Beijing, China

Positions Held:*University of Maryland*

Lab responsibilities:	Research Assistant	2002-present
	Lab radiation safety officer	2002-present
	Lab computer consultant	2000-present
	Lab ordering	2000-present

Lab growth chamber monitor 2003-present

Teaching experiences:

Teaching Assistant

Introductory Botany 2001, 2002

Plant Physiology 2001, 2000

Technique training and demonstration

Pollen germination training and demo 2004

Protoplast transfection workshop 2005

Publications:

Book review:

Sze, H., Frietsch, S., **Li, X.**, Bock, K.W., and Harper, J.F. (2006). Genomic and molecular analyses of transporters in the male gametophyte. In *The pollen tube : a cellular and molecular perspective*, R. Malho, ed (Berlin ; New York: Springer), pp. x, 295.

Research articles:

Sze, H., Padmanaban, S., Cellier, F., Honys, D., Cheng, N.H., Bock, K.W., Conejero, G., **Li, X.**, Twell, D., Ward, J.M., and Hirschi, K.D. (2004). Expression patterns of a novel AtCHX gene family highlight potential roles in osmotic adjustment and K⁺ homeostasis in pollen development. *Plant Physiol* 136, 2532-2547.

Zhang, D.P., Wu, Z.Y., **Li, X.Y.**, and Zhao, Z.X. (2002). Purification and identification of a 42-kilodalton abscisic acid-specific-binding protein from epidermis of broad bean leaves. *Plant Physiol* 128, 714-725.

Li, X., Romanowsky, S., Harper, J.F., Sze, H. (2006) A thapsigargin-sensitive Ca²⁺/Mn²⁺ pump AtECA3, supports pollen tube growth and male fertility. In preparation.

Li, X., Sze, H. (2006) A Golgi Ca²⁺/Mn²⁺ pump affects root growth through secretion. In preparation.

Meeting Presentations:

Li, X., Harper, J.F., Romanowsky, S., Sze, H. 2006. "A Golgi-localized Ca²⁺/Mn²⁺ pump supports root and pollen tube growth". 2nd Pan American Plant Membrane Biology Workshop, South Padre, TX (US). May 17th-21st. Oral presentation.

Padmanaban S., **Li X.**, Kwak J.M., Sze H. 2006. "Participation of an endomembrane Cation/H⁺ exchanger in guard cell movement" 2nd Pan American Plant Membrane Biology Workshop, South Padre TX (US). May 17th-21st. Poster presentation.

Li, X., Harper, J.F., Romanowsky, S., Sze, H. 2004. "Calcium ATPase AtECA3 shows tissue-specific expression and supports root and pollen tube growth". Minisymposium 24: Membrane transport at ASPB Plant Biology 2004, Orlando, FL (US). July 24th-28th. Oral and poster presentation.

Li, X., Sze, H. 2003-2006. "Arabidopsis 2010: Functional Genomics of Cation Transporters annual collaborative joint lab meetings". Oral presentation.

Scientific society:

Member of American Society of Plant Biologists, 2003-present